

DISERTATIONES GEOLOGICAE UNIVERSITATIS LATVIENSIS

Nr. 18

**ANDIS KALVĀNS**

**MORĒNAS UN LEDĀJA DEFORMĒTU  
NOGULUMU MIKROMORFOĻĪJA UN  
MIKROLINEARITĀTE BALTIJAS  
PIEKRASTES LĪDZENUMĀ RIETUMLATVIJĀ**

**PROMOCIJAS DARBS**

RĪGA 2010

DISERTATIONES GEOLOGICAE UNIVERSITAS LATVIENSIS  
Nr. 18

**ANDIS KALVĀNS**

**MICROMORPHOLOGY AND MICROFABRIC  
OF TILLS AND GLACIALLY DISTURBED  
SEDIMENTS, BALTIC COASTAL PLAIN,  
WESTERN LATVIA**

**DISERTATION**  
IN PARTIAL FULFILLMENT OF THE REQUIREMENTS  
OF THE DOCTOR DEGREE IN GEOLOGY  
SUBDISCIPLINE OF QUATERNARY GEOLOGY AND  
GEOMORPHOLOGY

UNIVERSITY OF LATVIA



The doctoral thesis was carried out: Chair of Geomorphology and Geomatics, Faculty of Geography and Earth Sciences, University of Latvia

Supervisor:

Vitālijs Zelčs, Professor, Dr. geol. (University of Latvia)

Reviewers:

Ojārs Āboltiņš, Professor Em., Dr. habil. geol., University of Latvia

Volli Kalm, Professor Ph. D., Tartu University

Valdis Segliņš, Professor, Dr. geol., University of Latvia

Doctoral Committee:

Vitālijs Zelčs, Professor, Dr. geol. – chairman

Ervīns Lukševičs, Professor, Dr. geol. – deputy chairman

Laimdota Kalniņa, Assoc. Professor, Dr. geogr.

Valdis Segliņš, Professor, Dr. geol.

Aija Dēliņa, Dr. geol.

Ivars Zupiņš, Dr. geol.

Ģirts Stinkulis, Assoc. Professor, Dr. geol. – secretary

This thesis is accepted for the commencement of the degree of Doctor of Geology (in Quaternary Geology and Geomorphology) on October 12, 2010, Protocol No. 07/2010 by the Doctoral Committee of Geology, University of Latvia.

The thesis will be defended at the public session of the Doctoral Committee of Geology University of Latvia, at 10:00 on December 10, 2010 Alberta Street 10, Jāņa un Elfrīdas Rutku auditorium (Room 313).

The publication of this summary of doctoral thesis is granted by the University of Latvia.

The thesis is available at the Scientific Library of the University of Latvia Kalpaka Blvd. 4, Rīga, and Academic Library of Latvia, Lielvārdes Street 24, Rīga.

Address for submitting of comments:

Dr. Ģirts Stinkulis, Department of Geology, University of Latvia, Rainis bulvāris 19, LV-1586, Rīga. Fax: +371 733 2704, e-mail: Girts.Stinkulis@lu.lv

© Andis Kalvāns, 2010

Latvijas Universitāte

[www.lu.lv](http://www.lu.lv)

## Contents

Contents .....	3
Abstract .....	5
Anotācija .....	6
Introduction.....	7
The motivation.....	7
Hypothesis .....	8
The aim .....	8
Main tasks .....	8
Theses to be defended.....	8
Novelty of the research .....	8
Study region .....	9
Approbation of results .....	9
Acknowledgements.....	13
Symbols .....	13
1. Subglacial environments and till micromorphology.....	16
1.1. Pleistocene sediments in Western Latvia.....	16
1.1.1. Sedimentology and stratigraphy .....	17
1.1.2. Structural geology.....	18
1.2. Subglacial environment .....	19
1.3. Shear zone development in granular material.....	20
1.4. Till fabric .....	24
1.5. Till macrofabric statistics and classification.....	26
1.6. The till micromorphology and microfabric .....	27
1.6.1. The till micromorphology.....	28
1.6.2. Micromorphology semi-statistics .....	29
1.6.3. Till microfabric .....	29
1.6.4. Grain size and shape .....	32
2. Methods and materials .....	33
2.1. Samples, data, analysis: the literature overview .....	33
2.1.1. Thin section preparation .....	33
2.1.2. Microfabric data acquisition .....	34
2.1.3. Other image analysis procedures .....	36
2.1.4. Analysis of circular data .....	37
2.1.5. Analysis of spatial distribution of circular data .....	38
2.1.6. Visualization .....	39
2.2. The methodology of this study .....	39
2.2.1. Fieldwork and sampling.....	39
2.2.2. Thin section preparation .....	41
2.2.3. Digital image acquisition.....	43
2.2.4. Microfabric measurement .....	44
2.2.5. Image processing and automated grain orientation measurement .....	45
2.2.6. Statistical procedures .....	49
2.2.7. The methodology testing: experimental sedimentology.....	50
3. The results.....	55
3.1. Ziemeupe site.....	58
3.1.1. The samples .....	59

3.1.2.	Microfabric and macrofabric comparison.....	60
3.1.3.	The micromorphology .....	60
3.1.4.	Upper Till: Sample ZP2.....	62
3.1.5.	Upper till: Sample ZP5 .....	62
3.1.6.	Shear zone between the tills: Sample ZP1 .....	62
3.1.7.	The sandy shear zone: Sample ZP6 and Sample ZP7.....	67
3.1.8.	Lower Till: Sample ZP3 .....	73
3.1.9.	Lower till, sample ZP4 .....	73
3.2.	Plašumi gully site.....	76
3.2.1.	The Samples.....	78
3.2.2.	Till micromorphology.....	78
3.2.3.	The preferred apparent orientation of different size grains .....	79
3.2.4.	The microfabric and joint system .....	80
3.2.5.	The microfabric strength and relationship to macrofabric.....	83
3.3.	Strante site.....	86
3.3.1.	The samples .....	87
3.3.2.	The summary preferred microfabric orientation.....	89
3.3.3.	The preferred orientation of different-size grains.....	89
3.3.4.	The spatial distribution of microfabric .....	92
3.3.5.	Grain shape considerations .....	98
3.4.	Sensala site.....	99
3.4.1.	The samples .....	101
3.4.2.	Upper till, samples Nos. 043 and 044.....	102
3.4.3.	Upper till, samples Nos. 072, 076b and 071 .....	105
3.4.4.	Upper till, samples Nos. 091 and 092.....	111
3.4.5.	Waterlain till – samples Nos. 042 and 017 .....	111
4.	Discussion and interpretation.....	118
4.1.	Microfabric in a distinct shear zone, Ziemupe case.....	118
4.2.	Origin of diamicton spherules at Plašumi gully site.....	119
4.3.	The origin of sandy diamicton at Strante site .....	119
4.4.	The microfabric strength and till fabric across different scales.....	120
4.5.	Microfabric distribution around gravel grains .....	127
4.6.	The methodological considerations .....	134
	Conclusions.....	137
	References.....	138
	Appendix 1.....	I
	Appendix 2.....	X
	Appendix 3.....	XI
	Appendix 4.....	XII
	Appendix 5.....	XVII
	Appendix 6.....	XIX
	Appendix 7.....	XX
	Appendix 8.....	XXIII
	Appendix 9.....	XXV

## **Abstract**

The till micromorphology examination in thin sections are routinely used tool to study the formation of subglacial sediments processes, but the microstructures are described in subjective terms, and objective research methods are sparse. A spatial distribution of microfabric is examined in tills outcropping along costal cliffs of Baltic Sea in Western Latvia, using especially developed automated toll. A varied microfabric distribution in tills is found: domain-like, well developed unimodal or distinctly bimodal. It is concluded that microfabric usually is similar to the macrofabric orientation, but the microfabric strength is significantly lower. Results indicate that the till microfabric distribution can indicate the processes active in the last stages of till formation.

Keywords: Subglacial environment, micromorphology, till microfabric, image analysis, Latvia.

## **Anotācija**

Morēnas mikromorfoloģijas analīze plānslīpējumos tiek tradicionāli izmantota zemledāja nogulumu veidošanās pētījumos, tomēr mikrostruktūras tiek aprakstītas subjektīvi un reti tiek izmantota objektīvas izpētes metodes. Darbā ir pētīts mikrolinearitātes telpiskais sadalījums morēnās, kas atsedzas Baltijas jūras stāvkrastos Rietumlatvijā, izmantojot īpaši izstrādātu automatizētu paņēmienu. Ir konstatēts, ka morēnām raksturīgs daudzveidīgs mikrolinearitātes sadalījums: domēnu tipa, labi izteikts vienmodāls vai izteikti divmodāls. Vidējā mikrolinearitātes orientācija ir līdzīga makrolinearitātes virzienam, tomēr mikrolinearitāte ir būtiski vājāk izteikta. Rezultāti liecina, ka analizējot morēnas mikrolinearitātes telpisko sadalījumu, ir iespējams raksturo morēnas veidošanās pēdējās fāzes.

Atslēgas vārdi: zemledāja vide, mikromorfoloģija, morēnas mikrolinearitāte, attēla analīze, Latvija

## **Introduction**

In the last decades the micromorphology is an established tool in the glacial geology. Large size thin section from glacial tills are prepared on the routine basis and examined under the polarised light, stereo or electron microscopes. However the terms used to describe the till micromorphology are largely subjective and statistically based approaches are rare. In the thesis method is develop to analysed the till microfabric, by measuring most of the elongated sand grains visible in the thin section. Thus more objective parameters of till micromorphology than visual identification of certain arrangements of the particles can be determined.

The investigations of tills are conduced across all scales: the global and regional scale for ice sheet and ice lobe perspective; the local and outcrop scales for glaciotectonic and glacial dynamic perspective (e.g. Hart, 2006) and the microscale to study the processes behind the ice sheet dynamics and till formation. This dissertation falls in the latest category – studies of tills in microscale by preparing thin sections and investigating them in optical microscope. The apparent (in two-dimensional sections) preferred orientation of sand size particles in tills and glacially disturbed sediments is in the focus of this dissertation.

The dissertation is elaborated in the Rock Research Laboratory at Faculty of Geography and Earth Sciences of the University of Latvia.

## **The motivation**

Most of the till micromorphology studies relay on highly subjective identification of existing microstructures. For example, galaxy or rotation structures (Menzies, 2000a; van der Meer, 1997) and grain stacks (Larsen et al., 2007) are identified from visual assessment of spatial arrangement of few skeleton grains. This approach can easily lead to over estimation of abundance of these structures as random sand grain arrangements can produce similar structures. Therefore statistically based approach is needed to study the till microstructure.

Carr (1999) suggested a semi quantitative method: comparing the relative abundance of all the different microstructures in observed in thin sections from different sediment types. Unfortunately the subjective perception and wishful thinking of the researcher can affect the results using this approach as well.

One of the till micro-scale properties that can be statistically analysed in non-subjective manner is the orientation of elongated sand grains – the microfabric. General data about till microfabric in scientific literature is relatively sparse (Chaolu, Zhijiu, 2001; Stroeven et al., 2005; Carr, Rose, 2003; Zaniewski, van der Meer, 2005; Roberts, Hart, 2005; Thomason, Iverson, 2006, 2009), so the need for in-depth analysis of this till property is clearly demonstrated.

It shall be noted that in thin sections only the orientation of apparently elongated sand grains can be measured as the true three-dimensional grain shapes is not known (Chaolu, Zhijiu, 2001).

## **Hypothesis**

It is suggested that the till microfabric – its preferred orientation, fabric strength and especially spatial distribution – hold indications of till formation and thus can be used to reconstruct the subglacial process active at the last stages of till formation.

## **The aim**

The aim of the dissertation is to study deformation of unconsolidated sediments and till formation under active, polythermal to warm-based glacier by analyzing microfabric spatial distribution.

## **Main tasks**

The main tasks for elaboration of the thesis are:

1. Comprehensive literature review about till microfabric, its measurement methods and best practices of statistical treatment and visualization of orientation data in geology to identify most suitable research methods and acquire the state of the art understanding about till micromorphology and particularly – microfabric.
2. Implement relevant methods for: thin section image acquisition and processing; image analysis tools for measurement the orientation of apparently elongated sand grains in thin sections; visualization and statistical analysis of two-dimensional apparent microfabric data.
3. To study the microfabric distribution in tills and glacially disturbed sediments in four key locations: Sensala site, Plašumi gully site, Strante site and Ziemupe site.
4. To discuss the results, particularly, characterize the nature of microfabric spatial distribution in tills and any evidence for identifying till forming processes in spatial arrangement of preferred microfabric orientation.

## **Theses to be defended**

Theses to be defended are:

1. The till microfabric – strength, preferred orientation and its distribution – is highly variable. It can be strong and consistent unidirectional, generally weak and in domains distributed as well as uniformly bidirectional. Generally largest grains exhibit strongest preferred orientation, and summary microfabric usually is consistent with macrofabric orientation but is generally weaker, especially in horizontal sections.
2. It is suggested that the spatial arrangement of microfabric, for example, its arrangement around a gravel grains, can be used to reconstruct the processes active during till formation.

## **Novelty of the research**

In comparison to other similar studies in the world, this study is distinguished by considerably higher level of resolution and volume of acquired data. The microfabric

distribution in full thin section area is studied, considering most of the sand grains visible that may reach several tens of thousands.

In the study it is demonstrated that subglacial sediments are characterised by diversified microfabric distributions, supplementing and expanding the limits of current understanding about till fabrics. On the basis of acquired results it is suggested to analyze the microfabric distributions around gravel grains that will help to better understand till formation processes.

Within the scope of the study new method is developed to be used in studies of glacial as well as non-glacial sediments in thin sections. The method can be used to study such homogeneous materials as tills or, for example, sandstones, acquiring new information about the inner structure of these sediments.

### Study region

The study region is costal plains of western Latvia, particularly bluffs along the Baltic Sea, where a sequence of last glacial cycle sediments are widely exposed. The ease of access to outcrops, diversity of glacial and non-glacial sediments and their internal structure, but most importantly the detail of present examination level of considered sequences combined with opportunity to conduce the research compatible to other scientific activities going on in the Faculty of Geography and Earth Sciences was the contributed in choosing the study sites.

### Approbation of results

The results of the research are presented in several scientific papers:

1. Saks, T., Kalvāns, A., Zelčs, V., 2007. Structure and micromorphology of glacial and non-glacial deposits in coastal bluffs at Sensala, Western Latvia. *Baltica* 20, pp. 19-27.
2. Kalvāns, A., Saks, T., 2008. Two dimensional apparent microfabric of the basal Late Weichselian till and associated shear zone: case study from Western Latvia. *Estonian Journal of Earth Sciences* 57, pp. 241–255.
3. Saks, T., Kalvāns, A., Zelčs, V., *in print*. OSL dating evidence of Middle Weichselian age of shallow basin sediments in Western Latvia, Eastern Baltic. *Quaternary Science Reviews* (*in print*).
4. Saks, T., Kalvāns, A., Zelčs, V., 2010b *accepted for publication*. Subglacial bed deformation and glacial dynamics of the Apriķi glacial tongue, Western Latvia. *Boreas* (*accepted for publication*).
5. Saks, T., Kalvāns, A., Zelčs, V., 2006. Stop 10: Clayey silt diapirs in the cliff sections at Ulmale. *In: Stinkulis, Ģ., Zelčs, V. (compilers), The Baltic Sea Geology: The Ninth Marine Geological Conference, August 27 – September 3, 2006 Jūrmala, Latvia. Pre-Conference and Post-Conference Field Excursion Guidebook*, Rīga, University of Latvia, pp. 54-59.
6. Kalvāns A., Saks T., Zelčs V., 2006, Stop 9: The Baltic Sea cliff section of glaciotectonically disturbed Weichselian deposits at Gudenieki. *In: Stinkulis, Ģ., Zelčs, V. (compilers), The Baltic Sea Geology: The Ninth Marine Geological Conference, August 27 – September 3, 2006 Jūrmala, Latvia. Pre-Conference and Post-Conference Field Excursion Guidebook*, Rīga, University of Latvia, pp. 49-53.



7. Dreimanis, A., Kalvāns, A., Saks, T., Zelčs, V., 2004. Introduction to Stops 6-9. In: Zelčs V. (ed.), *International Field Symposium on Quaternary Geology and Modern Terrestrial Processes, Western Latvia, September 12-17, 2004: Excursion Guide*. University of Latvia, Rīga, pp. 35-36.
8. Kalvāns, A., Saks, T., 2004. Stop 6: The Sensala cliff section. In: Zelčs, V. (ed.), *International Field Symposium on Quaternary Geology and Modern Terrestrial Processes, Western Latvia, September 12-17, 2004: Excursion Guide*. Rīga, University of Latvia, pp. 37-42.
9. Zelčs, V., Kalvāns, A., Saks, T., Ceriņa, A., 2004. STOP 7: The Cliff Section between Gullies at Plašumi and Gudenieki. In: Zelčs V. (ed.), *International Field Symposium on Quaternary Geology and Modern Terrestrial Processes, Western Latvia, September 12-17, 2004: Excursion Guide*. University of Latvia, Rīga, pp. 43-47.
10. Kalvāns, A., Saks T., Zelčs, V., Kalniņa L., 2004. STOP 8: The Cliff Section between Ulmale and Jotiķi. In: Zelčs V. (ed.), *International Field Symposium on Quaternary Geology and Modern Terrestrial Processes, Western Latvia, September 12-17, 2004: Excursion Guide*. University of Latvia, Rīga, pp. 48-53.
11. Saks, T., Kalvāns, A., Zelčs V., 2004. STOP 9: The Cliff Section at Strante. In: Zelčs V. (ed.), *International Field Symposium on Quaternary Geology and Modern Terrestrial Processes, Western Latvia, September 12-17, 2004: Excursion Guide*. University of Latvia, Rīga, pp. 54-56.

The results of the research are presented in several international scientific conferences as follows:

1. Kalvāns, A., Saks, T., 2002. Studies of glaciodynamic structures in Sensala outcrop. *Field symposium on Quaternary geology and Geodynamics in Belarus, May 20 – 25, 2002*. Grodno, Belarus. Minsk, pp. 26-27. *Poster*
2. Kalvāns, A., Saks, T., 2002. Studies of glaciodynamic structures and formation of glacial sediments in the Sensala outcrop. *NorFA seminar. Environment and settling along the Baltic Sea coasts through time. 3 – 6 October, 2002 in Parnu, Estonia*. NorFA, pp. 26-27. *Poster*.
3. Kalvāns, A., Saks, T., 2004. Till micromorphology and microfabric in the Sensala outcrop, Western Latvia. In: Zelčs, V., Segliņš V. (compilers), *International field symposium on Quaternary geology and modern terrestrial processes, Western Latvia, September 12-17, 2004*. Rīga, University of Latvia, pp. 24-26.
4. Kalvāns, A., Saks, T., 2005. Directional and structural analysis of diapir-like structures at Ulmale site, Western Latvia. *International Field Symposium on Quaternary Geology and Landforming Processes, Proceedings of the International Field Symposium, Kola Peninsula, NW Russia, September 4-9, 2005*, Apatity, Russian Academy of Sciences, p. 25-26.
5. Kalvāns, A., Saks, T., 2006. Sedimentology and structural geology of glacial sediments in Sensala outcrop, western Latvia. *Bulletin of the Geological Society of Finland. Special Issue 1, 2006. The 27<sup>th</sup> Nordic Geological Winter Meeting. Abstract Volume*. Oulu, p. 65.
6. Kalvāns A., Saks T., Zelčs V., 2007. 2D analysis of apparent till micro fabrics in thin sections: an example from Western Latvia. *Quaternary*

- International*, 167-168, Supplement 1. *Abstracts the XVII INQUA Congress 2007, Australia, 28 July - 3 August 2007*, 0656, p. 200. (0293)
7. Saks, T., Zelčs, V., Kalvāns, A., 2007. Towards revised Pleistocene stratigraphy of Western Latvia, the Eastern Baltic. *Quaternary International*, 167-168, Supplement 1. *Abstracts the XVII INQUA Congress 2007, Australia, 28 July - 3 August 2007*, p. 471 (0656).
  8. Saks, T., Zelčs, V., Kalvāns A., 2009. OSL dating evidence of Middle Weichselian age of shallow basin sediments in Western Latvia, Latvia. *In: Exploratory workshop on frequency and timing of glaciations in northern Europe (including Britain) during the Middle and Late Pleistocene, February 16-20, 2009, Freie Universität Berlin*. Deutsche Forschungsgemeinschaft, p. 13. *Poster*
  9. Saks, T., Zelčs, V., Kalvāns, A., 2009. A glacial dynamic study of Apriki tongue: implications for deglaciation history. *In: Kalm V., Laumets L., Hang T. (eds.), Extent and timing of Weichselian glaciation southeast of the Baltic Sea: Abstracts and Guidebook. The INQUA Peribaltic Working Group Field Symposium in southern Estonia and northern Latvia, September 13-17, 2009*. Tartu Ülikooli Kirjastus, Tartu, pp. 42-43.
  10. Saks, T., Zelčs, V., Nartišs, M., Kalvāns, A., 2009. The Oldest Dryas last significant fluctuation of the Scandinavian Ice sheet margin in Eastern Baltic and problems of its regional correlation. AGU fall meeting, 14 – 18 December, 2009. San Francisco, California, USA. *Poster*.
  11. Kalvāns, A., Saks, T., 2010. The spatial distribution of microfabric around gravel grains – indicator of till formation processes. *EGU General Assembly, Vienna, Austria, May 2010*. *Poster*.

The main results of the research are presented in the following local scientific conferences:

1. Saks, T., Kalvāns, A., 2001. Baltijas jūras stāvkrasta glaciotektonisks un litoloģisks raksturojums posmā starp Ventas un Užavas grīvām. *Krāj.: Ģeogrāfija. Ģeoloģija. Vides zinātne. Latvijas Universitātes 59. zinātniskā konference. Referātu tēzes*. Rīga, Latvijas Universitāte, lpp. 137-138.
2. Saks, T., Kalvāns, A., 2002. Sensalas atseguma glacigēno nogulumu mikrostruktūras. *Izd.: Ģeogrāfija. Ģeoloģija. Vides zinātne. Latvijas Universitātes 60. zinātniskā konference. Referātu tēzes*. Latvijas Universitāte, Rīga, lp. 163-165.
3. Kalvāns, A., Saks, T., 2003. Sensalas atseguma kvartāra nogulumu kartēšana un vizualizācija. *Izd.: Ģeogrāfija. Ģeoloģija. Vides zinātne. Latvijas Universitātes 61. zinātniskā konference. Referātu tēzes*. Latvijas Universitāte, Rīga, lp. 155.
4. Kalvāns, A., Saks, T., 2004. Ledāja nogulumu uzbūve mikro mērogā. *Izd.: Ģeogrāfija. Ģeoloģija. Vides zinātne. Latvijas Universitātes 62. zinātniskā konference. Referātu tēzes*. Latvijas Universitāte, Rīga, lp. 143.
5. Saks, T., Kalvāns, A., 2004. Ledāja dinamika Sensalas atsegumā un tam piegulošajā teritorijā. *LU Izd.: Ģeogrāfija. Ģeoloģija. Vides zinātne. Latvijas Universitātes 62. zinātniskā konference. Referātu tēzes*. Latvijas Universitāte, Rīga, lp. 164.
6. Saks, T., Kalvāns, A., 2005. Diapīru izvietojuma likumsakarības Rietumlatvijas piekrastes teritorijā. *Izd.: Ģeogrāfija. Ģeoloģija. Vides zinātne. Latvijas Universitātes 63. zinātniskā konference. Referātu tēzes*. Latvijas Universitāte, Rīga, lp. 164.

- zinātne. *Latvijas Universitātes 63. zinātniskā konference. Referātu tēzes.* Latvijas Universitāte, Rīga, lpp. 141-142.
7. Kalvāns, A., Saks, T., Nartišs, M., 2006. Smilts graudiņu orientācija ledāja nogulumos: problēmas pamatojums, pētījumu metodes un piemēri no Rietumlatvijas. *Izd.: Ģeogrāfija. Ģeoloģija. Vides zinātne. Latvijas Universitātes 64. zinātniskā konference. Referātu tēzes.* Latvijas Universitāte, Rīga, lpp. 174-175.
  8. Kalvāns, A., Saks, T., Zelčs, V. 2006. Pleistocēna nogulumu struktūrģeoloģija Baltijas jūras stāvkrastu atsegumos Ziemeļes apkārtnē. *Izd.: Ģeogrāfija. Ģeoloģija. Vides zinātne. Latvijas Universitātes 64. zinātniskā konference. Referātu tēzes.* Latvijas Universitāte, Rīga, lpp. 176-177.
  9. Kalvāns, A., Saks, T., Klimovičs, J. 2007. Subglaciālas bīdes joslas mikromorfoloģija: piemērs no Ziemeļes stāvkrasta. *Izd.: Ģeogrāfija. Ģeoloģija. Vides zinātne. Latvijas Universitātes 65. zinātniskā konference. Referātu tēzes.* Latvijas Universitāte, Rīga, lpp. 148-149.
  10. Kalvāns, A., Saks, T., 2007. Glaciodynamiskās struktūras un ledāja dinamika Ziemeļes stāvkrastā. *Izd.: Ģeogrāfija. Ģeoloģija. Vides zinātne. Latvijas Universitātes 65. zinātniskā konference. Referātu tēzes.* Latvijas Universitāte, Rīga, lpp. 146-147.
  11. Kalvāns, A., Stinkulis, Ģ., Klimovičs, J., Popovs, K., 2007. Iežu un nogulumu mikromorfoloģisko pētījumu iespējas Iežu pētījumu laboratorijā, Krāj.: *Ģeogrāfija. Ģeoloģija. Vides zinātne. Latvijas Universitātes 65. zinātniskā konference. Referātu tēzes.* Rīga, Latvijas Universitāte, lpp. 149-150.
  12. Saks, T., Kalvāns, A., Karvonena, I., 2008. Glaciotektoniska kroku-uzbīdījumu josla – Andomas kalns, Oņegas ezera austrumu krasts, ZR Krievija. *Izd.: Ģeogrāfija. Ģeoloģija. Vides zinātne. Latvijas Universitātes 66. zinātniskā konference. Referātu tēzes.* Latvijas Universitāte, Rīga, lpp. 218-219.
  13. Saks, T., Kalvāns, A., 2008. Morēnas nogulumu mikrolinearitātes īpatnības bīdes zonā: Ziemeļes atsegums, Rietumlatvija. *Izd.: Ģeogrāfija. Ģeoloģija. Vides zinātne. Latvijas Universitātes 66. zinātniskā konference. Referātu tēzes.* Latvijas Universitāte, Rīga, lpp. 217-218.
  14. Saks, T., Kalvāns, A., Zelčs, V., 2008. Apriķu ledāja mēles dinamika un gultnes apstākļi - rekonstrukcija no Baltijas jūras stāvkrastiem. *Izd.: Ģeogrāfija. Ģeoloģija. Vides zinātne. Latvijas Universitātes 66. zinātniskā konference. Referātu tēzes.* Latvijas Universitāte, Rīga, lpp. 220-221.
  15. Zelčs, V., Saks, T., Kalvāns, A., 2008. Baltijas jūras Kurzemes stāvkrastos atsegto baseina seklūdens nogulumu vecums un stratigrāfiskā interpretācija. Krāj.: *Ģeogrāfija. Ģeoloģija. Vides zinātne. Latvijas Universitātes 66. zinātniskā konference. Referātu tēzes.* Latvijas Universitāte, Rīga, lpp. 242-243.
  16. Kalvāns, A., Saks, T., 2009. Morēnas nogulumu mikrolinearitāte – piemēri no Baltijas jūras Kurzemes stāvkrastiem. *Izd.: Ģeogrāfija. Ģeoloģija. Vides zinātne. Latvijas Universitātes 67. zinātniskā konference. Referātu tēzes.* Latvijas Universitāte, Rīga, lpp. 198-199.
  17. Kalvāns, A., Popovs, K., Saks, T., 2009. Vienkārša autokorelācijas algoritma lietojums smilts un aleirīta graudu izmēru sadalījuma fotogrammetriskai noteikšanai. Krāj.: *Ģeogrāfija. Ģeoloģija. Vides zinātne.*

- Latvijas Universitātes 67. zinātniskā konference. Referātu tēzes. Rīga, Latvijas Universitāte, lpp. 201-202.*
18. Saks, T., Kalvāns, A., Zelčs, V., 2009. Diapīras kā ledāja dinamikas indikators: Rietumlatvijas piemērs. *Krāj.: Ģeogrāfija. Ģeoloģija. Vides zinātne. Latvijas Universitātes 67. zinātniskā konference. Referātu tēzes. Rīga, Latvijas Universitāte, lpp. 234-236.*
  19. Zelčs, V., Nartišs, M., Celiņš, I., Markots, A., Strautnieks, I., Krievāns, M., Saks, T., Kalvāns, A., 2009. Raunis paleoezera nogulumi, to izplatība un raksturs. *Izd.: Ģeogrāfija. Ģeoloģija. Vides zinātne. Latvijas Universitātes 67. zinātniskā konference. Referātu tēzes. Latvijas Universitāte, Rīga, lpp. 263-264.*
  20. Bethers, U., Dēliņa, A., Kalvāns, A., Saks, T., Vircavs, V., Virbulis, J., 2010. Pazemes ūdeņu modelēšanas projekts (PUMA). *Izd.: Ģeogrāfija. Ģeoloģija. Vides zinātne. Latvijas Universitātes 68. zinātniskā konference. Referātu tēzes. Latvijas Universitāte, Rīga, lpp. 275-276.*
  21. Kalvāns, A., Saks, T., 2010. Mikrolinearitātes sadalījums ap grants graudiem, kā morēnas veidošanās apstākļu indikators. *Izd.: Ģeogrāfija. Ģeoloģija. Vides zinātne. Latvijas Universitātes 68. zinātniskā konference. Referātu tēzes. Latvijas Universitāte, Rīga, lpp. 299-300.*

### **Acknowledgements**

This work was supported by several funding sources: European Social Fund projects „*Doktorantu un jauno zinātnieku pētniecības darba atbalsts Latvijas Universitātē*” (contract No. 2004/0001/VPD1/ESF/PIAA/04/NP/3.2.3.1/0001/0063) and „*Atbalsts doktora studijām Latvijas Universitātē*” (contract No. 2009/0138/1DP/1.1.2.1.2/09/IPIA/VIAA/004); Latvian Science Council funded projects of fundamental and applied research (No. 09.1420, 05.1498, 04.0147) and research projects funded by the University of Latvia (No. 2007/ZP-87 and 2006/1-229717). The laboratory equipment that allowed this study was purchased within EU funded project No. VPD1/ERAF/CFLA/04/NP/2.5.2./00008/016.

Special thanks go to becoming Dr. geol. Tomas Saks for effective cooperation in fieldwork and valuable discussions since the dawn of history in 1997. The support and understanding, but especially the baby-sitting of our son Daniels Jānis Kalvāns during 2009 and much of the 2010, my dear wife Gunta Kalvāne is deeply appreciated. The work of laboratory assistants Konrāds Popovs and Jānis Klimovičs are acknowledged for helping with preparation of thin sections. The contribution of the Norwegian government must be noted for funding the University Centre in Svalbard where the author had space and opportunity to nourish the most crucial ideas laying in base of this dissertation. Last but not least support of my supervision, Professor Vitālijs Zelčs is acknowledged, among other, especially for raising finances for establishment and furnishing the Rock Research Laboratory at the University of Latvia where all the lab-work was done. With out this the current study would not be possible.

### **Symbols**

The symbols used in thin section sketched images and microfabric distribution representation is summarised respectively in table 1 and table 2; most significant used abbreviations are collected in the table 3.

Table 1 Symbols used in sketched thin section images  
1. tabula. Skicētajos plānslīpējumu attēlos izmantotie simboli






Symbol	Explanation	Symbol	Explanation
	A silt or diamicton with contrasting content inclusion in till		Boundary between different lithologies
	A gravel grain		A scale, in a case of regular rose diagrams corresponding to 300 measurements evenly spread across sector of 30° (used in the Ziemeupe site description)
	A line indicating structure formed by the microfabric		

Table 2 Symbols used for microfabric distribution visualization  
2. tabula. Mikrolinearitātes vizualizācijai izmantotie simboli







Title	Strong fabric	Weak fabric	Method
Rose diagrams			Rose diagrams, with mode length proportional to the square root of the actual number of measurements in a single class. The fabric strength is evaluated by calculated the length of normalised resultant vector ( $R_n$ ; Davis 2002, p.322-330) and compared to critical values for 0.9 confidence level given by Davis (2002, p. 619) and indicated by green (dark grey in B& images) colour in case of strong fabric and grey in case of weak colour.
Density plot with summary orientation			Density plot of data distribution as used by Fisher et al (1985) – each line in diagram represents single measurement and its length represent the inverse of relative spacing between adjacent measurements. Normalised resultant vector $R_n$ is given as a green or grey single line for strong or weak fabric respectively. The fabric strings is evaluated as in case of Rose diagrams
Density plot with eigenvector indicated			Density plot of data distribution as used by Fisher et al (1985) – each line in diagram represents single measurement and its length represent the inverse of relative spacing between adjacent measurements. The single outstanding line is summary orientation – mean clustering direction ( $V_1$ – eigenvector) – as in Thomason and Iverson (2006). The different levels of darkness of summary orientation represent the relative fabric strength ( $S_1$ - eigenvalue).

Table 3 List of used abbreviations  
 3.tabula. Izmantoto saīsinājumi saraksts

<b>Abbreviation</b>	<b>Term</b>	<b>Explanation</b>
R	Radius	Distance between grid points in the images of the microfabric spatial distribution; with term “ <i>grid point</i> ” is understood the point that coincide with centre of microfabric diagram in the thin section image and simultaneously are in the centre of the thin section area from what the data are collected composing the respective diagram.
$V_1$	First eigenvector	indicating the direction of strongest clustering both for two dimensional and three dimensional data
$S_1$	First eigenvalue	indicates the strength of clustering around the direction of strongest clustering ( $V_1$ )

## 1. Subglacial environments and till micromorphology

The subglacial environment is place where most tills are formed and hence tills could bear some clues about the environment itself. Behaviour of ice sheets is largely controlled by the subglacial environments and reconstructing the subglacial environments of large past glaciers will contribute to the modelling efforts of development of the Pleistocene glaciations and understanding of the Earth climate evolution.

In “classical” sedimentology the term microfabric is used to describe arrangement of clay-size particles (e.g. Reynolds, Gorsline, 1992; Kuehl et al., 1988) or silt size particles (e.g. Francus, 1998, 2001). Mean while in glacial geology probably due to works of van der Meer who adopted terminology used in soil science the term plasmic structure or plasmic fabric is used to describe arrangement of clay-size particles. The term microfabric in glacial geology is more often used to refer to orientation of sand size particles (e.g. Evenson, 1970; Johnson, 1983). Hens in this study with term “microfabric” the preferred orientation of elongated sand grains will be understood.

It is understood that in thin sections only apparent microfabric can be observed. This is due to obvious fact that thin section is two-dimensional (2D) sections of three-dimensional (3D) till fabric (e.g. Chaolu, Zhijiu, 2001). For this reason sand grain appearing in thin section as elongated can actually be tabular or even cubic in three dimensions and but rod-shaped grains can appear spherical if the thin section plane is perpendicular to the longest axis of the grain. In the dissertation terms apparent microfabric and microfabric, if not stipulated differently, will be used as synonyms, understanding that only apparent microfabric can be directly measured in thin sections.

In this chapter first the geological background about study site are presented followed by review of the current scientific understanding of subglacial environments and associated till fabric in general. This includes short review of theoretical and experimental works on fabric formation in sheared granular materials like most tills probably are. At the last part of chapter short review of literature about till micromorphology and comprehensive review of available literature about till microfabric is give.

### 1.1. Pleistocene sediments in Western Latvia

At the study area up to 80m thick patch of glacial and basin sediments are presented. It is an extension of huge Quaternary deposit sequence at the depression of Baltic Sea (Juškevičs et al., 1997, 1998). The sedimentary sequence presents a rare opportunity for investigating the Quaternary history and the development of continental glaciations originating in Scandinavia.

The upper part of this section is exposed in about 10-18 m high bluffs between city Ventspils and the town of Liepāja. Dreimanis (1936) first studied coastal bluffs in the region along their entire length of more than 40 km, with main attention paid to the till layers and the orientation of the glaciotectionic deformation structures. He identified two till layers – grey and bluish grey – interbedded or underlain by stratified sand, silt, clay or gravel and assigned them to the penultimate glaciation. Since then the territory has been frequently revisited by numerous researchers: Ulsts, Majore, 1964; Konshin *et al.*, 1970; Veinbergs, Savvaitov, 1970; Danilāns, 1973; Meirons, Straume, 1979; Segliņš, 1987a; Kalniņa *et al.*, 2000; Kalniņa, 2001; Saks *et al.*, 2007 and others. They mostly focused on stratigraphic investigations attempting to establish the formation history of presented sequence.

During several campaigns of geological mapping of the Western Latvia, numerous boreholes have been logged, revealing complex succession of glacial and interglacial sediments as summarised in figure 2. The Quaternary sequence in the coastal area, according to borehole logs, is up to 70 m thick (Juškevičs, 1998).

The study area is located on the north eastern slope of the Baltic bedrock depression. The bedrock surface is dipping from 20 m in the southeast at the foot of Western Kursa upland down to 60 m below sea level near the sea coast with regional inclination 3.3 m/km to WNW. The bedrock surface is intersected by several paleoincisions, reaching up to 100 m below present sea level (Juškevičs *et al.*, 1998). The bedrock is formed by layered sequence of Middle Devonian sandstone, dolomitic marl, clay, dolomite and gypsum and overlaid by thick cover of Quaternary glacial, glaciofluvial, glaciolacustrine, lacustrine and marine deposits (Meirons, Straume, 1979; Juškevičs *et al.*, 1998).

The recent landscape of the mainland area is gently undulated sandy abrasion-accumulation plain of the Baltic Ice Lake to some extent altered by postglacial aeolian activity (Veinbergs, 1964).

### 1.1.1. Sedimentology and stratigraphy

In the patch of Quaternary sediments three glacial sediment levels, interlayered by warmer period marine silt and sand sediments are distinguished (Kalniņa *et al.*, 2000). At the very bottom reddish brown till is covering Devonian sandstones, earlier interpreted as Elsterian (Lētiža) till (Danilāns, 1973; Kalniņa *et al.*, 2000). This till unit is observed in most of the boreholes and usually it is 2-3 m thick.

The lowermost till is topped by some 25 – 30 m of silt and sandy silt sediments. The bottom of this sequence is mostly fine grained – silt, clayey silt and clay sediments rich in organic matter; the upward coarsening is observed (Segliņš, 1987b). Based on the macro faunal and palynological findings, this sedimentary sequence has been correlated with Pulvernieki (Holstenian) interglacial stratigraphic unit (Danilāns, 1973; Segliņš, 1987b; Kalniņa *et al.*, 2000; Kalniņa, 2001). However, no reliable absolute datings are available to prove previous interpretations, and other opinions exist on interpretation of the palynological and diatom records: Charamisinava (1971) based on diatom findings she correlated this silt sediment sequence to Eemian interglacial. Later Meirons and Straume (1979) doubted palynological data resemblance to Pulvernieki (Holstenian) type site, suggesting that pollen successions are more similar to Felicianova (Eemian) pollen record. Saks *et al.* (*in print*) have speculated that this sequence is of Eemian or Early Weichselian age.

The silt sediments are discordantly covered by thin, patchy till and glaciofluvial sediments, situated approximately in the middle of the Quaternary sediment body. The till is mostly reworked and susceptible just in few boreholes, and probably in some outcrop sections (Fig. 1 and 2). However it is not always recognised as a separate unit (Juškevičs *et al.*, 1998).

The top of quaternary sediment sequence is formed by silty sand and sand sediments with clay rich silt sediment interlayers covered by one or two till layers. The silt sediments in this level are often heavily dislocated due to diapirism and it is difficult to estimate correctly their initial position, distribution and thickness. The base of sandy sediments is approximately 20 m below present sea level (Fig. 2) and the upper part of it is outcropping in the coastal bluffs. This sedimentary sequence usually is correlated either with late Holstenian (Pulvernieki) or early Saalian time (Danilāns, 1973), or Eemian time (Kalniņa, 2001), marked as Jūrkalne formation (Segliņš, 1987b). However the new OSL



datings have demonstrated the Late Weichselian age of these sediments (Saks et al., *in print*).

Till layer at the top of the Pleistocene sequence earlier correlated to Saalian age (Danilāns, 1973; Kalniņa *et al.*, 2000) or a composite of Saalian and late-glacial till (Juškevičs, 1998, geological sections to Map of Quaternary Deposits). Its thickness varies being on average 2 m and reaching up to 7-8 m. The top of the till is eroded by Baltic Ice Lake, so in many places boulder pavements and Baltic ice lake sandy sediments are present instead of the till. The two-layer interpretation has been introduced by Dreimanis (1936), who assumed penultimate (Saalian) age of the upper till unit exposed in the Baltic Sea coastal outcrops. With limited critical evaluation this suggestion was preferred in later works by Konshin *et al.* (1970), Danilāns (1973), Juškevičs *et al.*, (1998) and others. This interpretation of the upper till has led to conspicuous situation, where main constituent of the Western Kursa upland is considered Saalian till, and Weichselian till plays only minor part in the Quaternary sequence (Meirons and Straume, 1979). The newest OSL datings and geomorphological investigations have revealed that the till is formed by the latest glaciation (Saks *et al.*, 2007, *in print, accepted for publication*). Segliņš (1987a) summarising the results of large number of grain size analysis concluded that the Late Weichselina (Latvian) till in western Latvia have predominantly of polymodal grain size distribution with dominant fractions of fine sands (0,25-0,1 mm), fine silt (0,02-0,01 mm) and clay (< 0,002 mm), with fine silt mode being the most prominent.

### **1.1.2. Structural geology**

From the structural geology perspective only the upper part of Pleistocene sediment sequence which is outcropping in the coastal bluffs, has been described. The structural architecture is dominated by glaciotectonically deformed three-layer system – the silt and clay sediments at the bottom, sandy sediments in the middle part and till at the top – complicated with density-inversion and glaciotectonically induced structures.

In general, all glaciotectonic deformation structures are attributed to deglaciation phase of the last Scandinavian ice sheet, when ice in the area was distributed in to active glacial tongues and areas of dead, probably frozen to its base ice (Zelčs, Markots, 2004). Two different sets of glaciotectonic assemblages have been described: Glaciotectonic structures associated with marginal position of the glacial tongues, and glaciotectonic structure assemblage associated with central parts of the glacial tongues. The marginal glaciotectonic structures include unidirectional thrusting and/or folding, with compressional stress direction being at the right angle to the overall glacial movement direction.

Deformation in the central parts of the glacial tongues comprises uplifted diapir structures, and accumulation of the till in inter-diapir spaces. Unlike in marginal position, glaciotectonic deformation of the subglacial sandy sediments is characterized mostly by vertical translation (rising diapirs and sinking inter diapir spaces), with little internal deformation.

Gaigalas *et al.* (1967) emphasized that during the last glacial maximum in the study region the glacier advanced from NNW direction out of the Baltic Sea depression which is supported by the palaeoglaciological reconstruction of the Scandinavian ice sheet dynamics through the Weichselian glacial cycle (Punkari, 1997; Boulton *et al.*, 2001a; Zelčs, Markots 2004; Saks, *et al.*, 2007; Saks *et al.*, *accepted for publication*).

## 1.2. Subglacial environment

There are vast literature on subject of subglacial environments, in fact most studies of till or glacial geomorphology are in some extent concerning the subglacial environment as well. Some of these studies are Glen *et al.* (1957); Dreimanis (1973, 1981, 1989), Stephan (1989), van der Meer *et al.* (1992, 2003), van der Meer (1993; 1997), Benn (1994), Wright (1995), Boulton (1996), Boulton *et al.* (2001b), Hart (1996, 1998), Hart *et al.* (2004), Hicock *et al.* (1996), Kjær and Krüger (1998), Alley *et al.* (1997), Hindmarsh (1997), Murray (1997), Piotrowski *et al.* (2001, 2006), Piotrowski, Kraus (1997), van der Wateren (1995, 1999), van der Wateren *et al.* (2000), Hiemstra and van der Meer (1997), Hiemstra and Rijdsdijk (2003), Knight (1999), Waller and Hart (1999), Hindmarsh and Rijdsdijk (2000), Hambrey *et al.* (1999), Carr (1999, 2001), Carr *et al.* (2006), Lachniet *et al.* (1999, 2001), Hambrey and Lawson (2000), Alley (2000), Menzies (2000a, b), Menzies and Taylor (2002), Menzies *et al.* (2006), Filler and Murray (2000), Fitzsimons *et al.* (2000), Knight *et al.* (2000), Phillips and Auton (2000), Siegert (2000), Chaolu and Zhijiu (2001), Ruszczynska-Szenajch (2001), Hoffmann and Piotrowski (2001), Larsen and Piotrowski (2003), Larsen *et al.* (2004, 2007), Mccarroll and Rijdsdijk (2003), Millar and Nelson (2003), Roberts and Hart (2005), Thomason and Iverson (2006, 2009), Hiemstra *et al.* (2006) and many others.

In short it is agreed that there is few dominant process that result in till formation (Table 1.1). It is agreed that rarely any of these process are acting alone (e.g. Piotrowski *et al.*, 2006), there is continuum among them (e.g. Hart, 1998) and till is the result of complex development history and only the last stages of till formation might be reflected in its structure and texture (e.g. Larsen *et al.*, 2004). It should be noted that till is formed as result of extremely complex interaction of processes connected to glacial dynamics, sediment availability, frost action, meltwater action, periglacial environment among which the movement of active glacial ice is the single most significant and genetically indicative process (e.g. Dreimanis, 1989). The described processes have to be seen as end members of the continuum (Dreimanis, 1989; Evans *et al.*, 2006).

It should be noted that some researchers point out that all of the tills have to have undergone some deformation in inter-grain scale (van der Meer *et al.*, 2003; Piotrowski *et al.*, 2004). Some researchers even call for total re-interpretation of till classification taking into account that in all tills micro-scale deformation structures can be observed (Menzies *et al.*, 2006). They argue that the best way to describe subglacial till is to call it glacial “tectomict” (*ibid*, see also Evans *et al.*, 2006).

Piotrowski *et al.* (2004) argues that subglacial till is formed as a cumulative effect of the local deformation spots of glacial bed and ploughing of boulders entrained in ice. The glacial bed is suggested to be in time changing mosaic of deforming and stable sediments. The ploughing of clasts thru the glacial bed is in agreement with Colombo-plastic rheology. They express a light scepticism about whether till micromorphology can be used to infer information about glacier-scale processes as all tills in micro-scale will exhibit some inter-grain movement and it will be more pronounced as the scale gets smaller.

The discussion among scientist are ongoing witch mechanisms of till formation and associated subglacial conditions are most dominant (e.g. Iverson *et al.*, 2003).

There is a view that many visually massive subglacial tills are a two-tear system, upper part being unconsolidated, with large water content and the lover part being highly consolidated and dense (e.g. van der Meer *et al.*, 2003; Evans *et al.*, 2006). The upper part is supposed to undergo penetrative deformation under active ice whilst the lover part

remains stable. This structure may be partly due to ploughing of boulders through the upper part of a till (Tulaczyk *et al.*, 2001).

Table 1.1 The summary of processes involved in till formation  
1.1. tabula. Kopsavilkums par morēnas veidošanās procesiem

Process	Description	Selected references
Melt-out	Slow melting of dead ice (stagnant) ice at the base due to geothermal heat flux or other heat sources resulting in gradual release of debris entrained in glacier.	Dreimanis (1989)
Soft and hard lodgement and ploughing	Melting-out particles from the base of the active ice are pressed against the substratum and eventually cease to move – decouple from the glacier. Sometimes soft and hard lodgement tills are distinguished given the amount of deformation that lodged particles have exerted on the substratum (usually till itself). The process of ploughing is the dragging of larger casts partly protruding from the glacier base through the underlying till layer introducing significant amount of deformation in the till.	Dreimanis (1989), Ruszczynska-Szenajch (2001), Tulaczyk <i>et al.</i> (2001)
Deformation of glacier bed	This is process when significant proportion of glacier movement is realised by deformation of sediments in its base. Sediments eventually are homogenised forming till.	Benn and Evans (1996); Boulton (1996)
Precipitation in water	If the glacier is overriding a body of water and due to melting at the base debris is released and regimented through the water column the waterlain till is formed.	Dreimanis (1989)

### 1.3. Shear zone development in granular material

In last decades the awareness of scientists on the role of soft sediment deformation in till formation has gradually raised from slight scepticism as demonstrated by Dreimanis (1989) to perception that all tills has undergone some deformation, particularly in the microscale, as concluded by Piotrowski *et al.* (2004). In this light the understanding of deformation process and its influence on particle orientation, which is in focus of this study, is crucial. Therefore, before focusing on the till fabric, the theoretical and experimental work about sheared granular materials should be briefly discussed.

In a simple approximation the subglacial deformed sediments are subject to simple shear in a continent-scale shear zone – the base of glacier (e.g. Boulton, 1996). However the deformation there is rather complex and variable in time and space, including, slipping of ice base over rigid bed, shearing of basal sometimes debris-rich ice itself, shearing of soft basal sediments, differentiated shearing of soft or partly frozen basal

sediments and ploughing of boulders partly frozen in the base of ice as recently was reviewed by Evans *et al.* (2006). Therefore it is necessary to remember that experimental (and theoretical as well) studies only partly resembles the deformation process imposed by moving glacier on its bed.

One of the first who mathematically described the behaviour of elongated particle immersed in viscous media was G.B. Jeffery (1922). The significance of his work is underlain by the fact that hardly any scientific paper dealing with the alignment of rigid elongated particles in deforming media is not referring to his pioneering work. It is worse noting that Jeffery (1922) says that he extended the work of Albert Einstein himself who described the increase of viscosity of liquid with immersed spherical particles. Jeffery suggested that particles immersed in viscose fluid that is undergoing laminar motion (simple shear) will periodically rotate with their axis aligned perpendicular to motion plane. Jeffery admits that his equations ignore the velocity gradients introduced by particle in sheared liquid and this is resulting in an uncertainty that can lead to preferred lodgement of particle axis along the direction of motion. Despite the probable alignment of particle axis the rotational movement of particles is expected to continue at any time during the shearing.

Latter March (1932) proposed competing theory – he suggested that rigid particles in deformed media will attain preferred, steady state orientation and will remain there as long as conditions do not change.

The two models usually are referred as Jeffery's models and March's model and this practice are followed there as well. The difference between March and Jeffery models is the character of particle surface-liquid (deforming media) interface. The Jeffery's model assumes no sliding on the interface; the March model – expects that sliding along the particle surface will occur. The rotation of particle in sheared media is induced by the traction of the flowing matrix on the surface of the rigid particle and the force of traction will be fundamentally different in case when the particle surface will be well lubricated (layer with smaller viscosity than the average matrix separating the particle from matrix).

The complex history of till development and the presence of all-size closely packed grains will significantly complicated the development of preferred orientation of elongated particles. As suggested by Carr and Goddard (2007) till fabric can not be explained neither by Jeffery nor March models as most experimental studies favour the March model but it does not explain the b-lineation often observed in a field. Therefore two basic mechanisms must be kept in mind in any study of preferred orientation of elongated particles in tills.

As suggested by recent studies most significant factors affecting preferred orientation of elongated particles in shear zone are interaction with other particles, the character of particle/matrix interface and the shear rate (the amount of displacement accommodated in the shear zone). The initial orientation of particles significantly controls the preferred alignment after the shear only in cases when shear rates are relatively low, interaction of particles is negligible and the particle/matrix interface is cohesive e.g. not lubricated.

Probably the first significant experimental work on high strain shear zone development in granular materials is that one of Mandl *et al.* (1977) who published results of extensive experiments with ring-shear apparatus started already in 1969. The ring-shear apparatus in contrast to standard geotechnical testing equipment can accommodated large strain rates and thus effects of prolonged shearing on geological materials can be studied. The first experimental work on the behaviour of elongated particles in sheared media however is dating back to beginning of previous century: Glen *et al.* (1957) is referring to

the experimental work of Taylor published in 1922, who studied behaviour of elliptic particles immersed in liquid glass and sheared between two rotation cylinders.

The particle/matrix interface is a key element in determining whether the particle in sheared media will behave according to Jeffery or March models. The contrasting behaviour of particles with sticky surface and well lubricated surface is demonstrated by the experimental studies. In ring-shear experiments of Ceriani *et al.* (2003), and Hooyer, Iverson (2000) rotation of elongated particles immersed in viscous, sticky gel corresponded well to theoretical calculations according to Jeffery's model. In case of well lubricated particles (using liquid soap) with initially horizontal position, antithetical rotation to 10-20° dip against the shear direction was observed (Mandal *et al.*, 2005a, 2005b; Ceriani *et al.*, 2003) corresponding to March model. Additionally if the interface is lubricate elongated particles will tend to rotate more quickly compared with the case of non-lubricated interface (Mandal *et al.*, 2005a). Hooyer and Iverson (2000) found that clasts embedded in till displayed rotation behaviour that was more similar to March model, however, the orientation of clasts did not followed the theoretical prediction as close as in case of putty.

The stable state orientation of 10-20° with lubricated particle/matrix interface corresponds to observed dip of preferred orientation of elongated pebbles in till (e.g. Dreimanis 1989; Āboltiņš, Dreimanis, 1995).

Particle elongation predominantly controls the swiftness of its reaction to shearing, but not the steady state orientation when it is attained. Cañón-Tapia, Chávez-Álavarez (2004) mathematically calculated the behaviour of elongated particles in sheared media according to Jeffery's theory. They found that in most geological settings elongated particles (short axis/long axis ratio  $\leq 0.5$ ) will attain steady state preferred orientation after strain rate of 4 to 10, that is close to somewhat large values (7-39) observed by Thomson and Iverson (2006) in their ring shear experimental studies of tills. However, Cañón-Tapia and Chávez-Álavarez (2004) saying "most geological settings" understood emplacement of various forms of magmatic rocks.

The interaction with other particles obviously is important in determining the steady state orientation. In physical model it is observed that denser populations of rigid elongated particles immersed in viscous matrix are reacting more swiftly to shearing and faster attain steady state orientation even if particle collisions is absent and antithetical non-linear rotation can be observed (Mandal *et al.* 2005b). This indicates that tills with large pebble and gravel-size grain content will have stronger preferred macro fabric orientation. In the field it is observed that glaciotectonically deformed gravel has stronger preferred orientation of skeleton grains than the diamicton does (Saks *et al.*, 2007)

Rosas *et al.* (2002) modelling the behaviour of parallelepiped-shaped amphibole crystals in shear zone in marble observed formation of the sheath folds above and below rotating intraclasts. This process inevitably has to affect the orientation of smaller particles which happens to be near the larger ones. Similar sheath-fold-resembling microfabric observed in till thin sections would be reliable indicator of particle rotation and hence the deformation of examined till. The similar configuration of microfabric around the rotating grains in deforming till was suggested by Thomason and Iverson (2006).

The strain rate or relative amount of shear accommodated in sediments undoubtedly is one of the most important factors contribution to fabric, including microfabric development. Large strain rates gives more time for particles to rotate to steady state orientation and the fabric strength is growing with increase of strain rate. However after certain threshold amount of strain is accumulated in sediments the fabric strength attains a steady state value that does not change with increased strain (Hooyer, Iverson, 2000; Thomason, Iverson, 2006).

The Riedel shears are associated with most of the shear zones and their presence will affect any small particles in their vicinity. For example, after prolonged shearing of sugar immersed in kerosene (to mimic the brittle behaviour of sand grains in natural shear zones but in smaller confining pressures), Mandl *et al.* (1977) observed sudden collapse of gradually widening shear zone to a single plane and a classical slickenside was produced with echelon or Riedel shear type slips dipping in direction of shearing at 20-25°.

Thomson and Iverson (2006) found in ring shear experiments with tills that two sets of Riedel shears (R1 and R2) manifested as latiseptic plasmic fabric developed – the R1 having low angles (~25°) against shear plane and R2 – wide angles (~75°). They suggest that most of the shear displacement was accommodated in Riedel shears and the particle preferred orientation can be explained as a result of competing action of both Riedel shear directions.

Kock and Huhn *et al.* (2007) used discrete element mathematical modelling method to determine behaviour of elongated clay and silt particles in shear box conditions. The model was run up to 200% of strain. After their experiment dip direction of most of particles was between minus 10° to plus 40° towards shear direction. Authors found that most of the local shear planes were deviated from horizontal direction usually no more than 20°. Exception was the case with spherical particles where several, equally strong, shear-plane orientation modes deviating from zero up to 50° were observed.

The slip localization in shear zone apparently can produce a plane of parallel-aligned elongated grains. The experimental studies with sufficiently large confining pressure to allow grain fracturing, sometimes result in slip localisation in single slickenside (e.g. Mandl *et al.*, 1977). However in other cases no shear localisation was observed, for example Mair, Hazzard (2007) in case of mathematical modelling. They argued that an analogue experimental study that shown shear localisation when the stress was sufficient for grain fracturing to occur, but in cases when stress was not sufficient for grain breaking, localised shear planes usually did not develop, as observed in their mathematical model.

Mandl *et al.* (1977) observed grain size segregation according to gravitational field – smaller particles tended to sink and large particles to float in case when the pore fluid was not as dense as the particles were and opposite effect when pore fluid was denser than the rigid particles. They report that similar particle behaviour have been observed in the field as well. Similar mechanism of formation of boulder pavements in subglacial tills has been suggested elsewhere.

In sheared granular media the formation of grain bridges that supports most of the shear resistance was observed already by Mandl *et al.* (1977). Rechenmacher (2006) used digital image correlation (DIC) technique to observe the emergence of shear zone in triaxial tests of granular materials. He found that in “matured” shear zones the local strains was highly non-uniform but it seems to suggest periodic pattern. He argued that this observation corresponded well with buckling of grains – forming of grain bridges suggested by others. Mair and Hazzard (2007) in three dimensions (3D) mathematically modelled found that in case of well sorted materials grain bridges (or force chains) were approximately oriented in direction of deformation and inclined some 50° from the plane of deformation; in case of unsorted material (like tills) grain bridges were significantly diverging from the direction of shear and much more branched than in the former case. Thus more chaotic orientation of elongated grains in diamictic materials could be expected in comparison to well sorted materials.

Hooyer and Iverson (2000) claimed to present the first report – on experimental studies of clast alignment in pervasively deformed till with high shear strain. They used a ring-shear apparatus and experimented with linear-viscosity putty as well as diamicton samples. The clasts embedded in putty, in no-surface slip environment displayed a rotation

behaviour as predicted by Jeffery (1922), in contrast clasts embedded in till displayed rotation behaviour that is more similar to that predicted by March (1932). However, the orientation of clasts did not follow the theoretical prediction as close as in case of putty. These results are in good agreement with other experimental studies with rigid particles immersed in plastic putty and lubricated surfaces (Cañón-Tapia, Chávez-Álvarez, 2004; Mandal *et al.*, 2005a). Hooyer and Iverson (2000) concluded that the strong till macrofabric was an indication of deformation till with considerable strain rate (5 or greater), that opposite to long standing perception that characteristic feature of deformation till was weak till fabric. They argued that many macroscale and microscale deformation features such as folds, shear bands, rotation structures could develop both in cases when strain rate from glaciological point of view was insignificantly small – 1 to 10 or in cases of significant strain rate exceeding 100, 1000 or 10000. The strong macrofabric would evolve gradually and remain stable and strong as long as shearing was continued. Benn (2002) strongly criticized the Hooyer and Iverson (2000) for exaggerating the significance and novelty of their findings, as similar thoughts have been expressed by other researchers before. Benn (2002) stressed that it has been demonstrated in the field that deformation tills could have significant local variations in fabric strength and local conditions such as pore water drainage and till volume changes could significantly affect the local fabric strength, nevertheless he did not dispute the validity of findings of Hooyer and Iverson (2000).

#### 1.4. Till fabric

The till fabric is defined as preferred orientation linear features of the till, that include the surface morphology of the till or its constituents, orientation of voids and fractures, arrangement of particles in the till, orientation of elongated or oblate particles and other anisotropic properties of the till. Most often the orientation of the elongated particles in the till is measured to determine the till fabric.

It is possible to distinguish megafabric, macrofabric and microfabric. The first being mostly orientation of glacier relief forms, the second – orientation of elongated pebbles and other structures of similar size and the latter is structural properties of sub-millimetre size, such as intergranular voids and orientation of elongated sand-size or silt-size particles.

The till microfabric is rather specific and relatively undeveloped field of research, therefore, to attain a better notion about the till fabric, macrofabric, of which many aspects are similar to the microfabric, will be considered in this chapter.

The till fabric is one of the most important till parameters measured in paleoglaciological studies. Already early workers suggested that it could be used as reliable ice flow direction indicator, however it was difficult to extract more information as it was influenced by many different factors (Glen *et al.*, 1957). Glen *et al.* (*ibid*) suggested that there were three main groups of till fabric sources: (1) incorporation of particles in the ice, (2) ice flow itself and (3) sedimentation of particles out of the ice with following soft sediment deformation.

On the basis on earlier works Glen *et al.* (1957) suggested that in the glacial ice particles behaved according to the Jeffery's model (*see below*) although the exact nature of ice flow was not known. They proposed that particles with elongation ration less than 1.5 would attain b-orientation. Glen *et al.* (1957) noted that collisions between particles in dens populations would ledwould led to development of the most energy efficient orientation – b-lineation. That is elongated particles with longest axis and tabular particles with shortest axis aligned according in plane of shearing and perpendicular to shear

direction. However this notion can be disputed as many studies have demonstrated that tabular particles tends to lie in the shearing plane with shortest axis oriented normally to the shearing plane (e.g. Chaolu, Zhijiu, 2001).

Referring to the paper of Holmes published in 1941 Glen *et al.* (1957) suggested that ice/sediment interface would be powerful clast re-orientation factor. The long axis or most profound edge of clasts would be aligned parallel to ice flow direction.

Glen *et al.* (1957) concluded that pebbles in tills would be aligned with their long axis either parallel or transverse to the ice-flow direction. They said that the ice flow direction could be reconstructed from the till fabric however it was difficult to extract any other information about till formation as there were too many factors contributing to the preferred alignment of elongated pebbles.

Lindsay (1970) presented a study of Permian tillite fabric and concept of how till fabric was formed by englacial deformation of sediment rich ice, deposition by lodgement and rolling or sliding of pebbles. He outlined that there might be fabric parallel to ice movement produced by sliding of clasts and fabric transfers to ice movement produced by rolling of clasts.

Li *et al.* (2006) studied macrofabric of glacial deposits in the Upper Urmi River valley, Tian Shan, China. They found that clast a-b planes had stronger fabric than the a-axis did. Additionally the a-axis fabric was at large non-right angles to the former ice flow direction. They emphasised the influence of glacial bed relief on the till fabric: smooth bed resulting in consistent, strong fabric and rough bed resulting in highly variable and weaker fabric.

Carr and Goddard (2007) reviewed the literature on till macrofabric and microfabric and concluded that there were several questions that have not been addressed in till fabric studies: the suitability of eigenvalue vector analysis method for studies of till genesis had been questioned; there was surprisingly little work done on the methodology of fabric analysis; there was no common understanding of fabric strength for different-sized particles. They studied the orientation of different-size particles in the field and in the horizontal thin sections. They found that the preferred orientation was contrasting for different-size particles and only the largest measured fraction (longest axis length 16 to 32 mm) corresponded to known local glacial stress direction.

Hart (1994) reviewed the macrofabric of deformation till and gave characteristic  $S_1$  and  $S_3$  eigenvalues for till fabric eigenvector analysis for various till types. She concluded that at low strains strong fabric should develop as a result of combination of melt-out and shearing. In contrast in high strain environment weaker strain-parallel fabric would develop largely due to partial transverse orientation of some of the pebbles. Additionally thin deforming layer would have stronger fabric and thick deforming layer – weaker. These findings have been later challenged by other researchers (e.g. Hooyer, Iverson, 2000) suggesting stronger till fabric for deformation till than other till types.

Dowdeswell, Sharp (1986) investigated the till fabric of modern glaciers using over 100 fabric measurement sets. They found that there was a general reduction in fabric strength and an increase in particle dip associated with the transition from melt-out tills, through undeformed and deformed lodgement tills, to sediment flow deposits and ice slope colluvium. They noted that there was considerable overlap of fabric strength between different sediment types. Additionally they suggested that deformed lodgement till had weaker fabric strength than the melt-out till or undeformed lodgement till. It has to be noted that concept of deformation till has evolved during the last few decades and the current understanding of deformation till (e.g. Evans *et al.*, 2006) might be different from that of the past, see Dreimanis (1989) for classification of tills agreed in INQUA Commission on Genesis and Lithology of Glacial Quaternary Deposits.



Thomason and Iverson (2006) modelled the deformation of subglacial tills in large ring shear apparatus. With help of a simple model they investigated whether the microfabric could be used as strain magnitude marker to investigate glacial tills. They found that sand size particle attain stable, 10° “up-glacier” dipping position after shear strain of 7 to 39. The steady fabric was moderately strong with eigenvalues of  $S_1 = 0.71$  to 0.74. For statistical analysis they used for two dimensions adapted eigenvalues method suggested by Mark (1973) Thomason and Iverson (2006) found that large particles exhibit slightly stronger preferred orientation than the smaller ones. They found that microshears manifested as unistrial plasmic fabric gradually appeared with increasing strain rate. Additionally they found only limited evidence that strain was accommodated by rotation of till aggregates as suggested by van der Meer (1997) – only few rotation (circum-grain plasmic fabric or circular arrangement of smaller grains around large ones) features were observed in thin sections.

### 1.5. Till macrofabric statistics and classification

The statistics for till fabric studies almost exclusively is calculated according to eigenvalues method proposed by Mark at 1973, that gained ground among geologists especially after the paper of Ballantyne and Cornish (1979) where previously widely used chy-square test method was proven to be biased by arbitrary chosen starting point for measurement grouping.

There have been several attempts to establish a till fabric classification system according to the shape of fabric diagrams and statistical parameter to allow identification of certain till formation mechanisms (e.g. Lindsay, 1970; Hicock *et al.*, 1996; Benn, Ringrose 2001; May *et al.* 1980). However no classification system has been widely accepted.

Benn and Ringrose (2001) tested the variance of till fabric samples from Breidamerkurjökull, Iceland, using ‘bootstrapping’ method. The bootstrapping method involves generation of large number of probable sample distributions from the initial set of measured data. They found that the sample size for till fabric analysis should be at least 50 and seemingly different sample distributions could come from the same real population of fabric data. They demonstrated that bootstrapping method could be used to assess whether the different fabric measurement sets could be attributed to the same population. Larsen and Piotrowski (2003, 2005) tested this method and did not reach any satisfactory results as fabric data for all three till units studied overlapped significantly. Larsen and Piotrowski (*ibid*) concluded that only 30 measured clasts were sufficient in a case of the strong fabric. However this is the minimum fabric sample size and generally at least 50 and preferably 100 measurements should be made.

Lindsay (1970) divided till fabric diagrams in several modal groups by visual inspection. This approach later was developed by Hicock *et al.* (1996) who proposed visual division of fabric diagrams in 5 modal groups and proposed a methodology for interpreting till fabric data by taking into account the modal types of fabric distribution: unimodal clusters (un), spread unimodal (su), bimodal clusters (bi), spread bimodal (sb) and polimodal to griddle-like fabrics (mm).

The methodology of Hicock *et al.* (1996) for identification of modal distribution of fabric data by visual interpretation seems to be too subjective as demonstrated in discussion arising after other researchers attempted to use it (Larsen, Piotrowski, 2003, 2005; Krüger, Kjær, 2005). Larsen and Piotrowski (2003) assigned their till fabric data to unimodal as well as bimodal distributions but Krüger and Kjær (2005) latter argued that fabric should be interpreted unimodal. This demonstrated that subjective criteria such as visual interpretation should be avoided in interpreting till fabric data.

Similarly Āboltniš already in 1986 proposed that the shape of fabric distribution visualized on the stereological net can be used to identify the till formation processes. As proposed elsewhere he adopted the view that tills can be considered. He proposed that three basic types of till macrofabric diagrams can be distinguished, corresponding to distinct modes of plastic deformation of the till: plastic laminar flow along, resulting to single fabric mode parallel to the ice flow direction (S-glacioteconite); fabric orientation transvers to the local ice flow resulting from displacement along to sets of planes in the till unit (B-glacioteconite) and griddle like distribution resulting from displacement along countless planes of the displacement (R-glacioteconite).

Larsen and Piotrowski (2003) extensively studied macrofabric of three till units exposed at an outcrop in Northern Poland. The three structurally distinct till units on the top of each other: (A) macroscopically deformed till at the bottom overlaying deformed outwash sand and interpreted as deformed glacial bed; (B) banded till unit at the middle interpreted as a result of combination of lodgement, deformation by ploughing of stones and melt-out; (C) homogenous till on top interpreted as melt-out till at the base of stagnant ice. They found surprisingly uniform strongly clustered (mean  $S_1=0.876$ ) macrofabric distribution in all three till units. They compared the results of the macrofabric measurements with interpretation suggested by May *et al.* (1980), Dowdeswell and Sharp (1986), Hart (1994), Hooyer and Iverson (2000), Benn and Ringrose (2001), and Hicock *et al.* (1996) diagram. They identified no significant macrofabric variation across all three till units or any dependency of macrofabric on considered grain size (0.7 to 5.6 cm). They found very strong fabric for the lower, deformation till unit (average  $S_1=0.879$ ). They claimed that their results suggested plastic rather than viscous behaviour of deforming till.

Bennett *et al.* (1999) examined the usefulness of till clast fabrics to identify facies of unknown origin. They analysed a set of 111 clast fabric measurements samples (each containing at least 50 measurements) and a number of data obtained by other researchers. They found that all the fabric for all studied till facies (basal ice, melt-out till, lodgement till, deformation till and flow till) did overlap and the variation between results of different investigations of the same till facies often were more dispersed than the results from one investigation of different till facies. Bennett *et al.* (1999) concluded that clast fabric alone was not sufficient for genetic fingerprinting the formation processes of tills and this parameter should be used with much more consciousness.

Possibly the till fabric measurements are more useful for understanding the built-up of glacioteconic structures as extensively used by e.g. by Āboltniš (1989), than in directly reconstructing the ice flow direction or unequivocally indicating mechanism of till genesis.

With discussion alive what fabric shapes are characteristic for what till formation processes (Larsen, Piotrowski, 2003, 2005; Krüger, Kjær, 2005) the conclusion of Glen *et al.* (1957) that till fabric is good for ice flow direction reconstruction have been disputed as well. It was demonstrated (e.g. Dreimanis, 1999; Zelčs, Dreimanis, 1997) that the till fabric reflects the local stress conditions. Often the local stress direction will coincide with the general ice flow direction; however there certainly are many cases when the local perturbations in shear strain will leave its imprint on the fabric distribution and orientation and it will not coincide with the general ice movement direction. Thus, in case when knowledge about any local perturbation in the glacial stress field are sparse an assumption must be made that the till fabric is not directly linked to the ice flow direction. Finally it shall be noted that this conclusion will be true in case of microscale as well.

## 1.6. The till micromorphology and microfabric

According to Glen *et al.* (1957) the first study of till micro fabric was published by Seifert in 1954: *Das mikroskopische Korngefüge des Geschiebemergels als Abbild der Eisbewegung, zugleich Geschichte des Eisabbaus in Fehmarn, Ost-Wagrien und dem Dänischen Wohld*. (The microscopic texture of glacial tills as a key to the reconstruction of the patterns of ice advance and retreat from Fehmarn, Ost-Wagrien and the Dänisch Wohld).-S. 124-190, 8 Abb., 6 Taf. (MEYNIANA, University of Kiel, 1954) In this paper it was noted that at the boundaries of a thick till layers a-lineation predominates and in the middle of till layer – b-lineation was observed.

The earliest studies of the till microfabric is from 50-ties of 20<sup>th</sup> century when Robert F. Sitler and Carleton A. Chapman (1955) studied North-American tills using thin sections and observing the preferred orientation of sand grains and clay particles as well. This work was followed by Sitler (1963) and few others. Probably due to slow and complicated sample preparation techniques, until 90-ties of 20<sup>th</sup> century little work was done in the field of till micromorphology. The “modern era” of till microscale studies was largely pioneered by the works of van der Meer (van der Meer, 1993, 1996, 1997; van der Meer *et al.*, 1992, 2003). Since many researches have studied till micromorphology (to name a few: Hiemstra, van der Meer, 1997; Hart *et al.* 2004; Menzies 2000a, b; Lachniet *et al.* 2001; Menzies, Zaniewski, 2003; Menzies *et al.*, 2006; Piotrowski *et al.* 2006; Thomason, Iverson, 2006; Larsen *et al.*, 2007).

### 1.6.1. The till micromorphology

There are developed a classification scheme of till micromorphology (see van der Meer, 1993; Figure 8 at Menzies, Zaniewski 2003). The classification is based on distinction between matrix and skeleton. In short, matrix is part of sediments that seems homogeneous in particular scale of exploration, e.g. in thin sections (microscopic scale) this usually will be fine silt, clay and amorphous material, such as disperse organic mater. Skeleton is material that appears particular in given scale of exploration, e.g. in thin sections (microscopic scale) it would be coarse silt particles, sand grains and other coarser material. In contrast, in macroscale matrix would be anything with grain size finer than gravel and skeleton – gravel, pebbles and cobbles.

There is notion of plasma – it is material with no observable particulate structure in given scale of exploration. Plasma usually consists of clay-size particles. If mineralogical axes of all clay particles in plasma are oriented in the same direction, then in polarisation microscope a birefringence is observed. These are regarded as plasmic fabric.

The structures formed jointly by matrix and skeleton grains are called as S-matrix structures. In case of tills they can be a result of plastic, brittle or polyphone deformation or formed by action of pore water.

Not all micro-structures observed by different scientist are included in the scheme. Particularly, grain stacks or bridges, defined as 3 or more skeleton grains in a line pressed to each and developed oblique to shear direction as a mean of stress support, observed in tills is missing (Larsen *et al.*, 2007). Although formation of grain stacks is similar to formation of crushed grains, the later often is an extreme way of grain stack collapse.

The till micromorphology has been used as on of the tools in many studies of glacial sediments (e.g. Carr, 1999, 2001; Carr *et al.*, 2006; Carr, Goddard, 2007; Carr, Rose 2003; Hart, 2006, 2007; Hiemstra, Rijdsdijk 2003; Hiemstra *et al.*, 2006; Johnson,

1983; Kalvans, Saks, 2008; Khatwa, Tulaczyk, 2001; Lachniet *et al.*, 1999, 2001; Larsen *et al.*, 2007; Menzies, 2000a; Menzies *et al.*, 2006; Menzies, Taylor, 2002; Piotrowski *et al.*, 2006; Roberts, Hart, 2005; Sitler, Chapman, 1955; Zaniewski, van der Meer, 2005). Due to scope limitations these will not be reviewed there.

### **1.6.2. Micromorphology semi-statistics**

Probably Carr (1999) was one of the first who introduced the counting of microstructures to gain semi statistical insight of their abundance in studied tills. He used four classes to quantitatively describe concentration of a set of microstructures: (1) not present; (2) particulate feature; (3) much more developed, and (4) common structure. Latter this approach was adopted by other researchers (e.g. Larsen *et al.*, 2007).

However it seems that there is large degree of uncertainty in till micromorphology studies as demonstrated by Khatwa and Tulaczyk (2001). They compared micromorphology of two tills that have to be known from other sources having formed as deformation tills. One till was of Pleistocene age from the United Kingdom and other – modern till from beneath Ice Stream B, West Antarctica. They found remarkable differences in abundance of microstructures indicative of deformation process in both tills. Other researchers have concluded that the till from Antarctica has had strain ratio of 1000 or more meanwhile the till from the United Kingdom only 10 or less, however the much more diverse microstructures are observed in the later one. They discuss that several factors are influencing this remarkable difference in till that both formed as the subglacial deformation tills: (1) the parent material – if the parent material available for till generation is heterogenous as in England, larger diversity of till microstructures is expected to be observed in comparison to case when parent material is homogenous as in Antarctica; (2) large strain magnitude will lead to homogenisation of sheared material, and little microstructures will be observable, in contrast moderate to small strain magnitude will preserve some initial inhomogeneities of parent material, and observer will see spectacular microstructures; (3) finally, subglacial water flow, when present, will produce some sorting of the till material and hence grain size differences need for manifestation of till microstructures, thus in case when more subglacial water will be available, it will be possible to observe more diverse set of till microstructures.

Similar observations were reported by Hart *et al.* (2004). They conclude that deformation is inhomogeneous in subglacial layer and more microstructures develop in coarse grained tills as there are more clasts to induce perturbations. Consequently microfabric is more heterogeneous in coarse grained tills.

### **1.6.3. Till microfabric**

In many studies the till microfabric is restricted to the orientation of the elongated sand size particles (see list of papers in Appendix 1). In this paper the same restriction is made.

It is sometimes referred to till microfabric as being roughly coincident with macrofabric (Dreimanis 1973, 1989). However, it has rarely been demonstrated with actual results. Only few attempts have been made to describe till microfabric – preferred orientation of elongated sand grains – using quantitative approaches (Chaolu, Zhijiu, 2001; Stroeven *et al.*, 2001, 2005; Carr, Rose, 2003; Zaniewski, van der Meer, 2005; Roberts, Hart, 2005; Thomason, Iverson, 2006, 2009). Additionally, it is understood that large clasts will significantly affect the orientation of elongated sand size particles (Thomason,

Iverson, 2006), and the depositional process for different size till particles will be different (Benn, 1994).

A conspectus of significant part of primary literature dealing with till microfabric studies are given in Appendix 1. In the next paragraphs a summary of literature review about till microfabric properties is drawn.

**Till type.** The sediments studied in 19 examined papers are: modern tills – three cases; subglacial tills in 17 cases out of which 11 were recognised as deformation tills; in one case experimentally deformed till and in four cases – glaciomarine sediments.

**Thin section orientation.** The study concentrate on the till microfabric as measured by apparent orientation of elongated sand size particles in till thin sections, therefore most of the studies reviewed uses this technique. There is rather large variety in the orientation of thin sections used in different studies: in four studies a set of three orthogonal thin sections are used; in six studies only vertical sections are studied (including two papers with few horizontal sections added) and in three papers only horizontal sections are addressed; three studies uses the approach of Evenson (1970) by cutting the vertical section in a direction of major microfabric mode of horizontal section; in one study thin sections is not used at all; in another study the thin section orientation is not specified and one study is using two vertical sections oriented in known, not-right angle to each other.

**Measurements.** The measurement techniques are diverse as well: in eight studies apparent orientation was measured in thin section projections; in two cases microscope with rotation stage is used; in three studies semi automated procedure are applied – manually selected grains in digital images are automatically measured; one study uses fully automated measurement procedure using digital thin section images; in another study (represented with two papers) automated and manual directed sets of secant intersections with grain boundaries are counted; in two studies anisotropy of magnetic susceptibility (AMS) of monolith till sample is measured. Only one paper (Thomason, Iverson, 2009) compares the results obtained by different measurement techniques: AMS and apparent sand grain orientation in thin sections. The number of measured grains in single data set ranges from few tens to unspecified very large numbers representing all the grains in microphotograph measured automatically.

**Statistical indicators.** Three of the studies uses only visual inspection of microfabric rose diagrams; four other studies uses a varieties of  $\chi^2$  tests in one case supplemented by the large fraction of measurements falling in 30° sector; in three papers a 2D variation of eigenvalue procedure proposed by Mark (1973) are used; resultant vector and vector magnitude are calculated in 4 papers; one study uses moving average technique; another – curve fitting regression and in one case the statistical procedure is not specified.

**Spatial distribution.** Most authors note variation of microfabric in relatively short distances, attributing it to effects of local deformation field of nearby prominent boulder (Hart *et al.*, 2004), different composition of till bands (Hart, 2006, 2007), changing local glacier advance direction and deformation mode as till is gradually accumulating (Thomason, Iverson, 2009) or with no evident explanation (Stroeven *et al.*, 2001, 2005). Although in experimental work of Thomason and Iverson (2006) shearing glacial till in ring-shear apparatus a consistent, steady-state and strong microfabric developed across the shear zone at moderate strain rate of 7 to 39. Chaolu and Zhijiu (2001) found that the microfabric strength is heavily affected by the near by landforms such as rock core of a drumlin and roche moutonnées: strong fabric in stoss and weak – in lees sides.

**Sorting effects.** Generally it seems that better sorted (smaller grain size variations) sediments has stronger microfabric if the dominant grain-size is measured (Johnson, 1983; Hart *et al.*, 2004; Hart, 2006, 2007). Hart (2007) notes that in banded tills

chalk-rich laminas have stronger microfabric than the sandy ones despite wider grain size distribution. This probably can be explained as a result of fine grained matrix of these tills and the estimation on sorting only from the length measured grain axis, that does not represent the real grain size distribution. Again the experimental work of Thomason and Iverson (2006) slightly contradict these findings, as the steady-state fabric was attained faster for less-well sorted sediments, although the resultant strength was similar.

**Micro fabric of different grain sizes.** The smaller grains tend to rotate around or to be plastered against surfaces (Hart *et al.*, 2004) of large grains, hence generally the large measured grains give stronger fabric results (Hart *et al.*, 2004; Carr, Rose, 2003; Thomason, Iverson, 2006; Carr, Goddard, 2007). Additionally it seems that matrix supported (in the microscale) sediments have stronger sand grain apparent preferred orientation (Hart, 2006, 2007). Similar results is presented in macrofabric studies of different-sized clasts, e.g. Kjær, Krüger (1998) found that in late Pleistocene tills in Denmark and recent tills in South Iceland clasts shorter than 2 cm usually exhibit significantly weaker ( $\Delta S1 \sim 0.1$ ) fabric than large clasts. Carr and Rose (2003) and Carr and Goddard (2007) observed that dominant orientation is related to size of measured grains with switching between parallel and transverse orientation in different size classes.

**Microfabric versus macrofabric and ice movement direction.** The results of reviewed papers are inconclusive as regards the preferred microfabric orientation and established ice movement direction: Carr and Rose (2003) as well as Carr and Goddard (2007) found that only in half of cases microfabric orientation coincided with reconstructed ice movement direction; Ostry and Deane (1963) found striking similarity between microfabric orientation and reconstructed ice movement direction; experimental work of Thomason and Iverson (2006) demonstrated that in simple shear conditions microfabric steady state orientation was similar but slightly weaker than the macrofabric (Hooyer, Iverson, 2000); Johnson (1983) in extremely clay rich tills found that in most cases microfabric was strong with major mode either parallel or transverse to established ice movement direction; Svärd and Johnson (2003) found that in general microfabric was similarly oriented but weaker than the macrofabric; Thomason and Iverson (2009) demonstrated that microfabric was directly related to ice advance direction. It could be concluded that microfabric is weaker than the macrofabric and most often similarly oriented as the macrofabric.

**Conclusions.** The results of most microfabric studies can be explained by the conclusions of Thomason and Iverson (2009): deformation via simple shearing do occur but is not the only process occurring in the glacier base and significant portions of deformation tills are subject to other modes of deposition or deformation. Likely candidates for deviation from simple shearing are pure shear occurring at the transition zones from patches of deformed bed and unreformed bed (e.g. Piotrowski, Kraus, 1997), rotating structures induced by clasts (e.g. Hart *et al.*, 2004) or ploughing boulders (Tulaczyk *et al.*, 2001).

Few papers deserve special attention. After experimentally investigating the development of macrofabric in ring-shear apparatus (Hooyer, Iverson, 2000), Thomason and Iverson (2006) used the same equipment to study the evolution of microfabric in tills sheared to large strain rates. They found that sand-sized size particle attain stable,  $10^\circ$  “upglacier” dipping position after shear strain of 7 to 39. The steady fabric was moderately strong with eigenvalues of  $S1 = 0.71$  to  $0.74$  (calculated for 2D data and, probably, not directly comparable to eigenvalues calculated from 3D data). Initially random microfabric ( $S1 = 0.53$  to  $0.56$ ;  $S1=0.5$  indicating uniform distribution in all directions of elongated particles in 2D) gradually become oriented as shearing progressed. Only few examples of rotational structures were observed in thin sections. It could be concluded that most of the

strain was accommodated by two sets of secondary steeply dipping and shallow Riedel shears. This study is followed up by other experimental investigations of till microfabric using AMS technique, and most recently extended to field studies (Thomason, Iverson, 2009).

A few studies have concentrated on fabric strength and shape, especially, elongation ratio. Millar and Nelson (2003) examined an extensive set of macrofabric data of slope deposits. They found that the minimal elongation ratio (longest axis to intermediate axis) should be at least 1.5 : 1 and it should be restricted to narrow interval. The first recommendation was followed in this study as well and only grains with apparent elongation greater than 1.5 : 1 were used.

Carr *et al.* (2000) concluded that in glaciomarine, mostly fine grained sediments, elongated sand grains poses subvertical preferred orientation, reflecting settling in a still water environment.

#### **1.6.4. Grain size and shape**

The descriptive, semi-quantitative micromorphological till characterisation and microfabric analysis are not the only information that can be extracted from till thin sections. The grain size and shape can be successfully studied as well, applying automated procedures if necessary.

Development of image capturing and computing technologies in the last decades of previous century enabled creation of automated image analysis techniques for grain size measurement (*e.g.* Harrell, Eriksson, 1979; Mazzullo, Kennedy, 1985; Francus, 1998). Until now they are not widely utilised, however the techniques are constantly improved, facilitated by onset of digital photography era (*e.g.* Rawling, Goodwin, 2003; Rubin, 2004; Seelos, Sirocko, 2005; Mertens, Elsen, 2006; Barnard *et al.*, 2007).

The image processing procedures developed within scope of this dissertation is adoptable for grain size distribution and shape evaluation using digital images (Kalvāns *et al.*, 2009).

## 2. Methods and materials

In this study a methodology of thin section preparation from weakly consolidated materials was implemented in The Rock Research Laboratory of Faculty of Geography and Earth Sciences at the University of Latvia; image acquisition and analysis techniques were developed for microfabric automated measurement; microfabric data statistical treatment and visualisation procedures adapted and implemented.

Samples from four study sites – Ziemepe, Strante, Plašumi gully and Sensala – are included in the dissertation. The site description is given in the 1. chapter “Subglacial environments and till micromorphology”. More than 77 thin sections of poorly consolidated sediments were prepared during the elaboration of the theses. All the thin section samples were collected and analysed by the author and majority of them were prepared by the author.

### 2.1. Samples, data, analysis: the literature overview

Four distinct methodological steps of the till microfabric studies using thin sections are identified: (1) thin section preparation; (2) microfabric data acquisition; (3) statistical analysis of data, that can be subdivided in analysis of circular and spatial distributions of preferred orientation, and (4) visualisation or presentation of results.

#### 2.1.1. Thin section preparation

The till thin section preparation process is a problem itself as diamicton sediments prior to thin-sectioning need to be impregnated with hardening agent (usually epoxy resin or polyesters sometimes plasticized with acetone) and often this is a difficult task. According to bibliographic list compiled by Prof. John Menzies<sup>1</sup> there are published more than 50 papers on the subject, some of which are discussed there.

For sample collection usually a Kubiena box – metal container, with both ends open (e.g. van der Meer, 1996) – is cut in the face of outcrop, removed with sample and wrapped in plastic for transportation to laboratory. In some cases, if long and possibly harsh transportation is expected, samples are immersed in quickly-curing glue – epoxy resin, polyester or acrylic resins (e.g. Baroni, Fasano, 2004; Chaolu, Zhijiu, 2001) – that is removed in laboratory. For collecting undistributed samples of loose sands more subtle techniques are developed that start with pre-hardening with agar in the field (Curry *et al.*, 2002).

In the laboratory samples are either air-dried (Carr, Lee, 1998), freeze-dried or water replaced with acetone (e.g. Jim, 1985; Camuti, McGuire, 1999). In subsequent steps the samples are impregnated with epoxy resin either directly in vacuum chamber or replacing the acetone in the sample with resin some times involving several steps. After impregnation and curing of resin samples are cut and checked the impregnation quality. Surface re-impregnation if the quality is not satisfactory is suggested by Carr and Lee (1998).

The further sample processing is much like dealing with hard rock and involves sample cutting in plates, grinding, polishing, mounting on glass slides, cutting off the

---

<sup>1</sup> Micromorphology Bibliography <http://spartan.ac.brocku.ca/~jmenzies/biblio.html> (2009.02.10.)



surplus sample, grinding, final polishing and covering with glass slips (e.g. Carr, Lee, 1998).

The optical microscopy of mineralogical materials often involves staining of the thin section for identification of certain minerals (e.g. Stinkulis, 1998) or etching to remove other minerals (fine-grained carbonate in particular, which is obscuring the plasmic fabric, (e.g. Thomason, Iverson 2006). For better void identification sometimes the sample is impregnated with epoxy that is coloured with fluorescent dye (e.g. Elsen, 2006; Kalvāns, Saks, 2008).

As regards the impregnation agents, the extremely viscous epoxy resin marketed under brand name of SPURR seems to be the best choice (e.g. Jim, 1985; Curry *et al.*, 2002). Unfortunately the SPURR resin is one of most expensive available in the market. Cheaper alternative are available for example Struers A/S (EpoFix resin and EpoDye fluorescent dye for it). It must be noted that satisfactory results can be obtained by using a low-grade transparent industrial epoxy resins plasticized with acetone as well.

### **2.1.2. Microfabric data acquisition**

Until recently till microfabric data was mostly acquired by visual identification of elongated grains and manual measurement of longest axis orientations in microscope (Ostry, Deane, 1963; Chaolu, Y., Zhijiu, C. 2001) or projected enlarged thin section images, e.g. using slide projector (Evenson, 1970) or projection microscope (Carr, 1999). In later works computer assisted measurement has been performed that involve manual selection of grains to be measured (e.g. Hart *et al.* 2004) or automated measurement of all grains present in several microphotographs (Thomason, Iverson 2006) or whole slide (Kalvāns, Saks, 2008). Some authors suggest that better results could be obtained by using scanning electron microscopy images as the contrast between skeleton grains and matrix is higher (Francus, 2001). The overview techniques used by different authors for microfabric – preferred orientation of long axis of sand grains – measurement is given in the Appendix 1. These methods are compared in Table 2.1.

There are principally different methods of microfabric measurement, for example, anisotropy of magnetic susceptibility (AMS; Principato *et al.*, 2005), but these are not widely used and will not be reviewed there.

Stroeven *et al.* (2001, 2005) have suggested a method of secants – counting the points of intersection between a set of parallel lines drawn in different directions and grain surfaces. The direction where the number of intersections is largest is perpendicular to preferred orientation of elongated grains. The difference between the preferred orientation direction and the less preferred directions obtained by this method however is small and therefore results are not convincing. The advantage of the approach is that it is not object based – it is not necessary to identify individual particles to obtain results so the approach should be more robust than object-based automated analysis procedures.

The fabric analysis is really done with help of the image analysis tools. But there are at least two fundamentally different approaches: (1) object based approach (Francus, 2001; Thomason, Iverson, 2006; Kalvāns, Saks, 2008) and (2) “statistical” approach (Stroeven *et al.*, 2001, 2005; Tovey, Dadey, 2002). In the first case individual particles are identified using colour threshold techniques, that usually involve creation of binary image, and particle geometrical parameters – size, elongation, orientation – are automatically measured. In the later case colour gradients or orientation of grain boundaries (image binarisation is necessary) is analysed.

Table 2.1 Overview of methods used for microfabric – orientation of long axis of sand grains – measurement in tills using thin sections

2.1. tabula. Morēnas mikrolinearitātes – smilts graudiņu garākās ass orientācijas – mērījumu, izmantojot plānslīpējumus, metodikas pārskats

Method	References	Advantages	Disadvantages
Manual measurement in thin section projection	Carr, Rose, 2003; Carr, 1999, 2001; Johnson, 1983; Evenson, 1970; Carr, Goddard, 2007	– Low-tech – low-cost technique; – Researcher has full control on his data	– Limited amount of data can be acquired (usually no more than 100 measurements in a single set)
Computer-assisted measurement with manual grain selection	Hart <i>et al.</i> , 2004; Hart, 2006, 2007; Sakai <i>et al.</i> , 2002	– Simple measurement procedures and data processing	– Limited amount of data that can be acquired; – Measurements can be subjective – the operator unintentionally may select grains aligned in on preferred direction
Computerised automated measurement	Thomason, Iverson, 2006; Kalvāns, Saks, 2008	– Easy to acquire and process very large (up to several thousands of measurements) data sets that are easily filtered according to selected parameters (e.g. elongation ratio or grain size); – Large, readily available data sets allows analysis of microfabrics spatial distribution	– Non-robust object based approach; – Required high and uniform thin section quality
“Secants” method	Stroeven <i>et al.</i> , 2001, 2005	– Not object-based image, hens more robust, analysis approach	– Usually the proportion of elongates particles is relatively small and it leads to small difference between preferred/non-preferred orientation directions – It seems that standard data statistical analysis procedures developed for circular data is not applicable – In both cited studies authors did not get satisfactory results with automated procedure and further improvements of methodology are needed.

Francus (2001) proposed an automated methodology for bioturbation detection in laminated sediments by analysing the microfabric. Detailed steps of image analysis are provided in author’s web page<sup>2</sup>. The image processing steps are contrast enhancement, median filter, sharpen filter, mediana hybrid filter (enhances linear features), image

<sup>2</sup> <http://www.geo.umass.edu/climate/francus/index.html>

binarisation – creation of black and white image, filing holes and removing particles that are too small and, finally, automated measurements.

Both Francus (2001), and Thomason and Iverson (2006) for automated microfabric measurement used public domain software NIH Image also named ImageJ, a Java program inspired by Image that “runs anywhere”. Kalvāns and Saks (2008) for the same purpose used ImageProPlus ® commercial software.

### 2.1.3. Other image analysis procedures

To highlight the possible applications and developments of image analysis procedures adapted and implemented with in this study a short overlook of other techniques is presented there.

Zaniewsky and van der Meer (2005) presented an attempt to extract some more quantitative non-subjective information about till micromorphology from thin sections with help of the image analysis procedures used in remote sensing. They stress the need for objective tools to evaluated plasmic fabric as routinely researcher is subjectively describing observed scene and adding descriptive labels. Authors like Sitler and Chapman (1955) used  $\lambda=1/4$  (gypsum) plate to enhance the colours of plasmic fabric. Zaniewsky and van der Meer (2005) acquired and processed 1280 to 1024 pixels large images (1.3 megapixels) with resolution of 2000 pixels/cm stored in 24-bit RGB format as TIFF files. For identifying skelsepic plasmic fabric Zaniewsky and van der Meer (*ibid*) evaluated the concentration of plasmic fabric domains in the proximity of skeleton grains; if it exceeded certain threshold they labelled plasmic fabric as skelsepic. Other types of plasmic fabric were identified by the orientation of plasmic fabric domains.

Mertens and Elsen (2006) proposed to use image analysis to determine the particle size distribution of sands used in ancient mortars. To maximise the contrast between aggregates and matrix they used average value of all three colour channels of RGB image and binarised resultant gray-scale image. Binary images were improved with filters despeckle for noise reduction, erosion and dilation to reduce noise and effects of touching grains and smoothing of grain boundaries. Binary images were cobined to increase the area covered by a single image file.

Hiemstra *et al.* (2006) used semi-automated multispectral image analyses technique utilising TNT™ image analysis package, involving visual enhancement and filtering, supervised classification and accurate measurements of plasma fabric orientation in a study of glaciomarine deposits form Alaska.

For analysis of air voids in lapped concrete samples there is developed hardware, controlled by personal computer – automated microscope RapidAir (Jakobsen *et al.*, 2006). This uses image analysis to determine the ration, specific surface and distribution of air bubbles in concrete. Analysis procedure involves concrete sample lapping, colouring with black ink, filing air voids with white powder (BaSO<sub>4</sub>) and acquiring digital image of the sample. The analysis is done according to standards ASTM C 457 (US) and EN 480-11 (EU).

Seelos and Sirocko (2005) describe a methodology to deterring grain size distribution in combined thin section images obtained by polarisation microscope with crossed niclos. The image processing is done by AnalySIS software. The data are processed in MatLAB. They used automated thin section scanning using software-controlled automatic microscope stage.

Allen *et al.* (2007) presented an apparatus for automated pollen recognition and counting. In core of it is a neural network that taking into account a number of mathematical parameters are recognising pollen species in images, obtained automatically.

Tovey and Dadey (2002) analysed anisotropy of deep sea sediments using colour gradient changes in scanning electron microscope images of thin sections. They tested several algorithms and found that the most robust are algorithm including identification of a colour gradient change for each pixel in centre of 5×5 pixels large square. This procedure does not require binarisation of the image and is not object based hence it should be more robust than other approaches are.

To study 3-D structure of pore space of sandy sediments Curry *et al.* (2002) repeated cycles of micro-photographing of polished slab and controlled polishing of the sample to remove constant thickness of the material. Obtained 2D images were combined in 3D computer models of sediment texture.

#### 2.1.4. Analysis of circular data

For statistical processing of microfabric data there is not established a single methodology. The methods used are modifications of ( $\chi^2$ ) test (Chaolu, Zhijiu, 2001; Hart *et al.*, 2004; Hart, 2006, 2007; Sakai *et al.*, 2002), resultant vector, and its magnitude (Carr, 1999; Carr, Rose, 2003; Carr, Goddard, 2007; Kalvāns, Saks, 2008), moving average (Johnson, 1983; Stroeve *et al.*, 2001, 2005), visual inspection of rose diagrams (e.g. Evenson, 1970), grain size and elongation ratio significance estimation in calculation specific statistical parameters (Francus, 2001), eigenvector analysis (Svård, Johnson, 2003; Thomason, Iverson, 2006).

Ballantyne and Cornish (1979) demonstrated that the chi-square test is very sensitive to initial conditions, such as the size of segment and initial point of segmentation given by researcher, and can give misleading results. The chi-square test in this aspect is not robust and for this reason it is not used in the current study.

The simplest way of analysing directional data is to calculate the orientation and magnitude (or normalised magnitude) of resultant vector (R) by summing all the sines and cosines of all measurements and calculating the orientation of R by *arctan* function (e.g. Davis 2002, p.322-330). However the correct result is obtained only for von Mises' distribution (normal distribution of circular data). The fabric strength can be calculated by normalising the R vector and comparing it to significance tables (e.g. given by Davis, 2002, p. 619).

The statistical method most used for three-dimensional till macrofabric processing is the eigenvector method proposed by Mark (1973). Its reduction for two-dimensions in analysing till microfabric was introduced by Thomason and Iverson (2006). Mark (1973) himself points out that the eigenvalue method proposed by him is a valid 3D extension of 2D orientation data analysis method proposed by Krumbein (1939) in late 30<sup>th</sup> of 20<sup>th</sup> century. The  $S_1$  value for 2D data is in range from 0.5 (isotropic distribution) to 1.0 (unidirectional distribution). Unfortunately as other relatively simple methods for circular data statistical analysis (e.g. Davis, 2002) this method assumes monomodal distribution. The eigenvector method should be preferred as it is statistical tool used in most modern till macrofabric studies.

Francus (2001) studied the microfabric of laminated sediments for specific purpose – to identify bioturbation. He developed several processing tools that considered the particles size and elongation ratio to give it a weight coefficient for calculation of the orientation statistics. To test the robustness of his method Francus (*ibid*) compared the observed H values to particle contents in sediments, roundness of particles (calculated as:  $R_i = 4A/\pi L^2$ ) and spread of grain size distribution ( $MD_0/sD_0$ ).

There is lack of simple and robust statistical analysis procedures for analysis of bimodal or multimodal data distributions. Jones and James (1969) described the methodology for analysing bi-modal orientation data. Their suggested algorithm calculates 5 parameters for bimodal orientation data assuming that data set is produced from mixture of two normal circular distributions.

### 2.1.5. Analysis of spatial distribution of circular data

In a simplest case it is assumed that there is no (or limited and foreseeable) variations in spatial distribution of microfabric (and macrofabric) in the same sedimentary unit. However often in glacial sediments it is not the case. It is suggested that spatial distribution of microfabric can give clues about the till formation processes (Thomason, Iverson, 2006). But it has not been demonstrated by actual results of the field investigations yet using un-subjective approaches.

However few authors have investigated the spatial distribution of till microfabric. Hart *et al.* (2004) studied till microfabric in three levels: (1) the thin section level – orientation of up to 100 randomly selected grains were measured over the whole area of thin section; (2) homogenous area on the thin section; (3) microfabric in selected structures – around gravel grains, in pressure shadows and others. Similar approach is used in the studies of Roberts and Hart (2005), and Hart (2006, 2007).

Thomason and Iverson (2006) analysed microfabric distribution across a shear band in till produced in ring-shear apparatus. They measured all the sand grains in 3 to 9 microphotographs taken in certain distance from the shear band. Similarly Stroeven *et al.* (2005) measured microfabric in vertical thin sections in closed areas and concluded that changes were due to local shear bands and structural boundaries.

If microfabric data is collected from whole area of the thin section, with coordinates of each measurement as demonstrated in latter chapters, it is worth trying to analyse the spatial distribution with the same resolution. Therefore two studies with similar approach are shortly discussed.

Yamamoto and Nishiwaki-Nakajima (1993) presented a study of computerized spatial dip-strike data analysis. For each measurement they calculated three normal components ( $l$ ,  $m$ ,  $n$ ) used those in further steps. They computed them moving average for a grid points by summing up all the data points falling within certain distance  $r$  from the grid point. The distance  $r$  used was several times large than the grid resolution in this manner greater smoothing of data was achieved. For visualization they plotted the summary arrows for each grid point with arrow length representing the dip of the plane.

Fisher *et al.* (1985) attempted to develop a technique for similarity analysis of orientation data and clustering it on the criteria of angular similarity as necessary, e.g., for analysis of spatial distribution. After data grouping in grid points, smoothed distributions were calculated, modal groups were identified manually and “bird feet” calculated. “Bird feet” is a kind of diagram showing the orientation and strength of each identified modal group. A principal component analysis (PCA) was applied to identify the domains to be grouped together.

Gumiaux *et al.* (2003) published a paper on the geostatistics best-fit interpolation of the orientation data demonstrating that it can be successfully applied to the directional data. Their procedure involved the calculation of variograms, followed by a kriging interpolation of the data. The circular properties of the directional data are avoided by using the direction cosines of double-angle values instead. The described methodology seems to be promising, but is not implemented in this study due to scope limitations.

### 2.1.6. Visualization

Traditionally two dimensional orientation data in geology is visualised in form of rose diagrams (e.g. Carr, 1999). However the appearance of rose diagrams is not robust regarding the chosen starting point and width of segments (e.g. Fisher *et al.*, 1985).

Fisher *et al.* (1985) suggested instead of rose diagrams use density plots. The density is defined as follows:

“Let  $\theta_1, \dots, \theta_n$  is  $n$  measurements (directions) in cyclic, regards as points on the circumference of unit circle. Let  $k$  be the integer part of  $\alpha n^{1/2}$ , where  $\alpha$  is some positive number to be specified. The for any strike  $\theta$ ,  $b_k(\theta)$  is inversely proportional to angular distance to the  $k$ th nearest strike.”

The  $\alpha$  values can be between 0.5 (little smoothing) to 2 (considerable smoothing). The algorithm is easy to be automated and gives nice smoothed results.

Fisher (1989) described a more elaborated procedure for smoothing circular data set with normal distribution. He suggested using it in stead of wide-spread rose diagrams, as a significant random error is introduced when splitting the real data in arbitral classes. He gave an algorithm in full details to be used for kernel density estimate for circular data. Unfortunately fellow researchers have paid little attention towards his suggestion. Due to scope limitations this algorithm is not implemented in current study instead more simple density calculation algorithm of same researcher (Fisher *et al.*, 1985) is used.

The visualisation of spatial distribution of orientation data is common in atmosphere sciences and oceanography. It is usually done by arrows arranged in a rectangular grid that representing the dominant direction in its vicinity, with arrows length describing the magnitude (e.g. speed). Similar approach was adopted by Yamamoto and Nishiwaki-Nakajima (1993), although the arrow length represented the dip angle.

In geology spatial distribution of orientation data usually are represented as a grid of diagrams (or its derivatives as “bird’s feet”, Fisher *et al.*, 1985).

## 2.2. The methodology of this study

The research methodology was largely developed for the elaboration of the thesis by the author. The overview of methodology implementation and development as well as references to first presentations in scientific papers and scientific events are given in Table 2.2. As of now in peer-reviewed literature results obtained by developed or implemented methodology are published in 2007 (Saks *et al.*, 2007) and 2008 (Kalvāns, Saks, 2008). The most significant methodology advances are illustrated in the Fig. 2.1.

In the next subchapters the methodology of current study is presented starting from field work and continuing to the sample treatment, thin section preparation, thin section image acquisition, image processing and analysis, microfabric data processing and visualisation.

### 2.2.1. Fieldwork and sampling

The outcrops of the Quaternary sediments were mapped usually in a scale of 1:100. Outcrops were photographed and images used as background for drawing full sketches after the fieldwork. Structural elements such as fold wings and hinges, shear plains and till macrofabric as indicated by elongated pebbles were measured in the field. Measuring the macrofabric only orientation of the longitudinal axis of pebbles with

elongation ratio larger than 1.5 (e.g. after Carr, Goddard, 2007) were recorded. Bulk samples were collected for grain size analysis.

Table 2.2. Chronology of the development and implementation of thin section preparation and analysis methodology

2.2. tabula. Plānslīpējumu izgatavošanas un izpētes metodoloģijas attīstīšanas un ieviešanas hronoloģija

<b>Procedure</b>	<b>External references (sources)</b>	<b>First published or presented results</b>
Sample cementation using acetone-epoxy resin mix, instead of colophony (rosin, Greek pitch) used before	Camuti, McGuire, Carr, Lee, 1998	Kalvāns, Saks, 2004a, 62 <sup>th</sup> Scientific Conference of University of Latvia
Thin section high-resolution scanning	–	Kalvāns, Saks, 2004a, 62 <sup>th</sup> Scientific Conference of University of Latvia
Manual measurement of elongated sand-sized particles in digital images	–	Kalvāns, Saks, 2004b, INQUA Peribaltic working group field symposium, Latvia
Use of dyed epoxy for sample impregnation, to improve void identification	e.g. Elsen, 2006	Kalvāns <i>et al.</i> , 2007a, b, 65 <sup>th</sup> Scientific Conference of University of Latvia; INQUA XVII Congress, Cairnes, Australia
Digital microphotography of thin sections and automated mounting of images ( <i>photomerge</i> ) to form all-slide-size composite image	–	Kalvāns <i>et al.</i> , 2007a, b, 65 <sup>th</sup> Scientific Conference of University of Latvia; INQUA XVII Congress, Cairnes, Australia
Automated sand-sized particle measurement in digital images	–	Kalvāns <i>et al.</i> , 2007a, b, 65 <sup>th</sup> Scientific Conference of University of Latvia; INQUA XVII Congress, Cairnes, Australia
Visualisation of microfabric preferred orientation across the thin section area in different scales (resolution levels) as simple rose diagrams	–	Kalvāns <i>et al.</i> , 2007a, b, 65 <sup>th</sup> Scientific Conference of University of Latvia; 65 <sup>th</sup> Scientific Conference of University of Latvia
Visualization of microfabric spatial distribution with fabric strength significance indicator according to summary vector length	Davis, 2002	Kalvāns, Saks 2009, 67 <sup>th</sup> Scientific Conference of University of Latvia
Visualization of microfabric spatial distribution using data density plot and summary vector as preferred orientation and fabric strength indicator	Fisher <i>et al.</i> , 1985; Davis, 2002	Kalvāns, Saks, 2009, 67 <sup>th</sup> Scientific Conference of University of Latvia

<b>Procedure</b>	<b>External references (sources)</b>	<b>First published or presented results</b>
Development of algorithm to identify preferred orientation modes in the data density diagrams using the given minimum modal strength and minimum distance between adjacent mode.	–	This dissertation
Visualization of the microfabric spatial distribution with significance indicator according to eigenvalue method	Mark, 1973; Thomason, Iverson, 2006	Kalvāns, Saks, 2010, 68 <sup>th</sup> of Scientific Conference of University of Latvia
The introduction of automated log-file – fixation of calculation parameters such as the grain size considered and aspect ratio.	–	Kalvāns, Saks, 2010, 68 <sup>th</sup> of Scientific Conference of University of Latvia
Mosaic image creation with “buffer lines” between individual images thus eliminating the source of systematic bias in the blended margins between two images	–	Kalvāns, Saks, 2010, 68 <sup>th</sup> of Scientific Conference of University of Latvia

Well-sorted fine sand samples were collected for the OSL age determination using cooper tubes that were hammered in the face of the fresh cleaned outcrop. The samples were processed using single-aliquot regeneration (SAR) OSL method with quartz (Murray, Wintle, 2000) in the Dating Laboratory of the Finnish Museum of Natural History at the Helsinki University.

Samples for thin section preparation were taken using a metal container. The container was cut into the deposits of the outcrop in a manner similar to that described by van der Meer (1996). In some cases the samples of well-consolidated diamicton were taken as single blocks. The upper face and northern direction were marked on each sample.

### **2.2.2. Thin section preparation**

The thin section preparation methodology was largely adopted from Carr and Lee (1998), and Camuti and McGuire (1999). In the laboratory the samples were air-dried and pre-impregnated with epoxy resin dissolved in acetone (in proportion usually 1:7) and after hardening cut into sections. In the second stage of cementation, the samples were impregnated with epoxy resin diluted with acetone in proportion usually 3:1. The two-step impregnation procedure was necessary as in a single step it usually was not possible to attain significant depth of resin penetration in the sample, reaching necessary high sample strength in the same time. This problem is described by Carr and Lee (1998) and their recommendation of surface-impregnation of poorly impregnated samples is followed in several cases. Visual sample inspection did not give any indication that the initial microfabric is significantly disturbed by the two-step impregnation procedure. There are three types of effects introduced by the described cementing methodology: (1) cracks formed as a result of acetone evaporation and resin-shrinkage; (2) weak birefringence of hardened resin as a result of large strains formed due to shrinkage, and (3) visible



boundaries between resin of different cementation steps. All these effects are easily identifiable and do not affect the microfabric studies significantly.

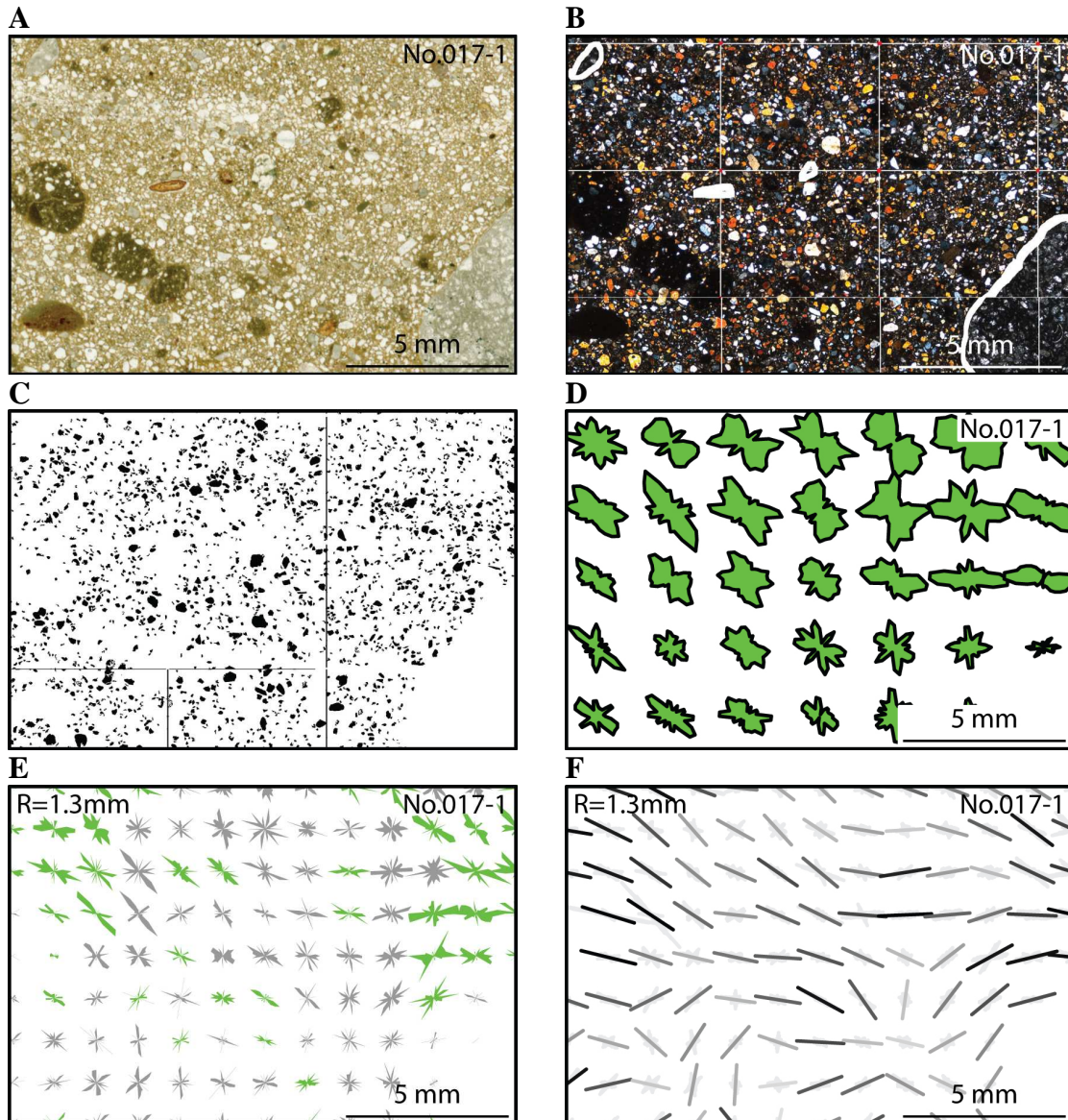


Figure 2.1 Illustration of microfabric measurement method and its development:  
 A – Scanned thin section image (as used in Kalvāns, 2004); B – Cleaned composite thin section image acquired in cross-polarised light and with buffer-lines separating individual microphotographs, the unwanted features of the image are deleted or encircled with white band, allowing their elimination during creation of the binary image; C – Binary image, all black objects with aspect ratio large than 4 or not matching the size criteria, e.g. lines that separated individual photographs in composite image (B) and any sand grains touching them, will not be measured. D – The first attempt of visualisation of the spatial microfabric distribution using simple rose diagrams; E – Visualisation using rose diagrams and indicating whether fabric strength is statistically significant with colour according to normalised resultant vector length and threshold values given by Davis (2002), published at Kalvāns, Saks (2008); F – Microfabric visualisation using data density plots (after Fisher *et al.*, 1985), with indicated eigenvector ( $V_1$ ) orientation and strength ( $S_1$ , after Thomason, Iverson, 2006; Mark, 1973, published at Saks *et al.* (accepted for publication).

2.1. attēls. Mikrolinearitātes mērījumu metode un tās attīstības piemērs: A – Ieskenēta plānslīpējuma attēls (Kalvāns, 2004); B – Salikts un attīrīts plānslīpējuma attēls, iegūts polarizētā gaismā. individuālas mikrofotogrāfijas ir nodalītas ar robežlīnijām, nevēlamās attēla daļas ir izdzēstas vai apvilktas ar baltu līniju, tādējādi izslēdzot tās no tālākas analīzes binarizējot attēlu; C – Binārais attēls, visi melnie objekti ar garākās/īsākās ass attiecību lielāku kā 4 vai neatbilstošu izmēru kritērijiem, piemēram, mikrofotogrāfijas atdalošās līnijas (B attēls) un smilšu graudi, kas tām pieskaras, tālākā analīzes gaitā netiks uzmērīti; D – pirmais mikrolinearitātes telpiskā sadalījuma vizualizācijas mēģinājums izmantojot rozes diagrammas; E – mikrolieneartātes telpiskā sadalījuma vizualizācija izmantojot rozes diagrammas un ar krāsa norādot vai linearitāte ir statistiski nozīmīga pēc normalizēta summārā vektora garuma atbilstoši Davis (2002) dotajām kritiskajām vērtībām, publicēts, Kalvāns, Saks (2008); F – mikrolinearitātes vizualizācija izmantojot orientācijas datu blīvumu (pēc Fisher *et al.*, 1985), norādot eigeņvektora (V1) orientāciju un vērtību (S1; pēc Thomason, Iverson, 2006; Mark, 1973), publicēts Saks *et al.* (*accepted for publication*).

An EpoFix™ two-component epoxy resin obtained from the Struers AS produced for sample preparation purposes for microscopic investigations was used in most cases. Some large-volume samples were cemented with locally available low-cost transparent two-component epoxy resin.

In a latter stage an EpoDye obtained from the Struers AS – fluorescent colouring agent for epoxy resin – was used to improve the identification of voids in the sample, especially important to increase the colour difference between voids and quartz grains in plain-light images.

After cementation samples were cut and hand-ground in three stages or in single stage with Logitech CL40 grinding machine that was introduced in latter stage of thesis elaboration. At the last stage corundum grinding powder of around Grit P2500 was used. Ground samples were mounted on glass slides, and after cutting of bulk material, finished to reach the slide thickness around 30 µm, as indicated by the pale yellow interference colour of quartz grains. Three mutually perpendicular thin sections were prepared from each sample in all cases where it was possible.

Thin sections were examined using ore microscope MBS-10 and polarized light mineralogical microscope MIN-8. In later stage of thesis elaboration Leica DMLA polarisation microscope and Leica polarisation stereomicroscope were introduced. Recommendations for thin section examination of van der Meer (1993, 1996, 1997), Hart and Rose (2001) were followed. The classification of microscale features of glacial sediments recommended by Menzies (2000a) and Menzies and Zaniewski (2003) were used.

### 2.2.3. Digital image acquisition

A set of overlapping thin section digital images was acquired with Leica DMLA microscope with magnification of 25 times and Leica DFC 480 digital camera with resolution of 1 mm = 460 pixels (2560×1920 pixels images). The fixed exposure was used for taking all images of single thin section. Exposure was adjusted so that to give best contrast between quartz grains and pores space filled with epoxy resin or sediment matrix. Images were saved using TIFF format. Plain as well as cross-polarised light was used. Images were resampled to 50% resolution using IrfanView Batch conversion tool.

The Photomerge function of Adobe Photoshop was used to create composite images. Later in the work (starting from June 2009) a new method of composite image

creation was adopted. The new method eliminated the need for extensive “image cleaning” by erasing the contact zones between images, where due to imperfect image alignment small but systematic distortions of thin section image was introduced. Microphotographs were taken in non-overlapping manner in rectangular grid, so that a “blank band” of known width separates them. Using the “Canava size” option of the IrfanView Batch conversation Advanced settings menu a white outline of corresponding width was added to each image. A composite image was created using the “Tile Images” command out of Process menu of ImageProPlus. In composted image thin lines were separating individual images resulting in insignificant lose of measured sand grain numbers and eliminating the need for extensive image cleaning.

Red, green or blue channel, what ever gave the best results of RGB image, was extracted using ImageProPlus®. The blue channel was best for thin sections that were prepared using epoxy resin coloured with yellow dye and images acquired in plain light. The green or sometimes red belt was best for images acquired using cross-polarised light. The matrix, if any, in cross-polarised light du to birefringence often was reddish; the blue colour gave light halo around brightest spots in the images. If thin section thickens was larger than normal or uneven, due to appearance of higher birefringence colours, the red colour often gave better contrast between the mineral grains and matrix than the green.

The cross-polarised light images were less sensitive to thin section thickness: strong and steady contrast between the mineral grains and pore space or matrix could be achieved for thin sections of uneven thickness as well. Significant proportion of mineral (quartz grains) was dark or grey-coloured and thus should not be measured in later stages. Additionally it was difficult to identify the thin-section quality problems in digital images. Finally, polymineral grains or lithoclasts could be misleadingly identified as separate grains and introduce additional error in the final microfabric data set. Both these obstacles could be avoided as the thin-section quality problems could be identified using the microscope and the lithoclasts could be easily identified and erased form the digital image manually.

In case of un-coloured samples with dark matrix digital images were acquired using plain light and blue channel of TIFF image was used to extract the microfabric information. Segliņš (1987a) has noted that the grains smaller than 2 mm in tills of western Latvia are predominantly of monomineral composition. So, possible bias that can be introduced in the data set by measurement of parts of polimineral grains instead of full grains are small.

#### **2.2.4. Microfabric measurement**

Several microfabric measurement techniques have been tested during the elaboration of this thesis. These including the one used for most of the data acquisition – automated object recognition – are described in this chapter.

Initially microfabric was measured manually on the digital images of the thin sections. These results are presented in Saks *et al.* (2007), Kalvāns, Saks (2004b) and Kalvāns (2004). The apparent orientation of elongated grains was marked with lines on the digital thin section images obtained by scanning in the CorelDraw environment. The line data, marking long axis of selected grains were exported as plotter file and the end-point data for each line were extracted and processed in MS Excel. The obtained orientation data were processed as usual two-dimensional orientation data with StereoNet for Windows 3.1 and represented as rose diagrams with 10° step. The length of longest, measure axis usually was between 0.05 mm and 1.0 mm. Usually two to four hundred grains were measured in

single thin section and 50 to 100, but in no case less than 30, in a detail of thin section except.

The problems associated with this approach are demonstrated in Fig. 2.2, where the same area of thin section is measured twice by the same operator (author) separated with some two years. The strikingly different results are obtained mostly due to problems outlined by Ballantyne and Cornish (1979) – the slight change of initial point of rose diagrams can lead to large apparent differences, especially in cases when samples are small. To overcome these problems automated microfabric measurement methodology was developed and density-based data visualisation procedures adopted (see next subchapters).

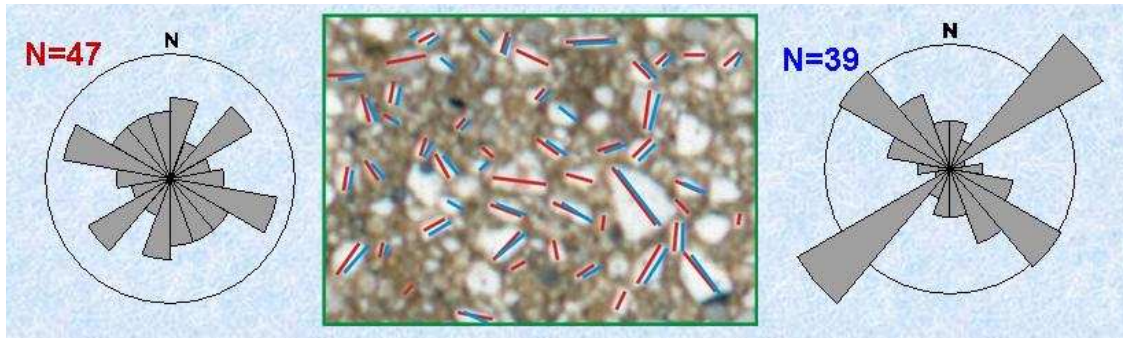


Figure 2.2. Two sets of manual microfabric measurement results visualized as traditional rose diagrams in the same fragment of thin section performed by the same author two years apart. The differences in appearance of both diagrams are mostly due to un-robust nature of rose diagrams in a case of small data sets: slight change in initial data can lead to relatively large differences in visualisation.

2.2. attēls. Viena un tā paša autora ar divu gadu starplaiku veiktas manuālas mikrolīnētātes uzmērīšanas rezultāti atainoti, kā tradicionālā rozēs diagrammas, nelielā plānslīpējuma attēla fragmentā. Atšķirības starp abām diagrammām pamatā ir neizteiksmīgie maksimumi rozēs diagrammās maza mērījumu skaita gadījumos, kā rezultātā nelielas atšķirības starp abām datu kopām var radīt relatīvi lielas atšķirības diagrammu izskatā.

Several software packages offer tools for automated image analysis including object recognition and measurement. The automated object recognition is simplest and best works for binarised – black and white – images. The binary images with one colour representing sand grains and other all the rest of thin section image are acquired as described in the next subchapter. The objects – sand grains – are automatically measured using the commercial software ImageProPlus by the Measure dialog box. Such parameters as object size, elongation ration, the X and Y coordinates and orientation of longest axis are measured and exported to the spreadsheet document for processing and storage.

### 2.2.5. Image processing and automated grain orientation measurement

The description of work steps of image processing used in elaboration of this thesis is given in Table 2.3. The image processing methodology is adopted from Francus (1998). The robustness of microfabric data acquired using this approach with good results was tested by Francus (1998) himself.

Table 2.3 Image processing steps used for automated microfabric measurement  
 2.3. tabula. Attēla apstrādes soļi mikrolīnētātes automatizētai uzmērīšanai

Procedure	Francus (1998)		Equipment and/or software used in this study	Description	Functions and comments
Image acquisition	Single microphotographs and SEM images	digital and	Leica polarisation microscope DFC480 digital camera; Leica IM50 Image Manager software	DMLA Acquisition of overlapping digital microphotographs (in an early stage) with crossed or removed Nicols, single image size: 2560×1920 pixels, with 2.5× objective; Starting from June 2009: Acquisition of non-overlapping, positioned in regular rectangular grid, digital microphotographs with crossed or removed Nicols, single image size: 2234×1784 (ROI settings in IM50: 2235×1788) pixels that correspond to 5×4 mm large thin section area including 8 pixels wide “buffer” that is not represented in any picture	Fixed exposition for all photos of single thin section; RGB images saved in TIFF format; Starting from June 2009: The region of interest (ROI) was defined so that images are regularly spaced with exactly known, small distance between each other
Image resampling	N/A		IrfanView	Image resolute reduction usually to 50% (1280×960 pixels), to improve computer-performance; Starting from June 2009: Additionally to this Canav size of 4 pixels in white colour is added, covering the “buffer” – separation between images.	File/Batch conversation
Composite image creation	N/A		Adobe Photoshop®  ImageProPlus®	Automated mounting of overlapping images in single composite image covering whole slide area; Starting from June 2009: Automated positioning of individual non-overlapping images in pre-defined grid exactly matching the position of individual images relative to other images.	Photoshop/File/Automate/Photomerge  ImageProPlus/Proces/Tile images
Image enhancement	Simple enhancement	contrast	ImageJ	Best Fit equalisation	Image/Adjust/Brightnes/Contrast

*To be continued in the next page*

<b>Procedure</b>	<b>Francus (1998)</b>	<b>Equipment and/or software used in this study</b>	<b>Description</b>	<b>Functions and comments</b>
Manual cleaning	N/A	Adobe Photoshop	Cropping out (substitution with background colour) any thin section image areas of poor image or thin section quality, defects or other patterns that do not characterise the till microfabric; In binary images the background colour will be the same as that of sand grains, thus it will be possible to exclude any boundary-touching grains from the statistic, so a potential source of systematic error is eliminated	
Creation of grey-scale image	N/A	ImageProPlus	Blue (or in some cases Green or Red – whatever gives the best contrast resolution) colour band extraction	Process/Colour channel
Noise reduction	Median filter (3*3)	ImageJ	Image noise reduction (Median filter, 3×3)	Process/Filter/Median (radius = 1.0)
Preservation of subtle details	Contrast kernel – average value of all slide pixels of 3×3 area multiplied by -1 and central pixel multiplied by 9 (the sum divided by 9)	ImageJ	Image detail enhancement (Sharpening)	Process/Sharpening (convolution kernel used: -1 -1 -1 -1 12 -1 -1 -1 -1)
Noise reduction while preserving linear features	Median of 3*3 area values of medians of “+” and “×”, and central pixel values	ImageJ	Enhancing the most expressed linear features	Plugins/Filters/ <u>Hybrid Median 2D filter</u>
Image binarisation	Selecting objects by finding appropriate threshold – binarisation at a cut-of level of minimum colour frequency	ImageJ	Creating a bi-colour (Black & White) image, with distinction between sand grains and matrix. The threshold level is manually selected comparing the preview with original image or thin section to attain best results	Image/Adjust/Threshold/ <i>Adjust</i> (manual)/Apply

*To be continued in the next page*

<b>Procedure</b>	<b>Francus (1998)</b>	<b>Equipment and/or software used in this study</b>	<b>Description</b>	<b>Functions and comments</b>
“Cleaning up”	Filling holes and removing too small (<20 pixels) objects	ImageJ	Filling holes; Removing too small (<125 pixels) objects Removing too big (<12,500 pixels) objects A plug-in Particle remover need top be installed; the colour of removed objects is reset to current background colour: Image/Colour/Colour picker)	Process/Binary/Fill holes Plugins/Analyse/ <u>Particle remover</u> ; Plugins/Analyse/ <u>Particle remover</u>
Smoothing the remaining objects	N/A	ImageJ	Smoothing remaining objects to improve particle recognition	Process/Noise/Despeckle
Verification	Visual verification	ImageJ	Visual verification and re-processing if large proportion (more than some 5%) of grains are not recognised correctly	Visual verification
Measurement	Tools in Analyze Menu of NIH Image	ImageProPlus	Count and measure objects, selecting object area, angle, centre (x-y) position, with 4-corer smoothing of sensitivity set to 2 and convex hull (in options submenu), size range usually 125 to 12500.	Measure/Count/Size



### 2.2.6. Statistical procedures

The task of the statistical analysis is to extract the information on microfabric spatial distribution across the area of the thin section and present in an easily-perceptible manner. Spatial orientation data, such as wind or ocean current direction, usually is represented in rectangular with arrow direction indicating the flow direction and arrow length – the flow speed. In geology the two dimensional orientation data is traditionally represented in a form of the rose diagrams, despite the weak point of rose diagrams is identified by Ballantyne and Cornish (1979), and demonstrated in Fig. 2.2). Obvious way forward is to combine the both approaches and represent the spatial distribution of microfabric as a grid of rose diagrams. During the dissertation elaboration the methodology has been modified as follows (see Table. 2.4 for method details):

- 1) Initially rose diagrams have been constructed from data that are within distance  $R$  (distance between two adjacent grid points) from the central grid point (Kalvāns, Saks, 2008). The developed algorithm was slow as large number of square-root calculation was involved and it was somehow difficult to visually identify area from what microfabric data were collected.
- 2) To reduce outlined problems a new algorithm was introduced, here called Large Squares algorithm. Instead of collecting the data form circle are around a grid point, data from the square outlined by the eight neighbouring grid points is collected. The algorithm is faster and area from what data in a single rose diagram is collected can be easily identified.
- 3) Algorithm using hexagonal (not orthogonal) grid and algorithm collecting data from small square (a half-distance to neighbouring eight grid points) were tested, but were considered not suitable for the reason of conformity to established modes of visualisation and maximum possible resolution where still sufficiently large number of measurements were in the neighbourhood of any give grid point.

During elaboration of dissertation, several approaches have been developed for the visualisation of preferred microfabric orientation in a single grid point:

- 1) initially simple rose diagrams constructed according to recommendations of Davis (2002), including use of the square root instead of real number to indicate the magnitude of a single class. The statistical significance at a 90% level were calculated assuming the von Miss (normal) distribution with resultant vector method, using parameters published by Davis (2002) and identified by the colour of rose diagrams – green or dark grey for statistically significant preferred orientation (Fig. 2.3) and light grey for insignificant preferred orietnation.
- 2) Latter a data density plot presented by Fisher et al. (1985) was implemented (Kalvāns, Saks, 2009). Instead of indicating the number of measurements in a given interval, the distance to  $n$ -nearest measurement is indicated in a rose-like diagram. This approach is believed to overcome the weak point outlined by Ballantyne and Cornish (1979) of traditional rose diagrams.
- 3) The mean fabric orientation initially was calculated as normalised summary vectors (Kalvāns, Saks, 2009). Latter more sophisticated algorithm of eigenvalues for 2D data as described and used by Thomason and Iverson (2006, 2009) is introduced (Kalvāns, Saks, 2008; Saks *et al.*, *accepted for publication*).



The data pre-processing tools used in elaboration the dissertation allow selection for the analysis only grains with certain parameters, such as given size range or the elongation ratio.

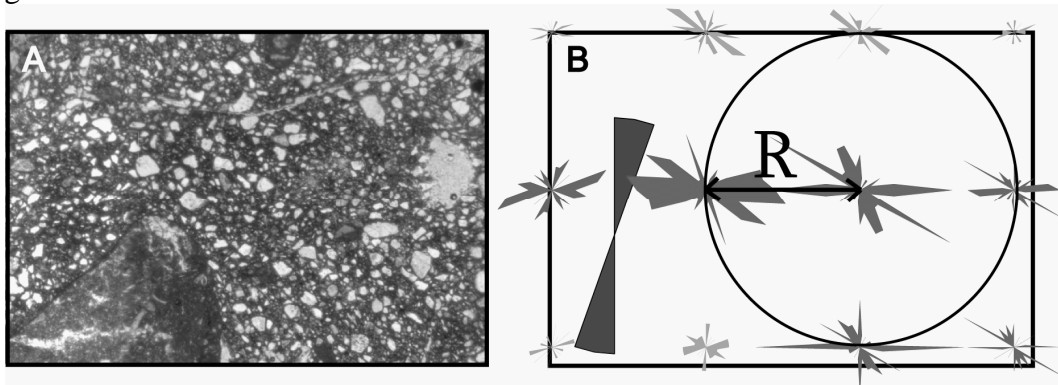


Figure 2.3. An example of visualization of the apparent microfabric. A – Original thin section image; B – microfabric image. Dark grey diagrams have statistically significant lineation assuming von Mises (normal) distribution, the light grey ones – denote cases with unreliable values; the circle indicates area from which data are plotted for single diagram, R is the distance between the centres of adjacent diagrams.

2.3. attēls. Mikrolinearitātes vizualizācijas piemērs. A – oriģināls plānslīpējuma attēls; B – mikrolinearitātes sadalījums, tumši pelēkajās diagrammās ir statistiski nozīmīga linearitāte, pieņemot von Misa (normālu) sadalījumu, gaiši pelēkajās – statistiski nozīmīga linearitāte nav konstatēta; riņķa līnija parāda laukumu, kurā esošie mērījumu punkti ir iekļauti centrālās diagrammas statistikā, R ir attālums starp līdzās esošo diagrammu centriem.

### 2.2.7. The methodology testing: experimental sedimentology

To test the methodology of thin section preparation, data acquisition and analysis artificially created sample was processed according to the methodology described above: suspended diamicton collected at the Jaunupe outcrop to the NE of Ventspils was sediment in a water-filled cylinder. For ease of removal sediment sample a smaller cylinder was inserted in the cylinder where sedimentation took place. The suspension was added several times and so lamination was created. At the latest stage a few gravel grains were dropt in the soft sediments to see the deformation effects. It must be noted that the suspension was extremely dens and the sedimentation time – short – if comparing to conditions likely to be observed in glaciofluvial or glaciolimnic situation where similar sedimentary conditions could be observed. A 0.5 kg diamicton sample was suspended in 5 l of water and the total sedimentation time, except the final settlement of fine particles, was 1 ½ hours. A 60 mm thick sediment pile was accumulated. When fine particles that apparently were coagulated, settled, excessive water was removed and the sediments – left for draying.

Sample was air-dried and impregnated with colour-less epoxy resin diluted with acetone in two steps, vertical thin section prepared and digital composite image created using the photomerge approach. The microfabric distribution was visualised using simple rose diagrams, with colour indicating whether the preferred orientation is statistically significant according to summary vector length method (Davis, 2002) using Radial data collection algorithm – that is all data within a distance R from the grid point are used to calculate its statistics.

Table 2.4. The statistical procedures for microfabric data analysis implemented and tested during thesis elaboration

2.4. tabula. Pētījuma gaitā ieviestās un pārbaudītās mikrolineariātes datu statistiskās apstrādes operācijas

Procedure	Method	Description
Grouping	Circles	All data points within the distance R, which is the distance between adjacent grid points arranged in an orthogonal grid, are included in the statistic of the give grid point. Each data point is included in the statistics of several – up to four – grid points. The data collection from circular area gives best representation of the microfabric in the vicinity of particular grid point and the overlapping of data collection areas ensures that no measurement is left out of the statistics.
	Hexagons	Grid points are arranged in a hexagonal grid and each data point are added to statistics of a single, nearest grid point. The hexagonal grid ensures the least variation of distance from grid point to the borders of data collection area.
	Large squares	Grid points are arranged in rectangular grid and data is collected from the square-shaped area outlined by eight neighbouring grid points. Each data point is included in statistics of four adjacent grid points. The inclusion of a single measurement in the statistics of several neighbouring grid points allow tracing of finer microfabric variations.
Visualisation	Rose diagrams	Data is visualized in the form of traditional bidirectional rose diagrams. The data is split into 10° classes. Square root instead of real number of measurements in every class is used to calculate the relative high of any data class in a diagram, thus avoiding the exaggerated size of the largest classes (Davis, 2002). The diagrams with statistically significant preferred orientation are plotted in another colour than the rest of diagrams.
	Density plots	A method used by Fisher <i>et al.</i> (1985) for calculating the relative density for angular measurement data defined as: if $\theta_1, \dots, \theta_n$ is the angular measurements, then the relative density for any measurement $bk(\theta)$ is inversely proportional to $k$ nearest measurement, were $k$ is the integer part of $\alpha n^{1/2}$ , where $\alpha$ is freely chosen from 0.5 until 2. This approach is believed to overcome the weak point outlined by Ballantyne, Cornish (1979) of traditional rose diagrams.
	The summary orientation – resultant vector	The summary orientation of each grid point is plotted as the normalized $R_n$ (resultant vector), that is additionally normalized against the threshold level of $R_n$ length for different classes of number of measurements, as, according to Davis (2002), for large numbers of measurements shorter $R_n$ values are considered statistically significant. The resultant vectors ( $R_n$ ) that are statsitcialy significant after Davis (2002) are presented in green or dark grey colour.

*To be continued in the next page*

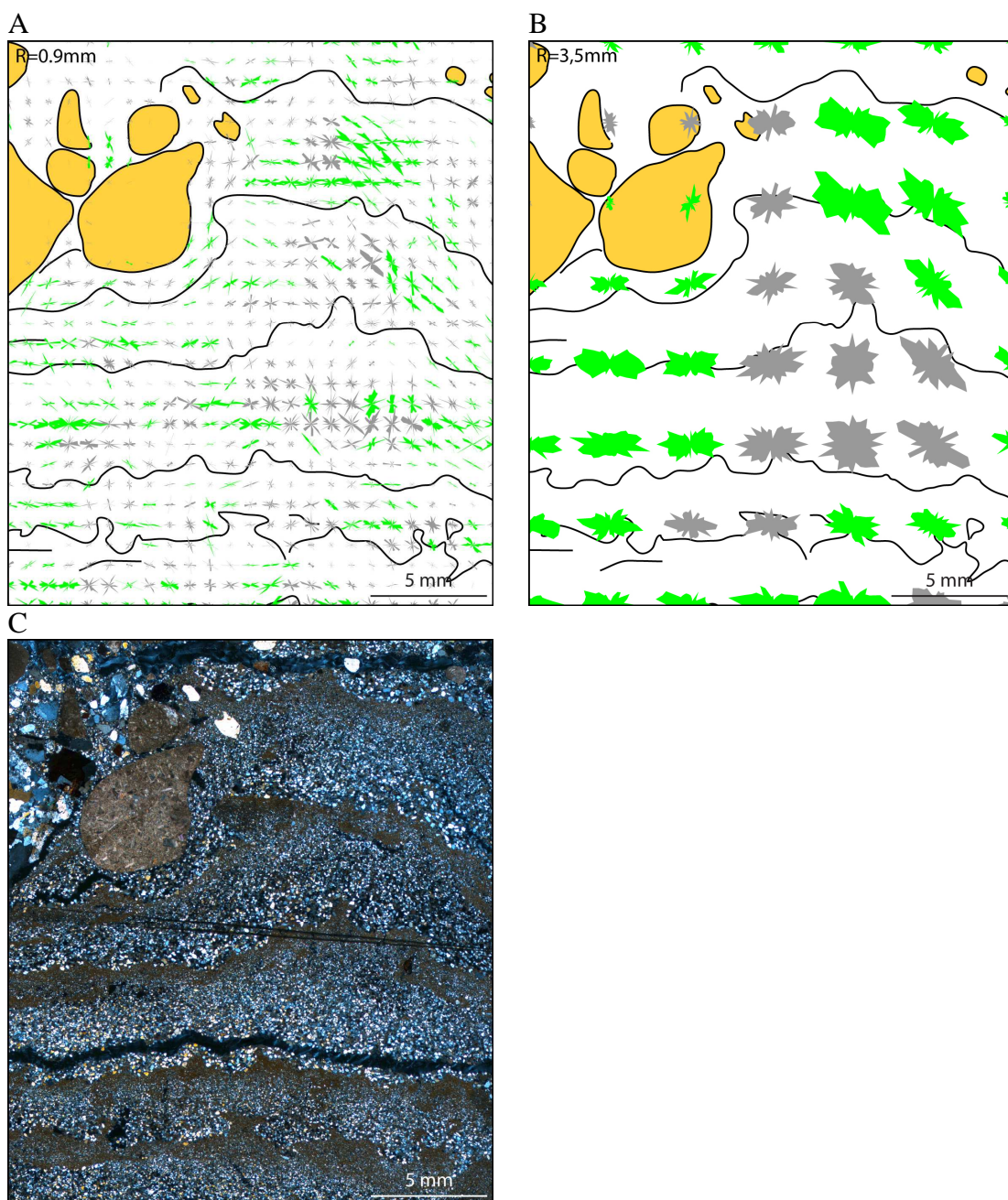
Procedure	Method	Description
	The summary orientation – eigenvector	Alternatively the direction of the strongest clustering ( $V_I$ ) and respective eigenvalue ( $S_I$ ) are used (after Mark, 1973; Thomason and Iverson, 2006) applying gray-scale colour coding and line length scaling.
Preferred orientation strength	Resultant vector	<p>Von Mises (normal, monomodal) data distribution is assumed and significance of preferred orientation is evaluated by calculating the length of the normalized resultant vector (<math>Rn</math>; Davis 2002, p.322-330) and comparing it to the critical values for 0.9 confidence level, as given by Davis (2002, p. 619):</p> $Rn = \frac{\sqrt{(\sum \sin 2\alpha)^2 + (\sum \cos 2\alpha)^2}}{n}$ <p><math>n</math> – number of measurements around the grid point;  <math>2\alpha</math> – doubled orientation value of measurement</p> <p>The measured tilt angle <math>\alpha</math> of a long axis before the statistical interpretation is doubled due to bidirectional nature of orientation data: a value <math>0^\circ</math> is actually identical value <math>180^\circ</math>, but in trigonometrically they are opposite to each other; by doubling both measurements we get <math>0^\circ</math> and <math>360^\circ</math> that are trigonometrically identical values (Davis 2002, p.316-322). Usually the dominant orientation using this method is calculated only if the number of measurements in a given grid point is 18 or more.</p>
	Eigenvalue	<p>The eigenvalue method for three dimensional directional data analysis in glacial geology was suggested by Mark (1973) is implemented as adopted for 2D by Thomason, Iverson (2006):</p> $S_1 = \frac{1}{n} \sum_{i=1}^n \cos^2 \phi_i .$ <p>The <math>\phi_i</math> is the difference between the direction <math>V_I</math> – the direction of data clustering – and observation <math>i</math>. The function is maximised <math>V_I</math> (the value of <math>V_I</math> found that corresponds to largest value of <math>S_I</math>). <math>n</math> – is the number of observations. In 2D if the <math>S_I=1</math>, all measurements are pointing in the same direction and <math>S_I=0.5</math> indicates random distribution. Usually the dominant orientation using this method is calculated only if the number of measurements in a given grid point is 30 or more, unless it is stated otherwise.</p>

A distinct lamination with well expressed water escape structures that do not exceed the borders of single lamina is observed in the thin section (figure 2.4). The microfabric is predominantly horizontal, although in fine resolution the fabric alignment along water-escape structures can be seen.

The “dropstones” that were introduced in the sedimentation last stage resulted in deformation of two laminas below them. Below the dropstones lamina thin and fabric

strengthening is observed. Material is pressed in a “pile” next to dropstones resulting in lamina thickening (layer parallel shortening) and sub-vertical reorientation and weakening of fabric. Fabric strengthening is observed in the opposite side to dropstones in the diapir-like bulge formed by the thinking stones (figure 2.4).

The eigenvector statistics for the sedimentation experiment thin section image that is acquired following the buffer-lines methodology is given in the Appendix 2 and 3. The fabric is rather strong and due to insufficient resolution the local variations introduced by fluidisation (flame) structures is not represented in the eigenvector data sets. The orientation of different-size grains is remarkably uniform (maximum spread only  $8^\circ$ , appendix 3). The fabric strength (eigenvalue) variations are moderate and large grains exhibit only slightly stronger fabric than the small ones. The water-escape (flame) structures are rather symmetrical, thus the summary preferred orientation is not affected, but can affect the fabric strength.



*See caption in the next page*

Figure 2.4 Strongly sub-horizontal microfabric distribution (A and B) and microstructure (C) in artificially sediment suspended till diamicton. The suspension was added to the sedimentation container in several portions resulting in distinct lamination and formation of water-escape structures at the interface between individual lamina. In fine resolution (A) microfabric strength weakening around water-escape structures can be observed. In the medium grid resolution (B) the fabric weakening as a result of formation of diapir-like structure is observed. The used symbols are explained in tables 1 and 2.

2.4. attēls. Mākslīgi izgulsnēta, suspendētas morēnas diamiktona izteikti sub-horizontālā mikrolinearitāte (A un B) un mikrostruktūra (C). Sedimentācijas traukā suspensija tika pievadīta atsevišķu porciju veidā, tādējādi veidojoties laminētai nogulumu uzbūvei un atūdeņošanās struktūrām uz individuālu laminu kontaktvirsmām. Attēlā ar augstu izšķirtspēju (A) var novērot mikrolinearitātes pavājināšanos ap atūdeņošanās struktūrām. Attēlā ar vidēju izšķirtspēju (B) var novērot mikrolinearitātes pavājināšamos diapīrveida struktūras kodolā. Izmantotie apzīmējumi ir paskaidroti 1. un 2. tabulās.

It was concluded that symmetrical sub-millimetre size structures, such as flame structures (Fig. 2.4), likely will not be identifiable in microfabric distributions calculated with present methodology. However the centimetre scale deformation structures are likely to be clearly manifested in the microfabric distribution.

### 3. The results

The study is part of wider examination of geological structure of quaternary sediments exposed in the bluffs along the Baltic Sea by research group lead by professor Vitālijs Zelčs. In four key locations at the bluffs along the Baltic Sea coast till micromorphology was examined and are included in this thesis: Sensala site, Plašumu gully site, Strante site and Ziemupe site (Figure. 3.1 and 3.2). The study sites were selected due to examined sated of the outcrops that are constantly renewed due to costal erosion and easy to aces.

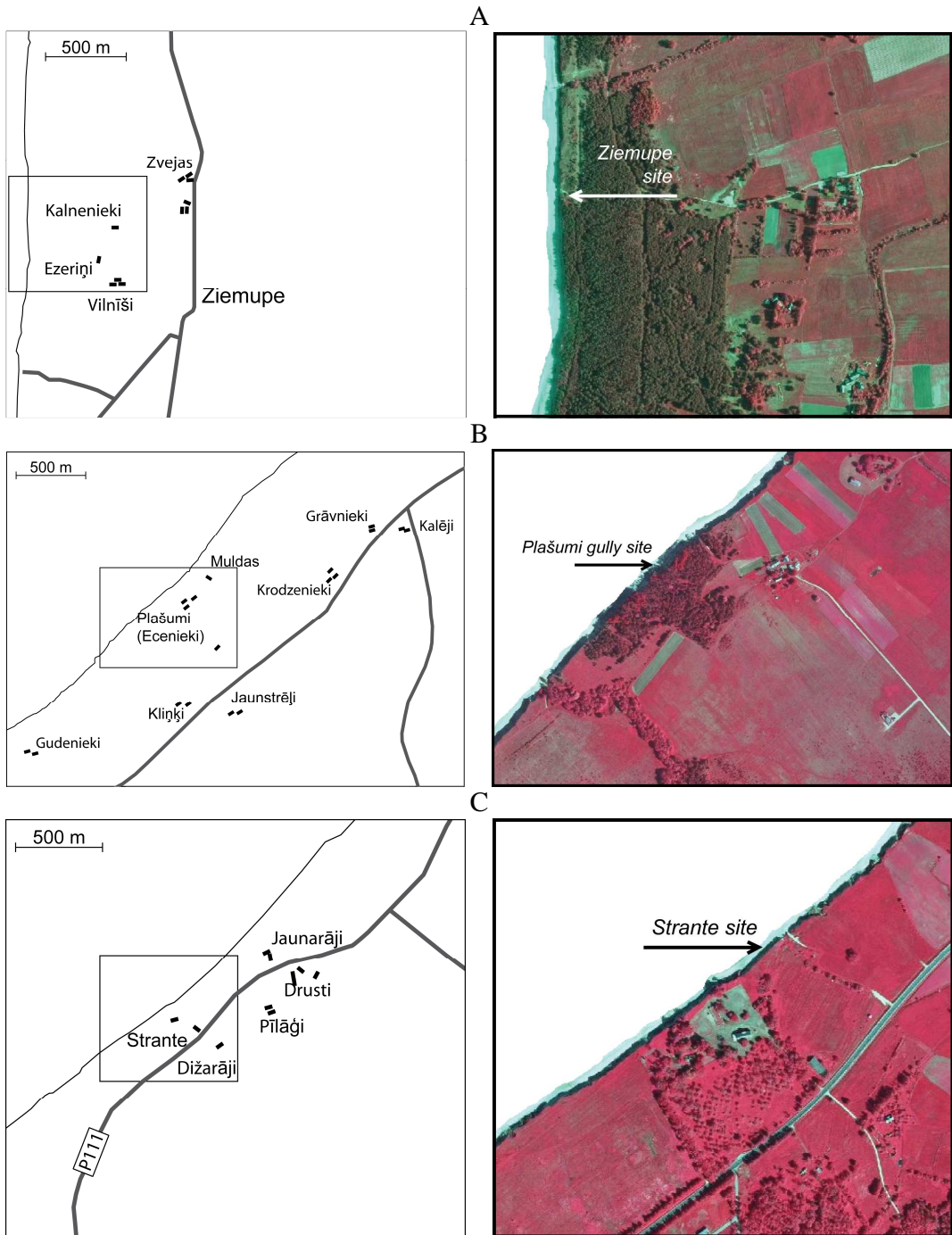
To identify any position at the costal bluffs an arbitrary starting point is defined already by Dreimanis (1936). Any position at the costal profile is described by single number identifying the distance from this starting point in meters. It is referred to this profile in the current dissertation as well to indicate the location of certain geological structures.

In the following subchapters findings of individual site investigation are described. The description in Sensala site and Ziemupe site more than one till unit was identified. They usually are marked as upper till and lower till. These names are used only to explain they relative position in the outcrop and contains no general indication about their age or genesis.



Figure. 3.1. The overview cartogram of the location of study sites.

3.1. attēls. Pētījuma objektu novietojuma pārskata kartogramma.



*To be continued in the next page*



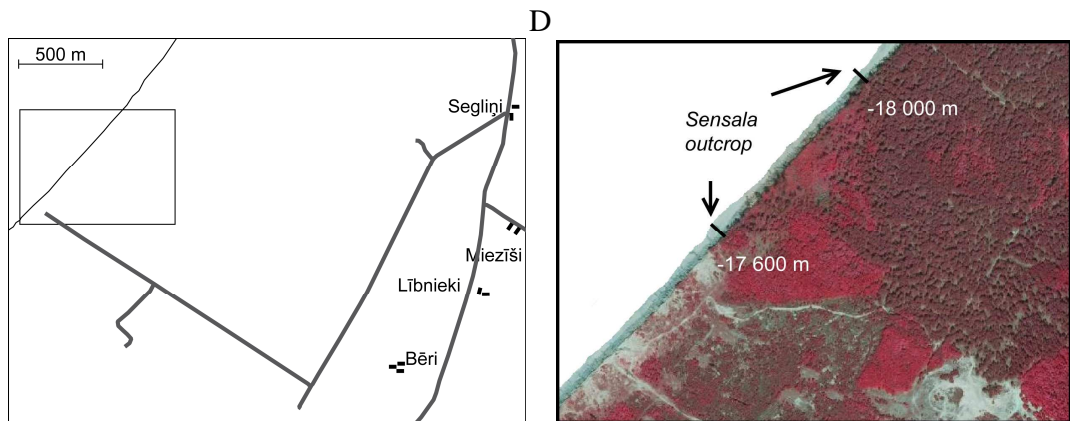


Figure. 3.2 The location of study objects shown in cartograms and ortofoto pictures: A – Ziemupe site; B – Plašumi gully site; C – Strante site; D – Sensala outcrop. © 2009 LU ĢZZF, kartes.geo.lu.lv; Ortofoto © 2009 Latvian Geospatial Information Agency

3.2. attēls. Pētījuma objektu atrašanās norādītas pārskata kartogrammās un ortofoto attēlos: A – Ziemupe; B – Plašumi grava; C – Strante; D – Sensalas atsegums. © 2009 LU ĢZZF, kartes.geo.lu.lv; Ortofoto © 2009 Latvijas Ģeotelpiskās informācijas aģentūra



### 3.1. Ziemupe site

The outcrop at Ziemupe is located at the Baltic Sea cliff, approximately 30 km N of the Liepāja Town, in Western Latvia (Figs. 4.1 and 4.2); the geographical coordinates are X = 003-20-261E and Y = 062-93-812N in LKS92 reference system.

At nearly 600 m long bluff section the complex sequence of Pleistocene marine and glacial sediments, common for this region, are exposed (Kalniņa *et al.*, 2000; Segliņš, 1987b; Saks *et al.*, 2007; Kalvāns, Saks, 2008).

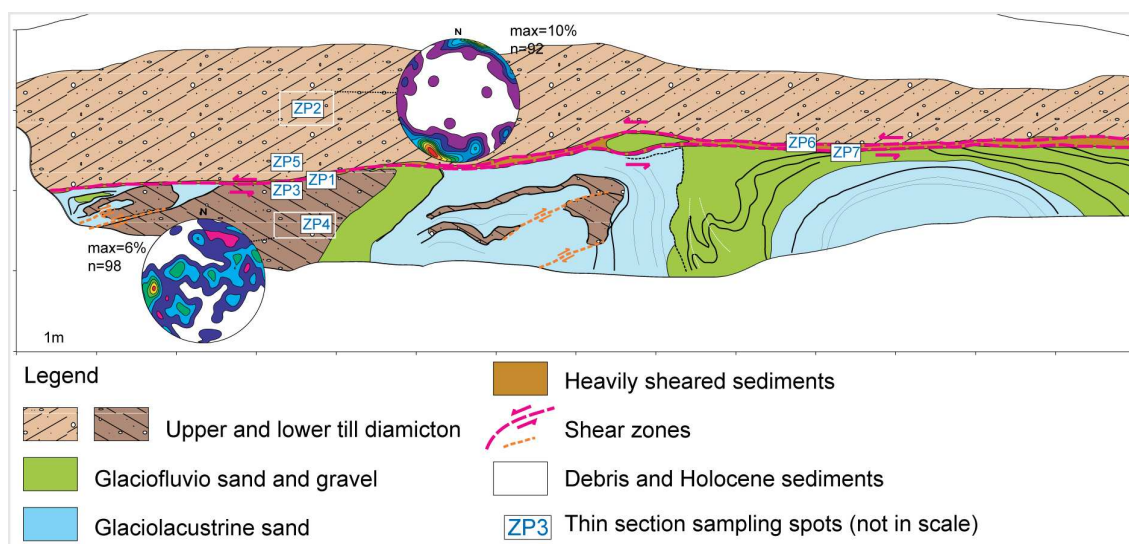


Figure 3.3. Geological structure and location of the sampling sites for thin section preparation at the Ziemupe outcrop. The macrofabric measurement sites are indicated by white rectangles and results are shown in the lower hemisphere of the Schmidt net: n denotes number of measured clasts, maximum orientation concentration (max) is given in %.

3.3. attēls. Ziemupes atseguma ģeoloģiskā uzbūve un paraugu ievākšanas vietas plānslīpējumu pagatavošanai. Oļu linearitātes rezultāti apkopoti Šmita projekcijā uz apakšējās puslodes: n norāda mērījumu skaitu, maksimālā koncentrācija (max) ir dota %.

At investigation site glaciotectionally deformed fine sand and silt sediments as well as glaciofluvial coarse sand and gravel topped by the basal till unit (referred here as the upper till unit) was exposed (Fig. 3.3). Additionally a second diamicton unit (referred here as the lower till unit) below the upper till was observed in some places along the outcrop. A distinct shear zone was observed at the base of upper till unit (Fig. 3.4).

The deformation style of the sedimentary strata can be described as a result of two factors: (1) density inversion that resulted in formation of fine sand diapir structures and sinking of denser glaciofluvial sand and gravel, and (2) glaciotectionic compression and dragging of material at the glacier bed in the SSE direction. The formation of gravity-driven structures likely was triggered by dramatic loss of sediment strength at some point when pore water pressure at a glacier sole reached the floatation point. The origin of the lower till unit at this site may be explained by detachment and sink in loose sediments of slab of basal till simultaneously with formation of other gravity-driven structures. Alternatively it could be an older till unit from earlier glacial phases. The top of structural

complex is cut by the shear zone at the base of the upper till, suggesting decoupling of the glacier from its bed.

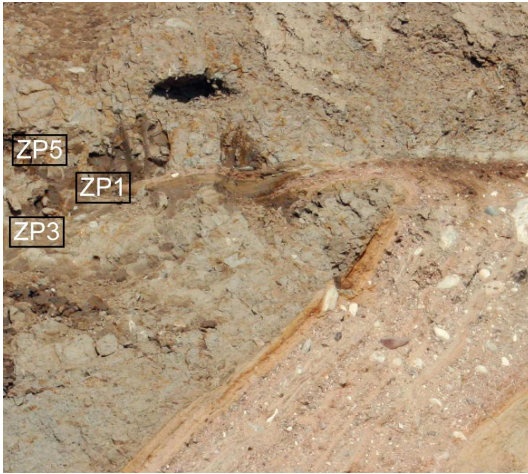


Figure 3.4. The shear zone at the base of upper till. The image is 0.5 m wide. Sample ZP1, ZP3 and ZP5 collection sites are indicated.

3.4. attēls. Bīdes josla augšējās morēnas pamatnē. Attēla paltums ir 0,5 m. Ir norādītas paraugu ZP1, ZP3 un ZP5 aptuvenās ievākšanas vietas.

The upper till macrofabric has a well developed NNE to SSW orientation (Fig. 3.3; with eigenvalues  $S_1 = 0.675$  and  $S_2 = 0.256$ ). This is somewhat different than suggested in studies on regional ice movement direction (Gaigalas *et al.*, 1967; Punkari, 1997; Boulton *et al.*, 2001a; Zelčs, Markots, 2004).

The interpreted shear direction in the shear zone beneath the upper till is roughly from S to N.

The macrofabric of the lower diamicton is not as well developed (Fig. 3.3; with eigenvalues  $S_1 = 0.443$  and  $S_2 = 0.370$ ). Relatively high  $S_2$  value suggests more grid-like distribution that can be interpreted as result of the initial fabric re-orientation due to penetrative deformation. The mean macrofabric orientation is from NEE to SWW.

The results of the microfabric investigation at the Ziemeupe site are partly published at Kalvāns and Saks (2008). The dissertation is supplemented with results of the samples from the shear zone at the base of the upper till (ZP6 and ZP7) and missing sections of the sample ZP4 of the lower till.

### 3.1.1. The samples

Seven samples have been collected for micromorphological examination. Two of them were taken above, three – within and two – below the shear zone, separating upper and lower till units (Fig. 3.3.). Sample ZP1 is taken directly from the shear zone. Samples ZP2 and ZP5 are taken from the upper till respectively 1 m and 10 cm above the shear zone. Sample ZP3 is taken directly below the shear zone and sample ZP4 is taken 0.5 m below the shear zone from the lower till. Samples ZP6 and ZP7 are collected from the sandy shear zone at the contact of upper till and underlain sand and gravel.

The thin sections were prepared using colourless (samples ZP3, ZP4 and ZP5) and dyed (samples ZP1, ZP2, ZP6 and ZP7) epoxy resin for sample hardening. Digital images were acquired using plain light; mosaic images were obtained using the photomerge function of Adobe Photoshop.

In the samples ZP1 to ZP5 the microfabric distribution is visualised using simple rose diagrams, with colour indicating whether the preferred orientation is statistically significant according to summary vector length method with level of certainty 90% (Davis, 2002) using Radial data collection algorithm – that is all data within a distance R (equal to the spacing of grid points) from the grid point are used to calculate its statistics.

The samples ZP6 and ZP7 as well as two sections of sample ZP4 have been analysed using visualisation of microfabric spatial distribution as data density (Fisher *et al.*, 1985) and summary vector as preferred orientation and fabric strength indicator (Davis, 2002) with a single colour indicating whether the preferred orientating is statistically significant, assuming von Miss (unimodal) distribution (Davis, 2002). A “large squares” method was used to collect all the data points that fall with the square outlined by the neighbouring grid points, with square sides  $2 \times R$  long. Additionally on a latter stage the eigenvalue statistics were calculated for grid resolutions  $R = 20.8$  mm, 2.6 mm and 1.3 mm according to method used by Thomason and Iverson (2006).

### 3.1.2. Microfabric and macrofabric comparison

The macrofabric data is three-dimensional (3D), meanwhile the microfabric data is two-dimensional (2D), but represented in three perpendicular sections. It is hard to reconstruct true 3D pattern of microfabric from thin sections, therefore, in Fig. 3.5 the macrofabric data in the same form as microfabric data in three mutually perpendicular plains, corresponding to orientation of thin sections.

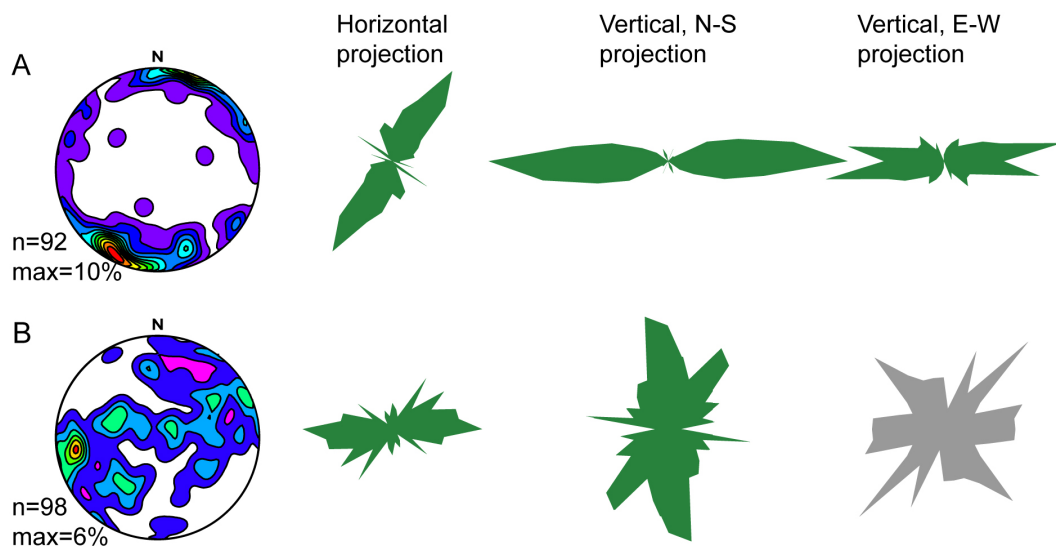


Figure. 3.5. Macrofabric lineation of upper (A) and lower (B) till units and its projections to single planes. See Fig. 3.3 for location of the sampling site.

3.5. attēls. Augšējās (A) un apakšējās (B) morēnas makrolinearitātes hipotētiskās projekcijas uz trīs savstarpēji perpendikulārām plaknēm. Paraugu ievākšanas vietas izvietojumu atsegumā skat. 3.3. att.

Calculating the projections of macrofabric to the plains it is assumed, that macrofabric is formed by perfect rod-like particles, with no flattening. Unfortunately flattening of the pebbles has not been recorded in the field. This introduces some level of uncertainty in projected data.

### 3.1.3. The micromorphology

Semi-statistical micromorphological analysis was done following methodology introduced by Carr (1999). A simplified set of four microstructure categories was adopted

from Larsen *et al.* (2007): (1) turbate structures, also known as galaxy or rotation structures, are circular grain alignments that occur both with and without a core stone; (2) lineations comprising three or more aligned elongated grains; (3) grain stacks are micro-scale equivalents of grain bridges consisting of stacks of at least five equal-sized sand grains; (4) intra-clasts and domains are inclusions or zones of sediment with unique textural characteristics that can be distinguished from the surrounding sediment. Due to low clay contents of the studied tills no plasmic fabric structures (i.e. clay-sized particle arrangement observable in cross-polarised light) were observed.

The microstructures have been counted in the thin section area of 23×16 mm. Results of microstructure counts are presented in Fig. 3.6. For each sample number of counted microstructures in each thin section are standardized to proportion of glacial diamicton to other material (like sand lamina, gravel grains of significant size or technical defects) in analysed area of thin section and summed together.

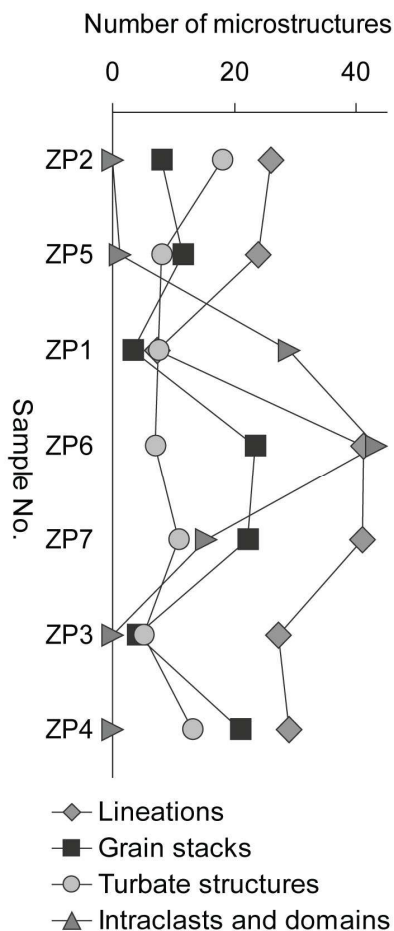


Figure 3.6. Synoptic results of the microstructure counting. Note that the samples collected from the shear zone at the base of upper till (ZP1, ZP6 and ZP7) have a distinctly different set of microstructures than samples collected elsewhere. See Fig. 3.3 for location of the sampling site.

3.6. attēls. Mikrostruktūru skaitīšanas rezultātu kopsavilkums. Paraugos, kas ievākti no bīdes joslas augšējās morēnas pamatnē (ZP1, ZP6 un ZP7), ir novērojams atšķirīgs mikrostruktūru komplekts, salīdzinot ar tiem, kas ir ievākti citur. Paraugu ievākšanas vietas izvietojumu atsegumā skat. 3.3. att.

It can be seen (Fig. 3.6.) that the samples collected from the sandy shear zone (No. ZP6 and ZP7), as expected, have similar microstructure sets excepting the number of intracalsts with high number of grain stacks and lineations. In contrast the sample ZP1 that is believed to be collected from the shear zone between upper and lower tills has very small numbers of lineations and grain stacks.

It is visually assessed that the much greater amount of displacement has occurred in the sandy shear zone than between the both till units. Thus different microstructure sets is understandable.

### **3.1.4. Upper Till: Sample ZP2**

Both in macroscale and microscale the upper till has uniform composition with dominantly sand and silt matrix and occasional gravel grains. The sample ZP2 taken well above (1 m) the basal shear zone has microfabric orientation close to that of macrofabric orientation in both vertical and horizontal sections (Figs. 3.5 and 3.7). However in horizontal plane (Fig. 3.7.a) multiple domains of different orientation can be observed and in large generalisation levels (greater than  $R = 1.4$  mm) the statistically significant lineation has not been detected. Overall shape of the diagrams indicate N-S trend.

In vertical section parallel to macrofabric (Fig. 3.7.b) microfabric is well developed, and in all resolutions statistically significant lineation domains are observed, coinciding with macrofabric. Several curved microfabric structures associated with gravel grains are present, and discontinuous microfabric can be observed. In the section that is transverse respective to macrofabric (Fig. 3.7.c) several domains with statistically significant lineation are observed. However, in large generalisation the microfabric is not as strong as in section parallel to macrofabric. As demonstrated in Fig. 3.5a macrofabric in the upper till is distributed in subhorizontal plane, and this corresponds to microfabric distribution in the horizontal plane (Fig. 3.7.a) as well. Even the strength of macrofabric and microfabric is similar in both projections – larger in N-S projection (Fig. 3.5a, N-S projection and Fig. 3.7.b) and weaker in E-W projection (Fig. 3.5a, E-W projection and Fig. 3.7.c).

### **3.1.5. Upper till: Sample ZP5**

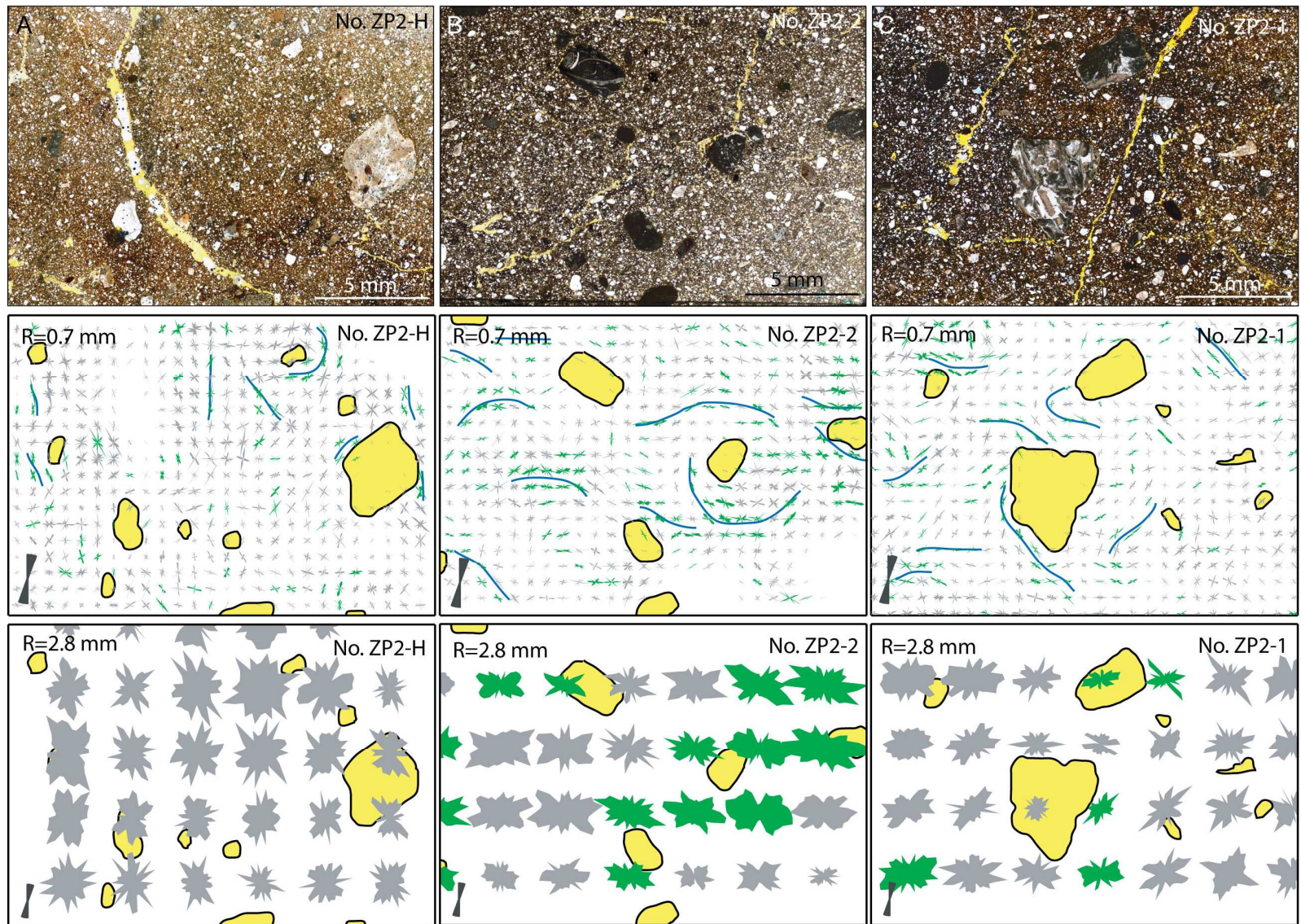
The sample is taken few cm above the extrapolated basal shear zone (Figs. 3.3 and 3.4). In general microfabric in this sample is in agreement with the macrofabric orientation of the upper till, especially in the horizontal plane. However, the vertical sections show preferred sand grain orientation dipping  $30^\circ$  to  $45^\circ$  from the horizontal plane. Similar, steeply dipping microfabric in basal tills with several orientation domains have been reported by other researches as well (Carr, 2001; Carr, Rose, 2003) deemed as an indicator of the large strain. The summary of the apparent microfabric in vertical sections has only weak subhorizontal maximum.

There is a zone of well developed microfabric in the horizontal section, which coincides with orientation of the macrofabric of the upper till, however it is situated near large gravel grain, and trend of microfabric is coinciding with observed trend of gravel grain surface. Elsewhere in horizontal section the domain pattern of microfabric is observed.

### **3.1.6. Shear zone between the tills: Sample ZP1**

The sample is taken so that to include a termination of the sand stringer that can be followed out to the basal shear zone of the upper till (Figs. 3.4 and 3.6). The horizontal thin section and one vertical thin section are cutting this stringer. In contrast to other samples this sample stacks as illustrated in Fig. 3.6 has plenty of silt intraclasts, smaller number of lineations, and grain. A sand lamina or stringer and silt nodules are signs of assimilation of subglacial material in deforming till due to shearing along the basal shear zone of the upper till. No “armour” of sand grains is observed on the surface of glacial diamicton and sand lamina. This indicates that contact is not of sedimentological character and has been formed or renewed during deformation.



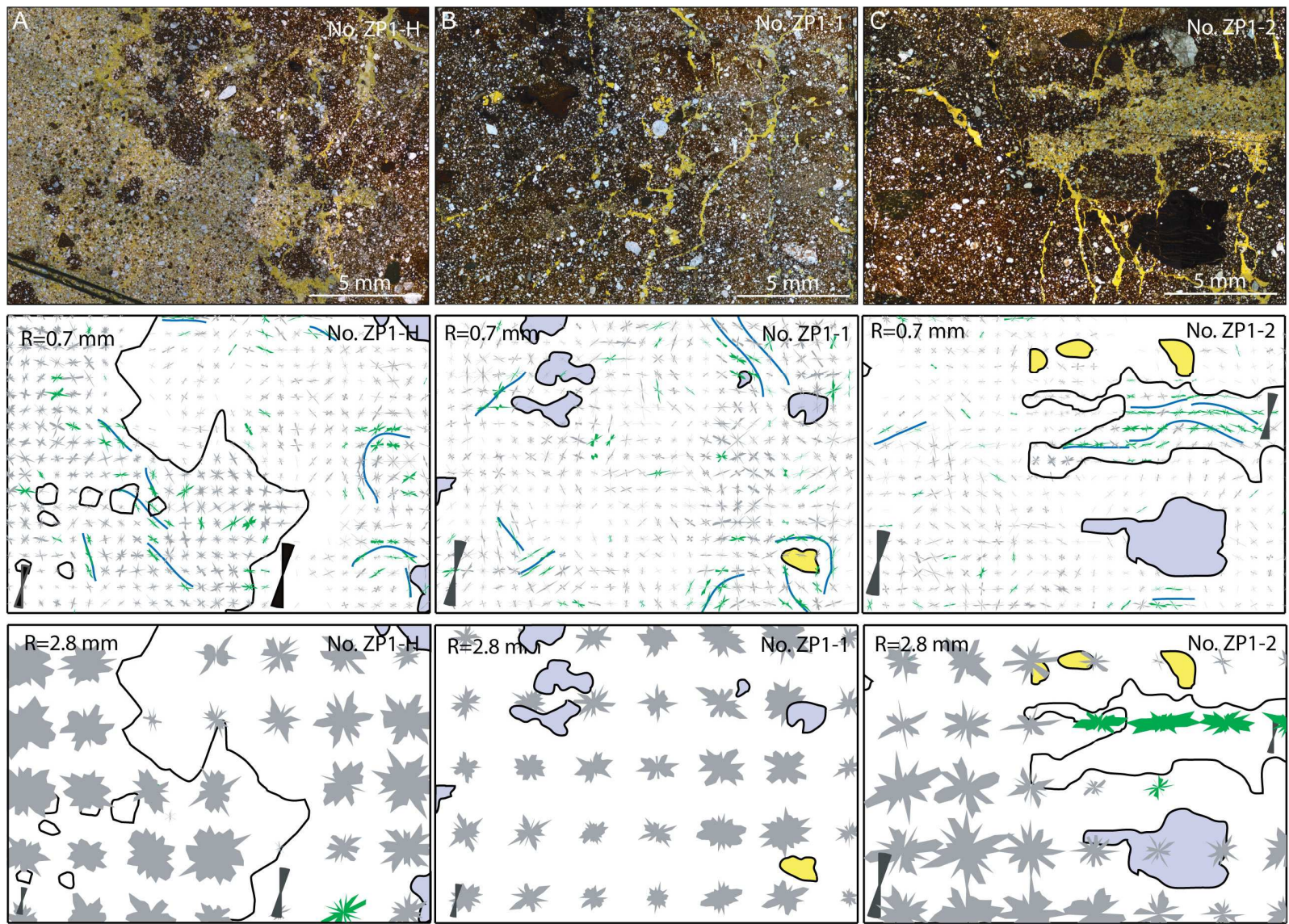


*See caption in the next page*

Figure 3.7. Photographs and apparent 2D microfabric of the thin sections from the upper till unit, sample ZP2; in columns: A – horizontal section No.ZP2-H; B – vertical section No.ZP2-2, sub-parallel to the upper till macrofabric, facing N; C – vertical section No.ZP2-1 sub-perpendicular to the upper till macrofabric, facing E. In general ( $R = 2.8$  mm) microfabric is in agreement with macrofabric (Fig. 3.5.a), however it is not always statistically significant. In B column image with grid resolution  $R = 0.7$  mm, discontinuous microfabric indicated by lines can be observed around a gravel grain, however, it is not recognisable in resolution  $R = 2.8$  mm image. Similarly in C column image with grid resolution  $R = 0.7$  mm, the alignment of the microfabric can be identified along gravel grains, while in grid resolution  $R = 2.8$  mm, image it is blur. Used symbols are explained in Tables 1 and 2. See Fig. 3.3 for location of the sampling site.

3.7. attēls. No augšējās morēnas parauga ZP2 izgatavoto plānslīpējumu mikrofotogrāfijas un šķietamā 2D mikrolinearitātes orientācija; kolonās: A – horizontāls griezum Nr. ZP2-H; B – vertikāls griezum Nr. ZP2-2, subparalēls augšējās morēnas makrolinearitātei, vērsts uz Z; C – vertikāls griezum Nr. ZP2-1, subperpendikulāri augšējās morēnas makrolinearitātei, vērsts uz A. Kopumā ( $R = 2,8$  mm) mikrolinearitātes orientācija līdzinās makrolinearitātei (3.5.a att.), tomēr tā ne vienmēr ir statistiski nozīmīga. B kolonas attēlā ar režģa izšķirtspēju  $R = 0,7$  mm ap grants graudu ir novērota, pārtraukta mikrolinearitātes orientācija, tomēr šī struktūra nav atpazīstama attēlā ar izšķirtspēju  $R = 2,8$  mm. Līdzīgi arī C kolonas attēlā ar  $R = 0,7$  mm var novērot mikrolinearitātes apliekšanos ap grants graudiem, savukārt, attēls ar  $R = 2,8$  mm ir daudz neskaidrāks. Izmantotie apzīmējumi ir paskaidroti 1. un 2. tabulās. Paraugu ievākšanas vietas izvietojumu atsegumā skat. 3.3. att.





See caption in the next page



**Figure 3.8.** Photographs and apparent 2D microfabric of thin sections prepared from sample ZP1, collected from the shear zone between the upper till and the lower till units, in columns: A – horizontal section No. ZP1-H; B – vertical section No. ZP1-1 sub-parallel to the upper till macrofabric, facing SEE; C – vertical section No. ZP1-2 sub-perpendicular to the upper till macrofabric, facing NNE. Microfabric with resolution  $R = 0.7$  mm shows some domains with statistically significant lineation (e.g. the lower left corner of the middle image in B column) that are not represented in grid resolution  $R = 2.8$  mm. Note the contrasting lineation patterns in the sand stringer and surrounding diamicton (images in C column) indicating either different modes of deformation or sand grain response to shear of the contrasting lithological environments. In neither diamicton nor sand part in the horizontal section, in A column any significant preferred orientation of sand grains could be observed. Used symbols are explained in tables 1 and 2. See Fig. 3.3 for location of the sampling site.

**3.8. attēls.** No bīdes joslas starp augšējo un apakšējo morēnu ievāktā parauga ZP1 plānslīpējumi, kolonās: A – horizontāls griezum Nr. ZP1-H; B - vertikāls griezum Nr. ZP1-1, subparalēls augšējās morēnas makrolienariatātei, vērsts uz DAA; C – vertikāls griezum, Nr. ZP1-2 subperpendikulārs augšējās morēnas makrolinearitātei, vērsts uz ZZA. Attēlos ar  $R = 0,7$  mm ir novērojami atsevišķi domēni ar statistiski nozīmīgu linearitāti, piemēram, B kolonas vidējā attēla apakšējais kreisais stūris, kas nav atspoguļota attēlos ar režģa izšķirtspēju  $R = 2,8$  mm. Ievērojiet, krasi atšķirīgo mikrolinearitātes raksturu smilts dzīslīņā un apkārtējā diamiktonā (C kolona), kas norāda uz atšķirīgu smilts un diamiktona deformācijas raksturu vai arī atšķirīgu smilts graudu uzvedību bīdes apstākļos, dažāda sastāva materiālos. Horizontālā griezumā (kolonna A) nedz smiltīs nedz arī diamiktonā nav novērots izteikt dominējošais mikrolinearitātes orientācijas virziens. Izmantotie apzīmējumi ir paskaidroti 1. un 2. tabulās. Paraugu ievākšanas vietas izvietojumu atsegumā skat. 3.3. att.

The margin between the sand stringer and diamicton is sharp and undulating perturbed by secondary shear structures such as echeloned joints and Riedel shears (Fig. 3.8.c). Similar to the structure described by Larsen *et al.* (2007) it has undulating boundaries and little mixing between contrasting lithologies can be observed. Only slight statistically insignificant lineation of NWW – SEE direction in large generalisation levels can be observed in the horizontal section of sand lamina (Fig. 3.8.a), however, strong subhorizontal sand grain lineation is observed in the vertical section (Fig. 3.8.c).

The microfabric of the diamicton in the horizontal plane has no significant orientation, however, in large resolution some circular structures can be traced (Fig. 3.8a). The domain-like microfabric pattern in large resolution is presented in the vertical section as well, but no preferred orientation can be traced in low resolution – large generalisation levels. The till microfabric observed in the sample ZP1 is not similar to neither of both till unit macrofabrics.

### 3.1.7. The sandy shear zone: Sample ZP6 and Sample ZP7

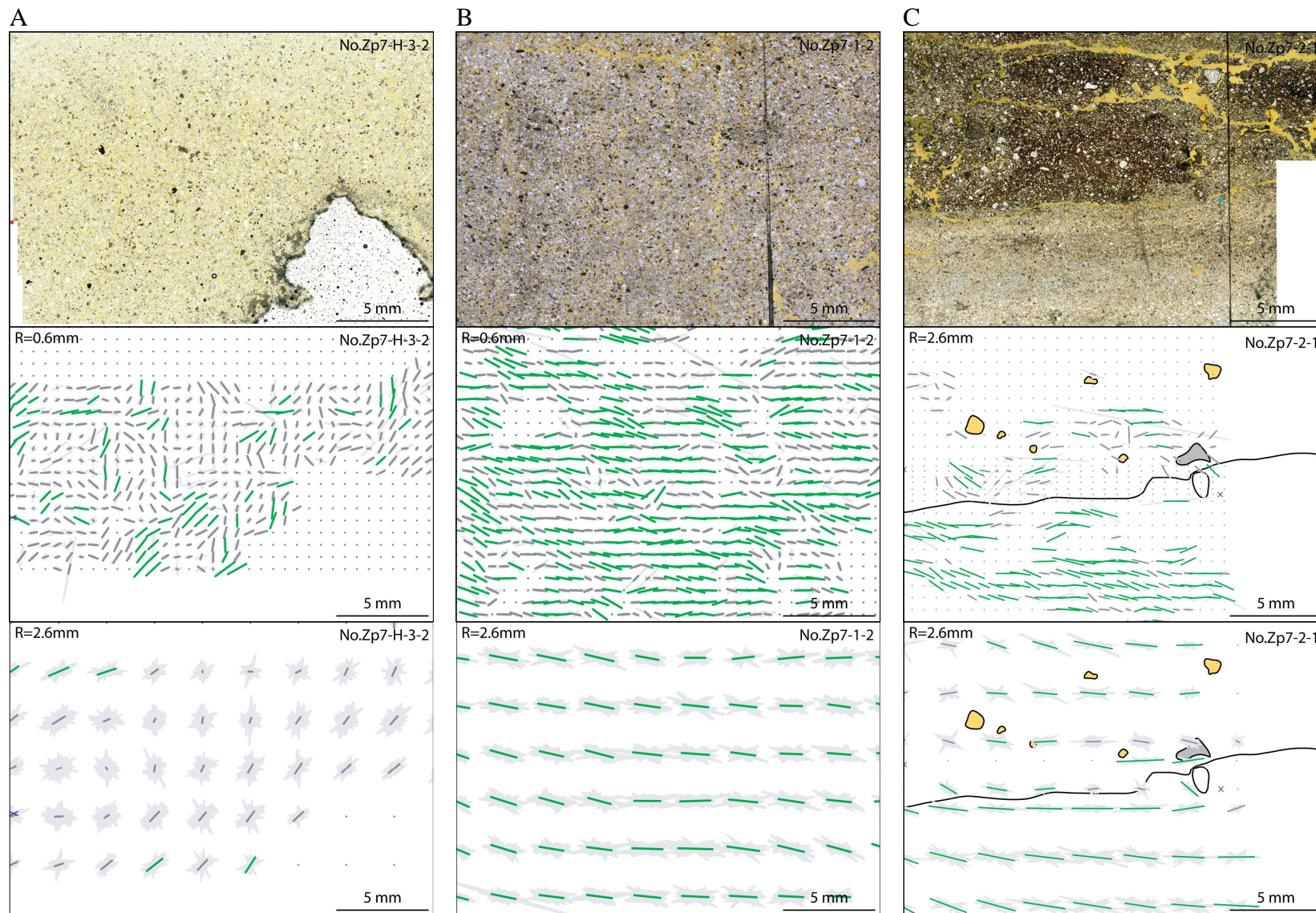
The shear zone in a base of the upper till (Fig. 3.9), composed of sandy and diamicton bands, has strong and uniform subhorizontal preferred sand grain orientation in vertical sections (Fig. 3.10) that is slightly dipping towards the shear direction.



Figure 3.9. The sandy shear zone and samples Nos. ZP6 and ZP7 at a base of the upper till at the Ziemupe site. The height of sampling box is 7 cm. See Fig. 3.3 for location of the sampling site.

3.9. attēls. Smilšainā bīdes josla un paraugu nr. ZP6 un ZP7 ievākšanas vietas augšējās morēnas pamatnē. Paraugu ievākšanas kastītes augstums ir 7 cm. Paraugu ievākšanas vietas izvietojumu atsegumā skat. 3.3. att.

In vertical sections sand bands and diamicton bands have different patterns of microfabric distribution. The sandy bands have the strong subhorizontal microfabric, while the bands of the heterogeneous material like the diamicton have markedly weaker microfabric, with noticeable domain-like distribution. In all parts of the shear zone the microfabric is stronger than in the overlying till.



*See caption in the next page*

Figure 3.10. Orthogonal thin sections from the sample ZP7, the lower part of shear zone at the base of the upper till at Ziemupe site, in columns: A – horizontal section No. ZP7-H-3-2; B – vertical section No. ZP7-1-2, facing NNW; C – vertical section No. ZP7-2-1, facing NEE; note that the vertical sections ZP7-1-2 and ZP7-2-1 are orthogonal but come from different heights of the sample. The microfabric in horizontal section No. ZP7-H-3-2 have a domain-like distribution and in lower grid resolutions (e.g.

R = 2.6 mm) only small number of diagrams show statistically significant preferred orientation. The top of the ZP7-H-3-2 section is to the 330° and the summary orientation is weakly expressed in N-S direction. Strong, consistent and in fine resolution, undulating microfabric in vertical section of sand bands are evident. The microfabric in vertical section of diamicton band (No.ZP7-2-1) is rather strong, but not as consistent as in the sand bands. Used symbols are explained in tables 1 and 2. See Fig. 3.3 for location of the sampling site.

3.10. attēls. Ortogonāli plānslīpējumi izgatavoti no parauga ZP7, kas ir ievākts no smilšainās bīdes joslas augšējās morēnas pamatnē, Ziemupes atsegumā, kolonās: A – horizontāls griezum Nr. ZP7-H-3-2; B – vertikāls griezum Nr. ZP7-1-2, vērsts uz ZZR; C – vertikāls griezum Nr. ZP7-2-1, vērsts uz ZAA; plānslīpējumi ZP7-1-2 un ZP7-2-1 ir ortogonāli, bet atbilst dažādiem līmeņiem bīdes joslā. Horizontālajā plānslīpējumā ZP7-H-3-2 ir novērojams domēnu tipa mikrolinearitātes sadalījums un gadījumā ar zemu režģa izšķirtspēju (R = 2,6 mm) tikai nedaudzas diagrammas uzrāda statistiski nozīmīgu linearitāti. Plānslīpējumu ZP7-H-3-2 augša ir vērsta uz 330°, un vāji izteikta summārā orientācija ir vērsta Z-D virzienā. Vertikālajos griezum ir novērojama stipra un vienmērīga mikrolinearitāte; pie augstas režģa izšķirtspējas ir novērojams (R = 0,6 mm) viļņots mikrolinearitātes sadalījums. Mikrolinearitāte vertikālā griezumā, diamiktona josliņa (plānslīpējums ZP7-2-1) ir relatīvi stipra, bet ne tik vienmērīgi orientēta, kā smilts josliņās. Izmantotie apzīmējumi ir paskaidroti 1. un 2. tabulās. Paraugu ievākšanas vietas izvietojumu atsegumā skat. 3.3. att.



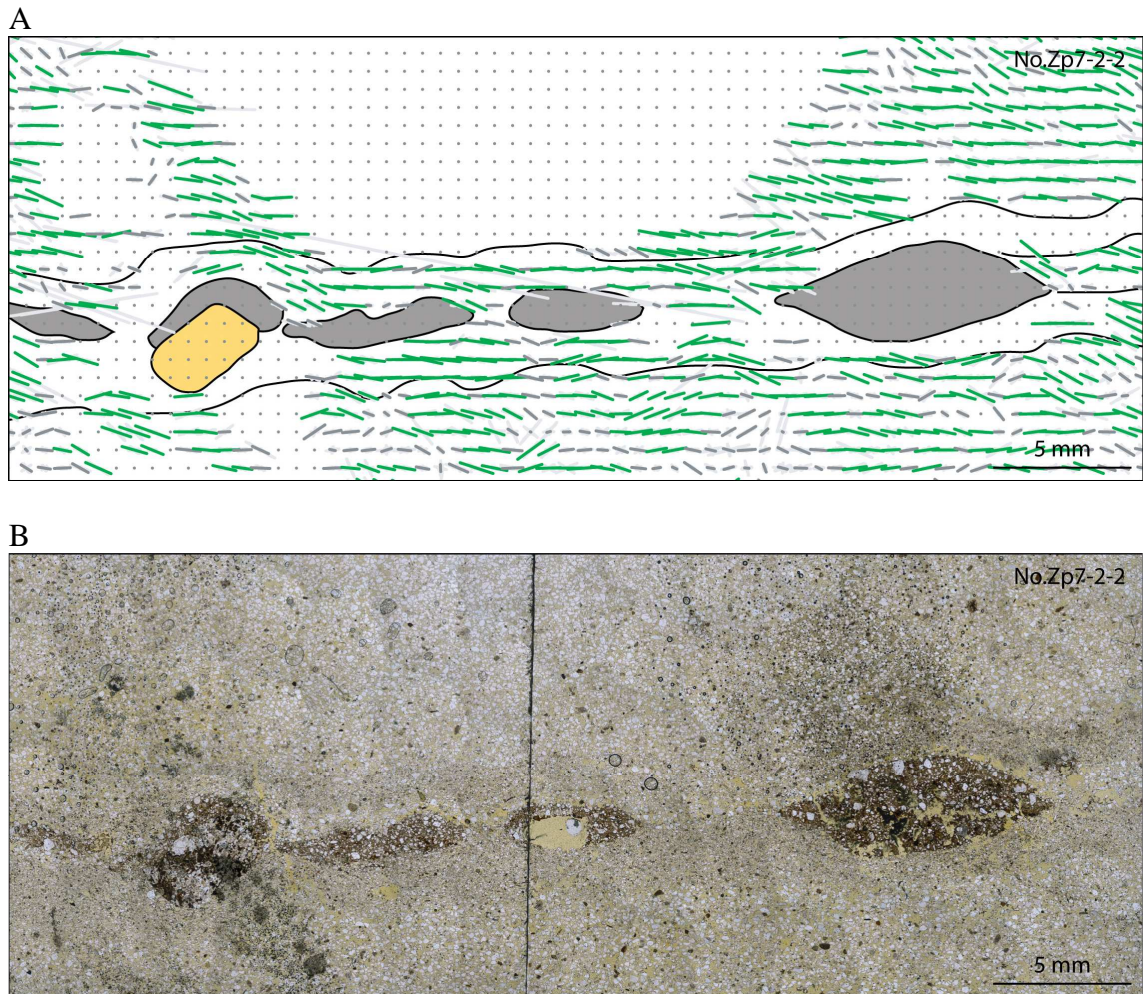


Figure 3.11. The microfabric distribution (A) in vertical thin section ZP7-2-2 (B), facing NEE, from the shear zone at the base of the upper till at the Ziemupe site. Observe the well developed preferred orientation in well sorted sands of the shear zone and wavy microfabric pattern. Used symbols are explained in Tables 1 and 2. See Fig. 3.3 for location of the sampling site.

3.11. attēls. Mikrolinearitātes sadalījums (A) uz ZZA vērsta vertikālā plānslīpējumā ZP7-2-2 (B), ka izgatavots Ziemupes atsegumā no bīdes joslas augšējā morēnas pamatnē.

Pievērsiet uzmanību labi izteiktajam mikrolinearitātei ar viļņoto sadalījumu. Izmantotie apzīmējumi ir paskaidroti 1. un 2. tabulās. Paraugu ievākšanas vietas izvietojumu atsegumā skat. 3.3. att.

In fine resolution a wavy pattern of microfabric distribution can be identified in vertical sections of the sand bands (Fig. 3.10). In sample ZP7-2-2 the microfabric waves can be correlated with diamicton boudins (Fig. 3.11). The wavy pattern can be resulted from secondary shears, cutting the general shear band in low angles in both upwards and downwards directions. Alternatively it can be the effect of stiff inclusions in the shear zone such as till boudins or gravel grains initiating something like standing waves or ripples in the shear zone.

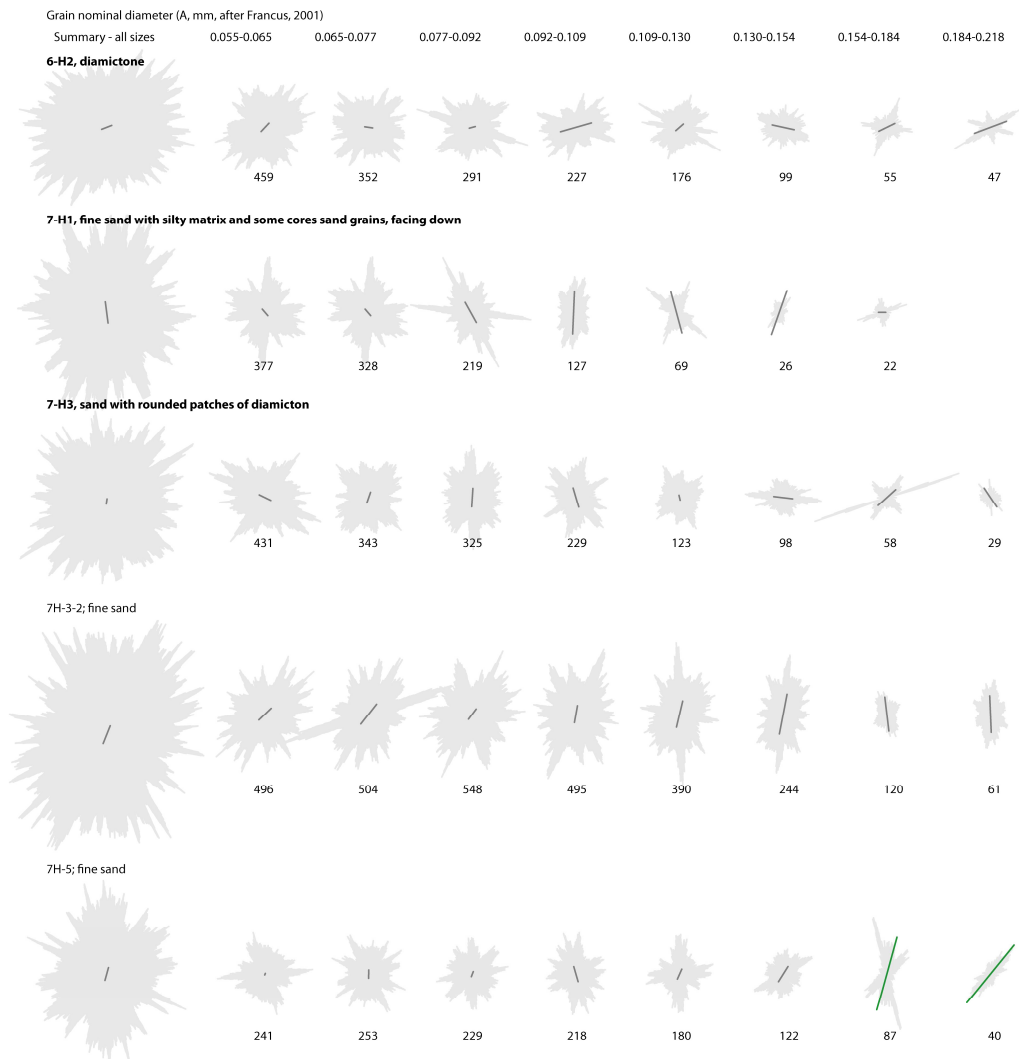


Figure 3.12. Orientation of different-size grains from the horizontal thin sections of the shear zone at the base of the upper till at the Ziemupe site. Thin section ZP6H-2 is from the diamicton band, thin sections ZP7H-1 and ZP7H-3 are from sandy bands with some inclusions of the diamicton, and thin sections ZP7H-3-2 and ZP7H-5 from the fine sand bands of the predominantly sandy shear zone. A stronger fabric is observed in the sand samples although statistically significant lineation is observed only for the coarsest grains in the thin section ZP7H-5. The dominant orientation is similar to that of the macrofabric of the upper till, that is trending in NNE-SSW direction. The top of diagrams is to the N; symbols used as in Table 2. See Fig. 3.3 for location of the sampling site.

3.12. attēls. Dažādu izmēru smilts graudu orientācija horizontālos plāslīpējumos, kas izgatavoti no Ziemupes atseguma augšējās morēnas pamatnē esošās bīdes joslas paraugiem. Plāslīpējums ZP6-H2 ir izgatavots no diamiktona josliņas, plāslīpējumi ZP7-H1 un ZP7-H3 ir izgatavoti no smilts josliņām ar atsevišķiem diamiktona ieslēgumiem, un paraugi ZP7H-3-2 un ZP7H-5 no smalkas smilts josliņām bīdes joslā. Izteiktāka linearitāte ir novērojama smilts paraugos, lai gan statistiski nozīmīga tā ir tikai rupjākajiem graudiem plāslīpējumā ZP7H-5. Dominējošais linearitātes virziens ir tuvs augšējās morēnas makrolinearitātei: ZZA – DDR. Diagrammu augša ir uz Z, apzīmējumi atbilstoši 2. tabulai. Paraugu ievākšanas vietas izvietojumu atsegumā skat. 3.3. att.

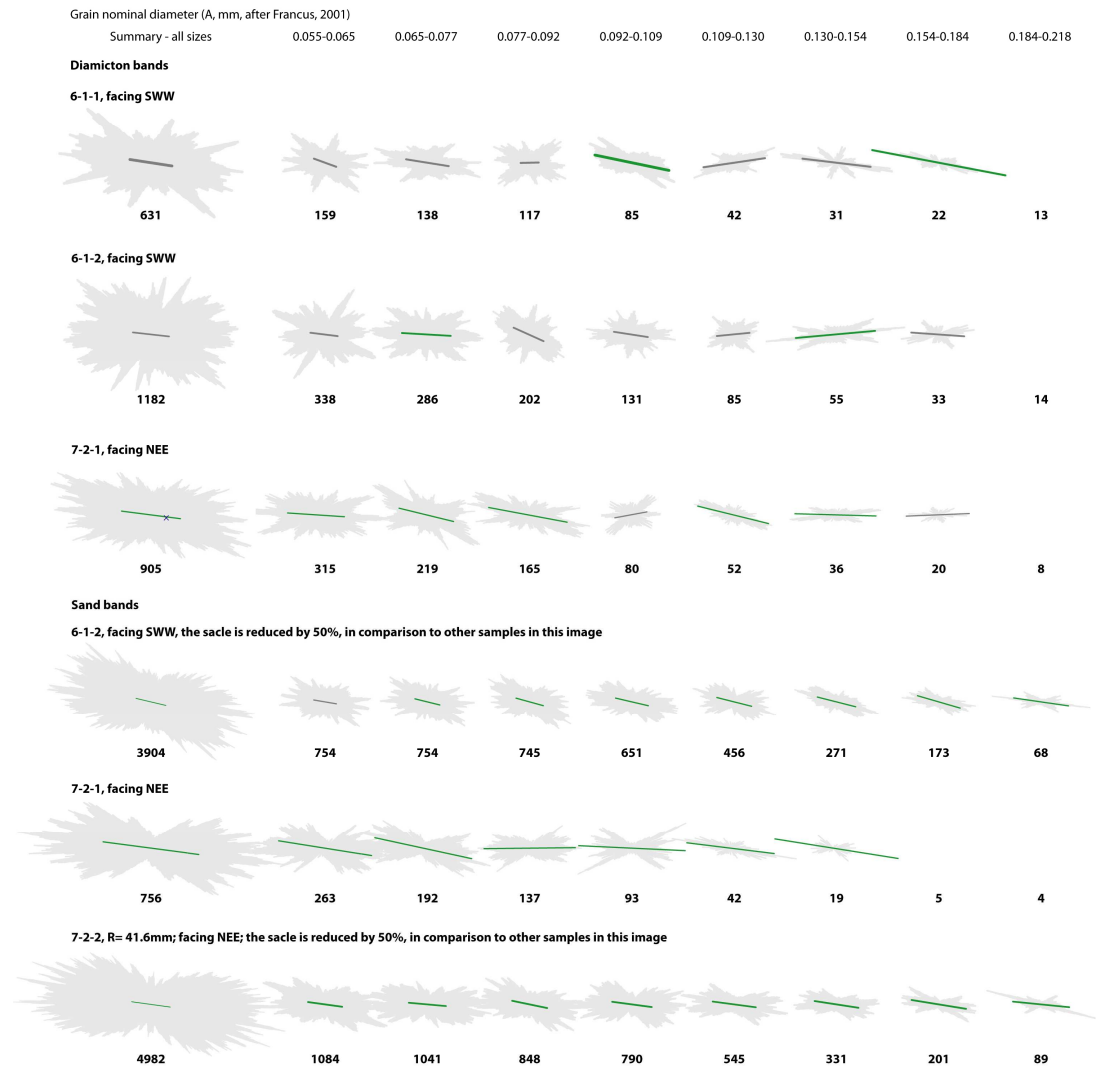


Figure 3.13. Orientation of different-size grains from the vertical thin sections of the shear zone at the base of the upper till at the Ziemupe site. Note the consistent orientation in sand bands and more heterogeneous orientation in the diamicton bands. The top of diagrams is to the N; symbols used as in Table 2. See Fig. 3.3 for location of the sampling site.

3.13. attēls. Dažādu izmēru smilts graudu orientācija vertikālos plānslīpējumos, kas izgatavoti no Ziemupes atseguma augšējās morēnas pamatnē esošās bīdes joslas paraugiem. Ievērojiet, ka smilts materiāli plānslīpējumos dažādu izmēru graudu orientācija ir līdzīga, savukārt diamiktonā tā ir mainīgāka. Diagrammu augša ir uz Z, apzīmējumi atbilstoši 2. tabulai. Paraugu ievākšanas vietas izvietojumu atsegumā skat. 3.3. att.

In horizontal sections larger grains has relatively stronger preferred orientation than the smaller ones. In vertical sections the variation of preferred orientation across different size classes, both for sand and diamicton bands, are smaller than in horizontal sections; the variation is large in diamicton bands than in sand bands (Figs. 3.12 and 3.13). In case of the horizontal sections almost transverse summary orientation in some cases is observed, but it is poorly developed and can not be regarded as a rule.

The wavy microfabric pattern is similar to echelon-type secondary shears observed by Mandl *et al.* (1977) in ring-shear experiments after the shear zone has collapsed into single plane producing slickenslided surface. Probably inclined microfabric

zones developed when shear displacement ceased in the particular part of the shear zone, and inclined zones of microfabric are artefact of ceasing shear displacement.

The microfabric in horizontal section is rather similar to the microfabric of till samples. It has domain-like distribution with rather low summary fabric strength and trending mostly in the N-S direction that is similar to preferred macrofabric orientation in the upper till. However in finer resolutions divergence between preferred, statistically significant orientation in individual domains can be more than 45°. Like in vertical sections it is observed, that bands of well sorted material – sands – have the stronger microfabric than those composed of the diamicton.

### **3.1.8. Lower Till: Sample ZP3**

The sample is taken from just below the position of the basal shear band of the upper till that can be interpreted by continuing the basal contact from parts of the section where sand is exposed below the upper till and the base of the upper till is identifiable.

The horizontal section has strongly developed sand grain apparent microfabric in E-W direction that is consistent with macrofabric of the lower till. In large resolution several well-developed lineation domains with discontinuous contacts can be identified.

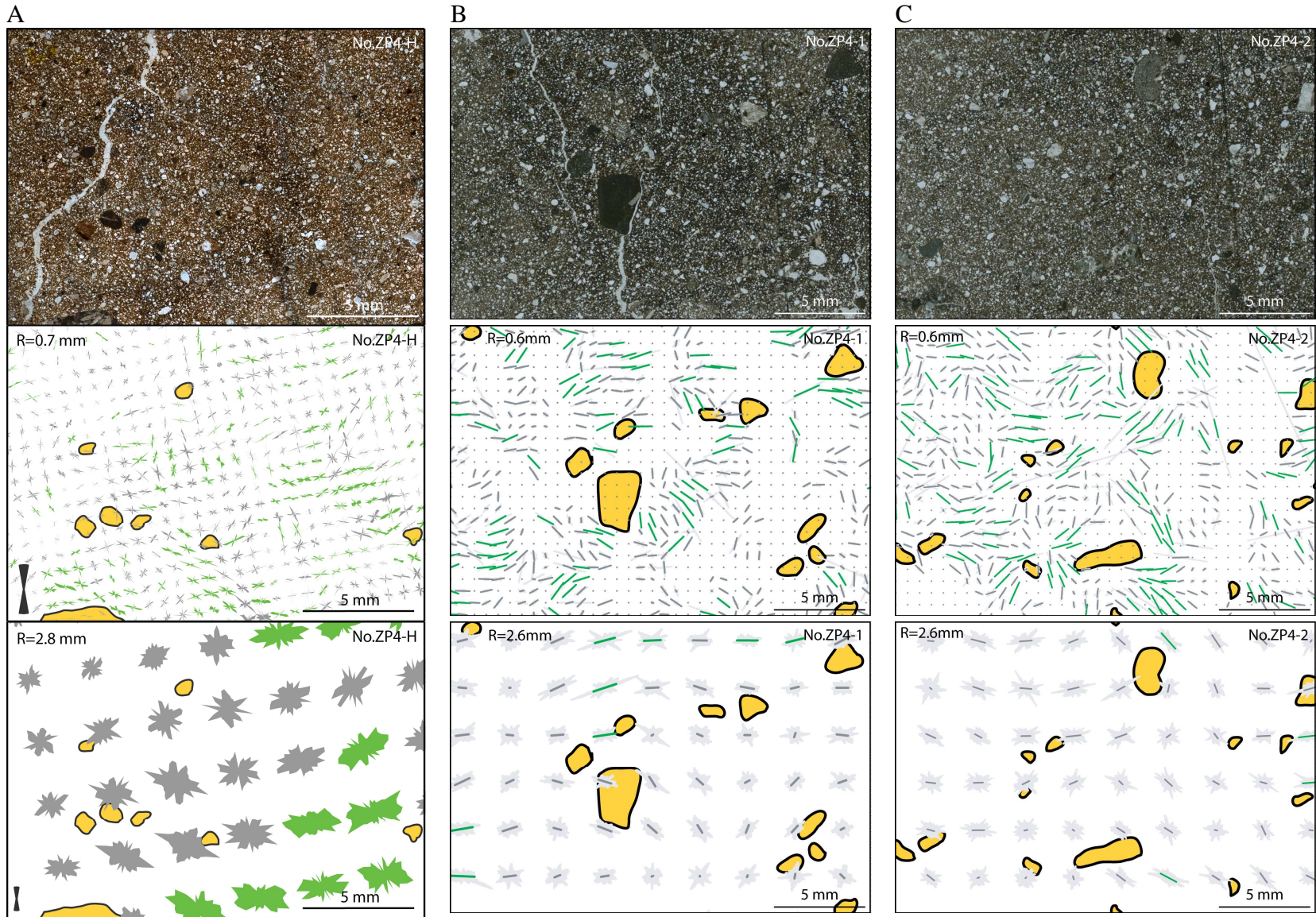
Several domains of well developed often steeply dipping lineation can be observed in vertical sections as well. In some cases lineation in domains is bending but it is difficult to identify any clear circular structure. In other cases contrasting (cross-cutting) lineation is observed in neighbouring lineation domains that probably are an indication of the brittle deformation. In large generalisation an irregular shape of the diagrams suggest the non-random orientation of the elongated grains and presence of the several distinctly oriented grain populations.

### **3.1.9. Lower till, sample ZP4**

The sample is taken from the lower diamicton unit. The microfabric in it is rather well developed with several distinct domains (Fig. 3.14). In low resolution microfabric is parallel to the macrofabric orientation. In finer resolution well expressed domain-like distribution is observed with fabric strength frequently reaching statistically significant values calculated according to Davis (2002). The observed microfabric is in a good agreement with calculated horizontal projection of macrofabric of the lower till, however the correlation in the vertical section is not so good. Microfabric bending and semicircular distribution is often observed in the vertical sections.

In the vertical sections, like in the horizontal section strong domine-like microfabric structure with statistically significant lineation is evident. Domains are up to several millimetres large. The lineation in domains is not consistent, and in large resolution horizontal as well as vertical and tilted microfabric in domains is manifested. In large generalisation ( $R = 2.6$  mm) only subhorizontal domains retain statistically significant lineation. Increasing generalisation level to  $R = 5.2$  mm or more the lineation domains become mixed up and not a single diagram shows statistically significant lineation.





See caption in the next page

Figure 3.14. The microfabric distributions in the thin sections of lower till sample ZP4; A – horizontal section No. ZP4-H; B – verticals section No. ZP4-1, facing S; C – vertical section No. ZP4-2, facing E. A domain-like microfabric picture is observed in fine grid resolution, however the lower resolution ( $R = 2.8$  mm) leads to more general micro fabric distribution that is similar to the macrofabric orientation trending in approximately E – W direction. Used symbols are explained in Tables 1 and 2. See Fig. 3.3 for location of the sampling site.

3.14. attēls. Mikrolinearitātes orientācija apakšējās morēnas parauga ZP4 plānslīpējumos; A – horizontāls griezum nr. ZP4-H; B – vertikāls griezum Nr. ZP4-1, vērsts uz D; C – vertikāls griezum Nr. ZP4-2, vērsts uz A. Attēlos ar smalku režģa izšķirtspēju var novērtot domēnu tipa mikrolinearitātes sadalījumu, tomēr samazinot režģa izšķirtspēju ( $R = 2,8$  mm) var novērot vienmērīgāku mikrolinearitātes orientāciju, kas līdzinās makrolinearitātes orientācijai apakšējā morēnā, kas tiecas aptuveni A – R virzienā. Izmantotie apzīmējumi ir paskaidroti 1. un 2. tabulās. Paraugu ievākšanas vietas izvietojumu atsegumā skat. 3.3. att.

### 3.2. Plašumi gully site

Plašumi gully site is located approximately 7 km SSW from town of Jūrkalne. The geographical coordinates of Plašumi gully site are X = 003-36-847E, and Y = 063-16-681N in LKS92 reference system, that is about 10 km NE of the town of Pāvilosta (Fig. 4.1 and 4.2).

The site is included in this study as the upper till is snug into diamicton spherules 1–3 cm in diameter at the top of the outcrop in few meters long section (at 23,540 m) (Fig. 3.15). In the field it has been supposed that the structures are denoted by cleavage that developed either due to rotation of diamicton domains in deforming bed, as proposed by van der Meer (1997) or as a result of some post-sedimental process. To gain any additional indication about the formation of this structure, samples for thin sectioning were collected there.

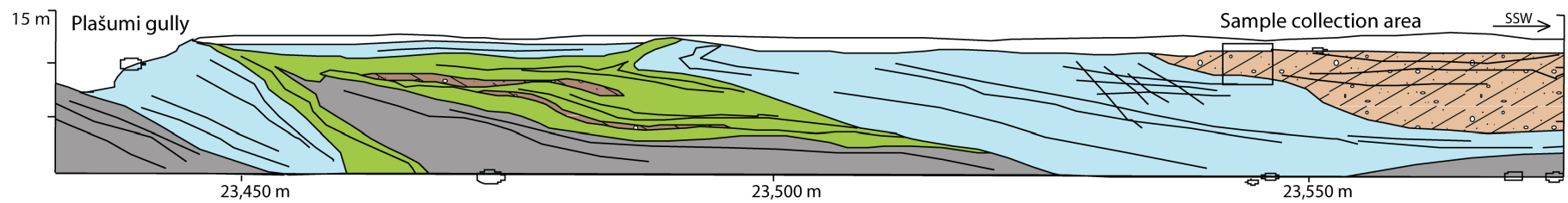
A common feature of the site is occurrence of the diapiric structures. Like in other sites, the diapirs are well pronounced apparent isometric structures. Diapirs are composed of brown silty and fine sand sediments as well as grey silt and clay. Some diapirs in this part of the cliff are composed of sandy silt and have complex deformational structures. Measurements of planar structural elements of the diapir show a slight offset of the structure in the direction close to the glacial shear direction, suggesting that after diapir formation it was deformed repeatedly due to direct glacial shearing. Some diapirs also contain more complex features, for instance, the so-called ‘mammoth trunk’ – a tilted dike structure originating from the upper part of the diapir (23,750-23,780 m). At another site (23,475 m) glaciotectonic rotation structures can be observed: silt and gravel material form concentric mélangé like structure. The outcrop sketch with indicated sample collection site is given in Fig. 3.16. The reader is redirected to the earliest works for more discussion on structural geology and stratigraphy of the site (Zelčs *et al.*, 2004).



Figure 3.15. Spherules in the upper till at the Plašumi gully site. The photograph is 15 cm high and was taken at the sample collection site, see fig. 3.16.

3.15. attēls. Sferoidāla augšējās morēnas struktūrā pie Plašumu gravas. Fotogrāfijas augstums ir 15 cm un tā tika uzņemta paraugu ievākšanas vietā, sk. 3.16. attēlu.

At the upper part of the outcrop in between diapir structures lie till sediments, which are forming lens-like beds. The preferred macrofabric orientation in the upper till is dipping predominantly to the W, with  $S_1$  values from 0.5 to 0.7 (Table 3.1).



**Legend**

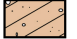



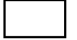


-   Till diamicton
-  Glaciofluvial sand and gravel
-  Glaciolacustrine sand
-  Debris and Holocene sediments
-  Structural elements
-  Sample collection area

Figure. 3.16. The sketch of geological structure observed at Plašumi gully site near thin section sample collection site.

3.16. attēls. Shematiska atseguma ģeoloģiskā uzbūve pie Plašumu gravas ap plānslīpējumu paraugu ievākšanas vietu.



Plant remains which are characteristic the Early and Middle Pleistocene as well as for interstadial subarctic or boreal flora (Cerina, 1999) are reported from layered sands containing at the site. The OSL age of fine-grained sand collected from this part of coastal bluffs is  $45 \pm 4.2$  ka (TL553) that is in good agreement with the OSL ages of fine-grained sand from other dating sites along the Baltic Sea cliffs of Western Latvia (Saks *et al.*, *in print*).

Table 3.1. Summary of the till fabric measurements at the Plašumi gully site (n – number of individual measurements;  $V_1$  – the mean clustering direction;  $S_1$ ,  $S_2$ ,  $S_3$  – eigenvalues)

3.1. tabula. Morēnas makrolinearitātes mērījumu pie Plašumu gravas kopsavilkums (n – individuālo mērījumu skaits;  $V_1$  – vidējais grupēšanās virziens;  $S_1$ ,  $S_2$ ,  $S_3$  – eigenvērtības)

Sample No	Description of position	n	$V_1$	$S_1$	$S_2$	$S_3$
L00	Upper till with spherules at thin section sampling spot (section position 23,540m)	60	277°/14°	0.695	0.229	0.076
L01	Basal part of upper till (section position 22,785 m)	130	292°/18°	0.533	0.327	0.140
L02	Sandy lacial diamictong and sand stretched fold below the upper till (section position 22,785 m)	104	284°/32°	0.630	0.232	0.138
L03	A melange-type sediments – mixture of gravel and dark grey silt below the upper till near rotation structure (section position 23,460 m)	100	290°/23°	0.642	0.185	0.173
L04	Upper till above banded glacial diamicton in base of upper till (section position 23,575 m)	101	186°/26°	0.502	0.344	0.154
L05	The upper part of the upper till (section position 23,895 m)	100	266°/30°	0.489	0.318	0.193

### 3.2.1. The Samples

The thin sections are prepared using non-coloured epoxy resin for impregnation, microphotographs are taken in non-polarized light, mosaic images are obtained using Photomerge technique, the large-square approach for data girding is used and the microfabric distribution statistics are plotted as data density plots (after Fisher *et al.*, 1985), and preferred orientation significance calculated assuming von Miss distribution after Davis (2002). Additionally on a latter stage the microfabric statistics was recalculated using the eigenvalue approach as suggested by Thomason and Iverson (2006).

Eight thin sections were prepared form the till with characteristic network of rectangular and spherical joints. Two microfabric aspects were studied in this case: the relationship of fractures or joints and microfabric preferred orientation and the dependence of considered grain size and apparent microfabric orientation. The boundaries of different size grains are set with step of  $2^{0.5}$  regarding the area of any grain as measured in the thin section. The grain size is expressed as A – equivalent circle diameter as used by Francus (1998).

### 3.2.2. Till micromorphology

Relatively straight vertical and horizontal as well as spherical joints are observed in thin sections. Except of one thin section no other peculiar structures on the background of massive diamicton is noted. The brief description of thin sections – the joint systems and microfabric – is given in Table 3.2. A general microfabric statistics is given in the

Appendix 5, the summary orientation of different size grains is given in Appendix 6 and visualised in Figs. 3.17 and 3.18.

In general – domain like microfabric preferred orientation is observed, with dominant moderately strong fabric in vertical sections and weak but consistent with macrofabric orientation in horizontal sections. In thin section Ps8-H a formation of authigenic minerals, likely carbonate precipitates, are observed.

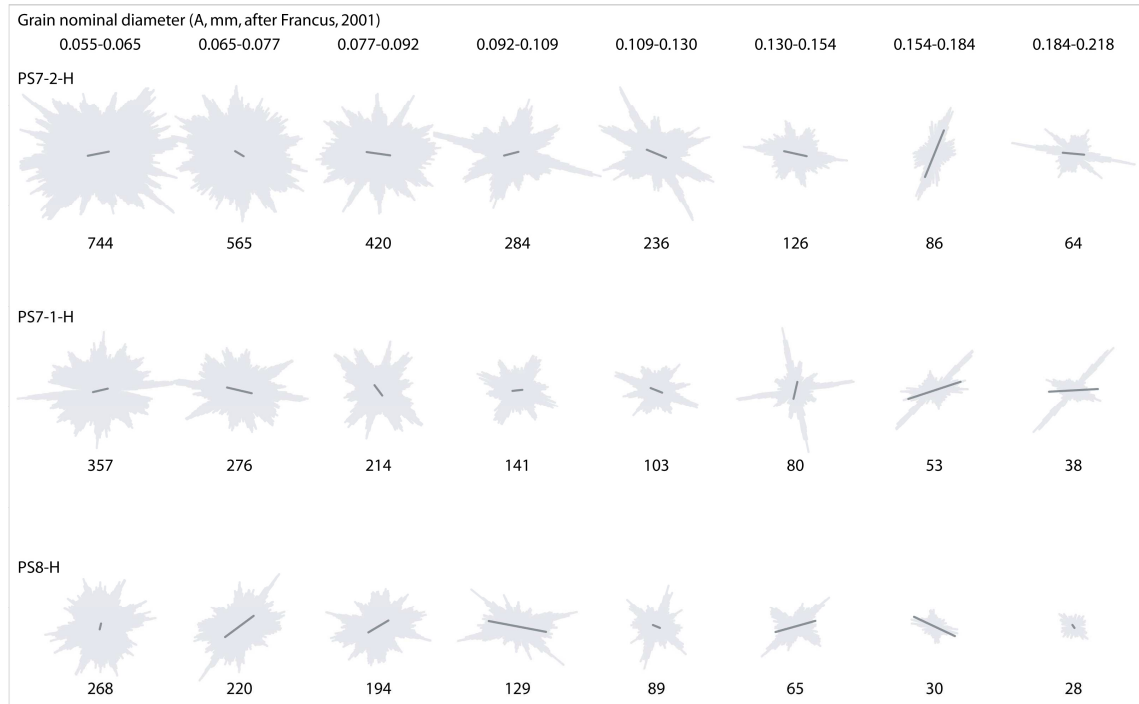


Figure. 3.17. The summary orientation data of different size classes in the horizontal thin sections from Plašumi gully site; the number beneath each diagram is the number of grains counted. The N is to the top. See Fig. 3.16 for location of the sampling site.

3.17. attēls. Dažāda izmēra smilts graudu summārā orientācija horizontālajos plānslīpējumos no Plašumu gravas; skaitlis zem katras diagrammas norāda mērījumu skaitu; ziemeļi ir uz augšu. Paraugošanas vietas izvietojumu atsegumā skat. 3.16. att.

### 3.2.3. The preferred apparent orientation of different size grains

In vertical sections usually the maximum spread of preferred orientation of different size groups is less than 20° (Appendix 6) and only in two cases the maximum spread of preferred orientation of different size groups is around 50°. There seems to be some systematic variation of preferred fabric orientation of different size groups (Fig. 3.21), but this appearance is not reliable as the fabric strength is low:  $S_1$  usually below 0.6. Particularly the size classes A from 0.065 mm to 0.077 mm and from 0.109 mm to 0.130 mm seem to have strongest deviation from average orientation to opposite directions.

The spatial distribution of microfabric in different size classes usually is similar but is not repeated exactly. Sometimes even strong orthogonal preferred orientation is observed (Fig. 3.20). At the section Ps7-1-H, in case of resolution  $R = 5.2$  mm, nearly orthogonal statistically significant microfabric is observed for size classes 0.092-0.109 mm, and 0.109-0.130 mm in one out of more than 10 grid points with sufficient number of measured grains. Similar picture is observed for thin section Ps7-1-2 in case of  $A = 0.055-0.065$  mm and  $A = 0.065-0.077$  mm. The most contrasting picture is observed in thin

section Ps7-2-H, where in size class A = 0.154-0.184 mm all five adjacent diagrams show rather strong preferred N-S orientation while in all other size classes E-W orientation is prevailing (Fig. 3.22).

### 3.2.4. The microfabric and joint system

The Plašumi gully vicinity study site was selected because of the particular globular or spherical till structure. Thin sections for the first instance were prepared to establish the relationship between the concave and straight vertical joints and the microfabric.

In the thin sections predominantly vertical and horizontal joints are observed, but the round joints (representing spherules) are rare, found only in three out of eight thin sections. This indicates relatively low numbers of spherical joints. Perhaps uncommon appearance of the spherical joints facilitates the overestimation of their proportion.

The distribution of preferred microfabric orientation does not seem to be associated with the orientation of any of the joints – nor the vertical or horizontal, nor the spherical ones. Few cases where the microfabric and joint orientation coincides seem to be coincidence rather than a rule (Fig. 3.20).

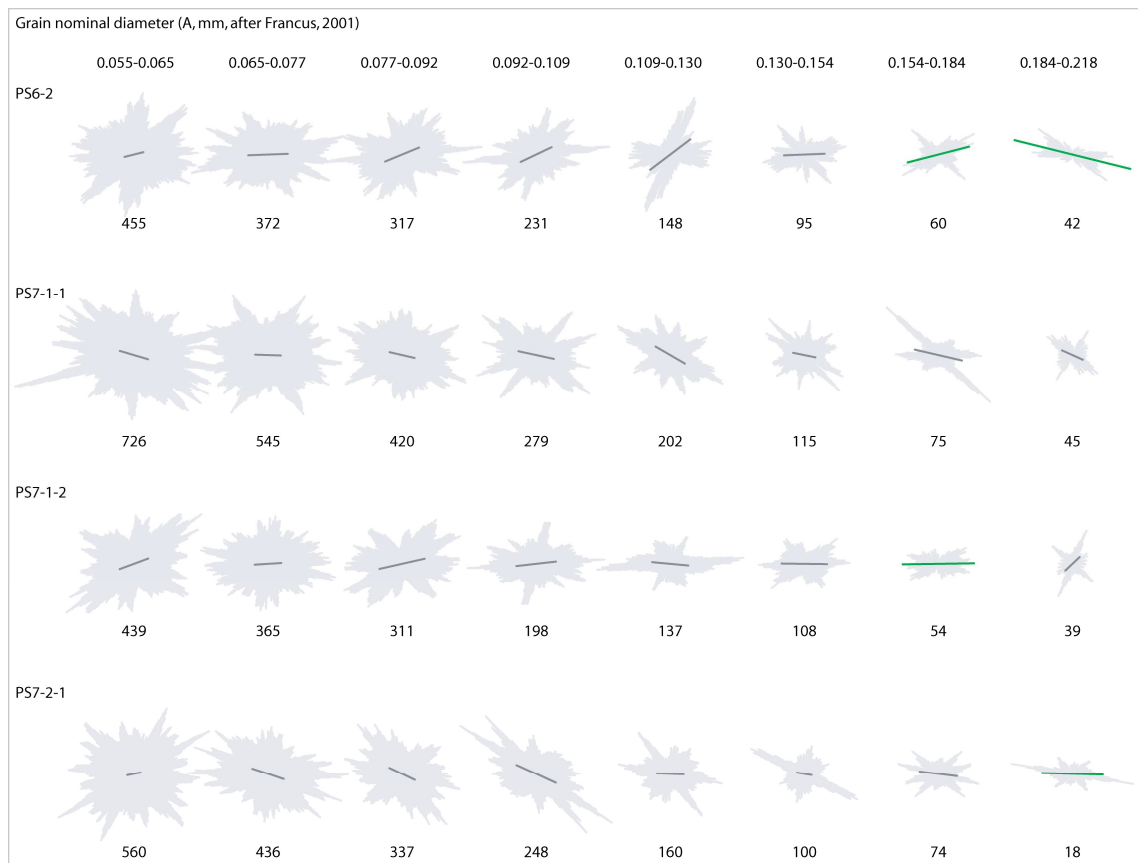


Figure. 3.18. The summary orientation data of different size classes in the vertical thin sections from the Plašumi gully site; the number beneath each diagram is the number of grains counted. See Fig. 3.16 for location of the sampling site.

3.18. attēls. Dažāda izmēra smilts graudu summārā orientācija vertikālajos plānslīpējumos no Plašumu gravas apkārtnes. Skaitlis zem diagrammas norāda mērījumu skaitu. Paraugu ievākšanas vietas izvietojumu atsegumā skat. 3.16. att.

Table 3.2. Summary description of the joint systems and microfabric in thin section samples collected at the Plašumi gully site  
3.2. tabula. Plašumu gravas atsegumā ievākto plānslīpējumu plaisu sistēmu un mikrolinearitātes apraksts

Sample No. and location	Thin section	Joints	Microfabric and micromorphology description
Ps6 Upper till near the 23,540 m costal profile mark, 2 m below the top of upper till	Ps6-1; facing N	No	The thin section quality is not suitable for automated microfabric studies
	Ps6-2; facing E	No	Microfabric is poorly developed however the subhorizontal to steeply dipping (around 45°) orientation is frequently observed in domains with statistically significant preferred orientation. Micro fabric for different grain sizes is rather different (R = 5.2 mm) sometimes statistically significant results are obtained in thin section areas where summary microfabric has no significant preferred orientation. The size fraction with equivalent circle diameter A = 0.109 mm to 0.130 mm has steeply dipping microfabric that is most different from other size classes, however, orthogonal orientation is not observed.
Ps7 Upper till near the 23,540 m costal profile mark, 1 m below the top of upper till	Ps7-1-H; facing up	Two straight joints with section angle 60° trending respectively to NNE and SWW	The general orientation of statistically significant microfabric domains is inconclusive. No direct association of joints and microfabric orientation is noted.
	Ps7-1-1; facing NE	A single horizontal joint	In general the domain-like pattern of microfabric is observed with domain size around few mm. The summary microfabric across the thin section for all size classes is subhorizontal but not statistically significant. Neither there is any grid points in R = 5.2mm resolution, where the orientation of elongated sand grains would be significantly depended on grain size. This is contrasting to horizontal thin sections where in some cases the preferred orientation is heavily depended on considered grain size.
	Ps7-1-2; facing SE	A network of vertical and horizontal orthogonal joints forming vertical brick-like structure, with joint spacing 1-2 cm, with horizontal joints ending at the intersections with vertical ones. A single circular joint with rotation radius ~1 cm, within borders of one "brick" delineated by orthogonal joints, (Fig. 3.19).	The microfabric dominant orientation is horizontal although in some domains statistically significant orientation other than subhorizontal is observed as well. It does not seem that microfabric would mimic the orientation of circular joints visible in this thin section. Summary diagrams (Fig. 3.18) shows that for all size classes microfabric is predominantly sub horizontal with better expressed preferred orientation in large size classes. In R = 5.2 mm comparing the microfabric of different size grains only one case of almost oblate statistically significant orientation between size ranges with A value 0.055 mm to 0.065 mm and 0.065 mm to 0.077 mm is observed. Taking into account the results of thin section PS7(1)2-1 it can be inferred that the microfabric in 3D is gently dipping towards the W, that is in good agreement with measured macrofabric orientation in the sampling site.

*To be continued in the next page*



<b>Sample No. and location</b>	<b>Thin section</b>	<b>Joints</b>	<b>Microfabric and micromorphology description</b>
	Ps7-2-H; facing up	Straight joints forming the sides of thin section trending towards N and NWW, and single circular joint that is not stained with iron hydroxides as the rest of joints are observed.	Any grain size when looking on the whole thin section demonstrated statistically significant preferred orientation and produced diagrams (Fig 3.17) are rather similar demonstration chaotic or multimodal distribution however the 0.154 mm to 0.184 mm size group demonstrates rather strong N-S preferred alignment that contrasts to predominately E-W orientation in al other cases. This difference is most striking when comparing the microfabric for resolution level R = 5.2mm, A = 0.154 mm to 0.184 mm, and 0.130 mm to 0.154 mm equivalent diameter where almost all grid points show rectangular microfabric (Fig. 3.20). Association of preferred microfabric orientation and joint system is not observed.
	Ps7-2-1; facing E	Two vertical joints connected with one horizontal and a circular joint with rotation radius ~2 cm between the vertical ones	The summary micro fabric orientation is sub-horizontal however only the coarsest size class (A from 0.184 to 0.218mm) with only 18 measured grains is displaying statistically significant preferred orientation.
Ps8 Upper till near the 23 540m costal profile mark, 0.4m below the top of upper till	Ps8-H; facing up	Clear joint system is not recognised, authigenic minerals are observed	There is no well developed microfabric general direction. However, the most of microfabric domains of the statistically significant preferred orientation are aligned in SWW-NEE direction. The microfabric in different scale resolutions does not repeated itself exactly, and sometimes orthogonal orientation of statistically insignificant mean alignment is observed. There is just one case from more than 10 grid points of nearly orthogonal statistically significant microfabric of different size classes (R =5.2mm, A is respectively 0.055 mm to 0.065 mm and 0.092 mm to 0.109 mm).

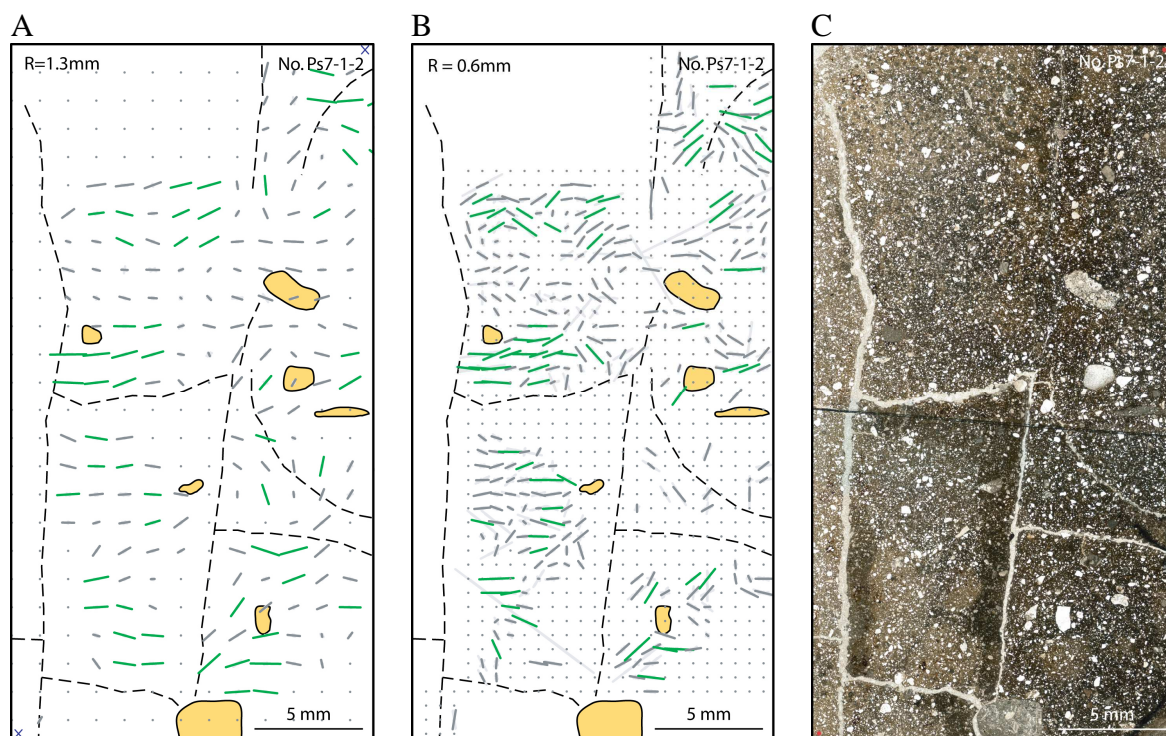


Figure 3.19. Position of joints and microfabric distribution. A and B – in the vertical thin section Ps7-1-2; C – from the upper till with spherical structure at the Plašumi gully site. The thin section is facing towards SE. Straight vertical and horizontal as well as spherical joints are observed in the section. The correlation of preferred microfabric orientation and the spherical joints is not observed. Used symbols are explained in Tables 1 and 2. See Fig. 3.16 for location of the sampling site.

3.19. attēls. Plaisu novietojums un mikrolinearitātes sadalījums. A un B – vertikālajā plānslīpējumā Ps7-1-2; C – no Plašumu gravas apkārtnes augšējās morēnas ar raksturīgu sfērisku struktūru. Plānslīpējums ir vērsts uz DA. Plānslīpējumā ir novērojamas taisnas vertikālas un horizontālas, kā arī sfēriskas plaisas. Plānslīpējumā nav konstatēta nozīmīga korelācija starp sfērisko plaisu un mikrolinearitātes dominējošo orientācijas virzieniem.

Izmantotie apzīmējumi ir paskaidroti 1. un 2. tabulās. Paraugu ievākšanas vietas izvietojumu atsegumā skat. 3.16. att.

It can be concluded that the spherical joints are not associated with processes associated to till sedimentation and deformation. It might be speculated that the desiccation of till in specific conditions could lead to formation of such a structure.

It was suggested (Stinkulis, *pers. com.*) that the spherules are formed as a result of carbonate recrystallization. Indeed on possible carbonate mineral precipitated was observed in the thin section Ps8-H; however it is unlikely that formation of such a small structures could result in development of spherical joints to extent observed.

### 3.2.5. The microfabric strength and relationship to macrofabric

At the thin section sampling spot macrofabric (elongated pebbles) is strong and unidirectional  $V_1$  dip of  $14^\circ$  to the W ( $277^\circ$ ) with three dimensional  $S_1=0.695$  and  $S_2=0.229$  (60 measurements). The dip angle probably is somewhat enhanced as a result of

simultaneous formation of diapirs as suggested by Saks et al (*accepted for publication*). The upper till macrofabric orientation in other measurement spots at this site is similar.

The apparent microfabric in general in all samples is similar (Appendix 5): in horizontal sections it has a weak E-W preferred orientation with  $S_1$  values 0.52 to 0.53; in vertical sections the microfabric is somewhat stronger ( $V_1=0.55$  to 0.56). The apparent dip angle in all cases is smaller than the  $20^\circ$  (referring to horizon), however the realistic 3D dip direction of microfabric can not be restored confidently as few studied samples give contrasting results.

Thus it can be concluded that the preferred microfabric orientation is similar to the macrofabric however much weaker than the macrofabric, especially in horizontal sections. Actually, given that the  $S_1$  value for microfabric in horizontal section is only slightly above the indication of random orientation – 0.5 – it is surprisingly that in all three cases the preferred microfabric orientation is in E-W direction and deviating less than  $20^\circ$  from thin section to thin section. It can be speculated that the microfabric in this site is strongly disturbed by some small-scale post-sedimentational process that left macrofabric largely intact.

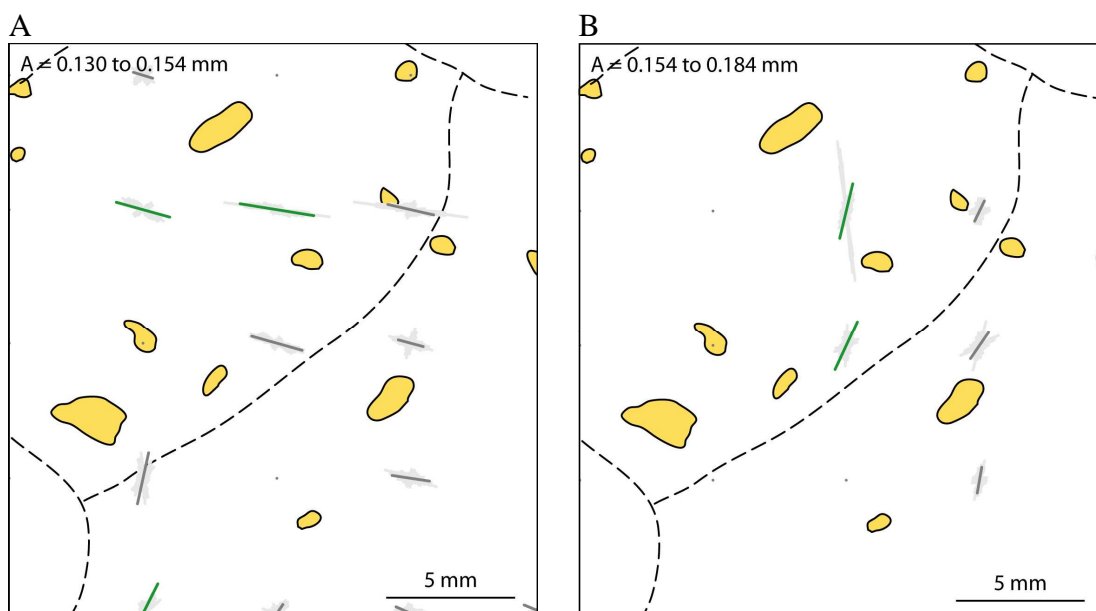


Figure 3.20. Comparison of the preferred orientation of the apparent microfabric in two neighbouring size classes – A and B – in horizontal thin section Ps7-2-H. The north is to the top of the image, the grid resolution –  $R=5.2$  mm. Note almost orthogonal microfabric differences in the central part of the image. Such distribution is an exception rather than a rule. Used symbols are explained in tables 1 and 2. See Fig. 4.1.8. for location of the sampling site.

3.20. attēls. Dominējošā mikrolinearitātes orientācijas virziena salīdzinājums divās līdzās esošās smilts graudu izmēru klasēs – A un B – horizontālajā plānslīpējumā Ps7-2-H, ziemeļi attēlā ir uz augšu, režģa izšķirtspēja –  $R=5,2$  mm. Ievērojiet gandrīz perpendikulāro mikrolinearitātes dominējošo virzienu attēla vidusdaļā. Šāds mikrolinearitātes sadalījums drīzāk ir izņēmums, nevis likumsakarība. Izmantotie apzīmējumi ir paskaidroti 1. un 2. tabulās. Paraugu ievākšanas vietas izvietojumu atsegumā skat. 3.16. att.

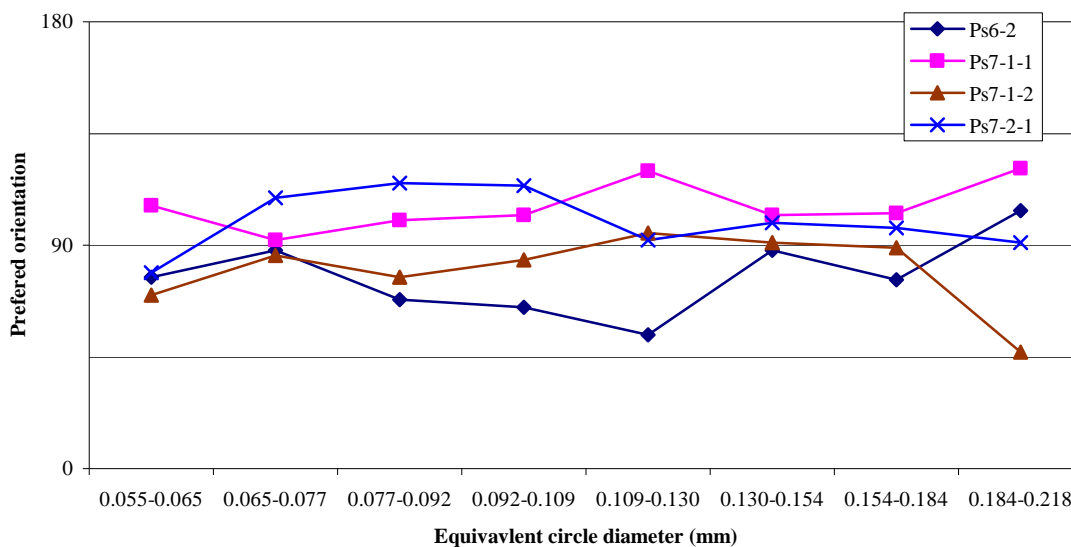


Figure 3.21. The preferred orientation of different size grains as observed in the vertical thin sections from samples collected at the Plašumi gully site. See Fig. 3.16 for location of the sampling site.

3.21. attēls. Dažādu izmēru smilts graudu šķietamā orientācija vertikālajos plānslīpējumos no paraugiem, kas ievākti Plašumu gravas apkārtnē. Paraugu ievākšanas vietas izvietojumu atsegumā skat. 3.16. att.

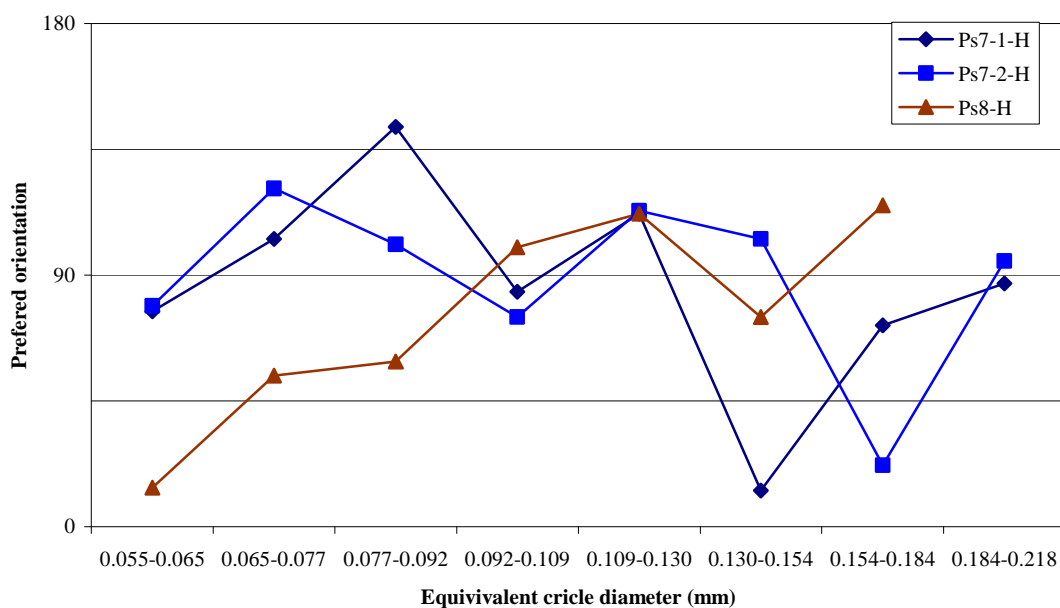


Figure 3.22. The preferred orientation of different size grains as observed in horizontal thin sections from samples collected at the Plašumi gully site. See Fig. 3.16 for location of the sampling site.

3.22. attēls. Dažādu izmēru smilts graudu šķietamā orientācija horizontālajos plānslīpējumos no paraugiem, kas ievākti Plašumu gravas apkārtnē. Paraugu ievākšanas vietas izvietojumu atsegumā skat. 3.16. att.

### 3.3. Strante site

The cliff section at Strante is located on the Baltic Ice Lake plain, approximately 5.0 km ENE of the town of Pāvilsta. The geographical coordinates of Strante site are X = 003-32-100E, and Y = 063-11-500N in LKS92 reference system. Here the maximum elevation of the plain is ca. 15 m. Glacial and glaciolacustrine sediments of the Middle Weichselian through the Late Weichselian age in places are overlain by a thin cover of younger glaciolacustrine and aeolian sediments, and occasional boulder pavements are outcropped in a distance of 0.6 km (Saks *et al.*, 2004). At the northern and southern flanks of the outcrop deformed sedimentary strata is overthrust by the series of till sheets. The thrusting surfaces are indicated by sandy stringers in the till (see Saks *et al.*, *accepted for publication* for more details).

Large portion of the section is built up by even 6 m thick, well consolidated sandy diamicton that contains fine grained sand, silt and occasional gravel grains (Fig. 3.23). This diamicton forms almost 120 m wide spans of the outcrop. Distinct planar foliation is traced within the diamicton and near diapir structures it becomes slightly bended. Rounded clasts of unconsolidated laminate sediments with signs of rotation are occasionally found within certain levels of sandy diamictone (Fig. 3.24). Preferred orientation of elongated gravel grains (macrofabric) due to very low gravel contents was done over 30 m long distance of the outcrop. The resultant preferred orientation has weak maxima in the NNE-SSW ( $n = 101$ ;  $S_1 = 0.393$   $V_1 = 268^\circ/35^\circ$ ) which is in good agreement with overall glacier movement directions in this area (Gaigalas *et al.*, 1967; Zelčs, Markots, 2004; Boulton *et al.*, 2001a). At the base of the sandy diamicton fine sand and coarse silt sediments are deformed into traction folds and rotation structures with dextral (top to the left) shear sense.



Figure 3.23. The sand rich overconsolidate diamicton interpreted as local deformation till at the Strante site. The stick at the hands of author is 5.0 m long. The location of the image is approximately at the 30,700 m profile mark indicated in the figure 3.25.

3.23. attēls. Smilšains, spēcīgi konsolidētais diamiktons Strantes atsegumā, kas ir interpretēts, kā lokāla deformācijas morēna. Lata autora rokās ir 5,0 m gara. Fotografija ir uzņemta aptuveni pie 30 700 m garkrasta profila atzīmes, kas ir norādīta 3.25. attēlā.





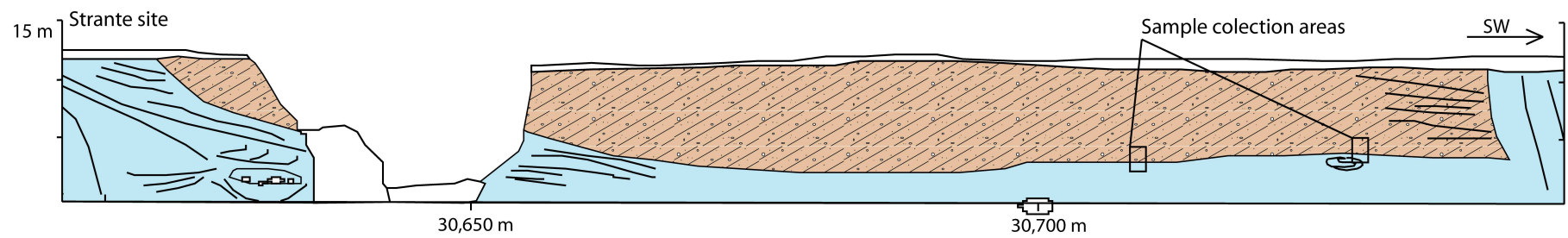
Figure 3.24. A soft sediment inclusion with signs of rotation and shearing in the sandy diamicton at the Strante site. The handle of knife is some 10 cm long. The structure was observed near 30,660 m profile mark indicated in the Fig. 3.25.

3.24. attēls. Nekonsolidētu nogulumu ieslēgums ar rotācijas un bīdes pazīmēm smiltšainajā diamiktonā Strantes atsegumā. Naža spals ir aptuveni 10 cm garš. Struktūra tika novērota aptuveni pie 30 660 m garkrasta profila atzīmes, kas ir norādīta 3.25. attēlā.

The origin of sandy diamicton was sedimentological clue: glaciolacustrine sedimentary processes as well as glaciotectonic origin was proposed (O. Āboltniņš, pers comm., 2003). To supplement ordinary field description a set of thin sections were prepared from these sediments. After several sessions of the fieldwork and considering the results of micromorphological investigation this unit is interpreted as a glaciotectonite, as described in Benn and Evans (1996) or deformation till according to Dreimanis (1989), Saks *et al.* (*accepted for publication*).

### 3.3.1. The samples

A set of four samples forming vertical profile was collected from the sandy diamicton assumed as the local deformation till, and the deformed sediments at its base at the 30,730 m of the coastal profile. Two additional samples are included in the study collected at the 30,710 m of the costal profile (Fig. 3.25). The samples are listed and shortly described as well as the summary microfabric statistics presented in the Appendix 7. The general statistics of the orientation of different-sized grains are summarised in the Appendix 8.



**Legend**

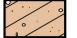



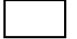


-   Till diamicton
-  Glaciofluvial sand and gravel
-  Glaciolacustrine sand
-  Debris and Holocene sediments
-  Structural elements
-  Sample collection area

Figure 3.25. Geological structure with indication of thin section sample collection places at the Strante site.

3.25. attēls. Strantes atseguma ģeoloģiskais griezum ar norādi uz plānslīpējumu paraugu ievākšanas vietām.

The thin sections are prepared both using non-coloured epoxy resin and coloured resin for impregnation. Microphotographs are taken in cross-polarized light and in some cases with plain light; mosaic images are obtained using Photomerge technique in the initial stage of the study and using “buffer lines” in a latter stage; the large-square approach for data grid is used and the microfabric distribution statistics are plotted as data density plots (after Fisehr *et al.*, 1985) and preferred orientation significance calculated according the eigenvalues method suggested by Thomson and Iverson (2006).

### 3.3.2. The summary preferred microfabric orientation

In all except one vertical sections two-modal nearly orthogonal preferred microfabric orientation is observed, and subhorizontal mode is the dominant one (Fig. 3.26). The exception is section No.5n-1 that comes from macroscopically deformed fine sand – coarse silt sediments below the considered sandy diamicton and thus represents a different sediment unit. In most sections the two modes are observed in all resolution levels (see Fig. 3.27), indicating that the bimodal distribution is not the product of combination of several pronounced preferred orientation domains, but rather is an intrinsic property of the microfabric preferred orientation of the sandy diamicton. Two-modal fabric is observed in the data sets obtained by different methods as well and is not observed in horizontal sections so the possibility that it is an artefact of the image processing can be excluded.

Due to bimodal nature of the microfabric neither  $V_1$  (summary orientation) nor  $S_1$  (fabric strength) correctly describe the microfabric data set as the statistical procedure used is designed for von Miss (unimodal, normal) distribution. As a result in most cases the eigenvalue statistics does represent the preferred orientation ( $V_1$ ) of the strongest mode but the fabric strength indication ( $S_1$ ) is not reliable.

In most of the horizontal sections rather weak microfabric ( $S_1 < 0.6$ ) trending in E – W direction is observed (Appendix 7). This coincides with the macrofabric orientation of the sandy diamicton ( $V_1 = 268^\circ$ ;  $S_1 = 0.393$ ;  $n = 101$ ). It must be noted, that due to very low gravel content in the sandy diamicton, macrofabric was measured across outcrop distance of nearly 80 m and likely is biased towards the orientation normal to the outcrop surface (e.g. Klein, 2002), that it is to the E – W direction.

The sample No. 5n, collected from the macroscopically deformed sediments at the base of the sandy diamicton, has the strongest observed microfabric. Often strongest microfabric is common in the sediments with most homogeneous grain size that is the case with this sample as well. Additionally the deformation porches, possibly, enhanced the initial sedimentary fabric, resulting in extremely strong microfabric.

### 3.3.3. The preferred orientation of different-size grains

Some variations of the preferred orientation and fabric strength of different size grains are observed, but the spread of dominant orientation rarely exceeds  $45^\circ$  (Appendix 8, Fig. 3.28).

It must be noted, that due to different image acquisition techniques (micro-photographing in plain or cross-polarised light), differed thin section thickness, variations of digital image exposure and thresholding levels, the grain size classes does not exactly mach for different thin sections as the grain boundaries because of mentioned factors may slightly migrate.



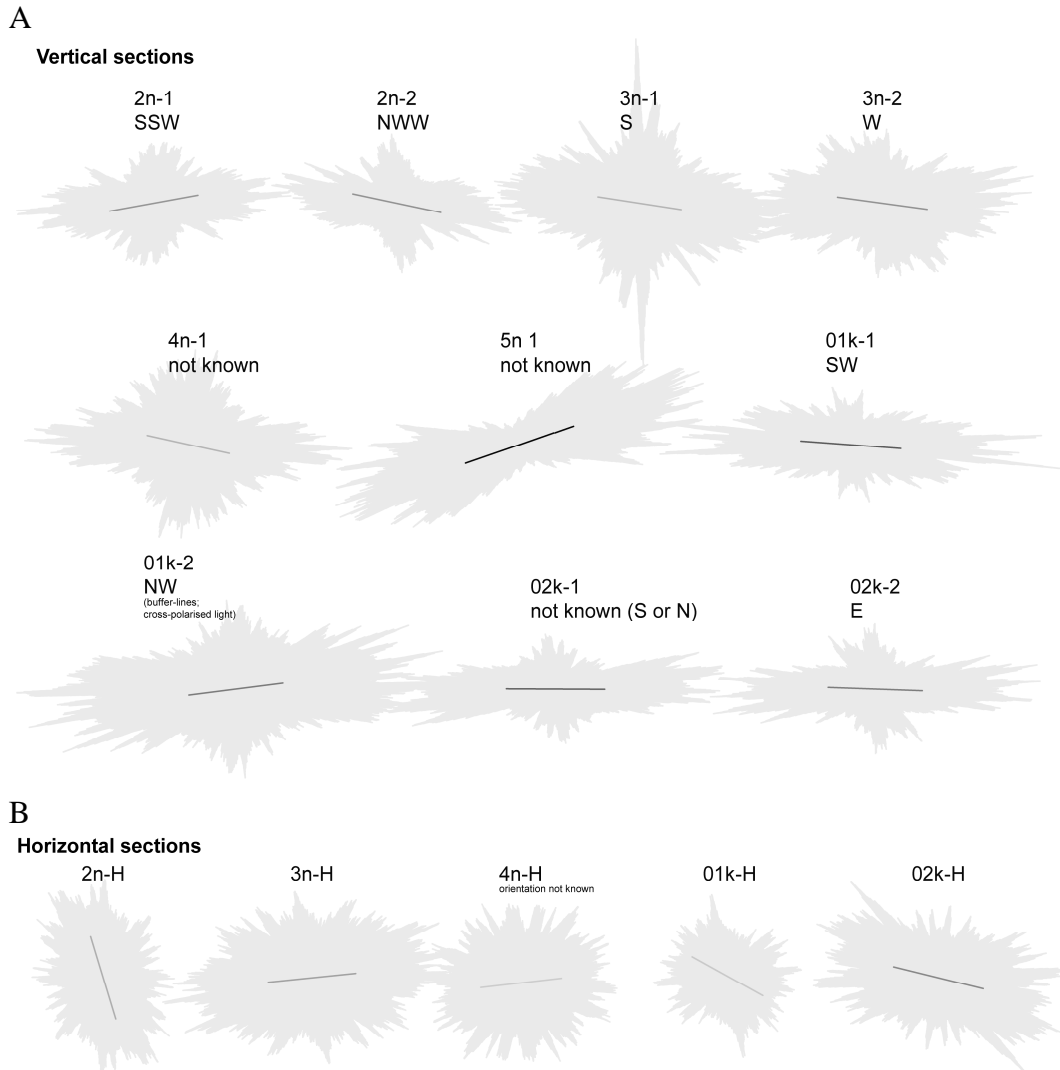


Figure 3.26. The summary microfabric preferred orientation in vertical (A) and horizontal (B) thin sections of the sandy diamicton at the Strante site. The number of measured grains in any diagram is at least 1000. The facing direction of the vertical sections is indicated below the section number; the orientation of the diagrams of horizontal sections is corrected so that the north is at the top. Note the two nearly orthogonal modes in almost all vertical sections and none in horizontal sections. Symbols are explained in Table 2.

3.26. attēls. Kopējā mikrolinearitātes orientācija vertikālos (A) un horizontālos (B) plānslīpējumos, kas izgatavoti no Strantes atseguma smilšainā diamiktona. Katrā diagrammā ir iekļauti ne mazāk kā 1000 graudu garenasu mērījumi. Vertikālo plānslīpējumu vērsums ir norādīts zem parauga numura, horizontālo plānslīpējumu diagrammu augša ir vērsta uz Z. Gandrīz visu vertikālo plānslīpējumu diagrammās ir novērojami divi, gandrīz ortogonāli mikrolinearitātes maksimumi, kas savukārt nav novērojami horizontālo plānslīpējumu diagrammās. Izmantotie apzīmējumi ir paskaidroti 2. tabulā.

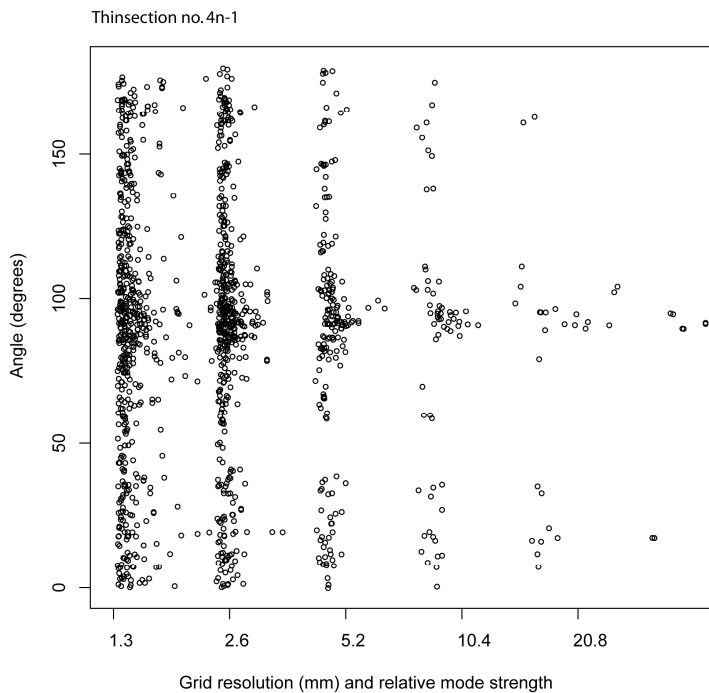


Figure 3.27. The orientation of microfabric modes, indicated on the vertical axis and their relative strength indicated on the horizontal axis of all diagrams in different grid resolutions grouped along horizontal axis in the thin section No.4n-1. The bimodal nature of the fabric distribution that is not manifested in a set of the summary orientation calculated according to eigenvalue method (Appendix 7 and 8). An orientation mode in here is defined as a mean direction of the sector in a diagram where data density exceeds 1 standard deviation for given diagram and modes that are less than  $15^\circ$  apart are merged together. The mode strength is defined as maximum data density with given mode.

3.27. attēls. Mikrolinearitātes modu orientācija uz vertikālās ass un to relatīvā izteiktība uz horizontālās ass visās diagrammās ar dažādiem režģa soļiem, kas ir grupēti pa vertikālo asi, plānslīpējumā Nr. 4n-1. Attēlā labi parādās mikrolinearitātes orientācijas bimodālā daba, kas nav redzama aprēķinot summāro orientāciju, izmantojot eigenvektoru paņēmieni (7. un 8. pielikumi). Šeit orientācijas moda ir definēta kā vidējais dominējošās orientācijas virziens diagrammas sektorā, kur datu blīvums pārsniedz vienu standartnovirzi šai diagrammai un modas, kas ir tuvāk kā  $15^\circ$ , ir sapludinātas kopā. Modas relatīvā izteiktība ir definēta, kā maksimālais datu blīvums dotajā modā.

Largest fabric strength variations in vertical sections are due to the relative strength variations of subvertical and sub-horizontal modes in different grain size fractions. These variations significantly affect the preferred orientation in only two vertical sections (Nos. 3n-1 and 4n-1) where the maximum spread of summary orientation approaches  $45^\circ$ .

In vertical section trend is observed that the bimodal distribution is more pronounced for largest grain sizes (Fig. 3.29). However it is difficult to assess whether this is due to clearer visualisation as a result of smaller numbers of grains and more precise fabric measurement for the largest grains or general trend towards stronger fabric for the largest grains noted elsewhere. The summary orientation is deviating from subhorizontal for medium to large grain size fractions in some sections and rarely in the fine-grained fractions. This is the result of stronger subvertical mode and there seems to be a trend that largest grains have better expressed subvertical mode.

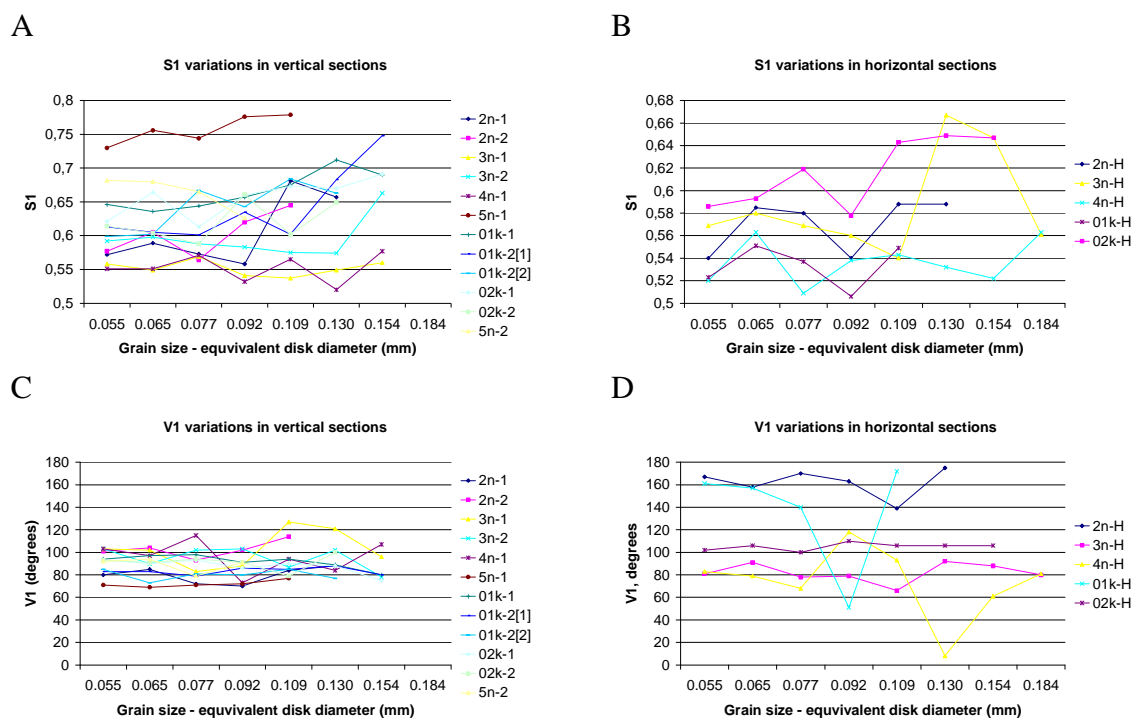


Figure 3.28. The microfabric preferred orientation (A and B) and respective fabric strength (C and D) for vertical and horizontal sections. Fabric strengthening for the largest grains and fabric strength minimum at 0.092 mm to 0.109 mm equivalent disk diameter for the horizontal section is noticeable. No systematic variations of the dominant orientation direction are noted.

3.28. attēls. Mikrolinearitātes dominējošais orientācijas virziens (A un B) un atbilstošā linearitātes izteiktība (D un C) vertikālajos un horizontālajos plānslīpējumos. Attēlos iespējams novērot linearitātes izteiktības pieaugumu virzienā no mazākajiem uz lielākajiem graudiem un izteiktības minimumu horizontālajiem plānslīpējumiem no 0,092 mm līdz 0,109 mm ekvivalenta diska diametra klasē. Dominējošā orientācijas virziena sistemātiskas novirzes nav novērotas.

In general the preferred orientation of different size grains in the horizontal section is more variable than in the vertical ones (Fig. 3.28). There are two horizontal sections (Nos. 4n-H and 01k-H) with large spread (up to 90°) of preferred summary orientation of different size grains. This is likely due to lower fabric strength in the horizontal sections.

In a background of the increasing fabric strength for the large grains in prominent 3 out of 5 horizontal sections a fabric strength minimum is observed at the grain size range of equivalent disk diameter 0.092 mm to 0.109 mm that corresponds to the extreme values of dominant orientation (Fig. 3.28). A similar trend is not observed in the vertical sections.

### 3.3.4. The spatial distribution of microfabric

Two microfabric spatial distribution patterns can be identified in the vertical sections: (1) fold-like distribution and (2) rather uniform bimodal distribution with local variations due to interplay of subhorizontal – subvertical mode strength.

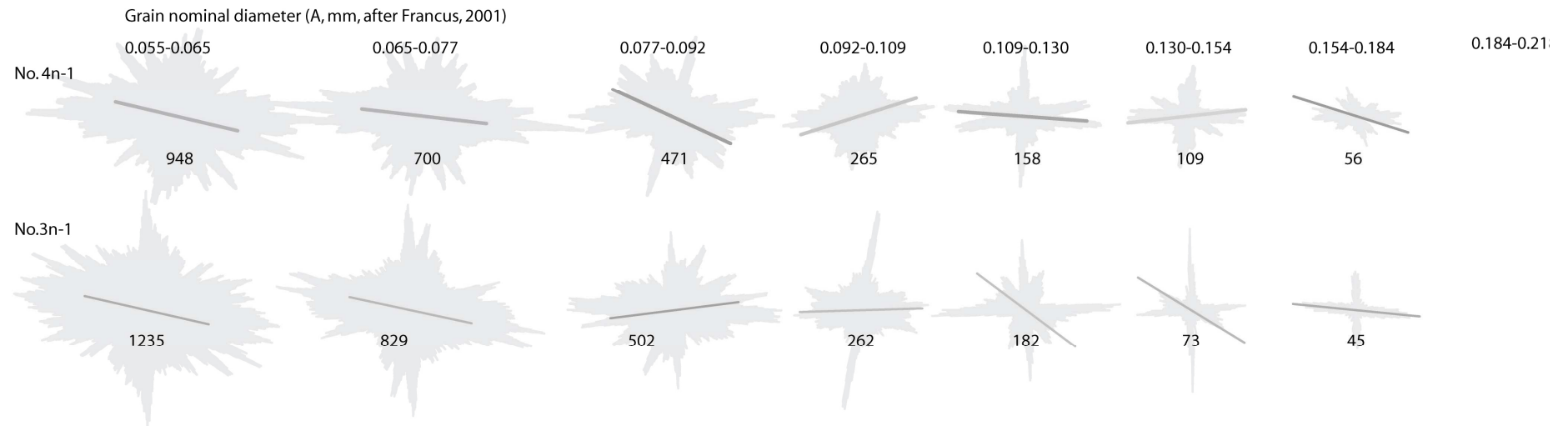


Figure 3.29. The summary orientation of different size grains in samples Nos. 3n-1 and 4n-1 from the sandy diamicton at the Strante site. A trend is observed that two orthogonal modes are more pronounced for larges grains. Used symbols are explained in Table 2.

3.29. attēls. Kopējā dažāda izmēra smilts graudu orientācija plānslīpējumos Nr. 3n-1 un 4n-1, kas izgatavoti no Strantes atseguma smilšainā diamiktona. Ir iespējams novērot tendenci, ka lielākajiem graudiem divas ortogonālās modas ir izteiktākas, salīdzinot ar mazākajiem graudiem. Izmantotie apzīmējumi ir paskaidroti 2. tabulā.

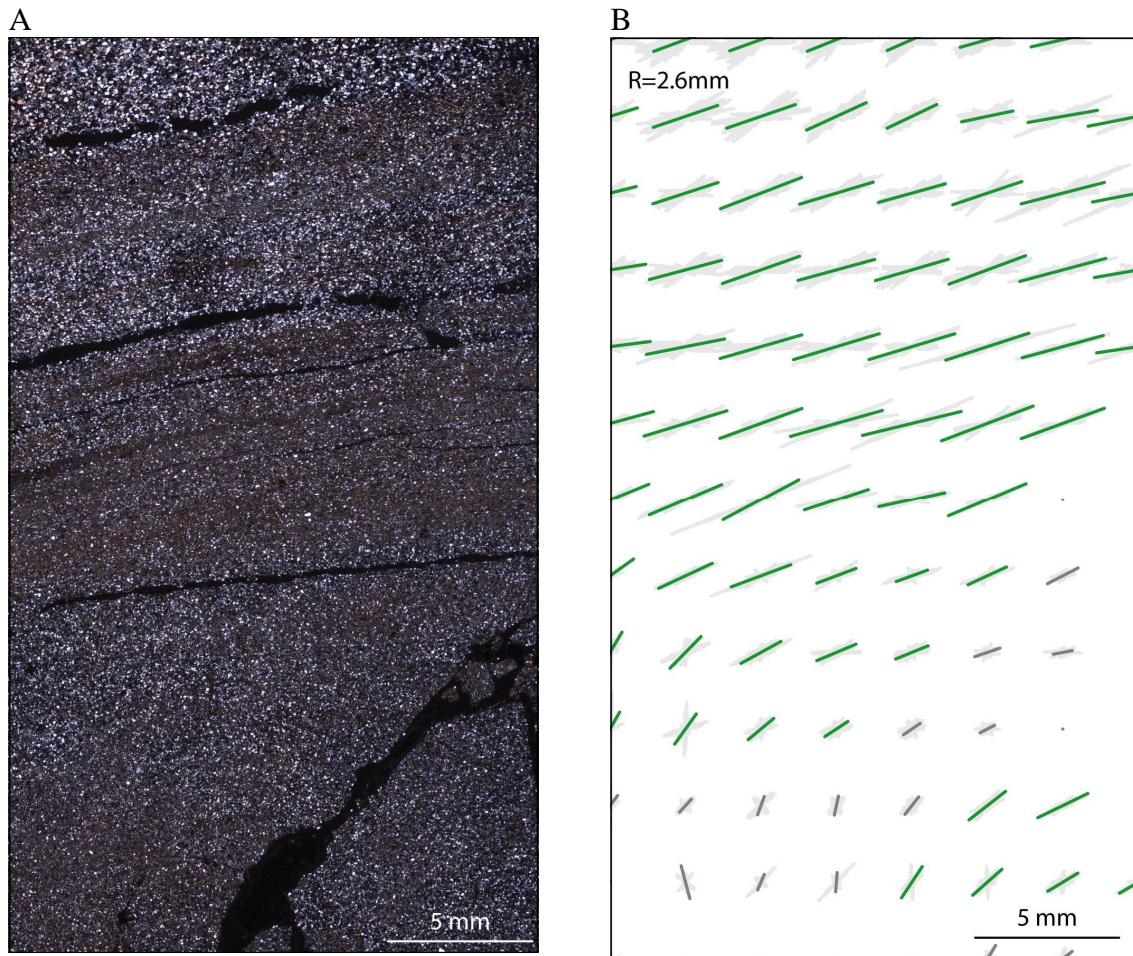
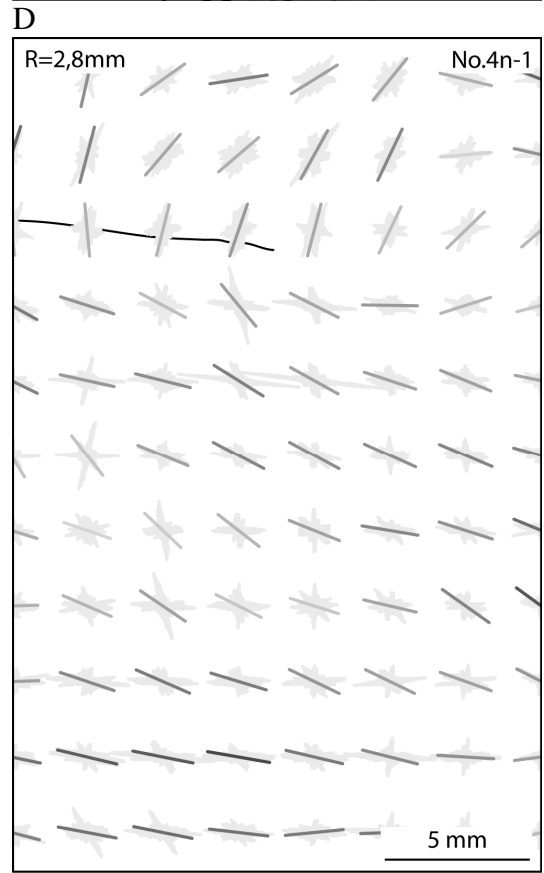
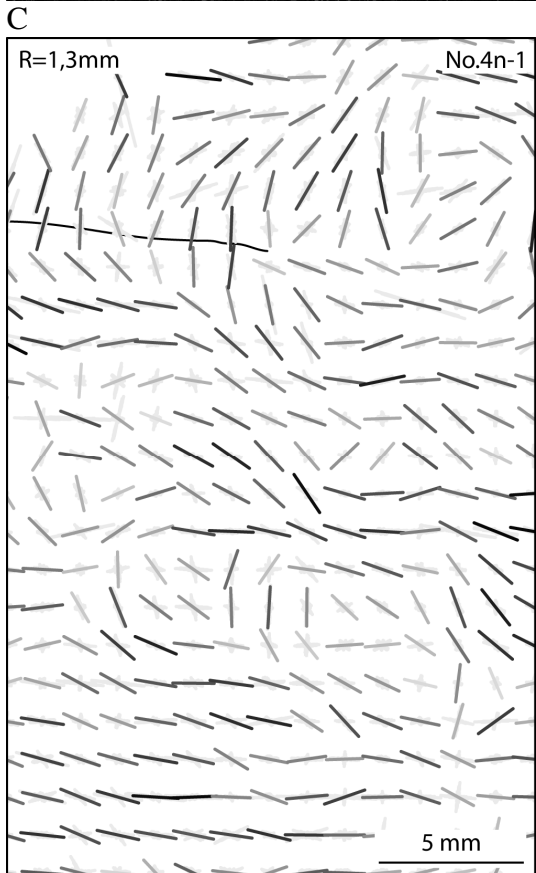
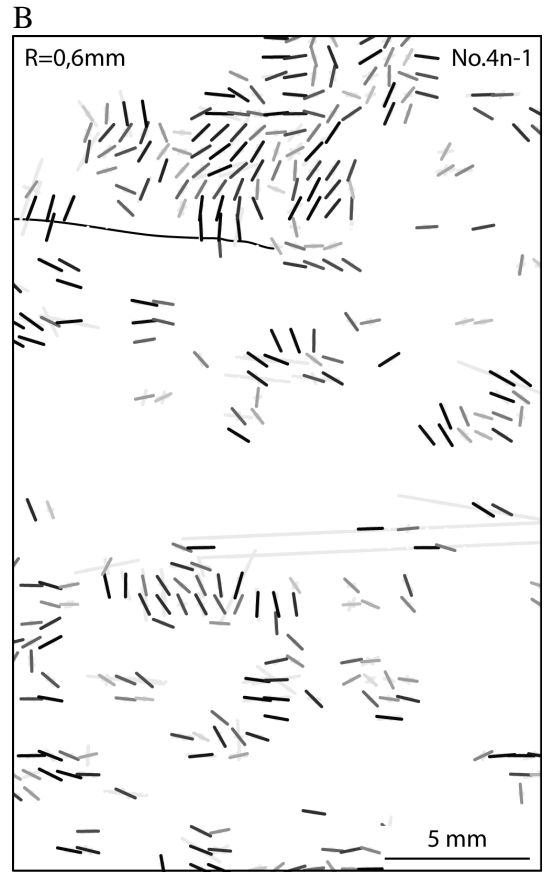
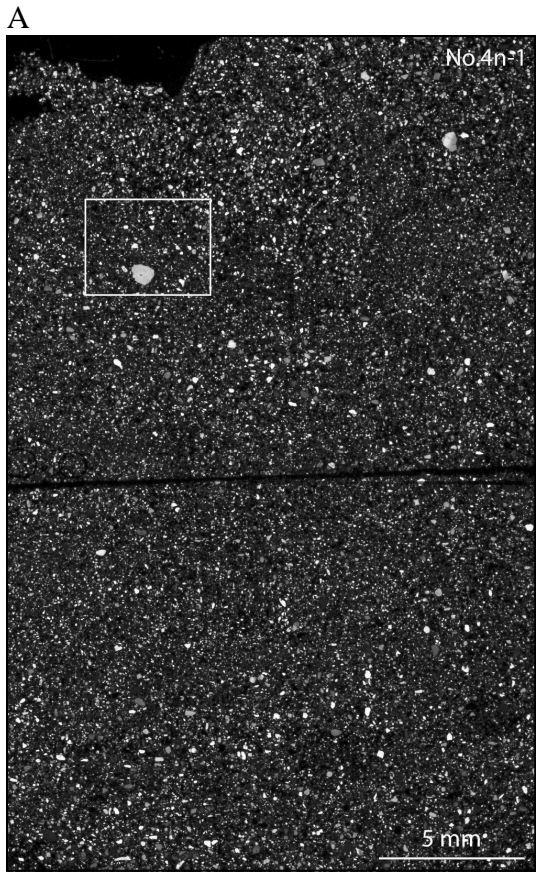


Figure 3.30. Microfabric in the deformed sandy silt sediments below the sandy diamicton at the Strante site, sample No. 5n-1: A – thin section microphotograph acquired with cross-polarised light; B – respective microfabric distribution. Observe the fold like distribution of microfabric in lower, homogeneous part of thin section that is probably formed due to reorientation of primary sedimentary microfabric during the deformation. Used symbols are explained in Table 2.

Attēls 3.30. Mikrolinearitāte deformētajos smilšaina aleirīta nogulumos, kas atrodas zem smilšainā diamiktona Strantes atsegumā (plānslīpējums Nr. 5n-1): A – plānslīpējumu attēls krustiski polarizētā gaismā; B – atbilstošais mikrolinearitātes sadalījums. Ievērojiet krokasveida mikrolineariātes sadalījumu apakšējā, homogēnajā plānslīpējuma daļā, kas domājams ir veidojies deformācijas rezultātā, kuras laikā tika pārorientēta primārā sedimentācijas mikrolinearitāte. Izmantotie apzīmējumi ir paskaidroti 2. tabulā.

The first case is observed in sections Nos. 4n-1 and 5n-1. The second case is observed in sections Nos. 01k-1, 01k-2, 02k-2, 2n-2 and 3n-2 with horizontal mode being the strongest one, and in thin sections Nos. 02k-2, 2n-1 and 3n-1 where strength of the subvertical mode is comparable to the strength of the horizontal one.

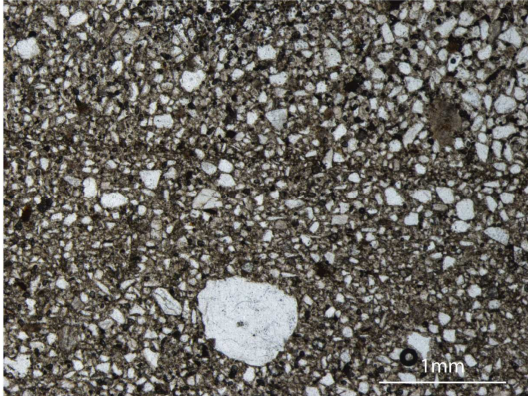
Microfabric parallel to the lamination visible in macroscale as well as in thin section is observed in section No. 5n-1. In the homogenous lower part of this thin section microfabric denotes fold-like structure (Fig. 3.30). This sample is from the macroscopically deformed sediments at the base of the sandy diamicton. The microfabric likely formed due to plastic sediment deformation, particularly – extension at the upper part of the section, and is superimposed on the sedimentational fabric.



*To be continued in the next page*



E



**Figure 3.31.** Microfabric distribution in the thin section No. 4n-1 from the lower part of the sandy diamicton: A – thin section microphotograph acquired with cross-polarised light; B, C and D – respective microfabric distribution with different grid resolution; E – close up view of the outlined square in image A. Domain-like distribution of preferred grain orientation is visible in case of grid resolution  $R = 0.6$  mm (B), but fold-like distribution emerges in case of grid resolution  $R = 1.3$ mm (C) and  $R = 2.6$  mm (D), that probably represents fine deformation structures in the sediments. The black line in images B, C and D indicates a possible plane of brittle rupture that does not affected microfabric distribution significantly, with close-up view in image E. Note that the microfabric distribution in images B is calculated with minimum number of measurements at the single grid point set to 10 that is too little for reliable estimation of preferred orientation strength. Used symbols are explained in Table 2.

**3.31. attēls.** Mikrolinearitātes sadalījumus plānslīpējumu Nr. 4n-1 no smilšainā diamiktona apakšējās daļas: A – plānslīpējumu attēls krustiski polarizētā gaisām; B, C un D – atbilstošais mikrolinearitātes sadalījums ar atšķirīgu režģa soli; E – pietuvināts skats A attēlā izzīmētajam laukumam. Gadījumā ar mazu režģa soli  $R = 0,6$  mm (B) ir redzams domēnu tipa mikrolinearitātes sadalījums, bet palielinot režģa soli (C un D) parādās krokveida mikrolinearitātes sadalījumus, kas domājams atspoguļo maza izmēra nogulumu deformācijas struktūras. Melnā līnija B, C un D attēlos norāda iespējamo trauša pārrāvuma plakni, kas nav būtiski ietekmējusi mikrolinearitātes sadalījumu, kas ir palielināta E attēlā. Mikrolinearitātes orientācija attēlos B aprēķināta katrā diagrammā iekļaujot ne mazāk kā 10 mērījumus, kas nav pietiekams liels skaits, lai ticami novērtētu linearitātes izteiktību. Izmantotie apzīmējumi ir paskaidroti 2. tabulā.

In the sample No. 4n-1 fold-like microfabric distribution is observed (Fig. 3.31). This sample was collected just above the base of the sandy diamicton. Probably at the base of the base of sandy diamicton traction folds developed and as a result fold-like microfabric deformation is observed in the thin section.

Foliation of the sandy diamicton that is detected in the field can also be observed in some thin sections either as laminas with increased content of the fines or bands of large concentration of the coarse sand grains. For example a foliation or attenuated fold structures are observed in thin section No. 01k-2, and the microfabric preferred orientation is partially coinciding with lamination.

In horizontal sections a domain-like microfabric distribution is observed with domain size just few mm. The exception is thin section No. 2n-H (figure 3.32) and to a lesser extent thin section No. In the vertical section of the same sample No. 2n microfabric distribution that could be connected to the microfabric distribution in the section No. 2n-H

is not noted. Similar but less pronounced distribution is observed in the thin section No. 02k-H, where half of the thin section has rather strong and uniform fabric (occasionally  $S_1 > 0.7$ ) trending approximately from N to S. The other half has less consistent and generally weaker ( $S_1 < 0.6$ ), with summary orientation in NE-SW. The summary preferred orientation in the section is at the right angle towards the dominant orientation in the most of other horizontal sections. In the vertical section of the same sample No. 2n microfabric distribution that could be connected to the microfabric distribution in the section no.2n-H is not noted. Similar but less pronounced distribution is observed in the section no.02k-H.

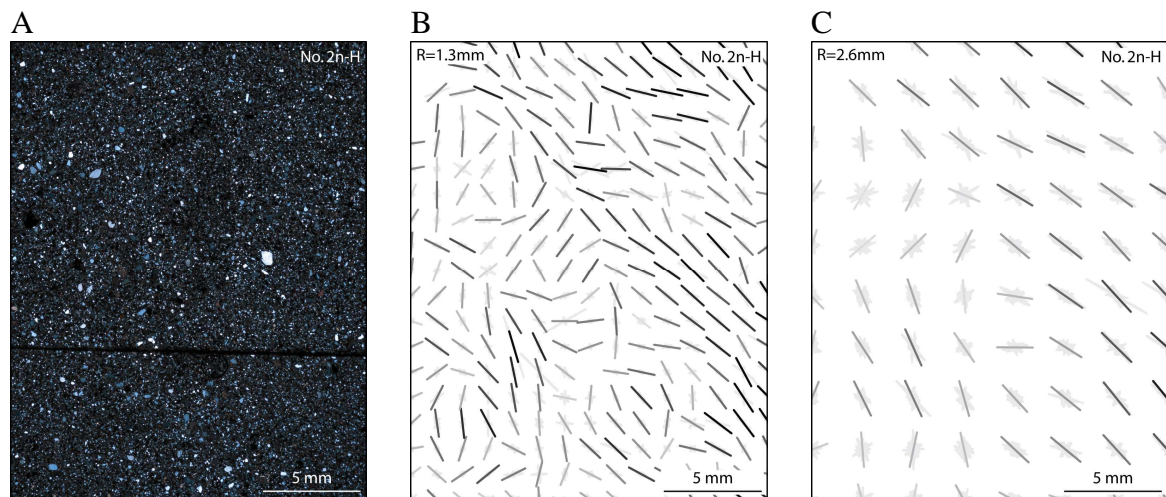


Figure 3.32. The horizontal thin section No. 2n-H: A – thin section microphotograph acquired with cross-polarised light; B and C – respective microfabric distribution with different grid resolution. Two distinct orientation domains are evident. The image top is to the  $330^\circ$ . Note that the microfabric distribution in images B are calculated with minimum number of measurements at the single grid point set to 10 that is too little for reliable estimation of preferred orientation strength. Used symbols are explained in Table 2.

3.32. attēls. Horizontālais plānslīpējums Nr. 2n-H: A – plānslīpējumu attēls krustiski polarizētā gaismā; B un C – atbilstošais mikrolinearitātes sadalījums ar atšķirīgu režģa soli. Divi krasi atšķirīgi orientācijas domēni ir redzami attēlos. Attēla augša ir vērsta uz  $330^\circ$ . Mikrolinearitātes orientācija attēlos B aprēķināta katrā diagrammā iekļaujot ne mazāk kā 10 mērījumus, kas nav pietiekams liels skaits, lai ticami novērtētu linearitātes izteiktību. Izmantotie apzīmējumi ir paskaidroti 2. tabulā.

In several cases feature that can be described as “glace ceiling” is noticed: a large number of diagrams from the same thin section with rather wide distribution of  $V_1$  values show fabric strength ( $S_1$ ) values up to certain level and very few or non diagram has higher  $S_1$  value (Fig. 3.33, Appendix 8). The  $S_1$  value for ceiling usually is close to 0.7. The origin of such distribution is not clear but it might be related to the maximum value of the shear deformation that the sediments have been subjected to. Alternatively the bimodal preferred orientation nature might preclude the  $S_1$  values for any single diagram to exceed the threshold value or the noise introduced by the data acquisition plays a role.



### 3.3.5. Grain shape considerations

Crude grain shape analysis was done using a stereomicroscope in order to assess the effects of the grain shape influence on the apparent microfabric. Three categories of grain shapes were defined: (1) isometric, (2) elongated, and (3) oblate (disk-shaped) grains respectively. Based on 199 counts, the size fraction 0.1-0.125 mm of the sandy diamicton consists of two thirds (68%) isometric grains, 16% of elongated and 16% – oblate grains.

Roughly 50% to 55% of all objects automatically measured and corresponding to the selected size criterion (125 to 2000 pixels or 0.055 mm to 0.220 mm equivalent disk diameter) have elongation ratio large than 1.5. This proportion, given the fundamental differences in estimation methods, is similar to the estimated summary proportion of elongated and oblate grains in the considered sediments. The large proportion of the apparently elongated grains in the thin sections most likely is a result using of the different methods. It must be noted that in case of thin sections the sample size is usually several thousand of sand grains.

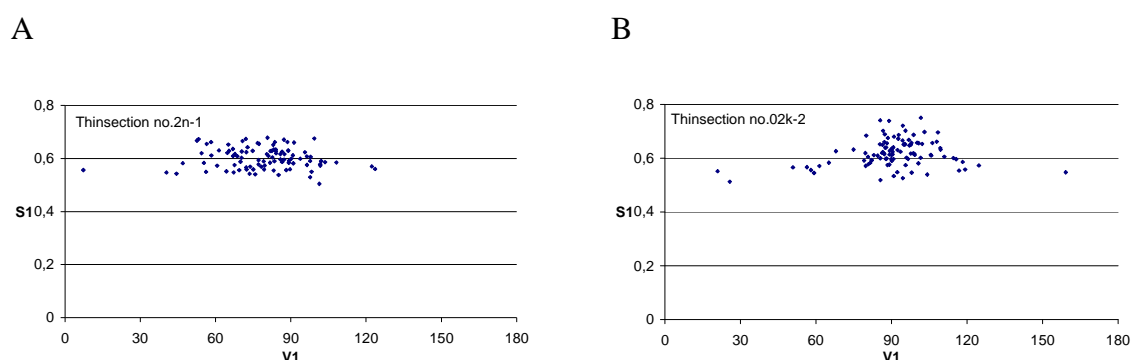


Figure 3.33. An example of the microfabric distribution with “glass ceiling” in the thin section No. 2n-1 (A); normal microfabric strength distribution in the thin section No. 02k-2 (B) in a case of grid resolution  $R = 2.6$  mm.

3.33. attēls. Mikrolinearitātes sadalījuma piemērs ar „stikla griestiem” plānslīpējumā Nr. 2n-1 (A) un normālais sadalījums plānslīpējumā Nr. 02k-2 (B), ar režģa soli  $R = 2,6$  mm.

If most of the oblate grains will lie in the horizontal plane as expected in a simplest case then in the horizontal sections compared to the vertical ones smaller proportion of measured grains will be apparently elongated. Indeed, in the vertical sections the average proportion of measured objects with elongation ratio larger than 1.5 is 54% (standard deviation,  $SD = 2.1$ ; 12 thin sections) comparing to around 50% ( $SD = 2.3$ ; 5 thin sections) in the horizontal thin sections. This slight difference might be of random origin, e.g. determined by thin section quality or measurement method. However if it is not an artefact of measurement inaccuracy, it supports the assumption that some part of oblate particles are lying in the horizontal plane, thus contributing to the fabric measured in vertical sections and not contributing to the fabric measured in horizontal sections.

The position of the oblate grains in the subhorizontal plane is supported by findings of Li *et al.* (2006) whose studies of the macrofabric of the glacial deposits in the Upper Urmi River valley, Tian Shan, China indicate that clast a-b planes have stronger fabric than the a-axis fabric.

### 3.4. Sensala site

The major Sensala site description and results of the paleo-glaciological studies are given in paper Saks *et al.* (2008). The Sensala site is located 10 km southwest of the town of Ventspils (Fig. 3.34). The geographical coordinates of Sensala site are approximately X = 003-46-100E, and Y = 063-44-900N in LKS92 reference system. It forms the northernmost stretch of the chain of the coastal bluffs along of the Baltic Sea coast of Western Latvia. Up to 18 m high coastal bluffs at Sensala provide insight into Pleistocene glacial and non-glacial deposits for about a distance of 3.5 km.

The exposed Quaternary sequence comprises six distinct lithofacies: (1) dark-greenish grey silt, (2) pinkish grey-fine grained sand with silt interbeds, (3) contorted lenses of sand and gravel, (4) lower and (5) upper till units, and (6) a continuous layer of sand and gravel. Glacioaquatic and marine deposits, as well as two different till units are encountered at the outcrop (Fig. 3.34).

Dark-greenish grey massive silt composes diapirs and partially overthrust slabs. On the faulting planes silt has been mixed with diamicton. The silt has a breccia-like microscale structure with angular to subrounded dark silt domains resting in a lighter colour matrix.

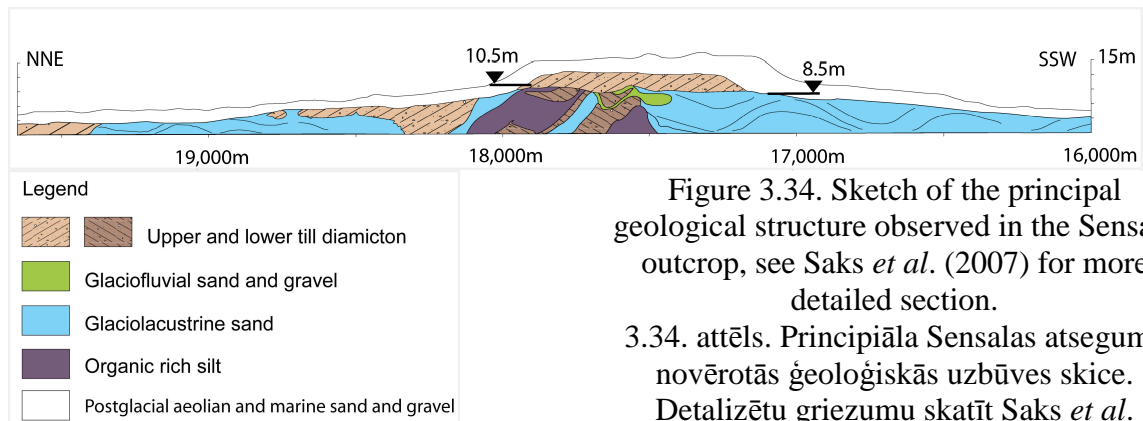


Figure 3.34. Sketch of the principal geological structure observed in the Sensala outcrop, see Saks *et al.* (2007) for more detailed section.

3.34. attēls. Principiāla Sensalas atsegumā novērotās ģeoloģiskās uzbūves skice. Detalizētu griezumu skatīt Saks *et al.* (2007).

Pinkish grey fine-grained sands is commonly present in the lowest part of the outcrop, particularly on either side of the complexly deformed and dark-greenish grey silt cored diapir at the central part of the section. The sediment sequence has a rhythmic structure with up to 1 m thick fine-grained sandy layers interbedded by approximately 20 cm thick silty material. Occasionally also brownish clay interbeds are found in the sand strata. In some layers wave current ripples, liquidification and water escape structures are common. Commonly fine-grained sand is deformed into 20 to 40 m long and up to a few m high gentle folds.

Sand wedge structures were found cutting through glaciotectonic structures. According to French and Guglielmin (2000) such structures indicate that the sediment surface has been exposed to a cold and dry non-glacial environment.

According to OSL dates, the fine grained sands were deposited around 40 ka BP. The OSL age for samples TL 501, TL 502 and TL 503 was determined as  $43 \pm 5.0$  ka,  $45 \pm 7.7$  ka and  $44 \pm 10$  ka accordingly (Saks *et al.*, 2007). A similar age of fine-grained sand

was obtained in three other places 20 to 40 km S, SW of the Sensala site (Saks *et al.*, *in print*).

Up to 20 m long and 5 m thick patches of intensively folded and distorted sand and gravel were observed in the highest part of the section. In most cases this unit overlaps both above-considered lithofacies.

Two types of diamicton are observed in the glaciotectonically contorted sequence: the lowermost loose and sandy diamicton considered as waterlain or flow till, and the upper one clay-rich diamicton resembling basal till. Pieces of these tills are also observed below the silt slab. Drag casts and folds and several tens of centimetres thick layers of very silty diamicton are observed on the contact of silt and diamicton revealing that the silt slab was dragged over the till.

The upper till unit is up to 4 m thick, continuous dark olive-grey diamicton – interpreted as basal till. Occasionally several metres long and a few millimetres to several centimetres thick sand or silt intercalations (stringers) are observed. Deformation of the till layer implies active glacier movement after deposition of the till. In places the uppermost part of the lower basal till has banded structure. Drag folds and boudinage structures are observed along with other minor shear zone structures and it is evident that the diamicton acted as more competent material

The mapping of the elevation of the upper till surface in the vicinity of the outcrop revealed a 500 m wide and almost 4 m high ridge stretching from W to E. The ridge stretches perpendicular to the main stress direction as shown by a glaciotectonic structure analysis at the outcrop. The outcrop itself intersects the ridge approximately under 80-100° angle. The most pronounced deformation with the deepest décollement surface is in the northern side of the outcrop. The décollement line gradually rises in the southern direction. The maximum thickness of till also occurs along the deepest deformation layer.

The section is covered by continuous layer of sand and gravel or fine sand. These are postglacial near shore nearshore sediments, in some places is covered by eolian sand with buried soil horizons.

The axis of folds and gravel grain fabric in the core of folds are oriented predominately in the NW-SE direction, suggesting NE – SW glacial stress direction. The décollement line of dynamic structures rises from NE to SW, suggesting a decrease of glacial stress to SW. The stretched nature of folds and the presence of augen-like structures indicate that folding was due to the drag of a moving glacier rather than lateral stress. Therefore it can be concluded that fold orientation represents the local direction of the ice movement.

Measurements of till macrofabric show inconclusive results with preferred orientation in W-E as well as N-S direction, however the strongest fabric ( $S_1$  values) are for diagrams with W-E preferred orientation (Table 4.11).

Saks *et al.* (2007) explained the formation of this complex situation as follows:

- 1) The silty sand sediments were deposited on top of fine grained basin sediments Middle Weichselian time;
- 2) At the ice margin water lain and flow till sequence formed;
- 3) Advancement of glacier and sole deformation forming diapir-like structures and folds;
- 4) Deposition of the upper till unit with stress direction different from that of previous phase;
- 5) Repeated deformation of the upper till layer imposing shearing structures and reorientation of till fabric.

During deglaciation in Western Latvia large Baltic ice stream split in to several ice lobes that terminate in smaller glacier tongues (Zelčs, Markots, 2004). The advance of

the tongues in the first phases occurred through several ice flows, which protruded into the terrain, and deformed the soft glacier bed. Evidently, the Sensala outcrop reflects the remains of an ice marginal formation – a lateral moraine. During glacier propagation all frontal topographic features were removed but the radial patterns as lateral moraines are partly preserved.

Glacier dynamics in the area have been mostly controlled by glacier bed rheology, which resulted in an assemblage of specific glacier landforms and glaciotectonic features (Saks *et al.*, 2007): overridden, partly preserved lateral moraine lineation and its unidirectional stress pattern, and diapiric structures formed at the glacier margin. From the outcrop studies it is concluded that since the glacier started to advance it became soon decoupled from the glacier bed, and the shear zone developed near the glacier bed. The upper till was deposited continuously, but the glacier was still active also after deposition of the till as in several places a comparatively thicker shear zone was developed in the till layer.

Table 3.3 Summary of till fabric measurements at Sensala site (n – number of individual measurements;  $V_1$  – the mean clustering direction;  $S_1, S_2, S_3$  – eigenvalues)

3.3. tabula. Sensalas atsegumā oļu garenasu mērījumu rezultātu apkopojums (n – individuālo mērījumu skaits;  $V_1$  – vidējais grupēšanās virziens;  $S_1, S_2, S_3$  – eigenvērtības)

Sample No.	Description of position	n	$V_1$	$S_1$	$S_2$	$S_3$
080	Upper till, at section position -17,443 m, stone-rich diamicton connected to sand-gravel lens in the upper till	60	308°/21°	0.487	0.339	0.174
009	Upper till, at section position -17,600 m	31	285°/21°	0.742	0.204	0.054
074	Upper till, at section position -17,600 m	100	256°/9°	0.618	0.285	0.097
013	Water-lain till, at section position -17,745 m	30	338°	0.659	0.245	0.096
045	Upper till, at section position -17,745 m, near palaeoslump structure of the till, at the middle of 4 m thick till unit	80	354°/24°	0.492	0.392	0.116
047	Upper till, at section position -17,805 m	70	160°/4°	0.587	0.305	0.108
029	Upper till, at section position -17,885 m	30	265°/14°	0.529	0.345	0.126
022	Upper till, at section position -17,925 m	31	272°/19°	0.751	0.184	0.068
077	Dark grey till unit at low laying outcrop 1.5 km to N of centrals Sensala outcrop - 19,600 m	62	287°/0°	0.646	0.213	0.141

### 3.4.1. The samples

Sample for thin section preparation from the upper till are collected near the till macrofabric measurement sites (samples Nos. 072, 076b, 071 at -17,600 m of coastal profile) or sandy interbeds in the upper till (samples Nos. 043, 044 at -17,550 m of coastal profile, and Nos. 091, 092 at -17,685 m of coastal profile). Two samples (Nos. 017 and 042) collected from lower, waterlain till at the Sensala site are included in this study as well.

The thin sections are prepared both using non-coloured epoxy resin but in some cases dyed resin is used for impregnation; microphotographs are taken in cross-polarized light and in some cases with plain light; mosaic images are obtained using Photomerge technique as well as the using “buffer lines” to separate individual images; the large-square approach for data girding is used and the macrofabric distribution statistics are plotted as

data density plots (after Fisehr *et al.*, 1985) and preferred orientation significance calculated according the eigenvalues method suggested by Thomson and Iverson (2006). The summary microfabric measurement results are presented in Appendix 9.

### 3.4.2. Upper till, samples Nos. 043 and 044

Samples Nos. 043 and 044 are taken from the middle part of the upper till bed, near the -17,550 m mark at the Sensala site. The samples are prepared using non-coloured impregnation epoxy resin and microfabric data are acquired using thin section images acquired with crossed polarised light. The eigenvalue method is used for calculation the microfabric statistics.

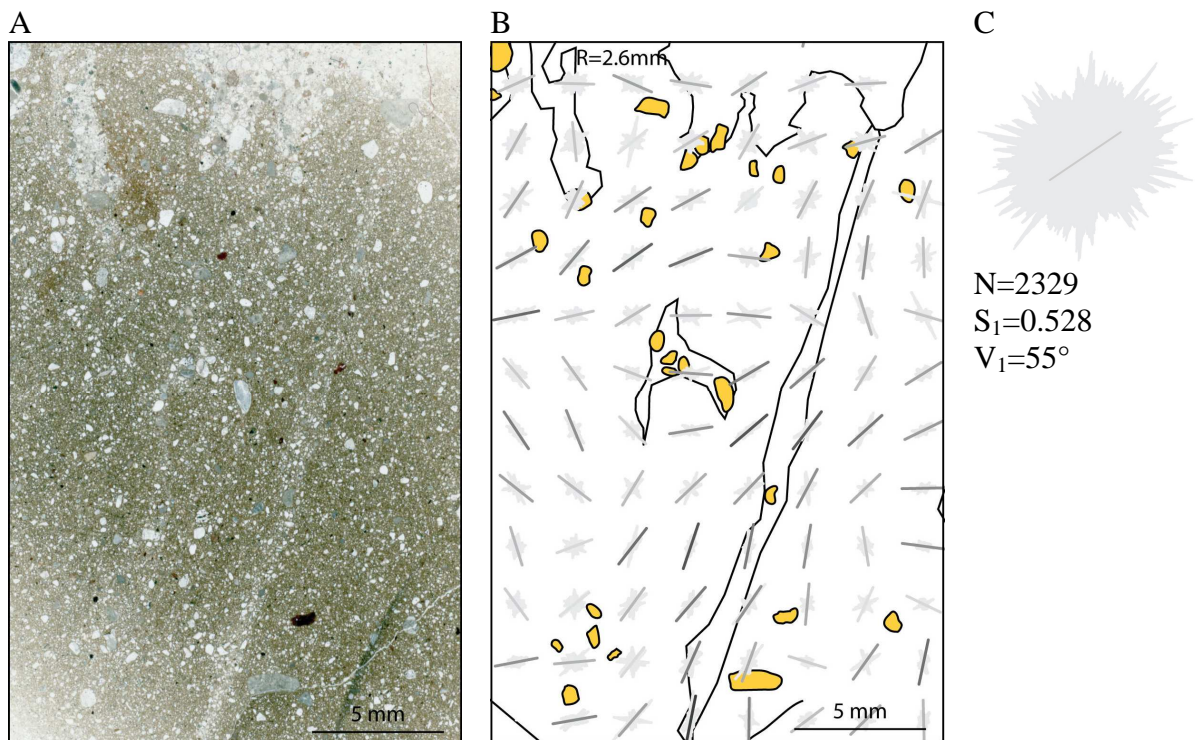


Figure 3.35. An image of horizontal thin section No. 043-1(H): A – scanned thin section image; B – microfabric distribution with grid resolution  $R = 2.6$  mm calculated according to eigenvalue method; C – summary microfabric orientation across the thin section calculated according to eigenvector method. The top of the image is to the N. Note the rather chaotic, domain-like preferred orientation with small proportion of strong fabric (indicated by the dark colour of summary orientation lines). The low  $S_1$  value for summary orientation indicates very weak fabric. Used symbols are explained in Tables 1 and 2.

3.35. attēls. Horizontālā plānslīpējuma Nr. 043-1(H) attēls: A – skenēts plānslīpējuma attēls; B – mikrolinearitātes sadalījums pie režģa izšķirtspējas  $R = 2.6$  mm aprēķināts izmantojot eigenvektoru paņēmieni; C – mikrolinearitātes summārā orientācijā visam plānslīpējuma laukumam, aprēķināta izmantojot eigenvektoru paņēmieni. Visos attēlos uz augšu ir ziemeļi. Ievērojiet visai haotisko domēnu tipa mikrolinearitātes sadalījumu B attēlā ar nelielu labi izteiktas linearitātes (tumšas summārās orientācijas līnijas) īpatsvaru. Zemā  $S_1$  vērtība C attēlā norāda uz ļoti vāji izteiktu linearitāti. Izmantotie apzīmējumi ir paskaidroti 1. un 2. tabulās.



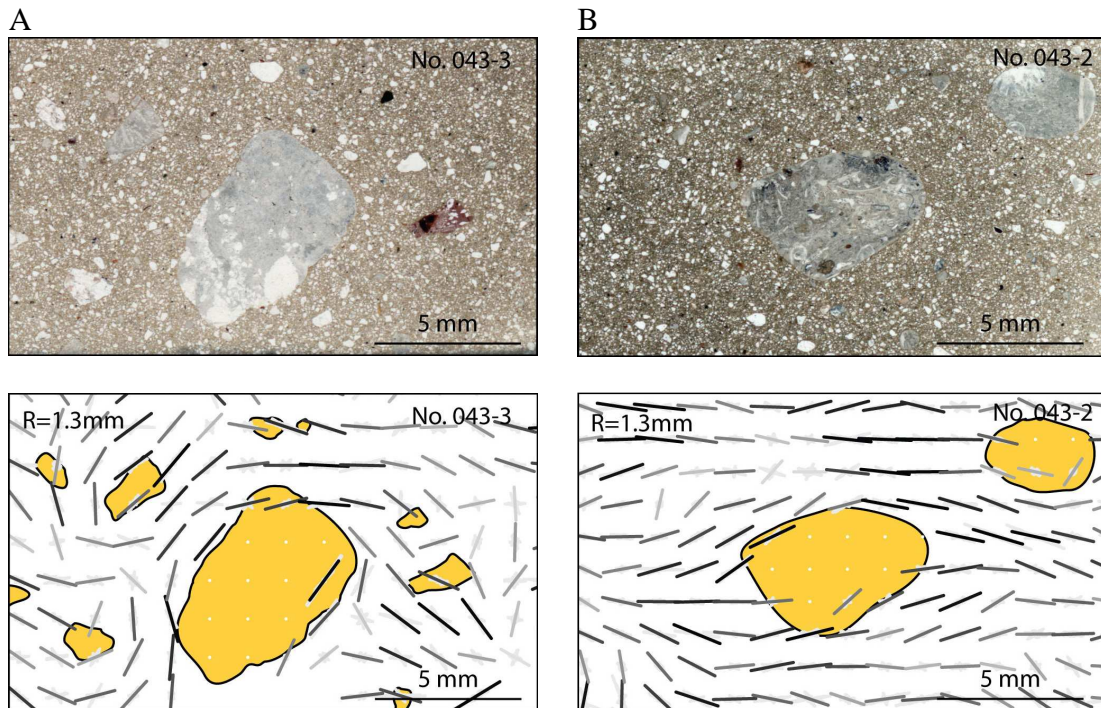


Figure 3.36. Two contrasting modes of microfabric distribution around gravel grain: A – circular microfabric arrangement around a gravel grain; B – microfabric gently bending around a gravel grain. Both thin sections are vertical, facing in the E direction and prepared from one sample. In the first case (A) gravel grain presumably has rotated, forming circular structure; in the second case (B) stable gravel grain position is suggested. Note that the microfabric distribution is calculated with minimum number of measurements at the single grid point set to 10 that is too little for reliable estimation of preferred orientation strength. Used symbols are explained in Tables 1 and 2.

3.36. attēls. Attēlā parādīti divi atšķirīgi mikrolinearitātes apliekšanās veidi ap grants graudu: (A) – mikrolinearitātes apļveida sakārtojums ap grants graudu; (B) – mikrolinearitāte apliecas ap grants graudu. Abi plānslīpējumi ir vertikāli un vērstu uz austrumiem. Pirmajā gadījumā (A) grants grauds, iespējams, ir rotējies veidojot apļveida struktūru, savukārt otrajā gadījumā (B), domājams, grants grauds atradās stabilā stāvoklī. Mikrolinearitātes orientācija ir aprēķināta katrā diagrammā iekļaujot ne mazāk kā 10 mērījumus, kas nav pietiekams liels skaits, lai ticami novērtētu linearitātes izteiktību. Izmantotie apzīmējumi ir paskaidroti 1. un 2. tabulās.

A single horizontal thin section is prepared from sample No. 044. The summary microfabric is extremely weak ( $S_1 = 0.532$ ;  $V_1 = 54^\circ$ ), however in grid resolution  $R = 2.6$  mm locally microfabric strength  $S_1$  is above 0.7 and  $V_1$  direction is around  $60^\circ$ . A well expressed domain like pattern is observed.

In the horizontal section of sample No. 043 weak preferred orientations is observed unfortunately only the N direction for the section is known. Well pronounced linear zone of coarse sand grains is present, that can be interpreted as marking direction of ice local movement or deformation during the till deposition (Fig. 3.35). The average microfabric strength  $S_1$  is only slightly above 0.5, indicating very weak fabric forming around  $30^\circ$  with the orientation of sand stringer observed in the thin section. The fabric

strength is low in individual domains as well – in grid resolution  $R = 2.6$  mm, the  $S_1$  value for individual diagrams in no case reaches 0.7 and typically is below 0.6 (Appendix 9).

The microfabric in the horizontal sections of both samples seems to coincide, being extremely weak and trending somewhere in the NE-SW direction.

Subhorizontal, moderately strong ( $S_1 = 0.613$  and  $0.557$ ) microfabric is observed in both vertical sections of sample No. 043. However, there is remarkable difference between microfabric arrangements around a gravel grain in both sections (Fig. 3.36): in one case gravel grain rotation is inferred; in the other – sediment compaction or gravel grain steady-state position in sheared till are the likely mechanisms of microfabric distribution formation. Both thin sections are facing to the E and the observation indicates that both rotation and steady-state position – sliding – of gravel grains in tills can occur simultaneously.

A microfabric distribution in fine resolution that resembles a water escape structure or microscale thrust in thin section No. 043-2 is observed (Fig. 3.37). Such structure can be produced as a result of minor till deformation and is compatible with observed microfabric distribution around gravel grains (Fig. 3.36).

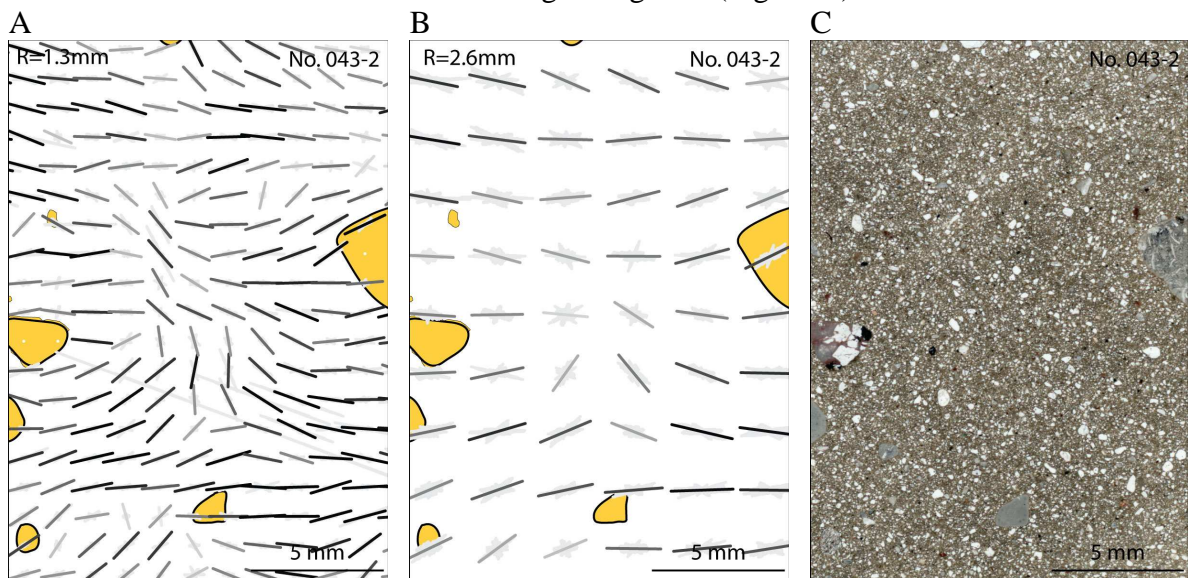


Figure 3.37. A microfabric distribution that resembles water escape structure or minor thrust in thin section No. 043-2 is evident in case of fine resolution of microfabric visualisation (A), barely identifiable in large resolution (B), and not seen in the scanned thin section image. Note that the microfabric distribution in image A is calculated with minimum number of measurements at the single grid point set to 10 that is too little for reliable estimation of preferred orientation strength. Used symbols are explained in Tables 1 and 2.

3.37. attēls. Plānslīpējumā Nr. 043-2 novērotais mikrolinearitātes sadalījums, kas līdzinās atūdeņošanās struktūrai vai mikromēroga uzbīdījumam ir labi redzams gadījumā ar augstu mikrolineartātes vizualizācijas izšķirtspēju (A), bet grūti pamanāms gadījumā ar zemu izšķirtspēju (B), un nav redzams skenētā plānslīpējuma attēlā (C). Mikrolinearitātes orientācija A attēlā ir aprēķināta katrā diagrammā iekļaujot ne mazāk kā 10 mērījumus, kas nav pietiekams liels skaits, lai ticami novērtētu linearitātes izteiktību. Izmantotie apzīmējumi ir paskaidroti 1. un 2. tabulās.



### 3.4.3. Upper till, samples Nos. 072, 076b and 071

Three samples (Nos. 072, 076b, 071) are collected at the -17,600 m mark of coastal profile, near the place where macrofabric measurements are made as well (Table 3.3). All the samples are collected from the middle part of the upper till. Samples Nos. 072 and 076b are collected 1.5 m below the top of this unit, and sample No. 071 – 2 m below its top. Few sand stringers and platy till structure noted observed at the sampling spot.

The sample No. 072 consists of massive diamicton with fine sand and silt stringer crossing it. Two vertical thin sections cutting the sand stringer and one horizontal – not cutting the stringer – are prepared from the sample (Appendix 9).

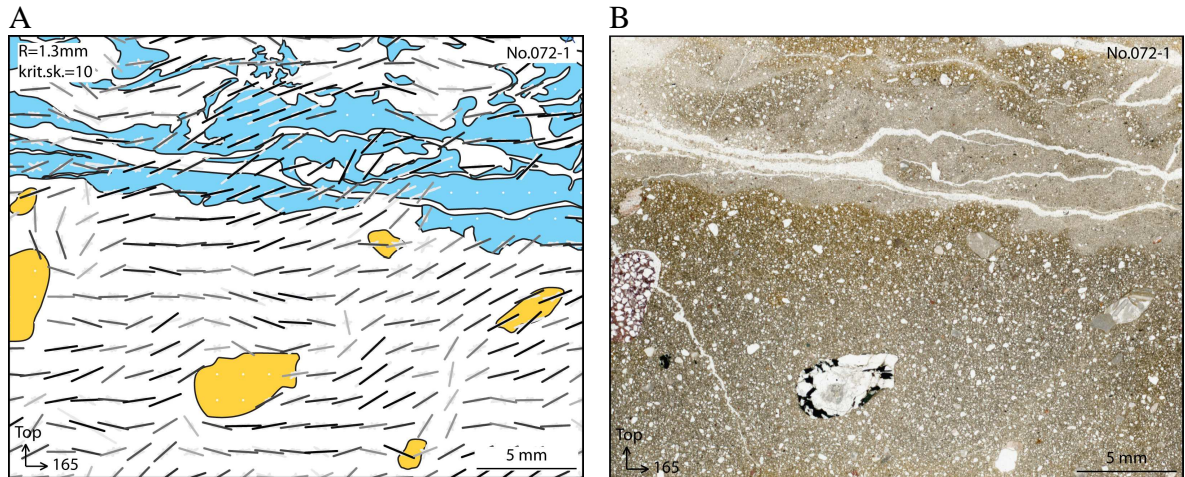


Figure 3.38. The sand stringer morphology and microfabric distribution in vertical thin section No. 072-1: A – scanned thin section image; B – thin section sketch and microfabric distribution. In image B the blue colour represents the sand stringer; other symbols are explained in Tables 1 and 2. The thin section is facing approximately to S. Note that the microfabric strength is indicative as the minimum number of measurement in each diagram is only 10. Mixing of sands and diamicton along their upper contact is observable. The gravel grain in the bottom-centre of the image introduces only minor perturbations in microfabric distribution, and it is likely associated with simple shear and steady state (as opposite to rotation) gravel grain position. Alternatively the microfabric distribution around the gravel grain can be interpreted as indicative of the lodgement.

3.38. attēls. Smilts josliņas morfoloģija un mikrolinearitātes sadalījumus vertikālajā plānslīpējuma Nr. 072-1: A – plānslīpējuma skenēts attēls; B – plānslīpējuma skice un mikrolinearitātes sadalījums. B attēlā ar zilu krāsu ir apzīmēta smilts josliņa, pārējie apzīmējumi ir paskaidroti tabulās 1. un 2. Mikrolinearitātes aprēķinā minimālais mērījumu skaits vienā diagrammā ir 10, kas ir par mazu, lai iegūtu statistiski ticamus rezultātus. Attēlā redzama smilts un diamiktona mehāniska sajaukšanās gar abu materiālu augšējo kontaktu. Mikrolinearitātes sadalījums ap grants graudu attēla vidējā daļā var tikt interpretēts kā vienkāršas bīdes rezultāts, bez grants grauda rotācijas vai arī kā veidojies sablīvējuma (*lodgement*) procesa rezultātā. Mikrolinearitātes orientācija ir aprēķināta katrā diagrammā iekļaujot ne mazāk kā 10 mērījumus, kas nav pietiekams liels skaits, lai ticami novērtētu linearitātes izteiktību.

The stringer has clear deformation marks (Saks *et al.*, 2007) – the upper part of it is mixed with glacial diamicton – the bottom boundary is undulated, but material mixing is limited (Fig. 3.38). A surface of till plate is observed some 2 cm bellow the sand stringer.

In vertical section No. 072-1 almost horizontal position of sand stringer and till plate is observed, in section No. 072-2 both are in inclined position. It is interpreted that the dip direction for both structures is to W.

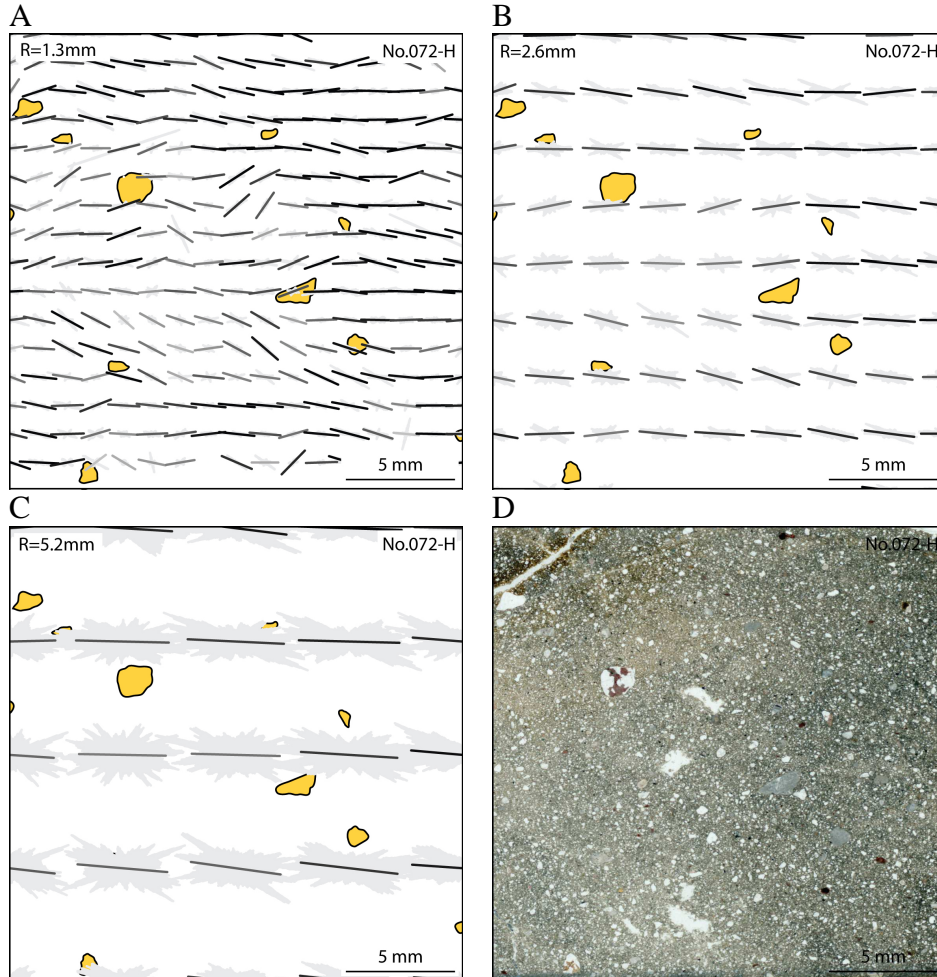


Figure 3.39. The microfabric distribution across different scales (images A, B, C) in thin section No. 072-H (D – scanned thin section image). Strong and consistent microfabric distribution is demonstrated. The thin section is facing down and north is approximately to the lower left corner of the image. Note that the microfabric distribution in image A is calculated with minimum number of measurements at the single grid point set to 10 that is too little for reliable estimation of preferred orientation strength. Used symbols are explained in Tables 1 and 2.

3.39. attēls. Mikrolineraritātes sadalījums dažādos mērogos (A, B, C) plānslīpējumā Nr. 072-H (D – skenēts plānslīpējuma attēls). Plānslīpējumā ir novērota labi izteikta un viendabīgi sadalīta mikrolineraritāte. Plānslīpējums ir vērsts uz leju, un ziemeļu virziens ir aptuveni uz kreiso apakšējo attēla stūri. Mikrolineraritātes orientācija A attēlā ir aprēķināta katrā diagrammā iekļaujot ne mazāk kā 10 mērījumus, kas nav pietiekams liels skaits, lai ticami novērtētu linearitātes izteiktību. Izmantotie apzīmējumi ir paskaidroti 1. un 2. tabulās.

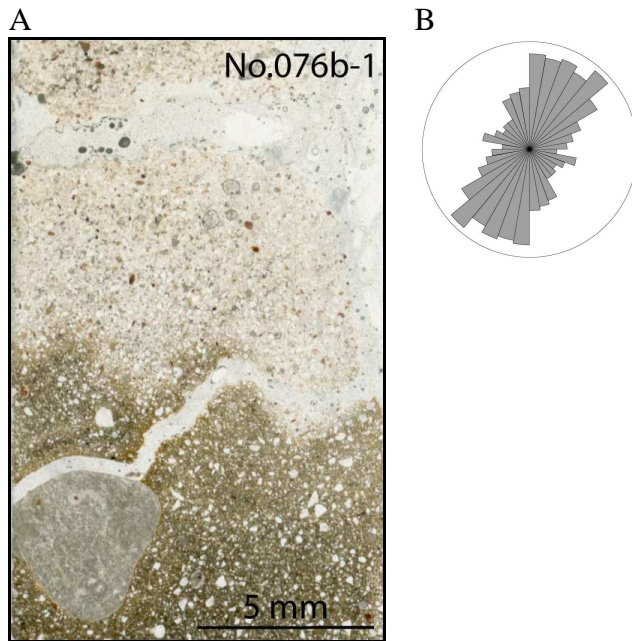


Figure 3.40 Scanned image of the thin section No. 076b-1 and summary preferred orientation of the 315 manually measured large sand grains in diamicton presented as a simple rose diagram (B).

3.40. attēls. Plānslīpējums Nr. 076b-1 skanēts attēls (A) un vienkāršas rozes diagrammas formā parādīta summārā manuāli uzmērītu 315 lielāko smilts graudu orientācija diamiktonā.

In vertical section No. 072-1 a gravel grain with surrounding microfabric distribution that can be interpreted as result of simple shear and gravel grain behaviour according to March model – stable state orientation – is observed (Fig. 3.38). Alternatively the microfabric distribution can be considered as indicative of lodgement as indicated by small microfabric “pinch” at the bottom – left corner of gravel grain). In first case dextral (top to the right) sense of shear is more likely, in the second – sinistral (top to the left) sense of shear is seen.

The rotation structures in thin section No. 072-1 sandy lamina indicate dextral (top to the right) shear sense. Given the overall microfabric dip direction to the left the dextral (top to the right) sense of shear is more likely. Microfabric overall dip angle in thin section No. 072-2 is slightly steeper ( $50^\circ$ ) than the dip angle of sand stringer in the same section.

The preferred microfabric orientation in the horizontal section is roughly perpendicular to the dip direction of the sand stringer and till plate. It is strong and uniform with no identifiable domain-like structure (Fig. 3.39). It is likely that the observed microfabric is a result of local small-scale folding within till unit as indicated by the steeply dipping sand stringer and till plate in the thin section No. 072-2. Extension, associated with folding could significantly contribute to the development of strong and uniform microfabric.

The summary microfabric strength ( $S_1$ ) in all three thin sections prepared from sample No. 072 is rather high – in all cases above 0.6.

Sample No. 076b include part of the coarse-grained sand lamina at the top, and diamicton – at the bottom (Fig. 3.40). Contact between sand and diamicton materials has a jig-saw form with preferred microfabric orientation in diamicton corresponding to the orientation of cutting lines, suggesting brittle sediment deformation due to extension or development of Riedel shears in consolidated till body that is reactivated by shearing. In both vertical sections (Nos. 076b and 076b-2) steeply dipping microfabric orientation is observed. In the horizontal section (No. 076b-H) strong unidirectional fabric is observed trending in NNE-SSW direction (Kalvāns, 2004). This is similar to the observation at the sample No. 072 and contrasting to the macrofabric orientation. Unfortunately only summary orientation of the largest sand grains with very limited details of the spatial distribution for this sample is available from Kalvāns (2004).



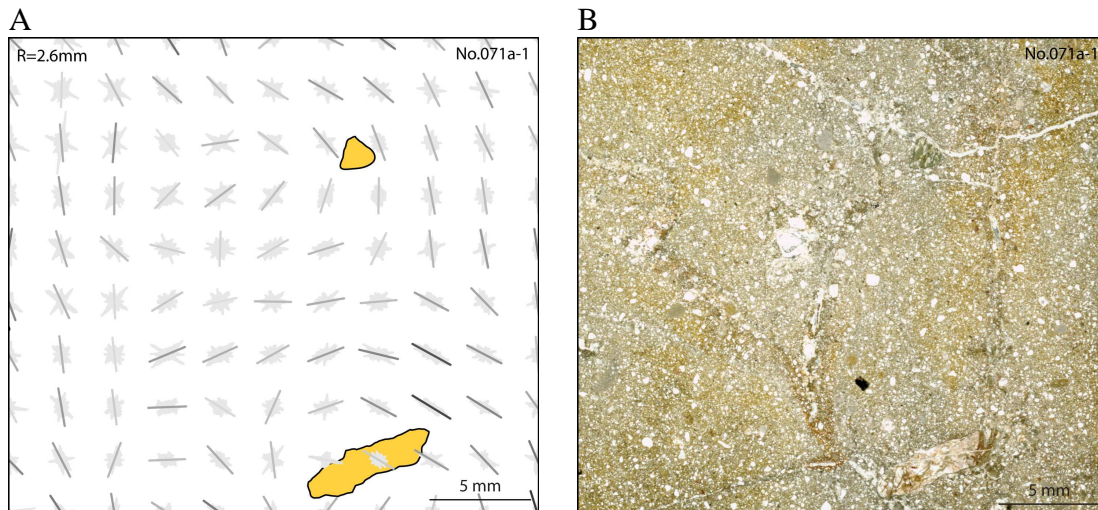


Figure 3.41 Microfabric distribution (A) and scanned thin section No. 071a-1 image (B). The microfabric is much weaker than in other orthogonal thin sections prepared from the same sample. Used symbols are explained in Tables 1 and 2.

3.41. attēls. Mikrolinearitātes sadalījums plānslīpējumā Nr. 071a-1 (A) un skenēts plānslīpējuma attēls (B). Mikrolinearitāte ir daudz vājāk izteikta, salīdzinot ar citiem ortogonālajiem plānslīpējumiem, kas izgatavoti no tā paša parauga. Izmantotie apzīmējumi ir paskaidroti 1. un 2. tabulās.

Two sets of three orthogonal thin sections are prepared from sample Nos. 071: 071a and 071b. Many of the smallest gravel grains in thin sections prepared from sample No. 071 have silt coatings and silt pebbles are present as well. Structures that are suggested to be calcite concretions formed after till deposition (Kalvāns, 2004) are observed.

The parallel vertical thin sections Nos. 071a-2 and 071b-1 as well as horizontal sections Nos. 071a-H and 071b-H have strong and uniform microfabric: the summary orientation  $S_1$  values respectively are above 0.6 (Appendix 9). Even in case of the finest grid resolution ( $R = 1.3$  mm) most of the diagrams indicate similar and strong preferred orientation.

In contrast the vertical sections Nos. 071a-1 and 071b-2 has poorly developed microfabric:  $S_1$  values respectively 0.533 and 0.559. Rather well developed domain-like distribution and fold-like bending of preferred microfabric orientation are observed (Fig. 3.41), but even in the grid resolution  $R = 1.3$  mm fabric strength  $S_1$  in no case reaches 0.7 (Appendix 9).

In summary one vertical (Nos. 071a-2 and 071b-1) and horizontal (Nos. 071a-H and 071b-H) sections demonstrate strong and uniform microfabric preferred orientation while the second vertical section in both sets have weak and domain-like preferred microfabric orientation. The observed microfabric distribution in sections prepared from sample No. 071 suggest strong uni-directional 3D microfabric dipping to the NWW with one vertical section roughly parallel and other perpendicular to this direction.

The till macrofabric measured near the sampling spot is strong as well ( $S_1 = 0.742$  and 0.618) but preferred orientation is in E-W direction rather than in N-S as in thin sections. Thus transverse microfabric – macrofabric orientation is suggested.

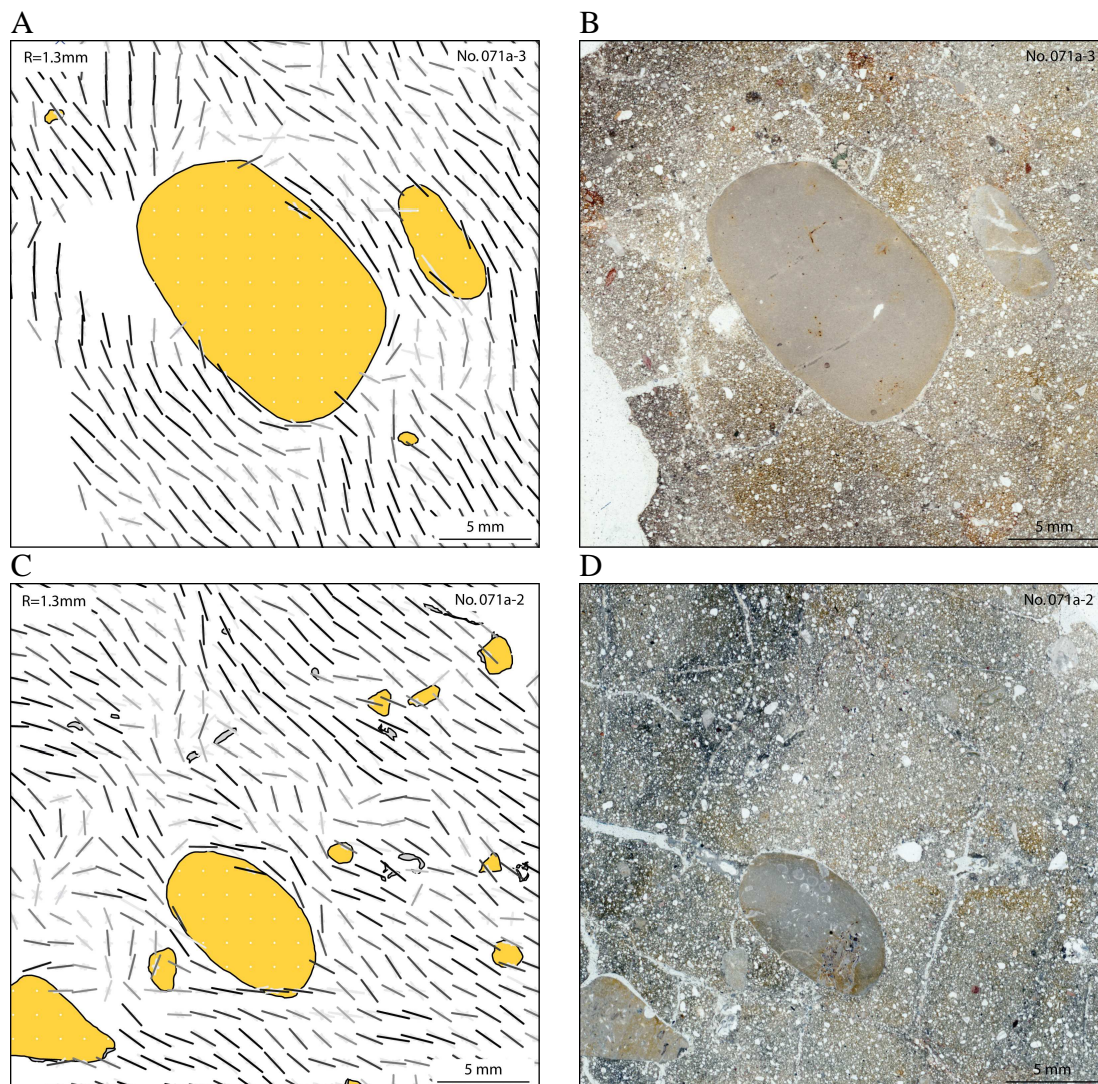


Figure 3.42 The preferred microfabric distribution (A and C) and respective scanned images of thin sections Nos. 071a-2 and 071a-3 (B and D). The asymmetric microfabric distribution relative to the longest axis of the largest gravel grains and discordances in microfabric distribution in both thin sections can be interpreted as indication of gravel grain lodgement, rather than simple shear. Note that the microfabric distribution is calculated with minimum number of measurements at the single grid point set to 10. That is too little for reliable estimation of preferred orientation strength. Used symbols are explained in Tables 1 and 2.

3.42. attēls. Mikrolinearitātes sadalījums (A un C) un attiecīgi plānslīpējumu Nr. 071a-3 un 071a-2 skenēti attēli (B un C). Asimetriskais mikrolinearitātes orientācija attiecībā pret lielāko grants graudu garāko asi un diskordances mikrolinearitātes sadalījumā, iespējams, liecina par grants graudu izgulsnēšanu sablīvējuma ceļā, nevis, piemēram, par morēnas vienkāršas bīdes deformāciju. Mikrolinearitātes orientācija ir aprēķināta katrā diagrammā iekļaujot ne mazāk kā 10 mērījumus, kas nav pietiekams liels skaits, lai ticami novērtētu linearitātes izteiktību. Izmantotie apzīmējumi ir paskaidroti 1. un 2. tabulās.



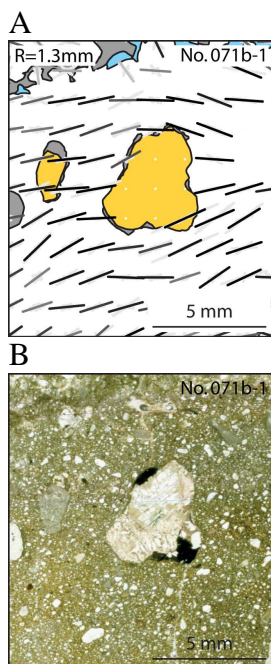


Figure 3.43. Microfabric distribution (A) around a gravel grain in thin section No. 071b-1 (B). The microfabric distribution is seemingly unaffected by the presence of gravel grain. Note that the microfabric distribution is calculated with minimum number of measurements at the single grid point set to 10. That is too little for reliable estimation of preferred orientation strength. Used symbols are explained in Tables 1 and 2.

3.43. attēls. Mikrolinearitātes sadalījums (A) ap grants graudu plānslīpējumā Nr. 071b-1 (B). Grants grauds, šķietami, nekādā veidā neietekmē mikrolinearitātes orientācijas virzienu. Mikrolinearitātes orientācija ir aprēķināta katrā diagrammā iekļaujot ne mazāk kā 10 mērījumus, kas nav pietiekams liels skaits, lai ticami novērtētu linearitātes izteiktību. Izmantotie apzīmējumi ir paskaidroti 1. un 2. tabulās.

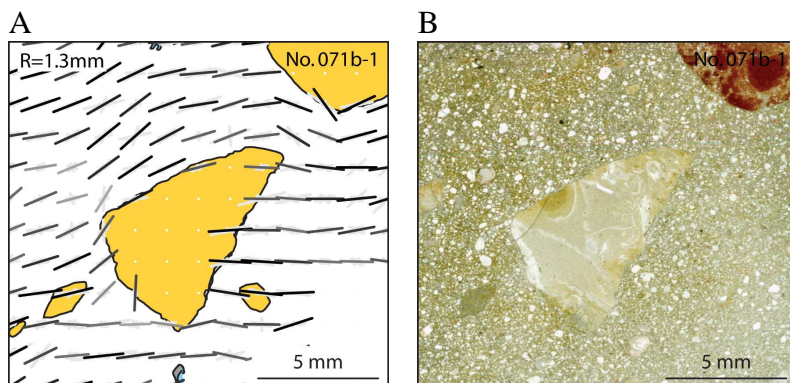


Figure 3.44. Strongly asymmetric microfabric distribution (A) around a gravel grain in thin section No. 071b-1 (B). Note that the microfabric distribution is calculated with minimum number of measurements at the single grid point set to 10. That is too little for reliable estimation of preferred orientation strength. Used symbols are explained in Tables 1 and 2.

3.44. attēls. Izteikti asimetrisks mikrolinearitātes sadalījums (A) ap grants graudu plānslīpējumā Nr. 071b-1 (B). Mikrolinearitātes orientācija ir aprēķināta katrā diagrammā iekļaujot ne mazāk kā 10 mērījumus, kas nav pietiekams liels skaits, lai ticami novērtētu linearitātes izteiktību. Izmantotie apzīmējumi ir paskaidroti 1. un 2. tabulās.

In sections with the strongest microfabric an asymmetric distribution of microfabric can be observed around large gravel grains. In section Nos. 071a-1 and 071a-2 structures that according to Thomason and Iverson (2006) can be interpreted as indicative of gravel grain lodgement rather than simple shear of sediments are observed (Fig. 3.42). In section No. 071b-1 one gravel grain seems not to affect the microfabric distribution at all (Fig. 3.43); around another gravel grain strongly asymmetric distribution across vertical axis is observed (Fig. 3.44).

#### 3.4.4. Upper till, samples Nos. 091 and 092

Samples Nos. 091 and 092 are collected from banded part of the upper till at the Sensala site, near the profile mark -17,685 m, 1 and 1.3 m respectively below the till surface. The banded structure is formed by diamicton bands and bands of silt-rich sand often with flowage structure. Both sandy-silty and diamicton bands are visible in the sample No. 092; in the sample No. 091 only diamicton is exposed.

Despite the different materials presented, the microfabric distributions in both sandy bands and diamicton bands are similar, though the microfabric in the sandy band seems to be more consistent than in the diamicton band. In the horizontal sections in both diamicton band (section No. 091-H) and sandy band (section 092-H) the summary microfabric are weak –  $S_1$  around 0.53 with dominant orientation roughly in N – S direction (Appendix 9). The vertical sections have only slightly higher microfabric strength with  $S_1$  in the range from 0.57 to 0.59 (Appendix 9). In vertical sections trending in N-S direction (091-2 and 092-1) subhorizontal orientation is observed; in sections trending in approximately E-W direction (Nos. 091-1 and 092-2) steeply dipping preferred orientation is observed. In 3D such an apparent microfabric distribution can be reconstructed as dipping towards the W and attributed, for example, to limb of fold-like structure with N-S axial direction.

The microfabric in the vertical section of sample No. 092 locally as well as in general follows the orientation of the boundary between sandy-silty band and diamicton band.

A sand intrusion in diamicton band is observed in sections Nos. 092-1 and 092-2 and the microfabric orientation locally follows the orientation of intrusions.

In section No. 092-2 comparing to section No. 092-1 the microfabric orientation in sandy part is more consistent, stronger and arranged in larger domains (Fig. 3.45), and a fold-like distribution is observed (Fig. 3.45). In section 092-1, in grid resolution  $R = 0.6$  mm, small scale fold-like microfabric distribution is observed. Two sub vertical fabric zones, possibly reflecting brittle deformation, are observed in the diamicton part.

Only in the sample No. 091-H a gravel grain of sufficient size to study the microfabric distribution around it is present (Fig. 3.46). Approximately in the direction of summary microfabric orientation from the gravel grain a domain of well expressed consistent lineation followed by a domain of fold-like microfabric distribution is observed. It can be speculated that the structure is a perturbation trail introduced in the sediments by the presence of rigid particle.

A keel-shaped band or domain of uniform preferred microfabric orientation is observed in the section No. 091-2 (Fig. 3.47). This represents a case of unusually large microfabric domains observed in other sections as well.

#### 3.4.5. Waterlain till – samples Nos. 042 and 017

The sample No. 017 is collected from the base of the water-lain till above its contact with fine sands near -17,940 m mark of the coastal profile. The single thin section (No. 017-1) prepared from this sample deserves special honour as it was the first thin section prepared in the scope of this study (Kalvāns, 2004) and have contributed in developing great deal of ideas in the base of this thesis. Fine lamination, matrix-rich diamicton pebbles and diamicton coatings around some of the gravel grains are observed in the section (Fig. 3.48). Subhorizontal (dip angle  $14^\circ$ ) and rather strong ( $S_1 = 0.601$ ) summary orientation of microfabric is observed in section No. 017-1 (Table 4.12).



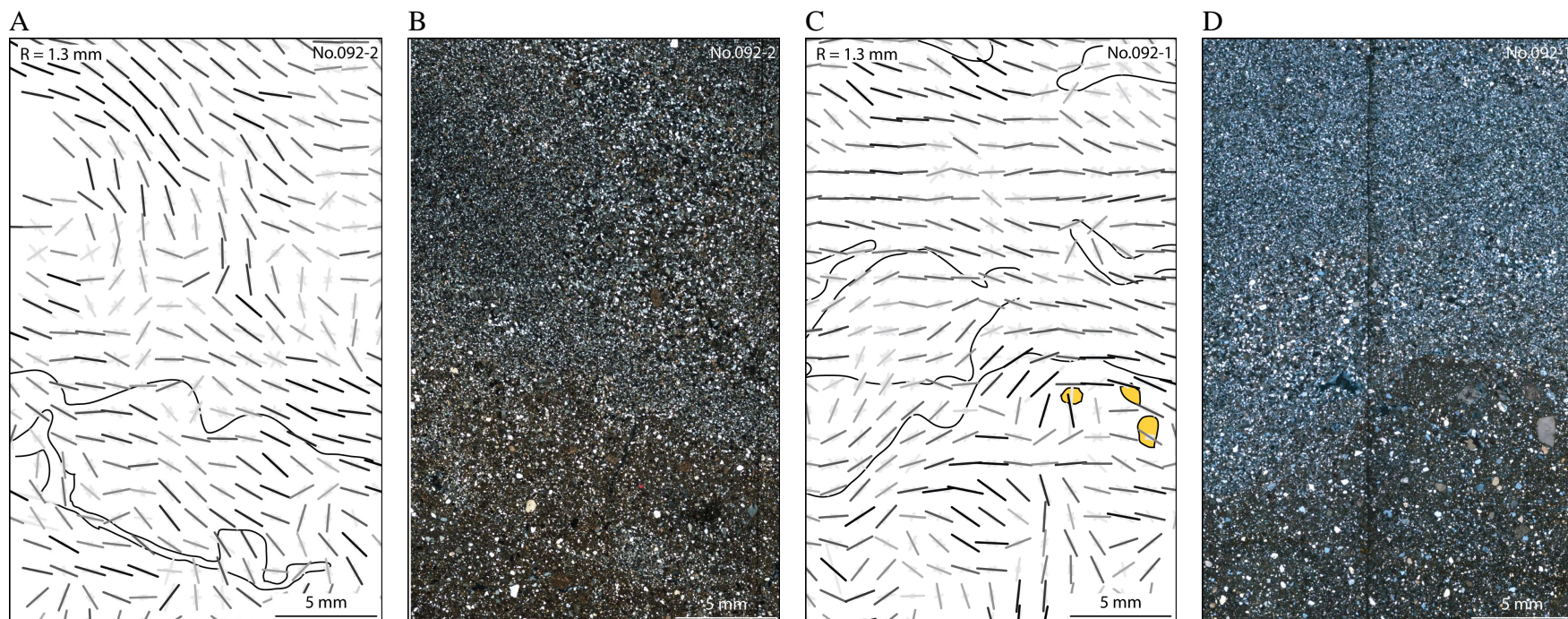


Figure 3.45. Orthogonal sections from the sample No. 092: microfabric distribution (A, C) and thin section images in cross polarised light (B, D). The lines in A and C images indicate boundaries of granulometrical composition. Note that the microfabric distribution is calculated with minimum number of measurements at the single grid point set to 10 that is too little for reliable estimation of preferred orientation strength.

Used symbols are explained in Tables 1 and 2.

3.45. attēls. Mikrolinearitātes sadalījums (A, C) un polarizētā gaismā uzņemtu no parauga Nr. 092 izgatavoto plānslīpējumu fotoattēli (B, D). Ar līnijām A un C attēlos ir apzīmētas granulometriskā sastāva robežas. Mikrolinearitātes orientācija ir aprēķināta katrā diagrammā iekļaujot ne mazāk kā 10 mērījumus, kas nav pietiekams liels skaits, lai ticami novērtētu linearitātes izteiktību. Izmantotie apzīmējumi ir paskaidroti 1. un 2. tabulās.

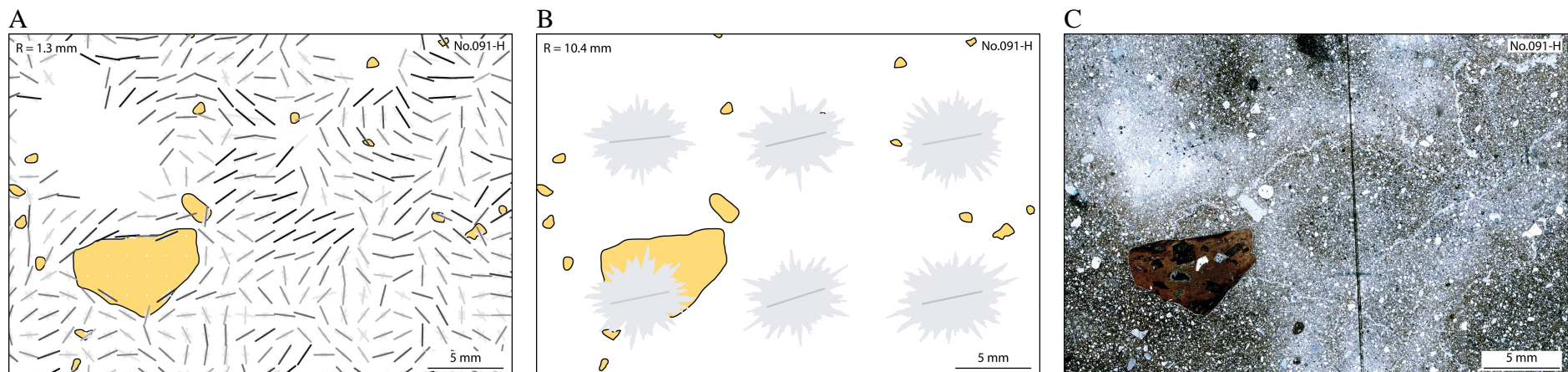


Figure 3.46. Microfabric distribution in a horizontal section No. 091-H around the gravel grain (A), summary fabric orientation (B) and thin section image in cross-polarised light (C). The N is to the lower left side of the image. A domain of consistent linear microfabric followed by the domain of fold-like microfabric distribution can be observed towards right, slightly up side of large gravel grain in the direction of summary microfabric orientation. Note that the microfabric distribution is calculated with minimum number of measurements at the single grid point set to 10 that is too small for reliable estimation of preferred orientation strength. Used symbols are explained in Tables 1 and 2.

3.46. attēls. Mikrolinearitātes sadalījums ap grants graudu plānslīpējuma 091-H (A), summārā mikrolinearitātes orientācija (B) un plānslīpējuma attēls, iegūts polarizētā gaismā. Z ir attēla uz attēla kreiso apakšējo stūri. Summārajā mikrolinearitātes orientācijas virzienā – pa labi un uz augšu no grants grauda – atrodas domēns ar labi izteiktu un vienmērīgi sadalītu mikrolinearitāti, kam seko domēns ar krokas veida mikrolinearitātes sadalījumu. Mikrolinearitātes orientācija ir aprēķināta katrā diagrammā iekļaujot ne mazāk kā 10 mērījumus, kas nav pietiekams liels skaits, lai ticami novērtētu linearitātes izteiktību. Izmantotie apzīmējumi ir paskaidroti 1. un 2. tabulās.



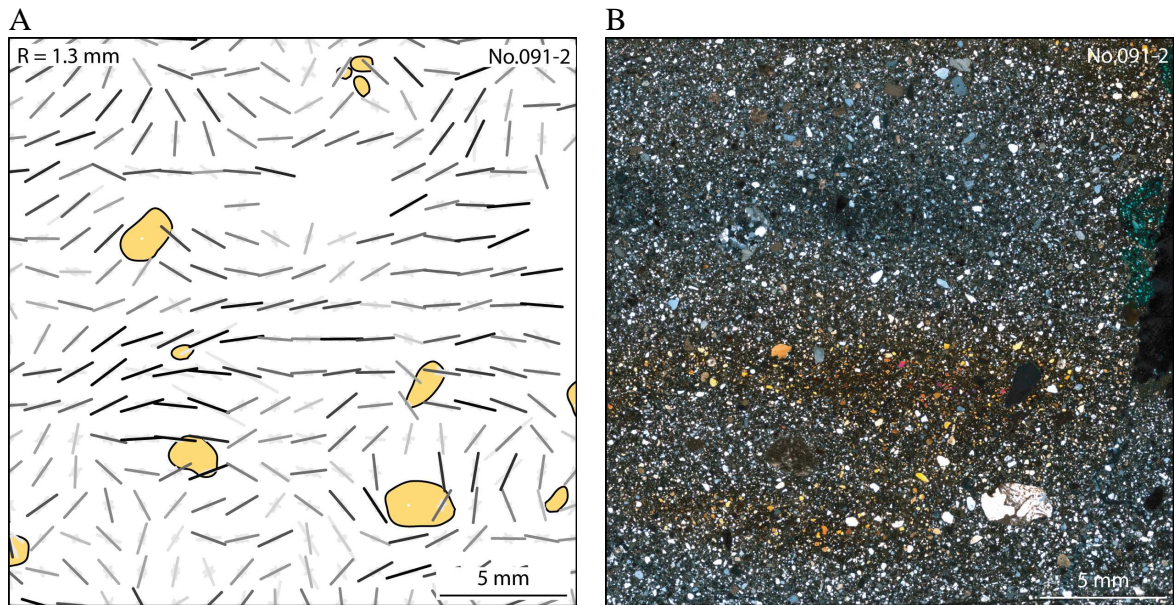


Figure 3.47. A keel-shaped microfabric domain with consistent orientation stands out on the background of rather chaotic preferred orientation in the section No. 091-2: A – microfabric distribution, B – thin section image acquired in cross-polarised light.

Note that the microfabric distribution is calculated with minimum number of measurements at the single grid point set to 10 that is too small for reliable estimation of preferred orientation strength. Used symbols are explained in Tables 1 and 2.

3.47. attēls. Ķīļa formas domēns plānslīpējumā Nr. 091-2 ar labi izteiktu, vienmērīgu mikrolinearitātes sadalījumu izceļas uz visai haotiska mikrolinearitātes sadalījuma fona: A – mikrolinearitātes sadalījums; B – plānslīpējuma attēls krustiski polarizētā gaisām. Mikrolinearitātes orientācija ir aprēķināta katrā diagrammā iekļaujot ne mazāk kā 10 mērījumus, kas nav pietiekams liels skaits, lai ticami novērtētu linearitātes izteiktību. Izmantotie apzīmējumi ir paskaidroti 1. un 2. tabulās.

The sample No. 042 is collected from uniform section of the waterlain till near the -17,550 m mark of the coastal profile. The orientation information of the individual sections is not retained. As the sample is taken from glaciotectionally disturbed sediments it is expected that the initial microfabric distribution has been reshaped to some extent.

The thin sections Nos. 042-1 and 042-3 have rather strong ( $S_1 = 0.571$  and  $0.603$  respectively) and relatively uniformly distributed microfabric that is usually characteristic for vertical sections. However in both cases the summary dip angle is quite steep ( $35^\circ$  and  $17^\circ$  respectively), probably indicating the glaciotectionic tilting of sediment patch. These values contrast to weaker microfabric in the section No. 042-2 ( $S_1 = 0.533$ ) that likely represent subhorizontal orientation.

Markedly for thin section Nos. 042-1 and 042-3 as well as No. 017-1 down to resolution of  $R = 1.3$  mm all diagrams with strongest microfabric have eigenvalue direction close to the mean value. That is not the case for thin section No. 042-2, where proportion of strong microfabric domains is significantly smaller than in other vertical sections and more chaotic orientation is observed (Fig. 3.49).

In the horizontal section No. 042-2 in sufficiently large generalisation level ( $R \geq 5.2$  mm) in all grid points  $V_1$  orientation is similar however the  $S_1$  value is low ( $<0.6$ ). This contrast to stronger microfabric in vertical sections where the  $S_1$  value in grid resolution  $R = 5.2$  mm remains relatively high (around 0.6).

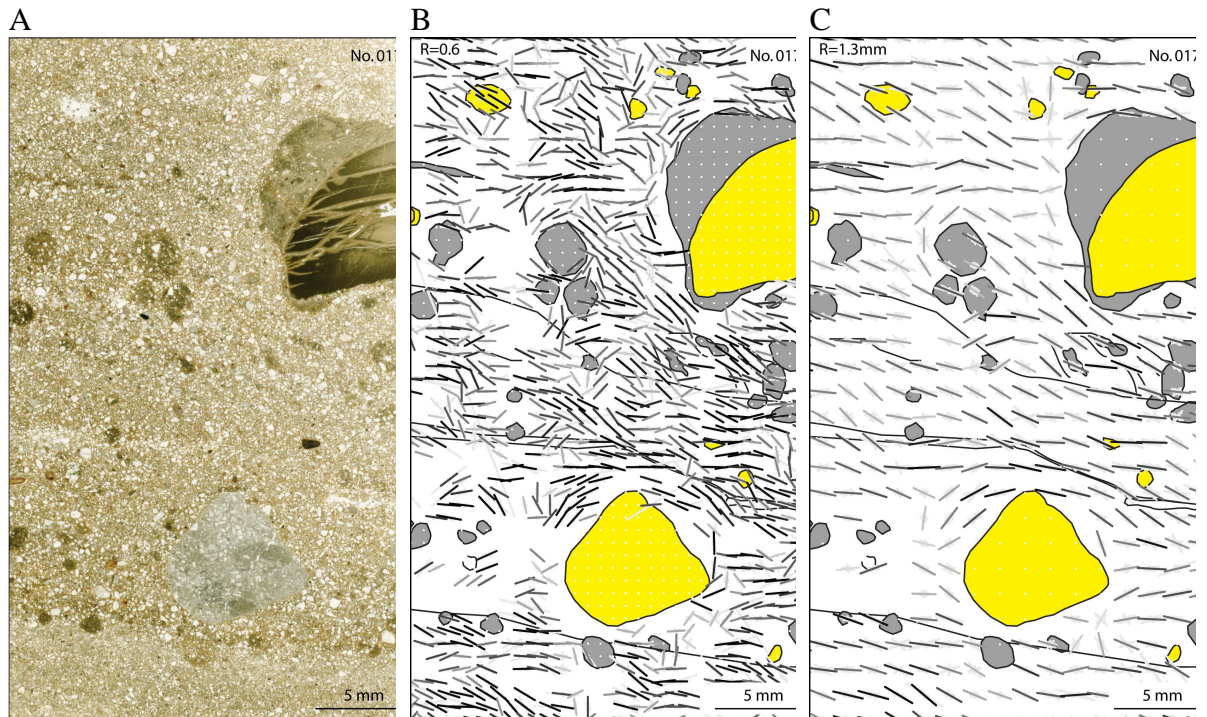


Figure 3.48. The vertical thin section No. 017-1 of the waterlain till: A – scanned thin section image; B, C – microfabric distribution. Faint lamination, matrix-rich diamicton pebbles and gravel grains with diamicton coatings are observed in the thin section. Microfabric bands dipping from the left top corner to the right of the image can be observed. This probably is a result of post-depositional brittle deformation. The microfabric is gently bending around tops of large gravel grains. This can be interpreted as a result of sediment compaction or, less likely, gravel grain rotation. Note that the microfabric distribution in image B is calculated with minimum number of measurements at the single grid point set to 10 that is too small for reliable estimation of preferred orientation strength. Used symbols are explained in Tables 1 and 2.

3.48. attēls. No ūdenī izgulsnētās morēnas parauga izgatavotais vertikālais plānslīpējums Nr. 017-1: A – skenēts plānslīpējuma attēls; B, C – mikrolinearitātes sadalījums. Plānslīpējumā ir novērojams neskaidrs slāņojums, ar matricu bagāta diamiktona oliši un grants graudi ar diamiktona apmalēm. Attēlā redzamas mikrolinearitātes joslas, kas tiecas no augšējā kreisā stūra uz apakšējo labo attēla stūri. Tās, iespējams, ir veidojošās trauklas deformācijas rezultātā pēc nogulumu izgulsnēšanās. Mikrolinearitāte applicas ap lielāko grants graudu augšējo malu. Tā var tikt interpretēta, kā nogulumu sablīvēšanās, vai, mazāk ticami, kā grants graudu rotācijas pazīme. Attēlā B mikrolinearitātes orientācija ir aprēķināta katrā diagrammā iekļaujot ne mazāk kā 10 mērījumus, kas nav pietiekams liels skaits, lai ticami novērtētu linearitātes izteiktību. Izmantotie apzīmējumi ir paskaidroti 1. un 2. tabulās.

In vertical thin sections No. 017-1, 042-1 and to a lesser extent in No. 042-3 in resolution  $R = 0.6$  mm fine zones of lineation crossing the full thin section area can be traced (Fig. 3.48 and 3.49). It is suggested that these structures are the result of brittle deformation, that occurred after sedimentation due to sediment compaction or glaciotectionic deformation.



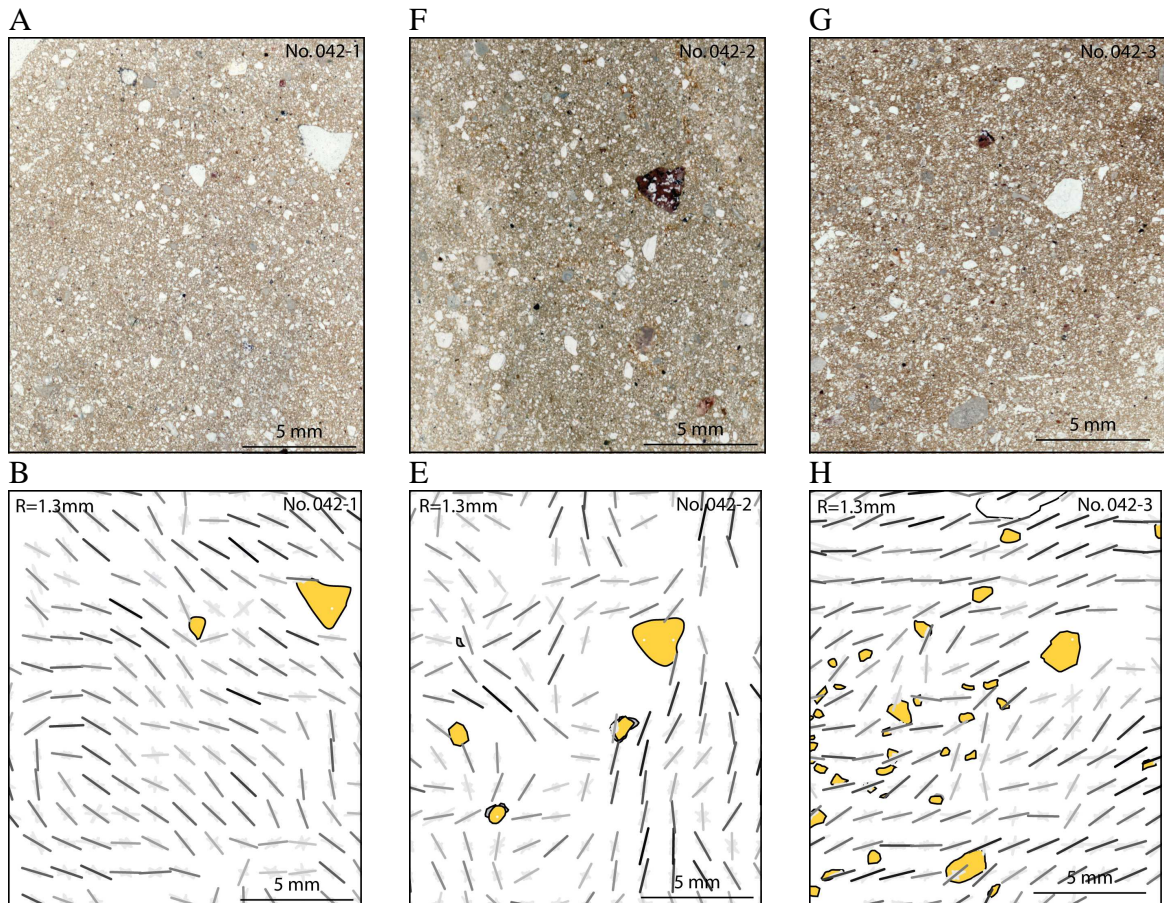


Figure 3.49. Comparison of microfabric distribution in three orthogonal thin sections prepared from the sample No. 042: A, F, G – scanned thin section images; B, E, H – microfabric distribution. Not the rather uniform and largely strong microfabric in the thin sections No. 042-1 and 042-3 compared to the thin section No. 042-2; the two first are likely representing the vertical orientation and the later one – horizontal. The steep microfabric dip in vertical sections probably is a result of the glaciotectionic tipping of the sediment patch. Used symbols are explained in Tables 1 and 2.

3.49. attēls. Mikrolinearitātes salīdzinājums trijos ortogonālos plānslīpējumos, kas izgatavoti no parauga Nr. 042: A, F, G – skenēti plānslīpējumu attēli; B, E, H – mikrolinearitātes sadalījums. Salīdzinot ar plānslīpējumu Nr. 042-2, plānslīpējumos Nr. 042-1 un 042-3 ir novērota vienmērīgi orientēta un labi izteikta mikrolinearitāte; Domājams, ka tas tas saistīts ar to, ka pirmais raksturo horizontālu griezumam, kamēr pēdējie divi – vertikālu. Stāvais mikrolinearitātes krituma leņķis plānslīpējumos Nr. 042-1 un 042-3 domājams atspoguļo nogulumu ķermeņa glaciotektonisku sašķiešanu. Izmantotie apzīmējumi ir paskaidroti 1. un 2. tabulās.

The waterlain origin of the sediments is supported by the microfabric distribution around a gravel grain at the thin section No. 017-1 (Fig. 3.48) as well as large number of fine-grained diamicton pebbles. The microfabric is symmetrically bending around a gravel grain suggesting material deposition on top of a bump created by buried gravel grain. Less likely explanation of such a microfabric distribution is gravel grain rotation in a process of the simple shear.

It can be concluded that waterlain till at the Sensala site is characterised by gently dipping microfabric in the vertical section. Perturbations in the microfabric around gravel grains are restricted to small area above them (thin section No. 017-1). No significant microfabric strength variation between sandy bottom part and diamicton part in thin section No. 017-1 is observed. This supports the assumption that the deposition in a water column is the main process involved in formation of these sediments as pervasive sediment deformation is likely to form different microfabric patterns in the materials of the different grain size.

## 4. Discussion and interpretation

The relatively large number of analyzed samples allow to draw some general conclusions about till microfabric as an important till characterization parameter, thus contribution to understanding of processes at the warm based active glacier bed. In this chapter first the object specific questions will be discussed followed by discussion about till microfabric in more general terms. At the concluding part some methodological questions will be considered as well.

### 4.1. Microfabric in a distinct shear zone, Ziemupe case

At Ziemupe site microfabric distribution was studied in the predominantly sandy shear zone and two till units above and below it. In till units contrasting macrofabric orientation was measured: NNE to SSW orientation in the upper till, and NEE – SWW orientation in the lower till. Although the microfabric strength in the horizontal sections is low the same trend was clearly identifiable: macrofabric and microfabric orientation is similar.

In vertical sections a very strong and uniform microfabric orientation of the sandy laminae from shear zone must be noted: in several thin sections the microfabric coincided within a single degree. In contrast the microfabric in bands of poorly sorted material is not as strong and less homogeneous. This indicates homogeneous nature of the microfabric in the shear zones composed from sediments with narrow grain size distribution in opposite to low fabric strength in heterogeneous – diamicton – sediments.

It can be expected that in sands subject to simple shear in case of low effective pressure sliding of similar size grains along each other will be the dominant form of grain interaction. In case of diamicton the same kind of interaction between similar size grains will take place, but the grains considerably larger than the mean size will disturb the deformation field and displacement directions around them. This will result in lower microfabric strength in diamicton compared to the sands and this is supported by the observations.

In mathematical modelling experiments it is demonstrated that the formation and collapse of grain bridges or force chains will support most of the stress in the shear zone (Mair, Hazzard, 2007). The same researchers demonstrated (*ibid*) that well sorted materials tend to have simple networks of strain chains (grain bridges) dipping around 50° in direction of the shear. Meanwhile the materials of power law distribution tend to have branched stress networks with significant proportion of weaker than average stress chains being oriented oblique or at large angles towards the shear direction. Assuming that the development of force chains is one of the mechanisms denoting microfabric development, described experimental results correspond well to the observations. This explains the relatively weaker microfabric of diamicton with characteristic power law grain size distribution (e.g. Hooke, Iverson, 1995; Benn, 2002) and stronger microfabric of well sorted sands.

It must be noted that the results present here and elsewhere (e.g. Thomason, Iverson, 2006, 2009) demonstrate that in tills rather strong microfabric can be observed as well. Thus different pattern of fabric strength development is expected for materials with different grain size composition undergoing similar deformation.



## 4.2. Origin of diamicton spherules at Plašumi gully site

A till at the Plašumi gully site with peculiar network of long vertical, short horizontal and spherical joint structure was studied in thin sections. Examination did not reveal any significant correlation between microfabric and spherical joint systems. Therefore is suggested that the odd spherical structure of the till is due to post-sedimentation processes, for example, repeated desiccation or frost action, rather than the genesis of till unit itself.

## 4.3. The origin of sandy diamicton at Strante site

The sandy diamicton at Strante site initially was chosen for microscale studies due to its unclear genesis, both glacioaquatic and subglacial origin were suggested. The repeated fieldwork sessions, mostly due to the presence of rounded soft sediment (mostly fine sand) clasts with preserved, slightly deformed primary sedimentary structure concentrated in certain levels it was concluded that present sediment are a local till. Similar inclusions are often found in basal tills (Evans *et al.*, 2006) and are interpreted as being incorporated in till in a frozen state.

An odd microfabric distribution is observed in the thin sections: rather weak preferred orientation in the horizontal sections and distinct bimodal distribution in the vertical sections with primary (dominant) subhorizontal and secondary subvertical modes. In three dimensions this can be imagined as a single subvertical mode rising above dominant orientation laying in horizontal plane with weak maxima roughly in E-W direction.

Several mechanism of observed preferred microfabric formation is considered: (1) rotation of oblate (disk-shape) sand grains in shear zone according to the Jeffery's model (Jeffery, 1922) around shortest axis positioned in horizontal plane normal to shear direction, (2) raining down of sand grains in a water column and "pricking" in soft substrate (like described by Carr, 1999, 2001) or (3) vertical loose sediment compaction – pure shear. The first case implies subglacial origin; the second – glacioaquatic origin and the third can be attributed both for subglacial sediments and glacioaquatic sediments

In a case of shearing origin, if Jeffery's model is assumed, oblate particles are expected to rotate with shortest axis in the plane of shearing and perpendicular to the shear direction and rod-like particles - are expected to roll, with longest axis laying in the plane of shearing, normal to the shear direction (forming b-fabric). If such position of oblate and rod-like grains are cut by randomly oriented vertical thin section plane that does not coincide with shear direction indeed two orthogonal modes of apparent microfabric orientation should be observed. The same should be the case for horizontal sections as well, with one mode representing rod-like particles and second – the oblate particles. But in horizontal thin sections monomodal, weak fabric is observed. Additional the evaluation of the grain shape indicates that a noticeable proportion of the oblate grains are lying in the horizontal plane as there are more apparently elongated grains in the vertical than in the horizontal sections. Thus observations do not confirm sand size particle behaviour according to Jeffery's model.

There is observed slight increase of subvertical mode strength for the largest grain sizes as should be expected in case of "pricking" (dropstones) mechanism. However, Carr (1999, 2001) examining glaciomarine sediments found only one subvertical not two orthogonal microfabric modes. The "pricking" (dropstones) mechanism is in line with weakly developed fabric in horizontal sections that could be shaped by dominant water or

wave movement direction. But formation of rounded inclusions of soft sediment clasts in such environment is unlikely.

The vertical compaction of loose sediments can result in formation of two orthogonal microfabric modes if sediments initially have random fabric orientation: all grains except those with longest axis parallel to the direction of compaction will be rotated to the plane normal to the compaction direction. However elongated grains will not reach this plane unless very large shortening rate is achieved. If the initial fabric will have any subvertical or subhorizontal mode, it will be enhanced during the compaction. It is likely that the bimodal fabric was enhanced due to sediment compaction, but was formed as a result of other processes.

These sediments likely accumulated in areas of ground subsidence between diapirs (see Saks *et al.*, *accepted for publication*, for discussion). New material was constantly added to the till accumulation area resulting in effective isolation of already present sediments from the glacial shear stress. The shear deformation likely resulted in development of subhorizontal mode, and the pore water upward or downward expulsion in the latter stage could produce the subvertical microfabric mode. The diamicton, likely, were gradually deposited as tectonic slices (as summarised by Evans *et al.*, 2006), and the compaction occurred gradually, rather than simultaneously for the full sediment pile of more than 6 m thickness. Thus it can be suggested that the material in the actively deformed layer was in viscous, flowing state effectively isolating the glacial shear stress from entering the deeper horizons of recently accumulated till where gradual compaction took place. However, this mechanism does not correspond to observations either, for examples, there is not observed any zones with stronger vertical mode, corresponding to possible pathway of more intense pore water expulsion.

#### **4.4. The microfabric strength and till fabric across different scales**

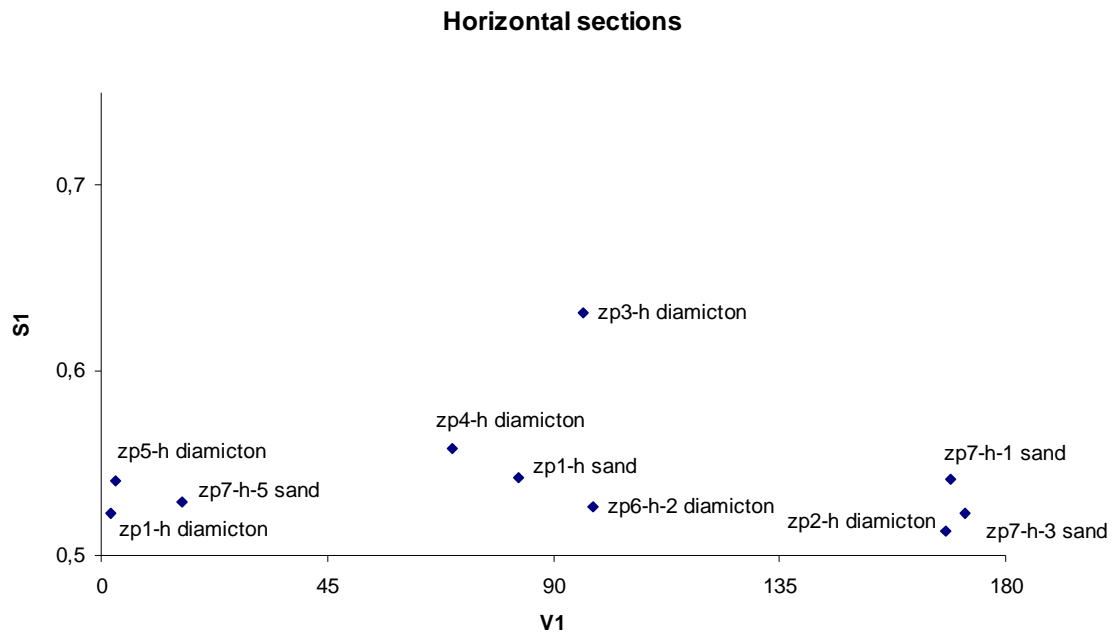
Thomason and Iverson (2006) in ring-shear experiments found that steady-state fabric strength of  $S_1$  around 0.71 to 0.74 after shear strains of 7–39 are established in some tills.

As demonstrated in the figures 4.1, 4.2, 4.3 and 4.4, the high fabric strength values  $S_1 > 0.7$  are approached only rarely. Even in the sandy shear zone below the upper till at Ziemupe site in only one case  $S_1$  is above 0.7, although relatively large shear strain are thought to be accumulated there. It is possible that the measurement of all small grains in contrast to manual selection of large grains as in most previous studies results in the lower summary fabric strength and thus the results need to be compared with caution.

Usually fabric strength in horizontal sections is lower than in vertical ones. It is likely due to relatively large proportion of the tabular grains as well as nature of the till emplacement processes. Tabular grains are expected to be aligned with longest axis close to horizontal plane, contributing significantly to the microfabric strength in the vertical sections and obscuring the microfabric signal associated with the rod-like grains in horizontal ones. Both shearing and compaction – the two dominant factors affecting grain orientation in tills – are expected to shift the longest axis of any grain towards the horizontal plane, thus strengthening the apparent subhorizontal microfabric observable in vertical sections. Additionally the compaction does not contribute to development of any preferred grain orientation in horizontal section and in numerous studies it is demonstrated that the shearing can produce transverse as well as parallel fabric. So both processes – the compaction and the shearing – can contribute to development of weak microfabric in horizontal sections and strong, subhorizontal fabric in vertical ones. The third major process affecting microfabric orientation in tills – plough associated with lodgement of the

large clasts – likely could produce more random or domain-like microfabric distribution in both horizontal and vertical sections.

A



B

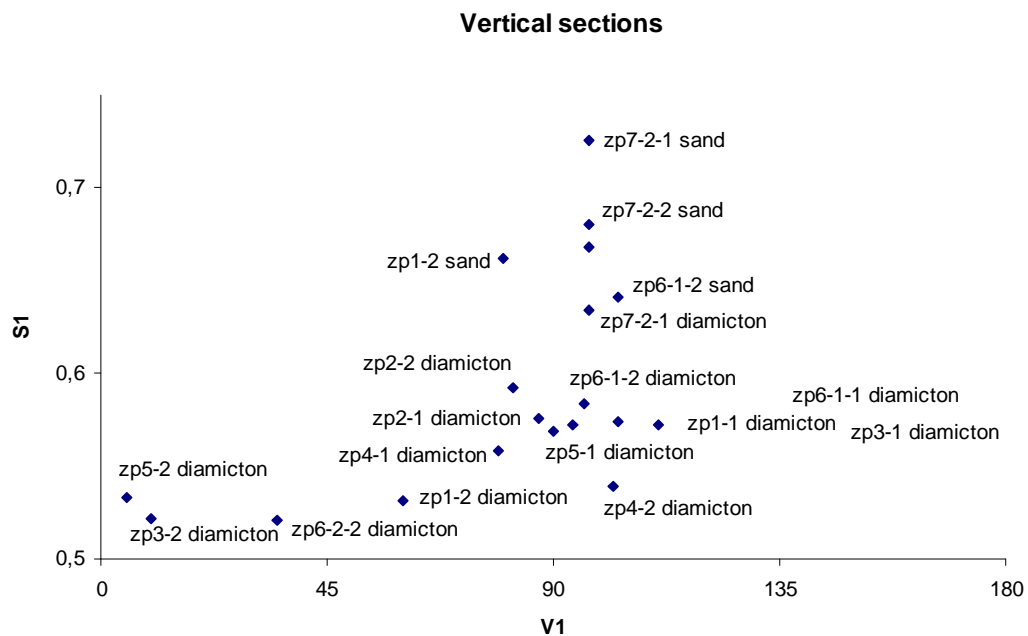
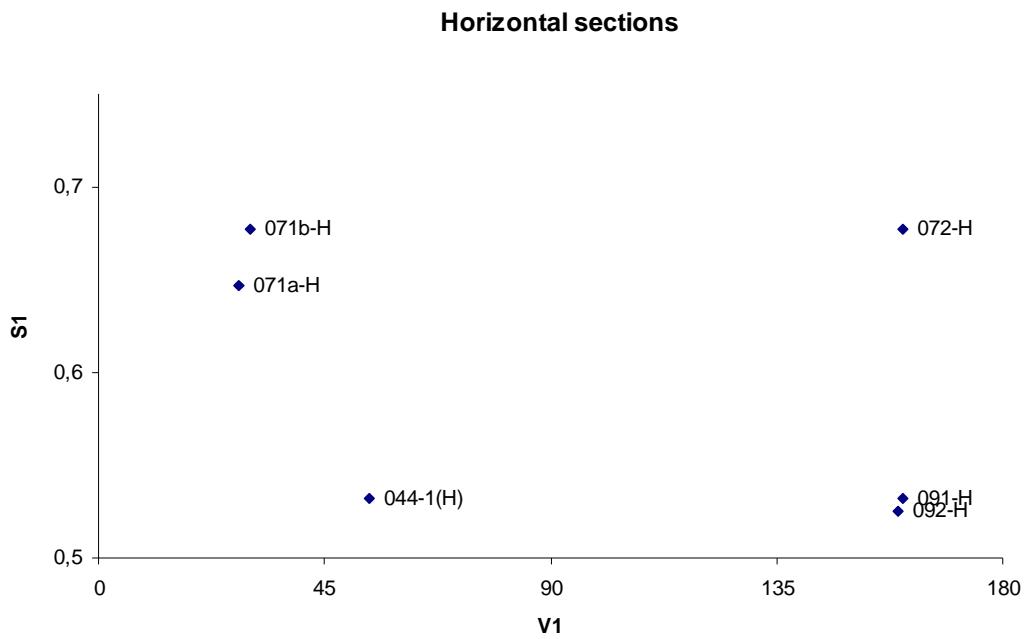


Figure 4.1 Summary microfabric from horizontal (A) and vertical (B) thin sections from the Ziemupe site.

4.1. attēls. Dominējošā summārā mikrolinearitātes orientācija paraugos, kas ievākti Ziemupes atsegumā, horizontālajos (A) un vertikālajos (B) plānslīpējumos.

A



B

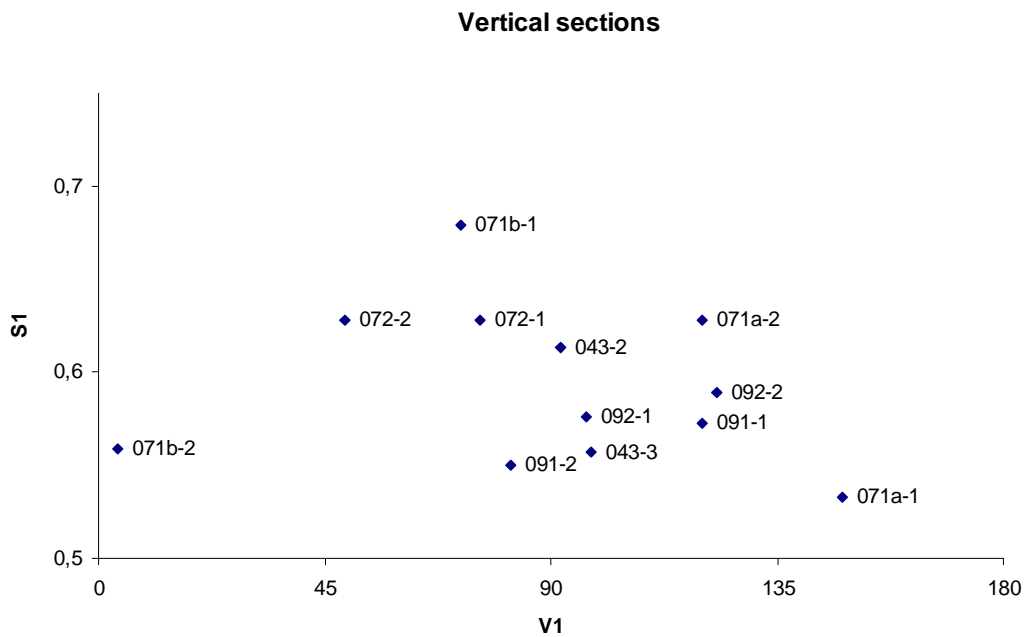
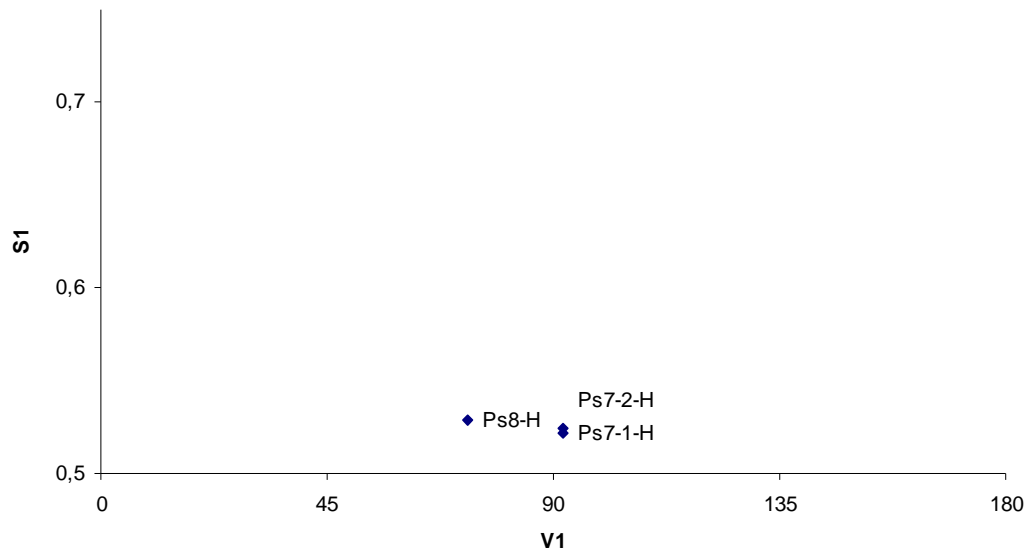


Figure 4.2 Preferred summary microfabric orientation and fabric strength in the horizontal (A) and vertical (b) thin section of the upper till at the Sensala site.

4.2. attēls. Dominējošā summārā mikrolinearitātes orientācija Sensalas atseguma augšējās morēnas horizontālajos (A) un vertikālajos (B) plānslīpējumos.

A

### Horizontal sections



B

### Vertical sections

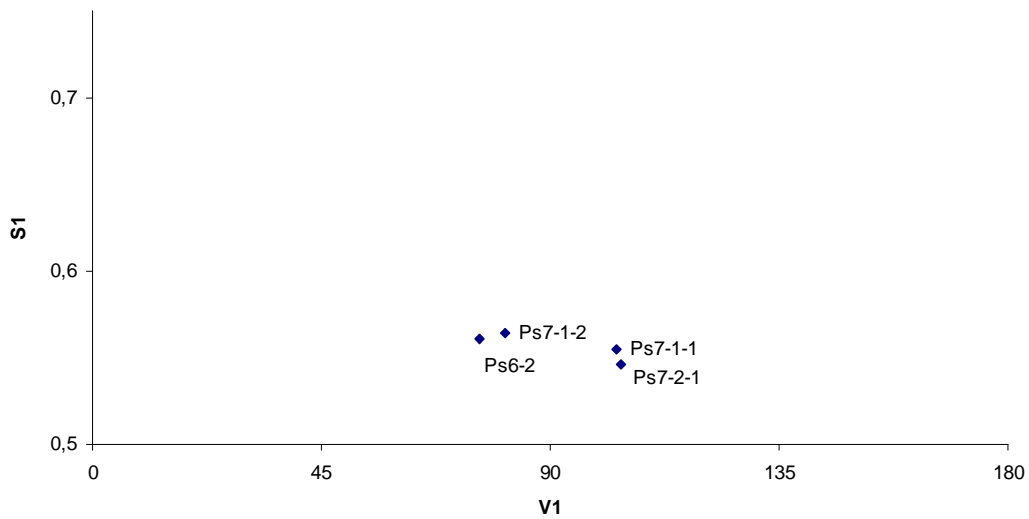
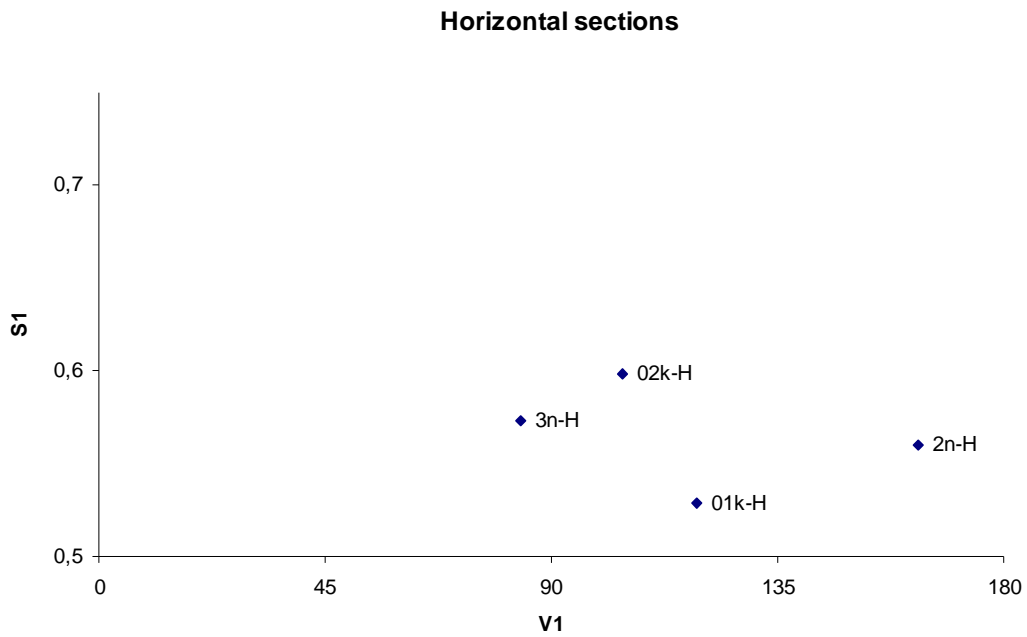


Figure 4.3 Summary microfabrics from horizontal (A) and vertical (B) thin sections from the upper till at the Plašumi gully site.

4.3. attēls. Dominējošā summārā mikrolinearitātes orientācija paraugos, kas ievākti no augšējās morēnas pie Plašumu gravas, horizontālajos (A) un vertikālajos (B) plānslīpējumos.

A



B

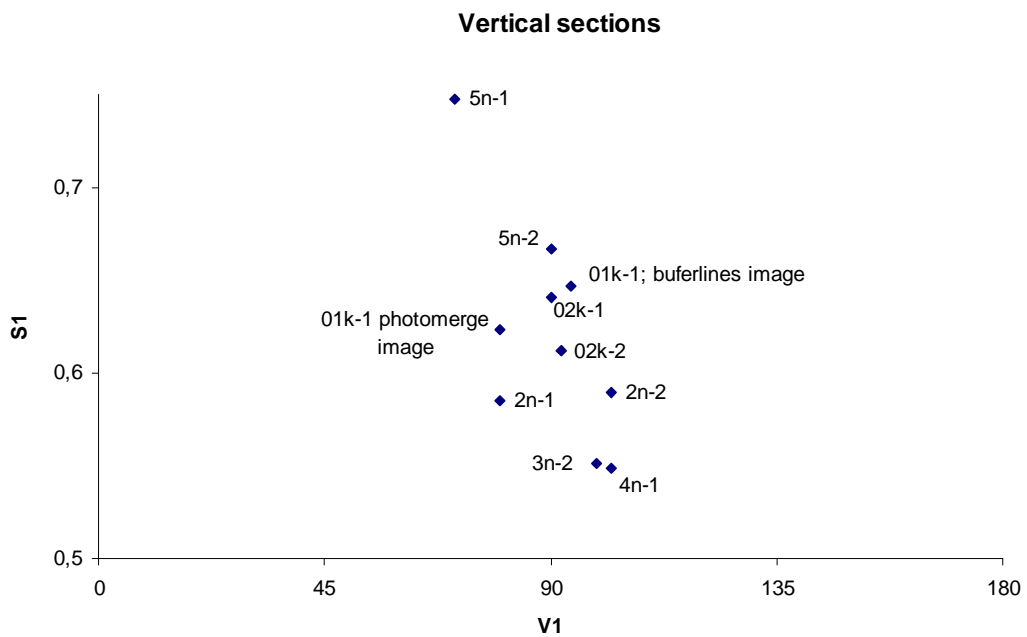


Figure 4.4 Summary microfabric from horizontal (A) and vertical (B) thin sections from the sandy diamictone at the Strante site.

4.4. attēls. Dominējošā summārā mikrolinearitātes orientācija paraugos, kas ievākti no smilšainā diamiktona Strantes atsegumā, horizontālajos (A) un vertikālajos (B) plānslīpējumos.



Analysing the results from Ziemupe site (see Appendix 4) it was found that in almost all cases the microfabric is relatively stronger if data are collected from smaller area of the thin section. When examining the microfabric spatial distribution a domain-like structure is apparent. If data from several orientation domains are collected in a single data set inevitably the summary preferred orientation strength will diminish. Usually the preferred orientation in individual diagrams with  $S_1 > 0.6$  in case of  $R = 1.3$  mm are spread across  $10^\circ$  to  $25^\circ$  wider sector than in case of  $R = 2.6$  mm, in the samples from sandy band of the shear zone.

Rather large variations of the microfabric strength are observed in the samples from the upper till at the Sensala site. The microfabric strength in horizontal sections is clearly divided in two groups (Fig. 4.1): (1) with relatively strong fabric ( $S_1 > 0.6$ ), and (2) with weak fabric ( $S_1 < 0.55$ ). No such microfabric strength modality is observed in vertical sections. The samples of similar fabric strength are collected from nearby locations. Samples Nos. 091 and 092, with weak fabric in horizontal sections, are collected from the relatively loose section of the upper till composed of bands of the diamicton and bands of the silt and sand with flowage structures at the -17,685 m of the coastal profile. The microfabric orientation there is similar to dominant macrofabric orientation in the upper till. In contrast samples Nos. 071, 072 and 076, having strong fabric in the horizontal sections, are collected from the well consolidate section of the till with few thin laminae of fine sands, at the -17,600 m of the coastal profile.

The banded structure and internal deformation features imply that both till varieties were formed or at least shaped by shearing, but the mode of deformation likely was different. In first case (-17,685 m of the coastal profile) less confined, viscous-like deformation with large water content resulting in low consolidation level, and weak grain alignment is likely. In the second case (-17,600 m of the coastal profile) plastic deformation is suggested resulting in strong preferred sand grain orientation. The rather steep dip of sand lamina and microfabric observed in the thin section No. 072-2 suggest that it is collected from some intertill deformation structure that formed after the emplacement of the sand lamina. Sediment extension – pure shear – not complicated by such process as lodgement or clast ploughing is a likely mechanism of the formation of the strong unidirectional microfabric there. The microfabric in the sample No. 071 is strong in four (out of six) thin sections and weak in the remaining two, additionally the dominant orientation is not subhorizontal. Such an apparent fabric distribution can correspond to strong unimodal real microfabric with one section orientated almost normal to the dominant fabric orientation.

The dominantly in E – W direction trending macrofabric at the respective site (upper till -17,600 m of the coastal profile) is oriented oblique to the microfabric orientation. It contrasts to the most of the observations where microfabric and macrofabric dominant orientation coincides. The assumption that the microfabric orientation was formed by small scale internal deformation of the sediments that did not affect the general macrofabric orientation can support this observation. However the identification of deformation structure in this case is not possible.

The fabric strength indicator  $S_1$  is not applicable to the vertical thin section samples from Strante site as distinctly bimodal nature of the microfabric is observed. The exception is the sample No. 5n, where strongest microfabric is observed with  $S_1 > 0.7$ . It comes from deformed fine sand sediments. The local nature of deformation of the sampled sediments likely was extension instead of simple shear that is expected in tills. Thus, like in the case of the Sensala site, the strongest microfabric is connected with local, small scale deformation structures.

The comparison of phenomena observed in different scales often is not straight forward. This is true for the tills as well: till fabric is known to be a good indicator of former ice movement direction. However the three dimensional analysis of fabric elements is required to reconstruct the glacier movement direction correctly (Dreimanis, 1999). It is even more so in case of microfabric, as the local dominant orientation are formed by structures from few mm size up to the scale of the ice sheet itself. The time transgressive till accumulation and late stage development of localised shears in the accumulated till body as outlined by Larsen *et al.* (2004, 2007) as well as perturbations in the microfabric distribution introduced by larger clasts are the obvious source of un-event microfabric distribution.

Only rarely the source of perturbations in microfabric orientation – e.g. a gravel grain – can be seen in the thin section, but more often it cannot be determined. Observed microfabric preferred orientation and its local spatial distribution can equally represent the general properties of particular till unit as well as local variability introduced by some large clasts or other unknown factors.

In scale of few millimeters there are higher fabric strength and higher variability of preferred orientation, compared to scale of few centimetres where low fabric strength and low variability of preferred orientation are observed.

It is suggested that all till formation processes (lodgement and ploughing, shearing and deformation, melt-out, sedimentation in the water) impose certain microfabric distributions. Due to heterogeneous nature of till grain size distribution all the microfabric distributions formed as a result of different till formation processes should be rather heterogeneous in a small scale (small measurement areas) and becomes more or less homogenous in large scale (large considered areas). The nature of heterogeneities and the level of homogenisation will depend both from till grain size distribution and till formation processes involved. Such an approach to till microfabric can be termed “threshold of homogeneity”. It predicts that tills with higher contents of large grains will have higher threshold of homogeneity, e.g. homogenous microfabric distribution will be observed if data were collected from larger area of the thin section.

Alternatively the microfabric distribution can be considered as being fractal-like. It is demonstrated that the grain size distribution for most tills are a fractal, with fractal dimension around 2.9 (Hooke, Iverson, 1995). Generally it is assumed that the till microfabric is formed by the interaction of different size grains, so it can be expected, that the microfabric distribution will have fractal-like (self similar at different scales) features as well. Such an approach to till microfabric can be termed “fractal like distribution”. It predicts that: (1) the same fabric distribution pattern should be observed across different scales, given that corresponding sized grains are measured for each scale; (2) the close correlation between grain size distribution and fabric strength across different scales should be observed

It is intuitively understood that till microfabric is determined by the behaviour of the larger clasts such as gravel grains or pebbles or cobbles and small grains will be aligned according to the surface orientation of the large ones. Such an approach to till microfabric can be termed “clast surface representation”. It predicts that: (1) the summary micro fabric orientation will represent the macrofabric, just in a blurred form, and, (2) the microfabric spatial distribution around large clasts will bear some information on the interaction or movements of the clasts in the last stage of the till formation. This concept was suggested by Thomson and Iverson (2006) emphasising that the pattern of microfabric around rotating clast in pervasively sheared till would be different from microfabric pattern around lodged clast in lodgement till.

#### 4.5. Microfabric distribution around gravel grains

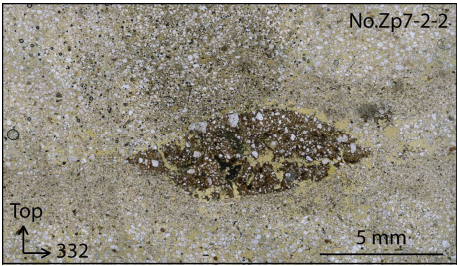
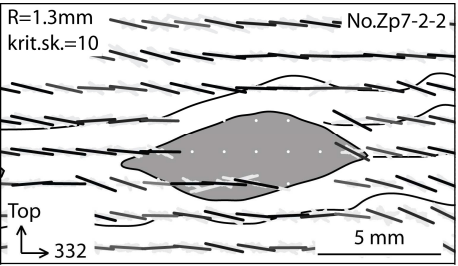
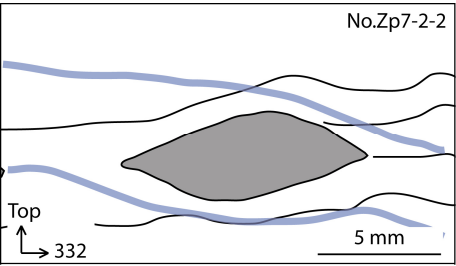
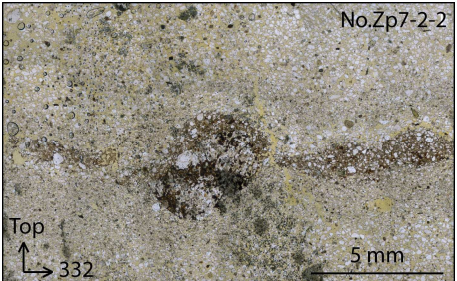
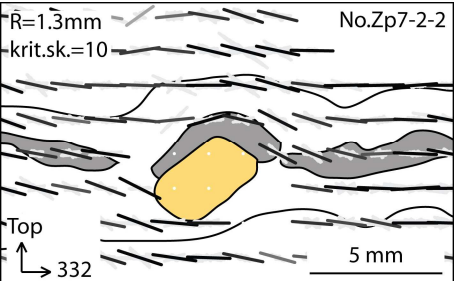
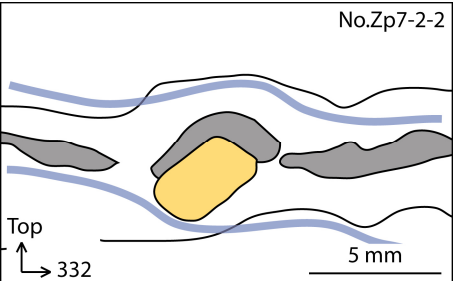
It is likely that clues about till formation can be found by studying the microfabric distribution around gravel grains. Four idealised basic microfabric distribution patterns around the gravel grain in a section parallel to local displacement direction are given in the Table 4.1. In the Table 4.2 a gallery of the microfabric distribution around gravel grains from vertical thin sections included in this study are presented.

Table 4.1. Idealised microfabric distribution patterns around a gravel grain in a vertical section parallel to the local displacement direction.

4.1. tabula. Idealizēti mikrolinearitātes sadalījuma veidi ap grants graudu, lokālajam pārvietojuma virzienam paralēlā, vertikālā griezumā.

Sketch		Name	Description
		Shearing without gravel grain	Microfabric distribution without gravel grain
		Shearing	Simple shear, steady-state gravel grain position (after Thomason, Iverson, 2006)
		Rotation	Simple shear, gravel grain rotation
		Lodgement	Lodgement – a discordance in microfabric distribution (after Thomason, Iverson, 2006)
		Compaction	Vertical compression due to pore water expulsion or debris rich ice melting – melt-out

Table 4.2. Gallery of microfabric distribution around gravel grains of vertical thin sections included in this study.  
 4.2. tabula. Mikrolinearitātes sadalījuma ap grants graudu šajā pētījumā izmantotajos vertikālajos plānslīpējumos.

Thin section identification	Thin section image	Microfabric distribution	Interpreted microfabric lines
<b>Shearing</b>			
Sandy shear zone in the base of the upper till at the Ziemupe site			
Sandy shear zone in the base of the upper till at the Ziemupe site			
<b>Rotation</b>			
<i>No certain cases found</i>			

*To be continued in the next page*

**Thin section identification**

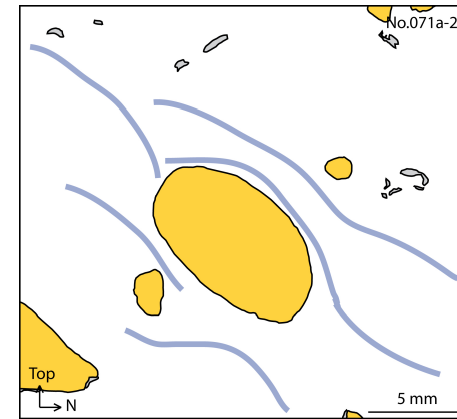
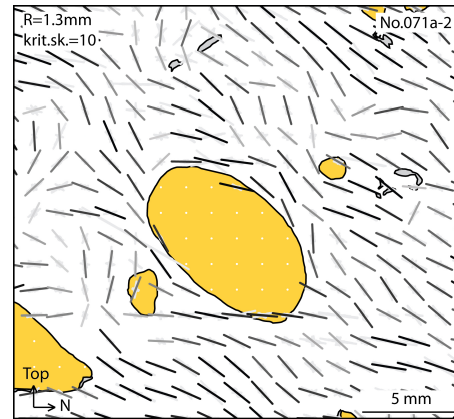
**Thin section image**

**Microfabric distribution**

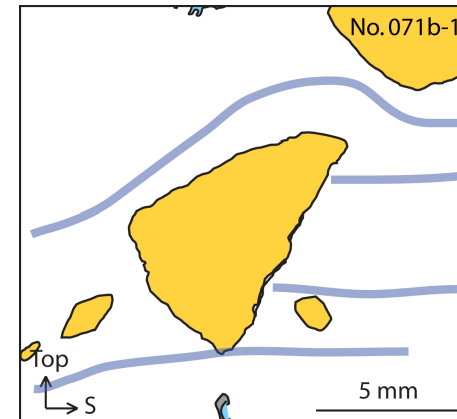
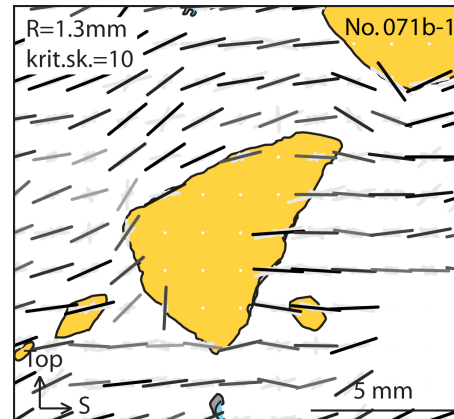
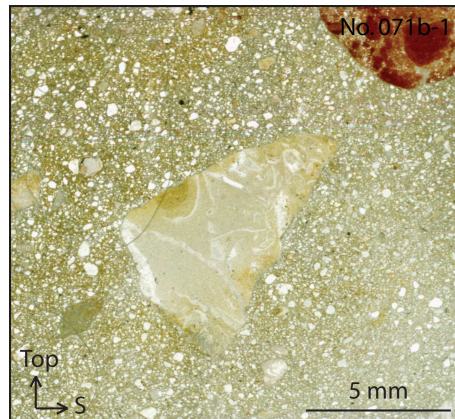
**Interpreted microfabric lines**

**Lodgement**

Upper till at the Sensala site



Upper till at the Sensala site



*To be continued in the next page*



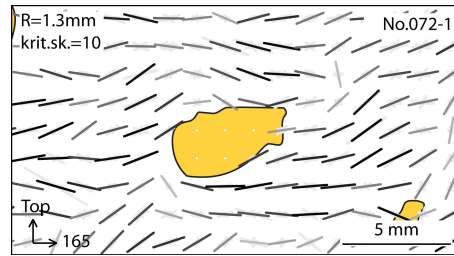
**Thin section identification**

Upper till at the Sensala site

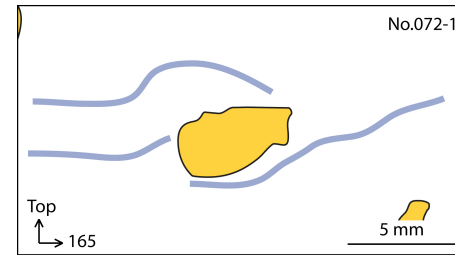
**Thin section image**



**Microfabric distribution**

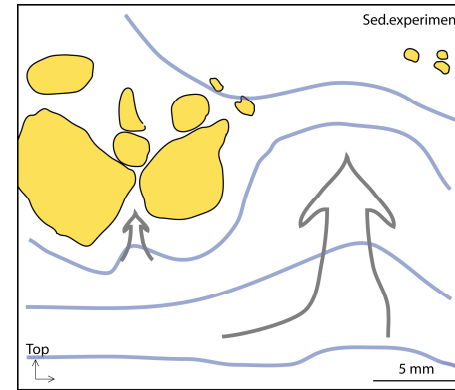
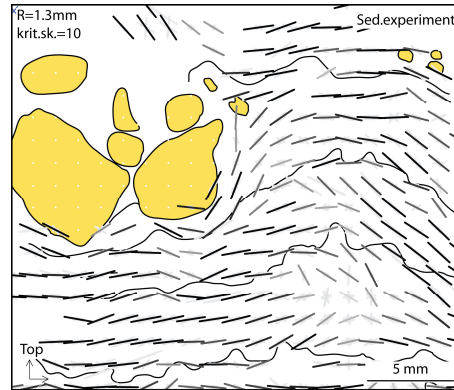
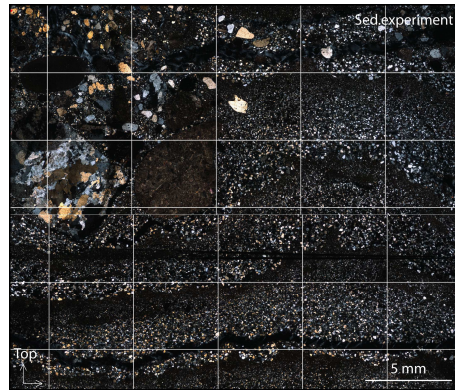


**Interpreted microfabric lines**



**Compaction**

Sedimentation experiment



*To be continued in the next page*



Thin section identification	Thin section image	Microfabric distribution	Interpreted microfabric lines
Waterlain till at the Sensala site			
Upper till at the Sensala site			
<b>Compaction or rotation</b>			
Waterlain till at the Sensala site			

*To be continued in the next page*

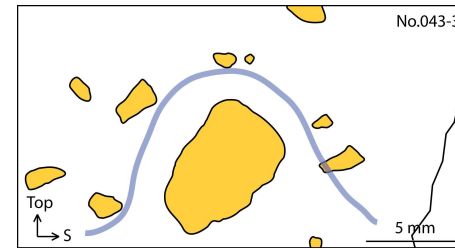
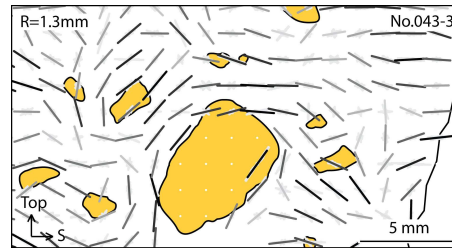
**Thin section identification**

**Thin section image**

**Microfabric distribution**

**Interpreted microfabric lines**

Upper till at the Sensala site



*To be continued in the next page*

**Thin section identification**

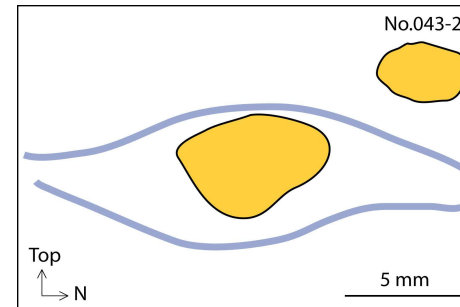
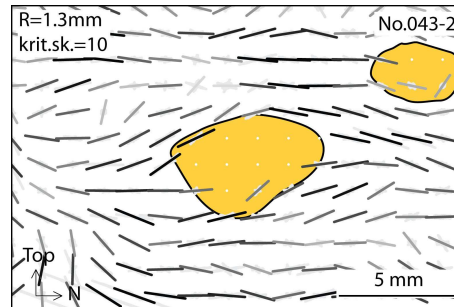
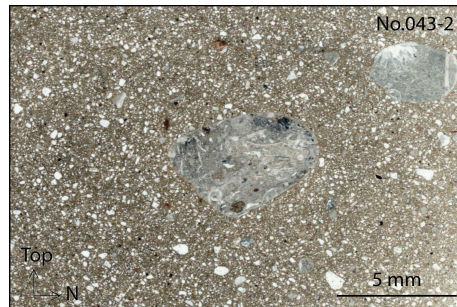
**Thin section image**

**Microfabric distribution**

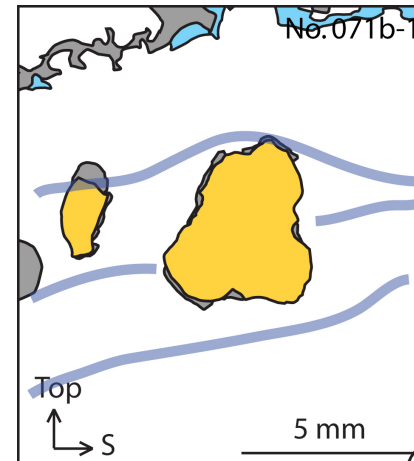
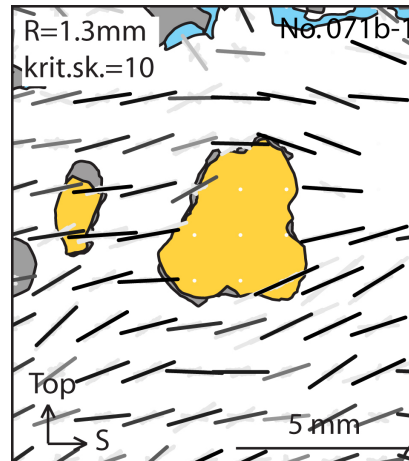
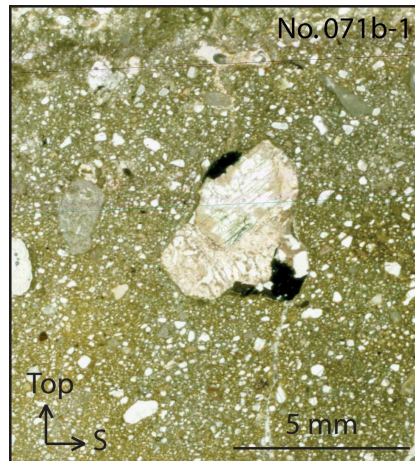
**Interpreted microfabric lines**

**Compaction or simple shear**

Upper till at the Sensala site



The upper till at the Sensala site



The identification of the sample orientation relative to former ice movement direction when a till was formed, the discrimination between different microfabric distribution patterns and collecting sufficiently large number of observations to perform at least semi-quantitative analyses are the most important problems encumbering the wider use of the presented approach of the till formation studies.

The Table 4.2 demonstrates that different microfabric distributions around gravel grains can be observed even in the parallel thin sections prepared from the same sample. It indicates that the presented methodology is not universal. It can be used only to collect semi quantities data to evaluated the till geneses as suggested by Carr (1999).

To use the described method for till formation studies, a good strategy for sample collection and thin section preparation must be elaborated. It is suggested that a hardened till sample need to be cut slice-by slice until sufficiently large gravel grain is exposed. Preparation of several parallel thin sections from single sample with different gravel grains exposed is favourable.

From the images presented in Table 4.2 conclusion about the till volume where orientation of the smaller particles is governed by the large one can be drawn. In most obvious influence of large clasts on orientation of sand grains is less than one diameter from the surface of the large clast.

Only from the Sensala site sufficiently large number of samples was collected to asses the abundance of different microfabric alignment patterns around gravel grains. In the sections of upper till mostly asymmetric microfabric distribution around gravel grains is observed. The spatial microfabric distribution structures around gravel grains in vertical sections in equal numbers are indicative of shearing as well as lodgement. The rotation structures are less common and compaction structures are not observed at all. The relatively small number of the studied cases (less than 10) does not allow drawing any firm conclusion.

As the compaction structures are not observed the melt-out genesis of the upper till unit can be excluded. Both the rotation and shearing structures can arise in deforming till in simple shear conditions. The same is true for lodgement as Evans *et al.* (2006) summarised that the lodgement can take place at the base of the deforming layer as well. It is unlikely that well expressed rotation or shear microfabric distributions would form if the dominant till formation process is lodgement and ploughing, that is inevitably accompanying lodgement.

Thus it can be concluded that the formation of the upper till at the Sensala site to some extent is a result of till deformation. Thus the motion of ice to some extent has been supported by substratum deformation. Lodgement, either at the base of deforming layer or at the sediment-ice interface, likely was one of the till accretion processes. However it must be noted, that a simple model of till formation in constant conditions is not likely as indicated by distinct microfabric strength separation in horizontal sections as well as inconsistent macrofabric at different measurement points.

#### **4.6. The methodological considerations**

To perform the microfabric distribution analysis of the till the need for automated methods are obvious as there are many thousands of elongated sand grains in a till volume as small as 1 cm<sup>3</sup> that can be measured.

There are several technically advanced analytical tools suitable for till microfabric analysis available such as X-ray tomography or magnetic susceptibility. There are published data regarding the use of X-ray tomography to analyses similar to tills (Videla *et al.*, 2007). However the tomography itself does not provide the microfabric data, a three

dimensional raster image is acquired instead. This three dimensional image needs further processing, possibly, using similar tools as in case two dimensional image. Actually the image analysis and data processing tools used for two dimensional images can be adopted for three dimensions images. However, the equipment for X-ray tomography with sufficient resolution is expensive and not readily available. A magnetic susceptibility are used to measure the till microfabric in some studies (e.g. Thomason, Iverson, 2009; Principato *et al.*, 2005). This method gives only summary microfabric orientation in a sample, not the spatial distribution of it additionally the individual particles contributing to the anisotropy of magnetic susceptibility can not be directly identified. Thus the thin section analysis, although somewhat old-fashion and comparably low-tech method, remain one of the most accessible tools for till microfabric spatial distribution studies.

The image analysis tools are the obvious solution for overcoming the labours manual measurements using microscope (e.g. Chaolu, Zhijiu, 2001) or digital images (e.g. Hart *et al.*, 2004). The image analysis methods can be divided in two groups: the object oriented approach – individual particles are identified for measurement – and statistical approach that involves determining some general statistical parameter of the image. The first one is straight forward extension of manual measurements of apparently elongated sand grains using microscope (e.g. Chaolu, Zhijiu, 2001) or macroscope (e.g. Carr 1999). The second approach has been tested with limited success by the Stroeven *et al.* (2001, 2005) by counting the number of the intersections of parallel lines (secants) crossing the image in different directions with the grain boundaries. The advantage of the later group of method is that the problems of identifying individual grains in images may be partly avoided.

It was possible to use the experience of manual microfabric measurement (Kalvāns, 2004) to develop procedures for microfabric data acquisition according to object oriented approach in an evolutionary manner. Therefore the object oriented approach was used in this study.

A simple colour thresholding is used to identify mostly quarts and feldspar sand-sized grains. However more sophisticated methods could be applied. The adopted approach is easily understandable and any problems with data quality that could arise from poor thin sections image quality or methodological shortcomings can be easily identified by visual inspection. The adoption of statistical approach would require more serious image analysis tools that could potentially lead to more complicated and inefficient image analysis and identification of methodological uncertainties.

Initiating the study author assumed that the use of dyed epoxy for the sample impregnation is the best approach to ensure easy thresholding in separating the sand grains and pores in the digital thin section images. In this case thin section images are attained using plain light, the pore space can be easily filtered out thanks to peculiar colour of dyed epoxy resin, the matrix can be separated due to its dark colour, and all the remaining light spots are sand-sized grains of transparent minerals (mostly quartz and feldspars). Thus, theoretically, parameters of almost all sand-sized particles can be included in the resultant data set. However the use acetone in case of several impregnation steps can result to diffusion of dye out of the already hardened resin producing uneven colouring that can hamper image thresholding.

Another approach is to acquire thin section images using cross polarised light. In this case all the pores and matrix are in dark colour as well as around half of the sand-sized particles. The remainder of sand-sized particles of most common minerals – quartz and feldspars – are in light colours and can be easily identified in digital images. The use of cross-polarised light reduces the number of grains appearing bright in a microscope however the contrast between these grains and the surrounding fine-grained matrix or pore

space is much larger than in the case of plain-light. Additionally the matrix colour in case of cross-polarised light is not as sensitive to thin section thickness as in case of plain light.

Theoretically more complete representation of microfabric is achieved using the first approach, but practically the image processing and thresholding procedures are more complicated and can introduce additional uncertainties in data set, so the second approach is considered to be superior. However in a different geological setting where dark mineral grains or polycrystalline grains dominate in sand size fraction is common this approach might not be the best one.

The composite image is best acquired by leaving buffer-lines between individual images rather than allowing touching or overlap of neighbouring images. Any grains cut by the buffer lines can be easily excluded from the data set, thus eliminating any distortion of calculated microfabric distribution that can arise due to tiny imperfections in alignment of individual images. It is found that due to spatially negligible fluctuations in image alignment joining or merging of overlapping image margins can produce linear zones across full thin section area of considerably and systematically distorted apparent microfabric representation. These zones can be eliminated manually – a cumbersome and time-consuming procedure. Thus the composite image acquisition with buffer-lines separating individual images is preferred.

For data visualisation the relative density plots (Fisher *et al.*, 1985) are preferred against traditional rose diagrams as the arbitrary chosen starting point of rose diagrams can introduce significant bias to the rose diagram appearance (Ballantyne, Cornish, 1979). For the same reason variations of the chi-square test as used by e.g. Hart *et al.* (2004) are not considered for data statistical analysis.

Finally, to evaluate fabric strength, the two-dimensional eigenvalue method re-introduced by Thomason and Iverson (2006) are preferred against the critical value of summary vector length as described by Davis (2002, pp. 322-330). Both methods give identical value of mean orientation and results can be visualized in a similar form. However the eigenvalue method is widely used to analyse the 3D macrofabric data in the glacial geology and thus are preferable for consistency reasons. Additionally the obtained value of fabric strength is not a simple “yes” or “no” as in case of summary vector length, but quantitatively describes data sets regardless of the number of measurements considered.



## Conclusions

Finally it can be concluded that the aim of the dissertation is reached and indicated tasks accomplished. As a result several important conclusions can be drawn, that are grouped there thematically:

### Study site-specific conclusions

- well sorted sediments, in a case of simple shear, are prone in developing considerably stronger and more uniform microfabric distributions than diamicton sediments;
- the odd joint system in a till at Plašumi gully site likely was developed in post-sedimentational processes that do not significantly affect the initial microfabric arrangement;
- the sandy diamicton at Strante site formed from sheared, with water oversaturated gradually deposited in form of tectonic slices, followed by vertical compaction due to pore water expulsion;
- the upper till at Sensala outcrop, at least partly, was formed as a deformation till;
- the till microfabric study results at Ziemupe, Strante and Sensala sites preclude existence of warm based glacier at the time.

### Till microfabric general characterisation

- a large diversity of microfabric distribution are found in the tills;
- summary microfabric orientation tend to be similar to the macrofabric orientation, however, the fabric strength is lower and usually microfabric strength in the horizontal sections are considerably smaller than in the vertical thin sections;
- a trend is observed that smaller particles tend to have lower fabric strength;
- four end members of the microfabric spatial distribution around gravel grains in the vertical thin sections are suggested: (1) shearing with stable gravel grain position; (2) shearing with gravel grain rotation; (3) gravel grain lodgement and (4) vertical compaction;
- The above described structures can be used for identification of till formation processes.

### Methodological considerations

- the best results for automated microfabric analysis can be achieved by obtaining thin section images using cross-polarised light;
- creating a composite thin section image it is advisable to introduce buffer lines between individual microphotograph, in order to avoid systematic errors in automatically measured microfabric that can arise from small errors in image alignment;
- the visualisation of measurements is best done using data density plots instead of traditional rose diagrams, and supplement it with the line indicating direction and strength of summary orientation;
- the orientation statistics shall be calculated using the eigenvalue method, so ensuring the compatibility with most macrofabric studies.

## References

- Āboltiņš, O., Dreimanis, A., 1995. Glacigenic deposits in Latvia. *In: Ehlers, J., Kozarski, S., Gibbard, P. (Eds.), Glacial Deposits in North-East Europe*. GA. A. Balkema, Rotterdam, pp. 115-124.
- Āboltiņš, O. P. Аболтиньш, 1986. Анализ трехосных линейных структурных элементов морен и интерпретация его результатов; Analiz tryokhosni'kh lineini'kh strukturni'kh elementov moren I interpretatsiya ego rezul'tatov. *In: Aboltins, O. P., Eberhards, G., Klane, V. (eds.), Морфогенез рельефа и палеогеография Латвии; Morfogenez rel'jefa i paleogeografiya Latvii.*, Латвийский государственный университет им. П. Стучки, Rīga, pp. 19-35.
- Āboltiņš, O. P. Аболтиньш, 1989. *Глациоструктура и ледниковый морфогенез*. Zinātne, Rīga, 284 c (in Russian)
- Allen, G. P., Hodgson, M. H., Flenley, J. R., Marsland, S. R., Flemmer, R. C., Arnold, G., Fountain, D. W., 2007. An Automated Pollen Recognition and Counting System. *Quaternary International 167-168, Supplement 1. Abstracts the XVII INQUA Congress 2007, Australia, 28 July - 3 August 2007*. 0910, p. 6.
- Alley, R. B., Cuffey, K. M., Evenson, E. B., Strasser, J. C., Lawson, D. E., Larson, G. J., 1997. How glaciers entrain and transport basal sediment: physical constraints. *Quaternary Science Reviews 16*, pp. 1017-1038.
- Alley, R. B., 2000. Continuity comes first: recent progress in understanding subglacial deformation. *In: Maltman, A. J., Hubbard, B., Hambrey, J. M. (eds.), Geological society special publication No. 176 "Deformation of glacial materials"*, London, pp. 171-179.
- Ballantyne, C. K., Cornish, R., 1979. Use of the chi-square test for the analysis of orientation data. *Journal of Sedimentary Petrology, 49*, pp. 0773-0776.
- Barnard, P. L., Rubin, D. M., Harney, J., Mustain N., 2007. Field test comparison of an autocorrelation technique for determining grain size using a digital 'beachball' camera versus traditional methods. *Sedimentary Geology 201*, pp. 180-195.
- Baroni, C., Fasano, F., 2006. Micromorphological evidence of warm-based glacier deposition from the Ricker Hills Tillite (Victoria Land, Antarctica). *Quaternary Science Reviews, 25*, pp. 976-992.
- Benn, D. I., Ringrose, T. J., 2001. Random variation of fabric eigenvalues: implications for the use of a-axis fabric data to differentiate till facies. *Earth Surface Processes and Landforms, 26*, pp. 295-306
- Benn, D. I., 1994. Fabric shape and the interpretation of sedimentary fabric data. *Journal of Sedimentary Research, 64*, pp. 910-915
- Benn, D. I., 2002. Discussion and reply: Clast-fabric development in a shearing granular material: Implications for subglacial till and fault gouge Discussion. *GSA Bulletin, 114*, pp. 382-384.
- Benn, D. I., Evans, D. J. A., 1996. The interpretations and classification of subglacially deformed materials. *Quaternary Science Reviews, 15*, pp. 23-52.
- Bennett, M. R., Waller, R. I., Glasser N. F., Hambrey M. J., Huddart D., 1999. Glacigenic clast fabrics: genetic fingerprint or wishful thinking? *Journal Of Quaternary Science 14*, pp. 125-135.
- Boulton, G., 1996. Theory of glacial erosion, transport and deposition as a consequence of subglacial sediment deformation. *Journal of Glaciology 42*, pp. 43-62.

Boulton, G. S., Dongelmans, P., Punkari, M., Broadgate, M., 2001a. Palaeoglaciology of an ice sheet through a glacial cycle: the European ice sheet through the Weichselian. *Quaternary Science Reviews* 20, pp. 591-625.

Boulton, G. S., Dobbies, K. E., Zatzepin, S., 2001b. Sediment deformation beneath glaciers and its coupling to the subglacial hydraulic system. *Quaternary International*, 86, pp. 3-28.

Camuti, K. S., McGuire, P. T., 1999. Preparation of polished thin sections from poorly consolidated regolith and sediment materials. *Sedimentary Geology*, 128, pp. 171-178.

Cañón-Tapia, E., Chávez-Álvarez, M. J., 2004. Rotation of uniaxial ellipsoidal particles during simple shear revisited: the influence of elongation ratio, initial distribution of a multiparticle system and amount of shear in the acquisition of stable orientation. *Journal of Structural Geology* 26, pp. 2073-2087.

Carr, S. J., Holmes, R., van der Meer, J. J. M., Rose, J., 2006. The Last Glacial maximum in the North Sea basin: micromorphological evidence of extensive glaciation. *Journal of Quaternary Science* 21, pp. 131-153.

Carr, S., 1999. The micromorphology of Last Glacial Maximum sediments in the Southern North Sea. *Catena* 35, pp. 123-145.

Carr, S., 2001. Micromorphological criteria for discriminating subglacial and glacial marine sediments: evidence from a contemporary tidewater glacier, Spitsbergen. *Quaternary International* 86, pp. 71-79.

Carr S. J., Hafliðason H., Sejrup H.P., 2000. Micromorphological evidence supporting Late Weichselian glaciation of the Northern North Sea. *Boreas* 29, pp. 315-328

Carr, S. J., Rose, J., 2003. Till fabric patterns and significance: particle response to subglacial stress. *Quaternary Science Reviews* 22, pp. 1415-1426.

Carr S. J., Holmes R., Van Der Meer J. J. M., Rose J., 2006. The last glacial maximum in the North Sea basin: micromorphological evidence of extensive glaciation. *Journal Of Quaternary Science* 2, pp. 131-153.

Carr, S. J., Goddard, M. A., 2007. Role of particle size in till-fabric characteristics: systematic variation in till fabric from Vestari-Hagafellsjó kull, Iceland. *Boreas* 36, pp. 371-385.

Carr, S. C., Lee, J. A., 1998. Thin-Section Production of Diamicts - Problems and Solutions. *Journal of sedimentary research* 68, pp. 217-220.

Ceriani, S., Mancktelow, N. S., Penacchioni, G., 2003. Analogue modeling of the influence of shape and particle /matrix interface lubrication on the rotation behaviour of rigid particles in simple shear. *Journal of Structural Geology* 25, pp. 2005-2021.

Cerina, A., 1999. Plant macrofossil assemblages of Eemian and Early Weichselian deposits in Latvia. In: *Field symposium on Pleistocene stratigraphy and glacial chronology. Southern Estonia, May 18-23, 1999, Estonia. Abstract volume*, University of Tartu, Tartu, pp. 26-27.

Chaolu, Y., Zhijiu, C., 2001. Subglacial deformation: evidence from microfabric studies of particles and voids in till from the upper Urumqi river valley, Tien Shan, China. *Journal of Glaciology* 4, pp. 607-612.

Charamisnava, A., 1971. Diatomavija vodarasci u marskix akladax Latvijskaj SSR. *Antropogen of Belarus. Navuka i Tehnika*, Minsk, pp. 213-219. (In Belarusian)

Curry, K. J., Abril, M., Avant, J. B., Curry, C., Bennett, R. H., Hulbert, M. H., 2002. A technique for processing undisturbed marine sand sediments and reconstructing fabric and porometry. *Journal of Sedimentary Research* 72, pp. 933-937.

Danilāns, I., И. Я. Даниланс, 1973. Четвертичные отложения Латвии. *Zinātne, Rīga*, pp. 312 (In Russian)

- Davis, J. C., 2002. *Statistics and data analysis in geology, third edition*. Mark Gerber (ed), John Wiley & Sons, pp. 638
- Dowdeswell, A. J., Sharp, M. J., 1986. Characterization of pebble fabrics in modern terrestrial glacial sediments. *Sedimentology* 33, pp. 699-710.
- Dreimanis, A. 1973. Tills, their origin and properties. In: Leggett, R. F. (ed.), *Glacial Till, Royal Society of Canada, Special Publication 12*, pp. 11-49.
- Dreimanis, A., 1981. The problems of waterlain tills. In: Mahoney, W. C. (ed), *Quaternary paleoclimate*, York Univ. GeoAbstrakts, Nowich, pp. 77-84.
- Dreimanis, A., 1989. Tills: Their genetic terminology and classification. In: Balkema, A. A. (ed), *Genetic classification of glacial deposits*, Brokfield, Rotterdam, pp. 17-83.
- Dreimanis, A., 1936. *Atšķirība starp augšējo un apakšējo morēnu Latvijā [Difference between upper and lower till in Latvia]*. University of Latvia, unpublished manuscript, pp. 126 (in Latvian)
- Dreimanis, A., 1999. A need of three-dimensional analysis of structural elements in glacial deposits for determination of direction of glacier movement. In: Mickelson, D. M., Attig, J. W. (Eds.), *Glacial Processes Past and Present. Special Paper 337*, Geological Society of America, Boulder, pp. 59-67.
- Elsen, J., 2006. Microscopy of historic mortars – a review. *Cement and Concrete Research* 36, pp. 1416-1424.
- Evans, D. J. A., Phillips, E. R., Hiemstra, J. F., Auton, C. A., 2006. Subglacial till: Formation, sedimentary characteristics and classification. *Earth-Science Reviews* 78, pp. 115-176.
- Evenson, E. B., 1970. A method for 3-dimensional microfabric analysis of tills obtained from exposures or cores. *Journal of Sedimentary Petrology* 40, pp. 762-764.
- Filler, S., Murray, T., 2000. Evidence against pervasive bed deformation during the surge of an Icelandic glacier. In: Maltman, A. J., Hubbard, B., Hambrey, M. J. (eds.), *Geological society special publication No. 176 "Deformation of glacial materials"*, United Kingdom Geological Society, London, pp. 181-190.
- Fisher, N. I., Huntington, J. F., Jackett, D. R., Willcox, M. E., Creasey, J. W., 1985. Spatial analysis of two-dimensional orientation data. *Mathematical Geology* 17, pp. 177-194.
- Fisher, N. I., 1989. Smoothing a sample of circular data. *Journal of Structural Geology*, pp. 775-778.
- Fitzsimons, S. J., Lorrain, R. D., Vandergoes, M. J., 2000. Behavior of subglacial sediments and basal ice in cold-based glacier. In: Maltman, A. J., Hubbard, B., Hambrey, M. J. (eds.), *Geological society special publication No. 176 "Deformation of glacial materials"*, United Kingdom Geological Society, London, pp. 181-190.
- Francus, P., 1998. An image-analysis technique to measure grain-size variation in thin sections of soft clastic sediments. *Sedimentary Geology* 121, pp. 289-298.
- Francus, P., 2001. Quantification of bioturbation in hemipelagic sediments via thin-section image analysis. *Journal of Sedimentary Research* 71, pp. 501-507.
- French, H. M., Guglielmin, M., 2000. Frozen ground phenomena in the vicinity of Terra Nova bay, northern Victoria land, Antarctica: a preliminary report. *Geografiska Annaler, Series A: Physical Geography*, 82, pp. 513-526.
- Gaigalas, A., Gudelis, V., Springis, K., Gaigalas, A., Gudelis, V., Springis, K., Konshin, G., Savvaitov, A., Veinbergs, I., Raukas, A. Konšins, Savvaitovs, Veinbergs, Raukas, A. Гайгалас, В. Гуделис, К. Спрингис, Г. Коншин, А. Савваитов, И. Вейнбергс, А. Раукас, 1967. Ориентовка длинных осей галек в моренах последнего

оледенения Прибалтики и ее связь с убиванием ледникового покрова. *Baltica 3*, "Academia", Vilnius, pp. 215-233.

Glen, J. W., Donner, J. J., West, R. G., 1957. On the mechanism by which stones in till become oriented. *American Journal of Science* 255, pp. 194-205.

Gumiaux, C., Gapais, D., Brun, J. P., 2003. Geostatistics applied to best-fit interpolation of orientation data. *Tectonophysics* 376, pp. 241-259.

Hambrey, M. J., Bennett, M. R., Glasser, N. F., Huddart, D., Crawford, K., 1999. Facies and landforms associated with ice deformation in a tidewater glacier, Svalbard. *Glacial Geology and Geomorphology*, 1999rp07, <http://boris.qub.ac.uk/ggg/papers/full/1999/rp071999/rp07.html>

Hambrey, M. J., Lawson, W., 2000. Structural styles and deformation fields in glaciers: a review. In: Maltman, A. J., Hubbard, B., Hambrey, J. M. (eds.), *Geological society special publication No. 176 "Deformation of glacial materials"*, London, pp. 59-83.

Harrell, J. A., Eriksson, K. A., 1979. Empirical conversion equations for thin-section and sieve derived size distribution parameters. *Journal of Sedimentary Petrology* 49, pp. 0273-0280.

Hart, J. K., 1998. The deforming bed/debris rich basal ice continuum and its implications for the formation of glacial landforms (flutes) and sediments (melt-out till). *Quaternary Science Reviews* 17, pp. 737-754.

Hart, J., Rose, J., 2001. Approaches to study of glacier bed deformation. *Quaternary International* 86, pp. 45-58.

Hart, J. K., 1994. Till fabric associated with deformable beds. *Earth surface processes and landforms* 19, pp. 15-32.

Hart, J. K., 1996. Subglacial deformation associated with a rigid bed environment, Aberdaron, North Wales. *Journal of Glacial Geology and Geomorphology*, RP01. <http://boris.qub.ac.uk/ggg>

Hart, J. K., 2006. An investigation of subglacial processes at the microscale from Briksdalsbreen, Norway. *Sedimentology* 53, pp. 125-146.

Hart, J. K., 2007. An investigation of subglacial shear zone processes from Weybourne, Norfolk, UK. *Quaternary Science Reviews* 26, pp. 2354-2374.

Hart, J. K., Khatwa, A., Sammonds, P., 2004. The effect of grain texture on the occurrence of microstructural properties in subglacial till. *Quaternary Science Reviews* 23, pp. 2501-2512.

Hicock, S. R., Goff, J. R., Lian, O. B., Little, E. C., 1996. On the interpretation of subglacial till fabric. *Journal of Sedimentary Research* 66, pp. 928-934.

Hiemstra, J. F., Rijdsdijk, K. F., 2003. Observing artificially induced strain: implications for subglacial deformation. *Journal Of Quaternary Science* 18, pp. 373-383.

Hiemstra, J. F., van der Meer, J. J. M., 1997. Pore-water controlled grain fracturing as an indicator for subglacial shearing in tills. *Journal of Glaciology* 43, pp. 446-454.

Hiemstra, J. F., Zaniewski, K., Powell, R. D., Cowan, E. A., 2006. Strain Signatures of Fjord Sediment Sliding: Micro-Scale Examples from Yakutat Bay and Glacier Bay, Alaska, U. S. A. *Journal of Sedimentary Research* 76, pp. 689-699.

Hindmarsh, R., 1997. Deforming beds: viscous and plastic scales of deformation. *Quaternary Science Reviews* 16, pp. 1039-1056.

Hindmarsh, R. C. A., Rijdsdijk, F. K., 2000. Use of a viscous model of till rheology to describe gravitational loading instabilities in glacial sediments. In: Maltman, A. J., Hubbard, B., Hambrey, M. J. (eds.), *Geological society special publication No. 176*

“*Deformation of glacial materials*”, United Kingdom Geological Society, London, pp. 191-201.

Hoffmann, K., Piotrowski, J. A., 2001. Till melange at Amdorf, central Germany: sediment erosion, transport and deposition in complex, soft-bedded subglacial system. *Sedimentary Geology* 140, pp. 215-234.

Hooke, R. LeB., Iverson, N. R., 1995. Grain-size distribution in deforming subglacial tills: Role of grain fracture. *Geology* 23, pp. 57-60.

Hooyer, T. S., Iverson, N. R., 2000. Clast-fabric development in a shearing granular material: Implications for subglacial till and fault gouge. *GSA Bulletin* 112, pp. 683-692.

Iverson, N. R., Cohen, D., Hooyer, T. S., Fischer, U. H., Jackson, M., Moore, P. L., Lappégard, G., Kohler, J., 2003. Effects of basal debris on glacier flow. *Science* 301, pp. 81-84.

Jakobsen, U., H., Pade, C., Thaulow, N., Brown, D., Sahu, S., Magnusson, O., De Buck, S., De Schutter, G., 2006. Automated air void analysis of hardened concrete – a Round Robin study. *Cement and Concrete Research* 36, pp. 1444-1452.

Jeffery, G. B., 1922. The motion of ellipsoidal particles immersed in a viscous fluid. *Proceedings of the Royal Society A (102)*, London, pp. 161–179.

Jim, C. Y., 1985. Impregnation of moist and dry unconsolidated clay samples using Spurr resin for microstructural studies. *Journal of Sedimentary Research* 55, pp. 597-599.

Johnson, M. D., 1983. The origin and microfabric of lake superior red clay. *Journal of Sedimentary Petrology* 53, pp. 0859-0873.

Jones, T. A., James, W. R., 1969. Analysis of Bimodal Orientation Data. *Mathematical Geology* 1, pp. 129-135.

Juškevičs, V., 1998. Kvartāra nogulumi. *Latvijas ģeoloģiskā karte. Mērogs 1:200000. 41. –Ventspils lapa. Paskaidrojuma teksts un kartes.* Valsts ģeoloģijas dienests, Rīga

Juškevičs, V., Kondratjeva, S., Mūrnieks, A., Mūrniece, A., 1997. *Latvijas ģeoloģiskā karte 1:200 000, 31. lapa - Liepāja, Paskaidrojuma teksts un kartes.* Valsts ģeoloģijas dienests, Rīga, pp. 48

Juškevičs, V., Kondratjeva, S., Mūrnieks, A., Mūrniece, A., 1998. *Latvijas ģeoloģiskā karte 1:200 000, 41.lapa - Ventspils, Paskaidrojuma teksts un kartes.* Valsts ģeoloģijas dienests, Rīga, pp. 48

Kalnina, L., 2001. Middle and Late Pleistocene environmental changes recorded in the Latvian part of the Baltic Sea basin. *QUATERNARIA Sre. A: Theses and Reserch Papers* 9, Department of Physical Geography and Quaternary Geology Stockholm University, Stoholma, pp. 173

Kalnina, L., Dreimanis, A., Murniece, S., 2000. Palynology and lithostratigraphy of Late Elsterian to Early Saalian aquatic sediments in the Ziemepe-Jurkalne area, Western Latvia. *Quaternary International* 68-71, pp. 87-109.

Kalvāns, A., 2004. Ledāja nogulumu mikromēroga uzbūve Sensalas atsegumā, Rietumlatvijā. *Maģstra darbs, Latvijas Universitāte, Rīga*, pp. 118. (in Latvian)

Kalvāns, A., Saks, T., 2004a. Ledāja nogulumu uzbūve mikro mērogā. *Izd.: Ģeogrāfija. Ģeoloģija. Vides zinātne. Latvijas Universitātes 62. zinātniskā konference. Referātu tēzes.* Latvijas Universitāte, Rīga, p. 143. (in Latvian)

Kalvāns, A., Saks, T., 2004b. Till micromorphology and microfabric in the Sensala outcrop, Western Latvia. In: Zelčs, V. (ed.). *International field symposium on quaternary geology and modern terrestrial processes, Western Latvia, Spetember12-17, 2004.* University of Latvia, Rīga, pp. 24-26.



Kalvāns, A., Saks, T., 2008. Two dimensional apparent microfabric of the basal Late Weichselian till and associated shear zone: case study from Western Latvia. *Estonian Journal of Earth Sciences* 57, pp. 241–255.

Kalvāns, A., Saks, T., 2009. Morēnas mikrolinearitāte – piemēri no Kurzemes Baltijas jūras stāvkrastiem. *Latvijas Universitātes 67. zinātniskā konference*. Latvijas Universitāte, Rīga, pp. 198-200. (in Latvian)

Kalvāns, A., Popovs, K., Saks, T., 2009. Vienkārša autokorelācijas algoritma lietojums smilts un aleirīta graudu izmēru sadalījuma fotogrammetriskai noteikšanai. *Krāj.: Ģeogrāfija. Ģeoloģija. Vides zinātne. Latvijas Universitātes 67. zinātniskā konference. Referātu tēzes*. Rīga, Latvijas Universitāte, pp. 201-202. (in Latvian)

Kalvāns, A., Saks, T., Klimovičs, J., 2007a. Subglaciālas bīdes joslas mikromorfoloģija: piemērs no Ziemeļpuses stāvkrasta. *Tēžu krāj. : Ģeogrāfija. Ģeoloģija. Vides zinātne. Latvijas Universitātes 65. zinātniskā konference*. Latvijas Universitāte, Rīga, pp. 148-149. (in Latvian)

Kalvāns, A., Saks, T., Zelcs, V., 2007b. 2D analysis of apparent till micro fabrics in thin sections: an example from Western Latvia. *Quaternary International* 167-168, Supplement 1. Abstracts the XVII INQUA Congress 2007, Australia, 28 July - 3 August 2007. 0293, p. 200.

Kalvāns, A., Saks, T., 2010. Mikrolinearitātes sadalījums ap grants graudiem, kā morēnas veidošanās apstākļu indikators. *Tēžu krāj. : Ģeogrāfija. Ģeoloģija. Vides zinātne. Latvijas Universitātes 68. zinātniskā konference. Referātu tēzes*. Latvijas Universitāte, Rīga, pp. 299-300. (in Latvian)

Khatwa, A., Tulaczyk, S., 2001. Microstructural interpretations of modern and Pleistocene subglacially deformed sediments: the relative role of parent material and subglacial processes. *Journal of Quaternary Science* 16, pp. 507-517.

Kjær, K. H., Krüger, J., 1998. Does clast size influence fabric strength?. *Journal of Sedimentary Research* 68, pp. 746-749.

Knight, J., 1999. Morphology and palaeoenvironmental interpretation of deformed soft-sediment clasts: examples from within Late Pleistocene glacial outwash, Tempo Valley, Northern Ireland. *Sedimentary Geology* 128, pp. 293-306.

Knight, P. G., Patterson, C. J., Waller, R. I., Jones, A. P., Robinson, Z. P., 2000. Preservation of basal-ice sediment texture in ice-sheet moraines. *Quaternary Science Reviews* 19, pp. 1255-1258.

Kock, I., Huhn, K., 2007. Influence of particle shape on the frictional strength of sediments — A numerical case study. *Sedimentary Geology* 196, pp. 217-233.

Konshin, G., Savvaitov, A., Slobodin, V., 1970. Marine intertill deposits of Western Latvia and some peculiarities of their development (Межморенные морские отложения западной Латвии и некоторые особенности их формирования). In: Danilāns, I. (ed.), *Questions of Quaternary Geology V (Вопросы четвертичной геологии, V)*, V. Zinātne, Rīga, pp. 37-48. (in Russian)

Krüger, J., Kjær, K. H., 2005. Fabric pattern in a basal till succession and its significance for reconstructing subglacial processes – discussion. *Journal of Sedimentary Research* 75, pp. 323–326.

Krumbein, W. C., 1939. Preferred orientation of pebbles in sedimentary deposits. *Journal of Geology* 37, pp. 673-706.

Kuehl, S. A., Nittrouer, C. A., De Master, D. J., 1988. Microfabric study of fine-grained sediments; observations from the Amazon subaqueous delta. *Journal of Sedimentary Petrology* 58, pp. 12-23.

- Lachniet, M. S., Larson, G. J., Lawson, D. E., Evenson, B. E., Alley, R. B., 2001. Microstructures of sediment flow deposits and subglacial sediments: a comparison. *Boreas* 30, pp. 254-262.
- Lachniet, M. S., Larson, G. J., Strasser, J. C., Lawson, E. D., Evenson, E. B., Alley, R. B., 1999. Microstructures of glacial sediment-flow deposits, Matanuska Glacier, Alaska. *Geological Society of America, Special Paper 337*, pp. 45-57.
- Larsen, K. N., Piotrowski, J. A., Kronborg, C., 2004. A multiproxy study of a basal till: a time-transgressive accretion and deformation hypothesis. *Journal of Quaternary Science* 19, pp. 9-21.
- Larsen, N. K., Piotrowski, J. A., 2003. Fabric pattern in a basal till succession and its significance for reconstructing subglacial processes. *Journal of Sedimentary Research* 73, pp. 725-734.
- Larsen, N. K., Piotrowski, J. A., 2005. Fabric pattern in a basal till succession and its significance for reconstructing subglacial processes – reply. *Journal of Sedimentary Research* 75 (2), pp. 323-326.
- Larsen, N. K., Piotrowski, J. A., Menzies, J., 2007. Microstructural evidence of low-strain, time-transgressive subglacial deformation. *Journal of Quaternary Science* 22, pp. 593-608.
- Li, D., Yi, C., Ma, B., Wang, P., Ma, C., Cheng, G., 2006. Fabric analysis of till clasts in the upper Urumqi River, Tian Shan, China. *Quaternary International* 154-155, pp. 19-25.
- Lindsay, J. F., 1970. Clast fabric of a till and its development. *Journal of Sedimentary Petrology* 40, pp. 629-641.
- Mair, K., Hazzard, J. F., 2007. Nature of stress accommodation in sheared granular material: Insights from 3D numerical modeling. *Earth and Planetary Science Letters* 259, pp. 469-485.
- Mandal, N., Misra, S., Samanta, S. K., 2005a. Rotation of single rigid inclusions embedded in an anisotropic matrix: a theoretical study. *Journal of Structural Geology* 27, pp. 731-743.
- Mandal, N., Samanta, S. K., Bhattacharyya, G., Chakraborty, C., 2005b. Rotation behaviour of rigid inclusions in multiple association: insights from experimental and theoretical models. *Journal of Structural Geology* 27, pp. 679-692.
- Mandl, G., de Jong, L. N. J., Maltha, A., 1977. Shear Zones in Granular Material. An Experimental Study of Their Structure and Mechanical Genesis. *Rock Mechanics* 9, pp. 95-144.
- March, A., 1932. Mathematische theorie der regelung nach der korngestalt bei affiner deformation. *Zeitschrift für Kristallographie* 81, pp. 285-297. (in German)
- Mark, D. M., 1973. Analysis of axial orientation data, including till fabrics. *Geological Society of America Bulletin* 84, pp. 1369-1374.
- May, R. W., Dreimanis, A., Stankowski, W., 1980. Quantitative evaluation of clast fabrics within the Catfish Creek Till, Bratville, Ontario. *Canadian Journal of Earth Sciences* 17, pp. 1064-1074.
- Mazzullo, J., Kennedy, S. K., 1984. Automated measurements of the nominal Section diameters of individual particles. *Journal of Sedimentary Petrology* 55, pp. 593-595.
- Mccarroll, D., Rijdsdijk, K. F., 2003. Deformation Styles as a Key For Interpreting Glacial Depositional Environments. *Journal of Quaternary Science* 18, pp. 473-489.
- Meirons, Straume, З. В. Мейронс, Я. А. Страуме, 1979. Cenozoic group (Кайнозойская группа). In: Геологическое строение и полезные ископаемые Латвии, Riga, pp. 176 – 264. (in Russian)

- Menzies, J., 2000a. Micromorphological analyses of microfabrics and microstructures indicative of deformation processes in glacial sediments. In: Maltman, A. J., Hubbard, B., Hambrey, M. J. (eds.), *Geological society special publication No. 176 "Deformation of glacial materials"*. United Kingdom Geological Society, London, pp. 245-257.
- Menzies, J., 2000b. Microstructures in diamictites of the lower Gowganda formation (Huronian), near Elliot Lake, Ontario: evidence for deforming-bed conditions at the grounding line?. *Journal Of Sedimentary Research* 70, pp. 210-216.
- Menzies, J., Taylor, J., 2002. Seismically induced soft-sediment microstructures (seismites) from Meikleour Western Strathmore Scotland. *Boreas* 32, pp. 314-327.
- Menzies, J., van der Meer, J. J. M., Rose, J., 2006. Till - as a glacial "tectomict", its internal architecture, and the development of a "typing" method for till differentiation. *Geomorphology* 75, pp. 172-200.
- Menzies, J., Zaniewski, K., 2003. Microstructures within a modern debris flow deposit derived from Quaternary glacial diamicton – a comparative micromorphological study. *Sedimentary Geology* 157, pp. 31-48.
- Mertens, G., Elsen, J., 2006. Use of computer assisted image analysis for the determination of the grain-size distribution of sands used in mortars. *Cement and concrete research* 36, pp. 1453-1459.
- Millar, S. W. S., Nelson, F. E., 2003. Influence of clast axial ratio on macrofabric strength in periglacial colluvium. *Journal of Sedimentary Research* 73, pp. 720-724.
- Murray, T., 1997. Assessing the paradigm shift: deformable glacier beds. *Quaternary Science Reviews* 16, pp. 995-1016.
- Murray, A. S., Wintle, A. G., 2000. Luminescence dating of quartz using an improved single-aliquot regenerative-dose protocol. *Radiation Measurements* 32, pp. 57-73.
- Ostry, R. C., Deane, R. E., 1963. Microfabric Analyses of Till. *Geological Society of America Bulletin* 74, pp. 165-168.
- Phillips, E. R., Auton, C. A., 2000. Micromorphological evidence for polyphase deformation of glaciolacustrine sediments from Strathspey, Scotland. In: Maltman, A. J., Hubbard, B., Hambrey, M. J. (eds.), *Geological society special publication No. 176 "Deformation of glacial materials"*. United Kingdom Geological Society, London, pp. 279-292.
- Piotrowski, J. A., Larsen, N. K., Menzies, J., Wysota, W., 2006. Formation of subglacial till under transient bed conditions: deposition, deformation, and basal decoupling under a Weichselian ice sheet lobe, central Poland. *Sedimentology* 53, pp. 83-106.
- Piotrowski, J. A., Larsen, N. K., Jungeba F. W., 2004. Reflections on soft subglacial beds as a mosaic of deforming and stable spots. *Quaternary Science Reviews* 23, pp. 993-1000.
- Piotrowski, J. A., Mickelson, D. M., Tulaczyk, S., Krzyszkowski, D., Junge, F. W., 2001. Were deforming subglacial beds beneath past ice sheets really widespread? *Quaternary International* 86, pp. 139-150.
- Piotrowski, J. A., Kraus, A. M., 1997. Response of sediments to ice-sheet loading in northwestern Germany: effective stresses and glacial-bed stability. *Journal of Glaciology* 43, pp. 495-502.
- Principato, S. M., Jennings, A. E., Kristjánssdóttir, G. B., Andrews, J. T., 2005. Glacial-marine or subglacial origin of diamicton units from the southwest and north Iceland shelf: implications for the glacial history of Iceland. *Journal of Sedimentary Research* 75, pp. 968-983.

Punkari, M., 1997. Subglacial processes of the Scandinavian Ice Sheet in Fennoscandia inferred from flow-parallel features and lithostratigraphy. *Sedimentary Geology* 111, pp. 263-283.

Rawling, G. C., Goodwin, L. B., 2003. Cataclasis and particle flow in faulted, poorly lithified sediments. *Journal of Structural Geology* 25, pp. 317-331.

Rechenmacher, A. L., 2006. Grain-scale processes governing shear band initiation and evolution in sands. *Journal of the Mechanics and Physics of Solids* 54, pp. 22-45.

Reynolds, S., Gorsline, D. S., 1992. Clay microfabric of deep-sea, detrital mud (stone)s, California continental borderland. *Journal of Sedimentary Petrology* 62 (1), pp. 41-53.

Roberts, D. H., Hart, J. K., 2005. The deforming bed characteristics of a stratified till assemblage in north East Anglia, UK: investigating controls on sediment rheology and strain signatures. *Quaternary Science Reviews* 24, pp. 123-140.

Rosas, F., Marques, F. O., Luz, A., Coelho, S., 2002. Sheath folds formed by drag induced by rotation of rigid inclusions in viscous simple shear flow: nature and experiment. *Journal of Structural Geology* 24, Pergamon, pp. 45-55.

Rubin, M. D., 2004. A Simple Autocorrelation Algorithm for Determining Grain Size from Digital Images of Sediment. *Journal of Sedimentary Research* 74, pp. 160-165.

Ruszczynska-Szenajch, H., 2001. "Lodgement till" and "deformation till". *Quaternary Science Reviews* 20, pp. 579-581.

Sakai, T., Yokokawa, M., Kubo, Y., Endo, N., Masuda, F., 2002. Grain fabric of experimental gravity flow deposits. *Sedimentary Geology* 154, pp. 1-10.

Saks T., Kalvāns a., Zelčs V., 2004. Stop 9: The cliff section at Strante. In: Zelčs V. (ed.), *International field symposium on quaternary geology and modern terrestrial processes, Western Latvia, Spetember12-17, 2004*, Latvijas Universitāte, Rīga, pp. 54-56.

Saks, T., Kalvāns, A., Zelčs, V., *in print*. OSL dating evidence of Middle Weichselian age of shallow basin sediments in Western Latvia, Eastern Baltic. *Quaternary Science Reviews (in print)*.

Saks, T., Kalvāns, A., Zelčs, V., 2010b *accepted for publication*. Subglacial bed deformation and glacial dynamics of the Apriķi glacial tongue, Western Latvia. *Boreas (accepted for publication)*.

Saks, T., Kalvāns, A., Zelčs, V., 2007. Structure and micromorphology of glacial and non-glacial deposits in coastal bluffs at Sensala, Western Latvia. *Baltica* 20, pp. 19-27.

Seelos, K., Sirocko, F., 2005. RADIUS – rapid particle analysis of digital images by ultra-high-resolution scanning of thin sections. *Sedimentology* 52, pp. 669-681.

Segliņš, V., 1987a. *Rietumlatvijas pleistocēna stratigāfija. Ģeoloģijas-mineraloģijas zinātņu kandidāta disertācija, Latvijas PSRS Ģeoloģijas pārvalde, Rīga*, pp. 285 (*in Russian*)

Segliņš, V., 1987b. *Стратиграфия плейстоцена западной Латвии. Автореферат диссертации кандидата геологических и минералогических наукю, Tallin*, pp. 14 (*in Russian*)

Siegert, M. J., 2000. Radar evidence of water-saturated sediments beneath the East Antarctic Ice Sheet. In: Maltman, A. J., Hubbard, B., Hambrey, M. J. (eds.) *Geological society special publication No. 176 "Deformation of glacial materials"*. United Kingdom Geological Society, London, pp. 217-229.

Sitler, R. F., Chapman, C. A., 1955. Microfabrics of till from Ohio and Pennsylvania. *Journal of Sedimentary Petrology* 25, pp. 262-269.

Sitler, R. F., 1963. Petrography of till from northeastern Ohio and northwestern Pennsylvania. *Journal of Sedimentary Petrology* 33, pp. 365-379.

Stephan, H. J., 1989. Origin of a till-like diamicton by shearing. *In: Goldthwait, R. P., Matsch, C. L. (eds.), Genetic Classification of Glacigenic Deposits.* Blakema, Rotterdam, pp. 93-96.

Stinkulis, Ģ., 1998. *Latvijas devona klastisko-karonātiežu un kaļķakmeņu pāreja zonu sedimentoloģija un mineraloģija. Promociajs darbs,* Latvijas Universitāte, Rīga, pp. 241 (in Latvian)

Stroeven, P., Stroeven, A. P., Dalhuisen, D. H., 2001. Image analysis of 'natural' concrete samples by automated and manual procedures. *Cement & Concrete Composites* 23, pp. 227-236.

Stroeven, P. A., Stroeven P., van der Meer J. J. M., 2005. Microfabric analysis by manual and automated stereological procedures: a methodological approach to Antarctic tillite. *Sedimentology* 52, pp. 219-233.

Svärd, N. M. M., Johnson, M. D., 2003. Micromorphology and fabric of sandy loam till, West-central Wisconsin. *The Geological Society of America, North-Central Section - 37th Annual Meeting (March 24-25, 2003), Kansas City, Missouri, USA, Paper No. 13-16,* [http://gsa.confex.com/gsa/2003NC/finalprogram/abstract\\_49197.htm](http://gsa.confex.com/gsa/2003NC/finalprogram/abstract_49197.htm) (skat. 07.09.2010.)

Thomason, J. F., Iverson, N. R., 2006. Microfabric and microshear evolution in deformed till. *Quaternary Science Reviews* 25, pp. 1027-1038.

Thomason, J. F., Iverson, N. R., 2009. Deformation of the Batestown till of the Lake Michigan lobe, Laurentide ice sheet. *Journal of Glaciology* 55, pp. 1-17.

Tovey, N. K., Dadey, K. A., 2002. Quantitative orientation and micro-porosity analysis of recent marine sediment microfabric. *Quaternary Science Reviews* 92, pp. 89-100.

Tulaczyk, S. M., Scherer, R. P., Clark, C. D., 2001. A ploughing model for the origin of weak tills beneath ice streams: a qualitative treatment. *Quaternary International* 86, pp. 59-70.

Ulsts, W., Majore, J., 1964. Roundness of hornblende grains as basis for stratigraphic subdivision of morainic deposits of the western part of the USSR (Стратиграфическое расчленение ледниковых отложений запада Европейской части СССР по окатанности зерен роговой обманки). *In: Danilāns, I. (ed.), Questions of Quaternary Geology III (Вопросы четвертичной геологии, III),* Zinātne, Rīga, pp. 33-61 (in Russian)

van der Meer, J. J. M., 1993. Microscopic evidences of subglacial deformation. *Quaternary Science Reviews* 12, pp. 553-587.

van der Meer, J. J. M., 1996. Micromorfology. *In: Menzies, J. (ed.), Past Glacial Environments: Sediments, Forms and Techniques.* Butterworth-Heinemann Ltd., Oxford, UK, pp. 335-355.

van der Meer, J. J. M., 1997. Particle and aggregate mobility in till: microscopic evidence of subglacial processes. *Quaternary Science Reviews* 16, pp. 827-831.

van der Meer, J. J. M., Menzies, J., Rose, J., 2003. Subglacial till: the deforming glacier bed. *Quaternary Science Reviews* 22, pp. 1659-1685.

van der Meer, J. J. M., Rabassa, J. O., Evenson, E. B., 1992. Micromorphological aspects of glaciolacustrine sediments in northern Patagonia, Argentina. *Journal of Quaternary Science* 7, pp. 31-44.

van der Wateren, F. M., 1995. Processes of glaciotectonism. *In: Menzies, J. (ed.), Modern glacial environments: processes, dynamics and sediments.* Butterworth-Heinemann Ltd., Oxford, UK, pp. 309-333.

van der Wateren, F. M., 1999. Structural geology and sedimentology of the Heiligenhafen till section, Northern Germany. *Quaternary Science Reviews*, 18, pp. 1625-1639.

van der Wateren, F. M., Kluiving, S. J., Bartek, R., 2000. Kinematic indications of subglacial shearing. In: Maltman, A. J., Hubbard, B., Hambrey, M. J. (eds.), *Geological society special publication No. 176 "Deformation of glacial materials"*. United Kingdom Geological Society, London, pp. 231-242.

Veinbergs, I., 1964. Coastal morphology and dynamics of the Baltic Ice Lake on the territory of the Latvian SSR (Морфология и динамика берегов Балтийского Ледникового озера на побережье Латвийской ССР). In: Danilāns, I. (ed.), *Questions of Quaternary Geology III (Вопросы четвертичной геологии, III)*. Zinātne, Rīga, pp. 331-369. (in Russian)

Veinbergs, I., Savvaitov, A., 1970. Текстурные особенности верхней части морских межморенных отложений участка Юркане – Улмале как показатели условий их образования (Teksturuie osobenosti verkhnei chasti morskikh mezhmornnuikh otlozhenii uchastka Yurkalne – Ulmale kak pokazateli uslovii ix obrazovaniya; Structural features of the upper part of marine intertill deposits in the Jurkalne-Ulmale area as indicators of the conditions of the deposition). In: Danilāns, I. (ed.), *Вопросы четвертичной геологии (Voprosy chetvertichnoj geologii 5 (Questions of Quaternary Geology V)*. Zinātne, Rīga, pp. 65-76. (in Russian)

Videla, A. R., Lin, C. L., Miller, J. D., 2007. 3D characterization of individual multiphase particles in packed particle beds by X-ray microtomography (XMT). *International Journal of Mineral Processing* 84, pp. 321-326.

Waller, R. I., Hart, J. K., 1999. Mechanisms and Patterns of Motion Associated with the Basal Zone of the Russell Glacier, South-West Greenland. *Glacial Geology and Geomorphology*, <http://boris.qub.ac.uk/ggg/papers/full/1999/rp021999/rp02.html>

Wright, J. S., 1995. Glacial comminution of quartz sand grains and the production of loessic silt: a simulation study. *Quaternary Science Reviews* 14, pp. 669-680.

Yamamoto, K., Nishiwaki-Nakajima, N., 1993. Automatic Analysis of Geological Structure from Dip-Strike Data. *Mathematical Geology* 25, pp. 819-832.

Zaniewski, K., van der Meer, J. J. M., 2005. Quantification of plasmic fabric through image analysis. *Catena* 63, pp. 109-127.

Zelčs, V., Markots, A., 2004. Deglaciation history of Latvia. In: Ehlers, J., Gibbard, P. L. (eds.), *Extent and Chronology of Glaciations, v. 1 (Europe)*. Elsevier, pp. 225-244.

Zelčs, V., Dreimanis, A., 1997. Morphology, internal structure and genesis of the Burtnieks drumlin field, Northre Vidzeme, Latvia. *Sedimentary Geology* 111, pp. 73-90.

Zelčs, V., Kalvāns, A., Saks, T. and Ceriņa, A., 2004. STOP 7: The Cliff Section between Gullies at Plašumi and Gudenieki. In: Zelčs V. (ed.), *International Field Symposium on Quaternary Geology and Modern Terrestrial Processes, Western Latvia, September 12-17, 2004: Excursion Guide*. University of Latvia, Rīga, pp. 43-47.



# Appendix 1

## A primary literature review of till micro fabric studies Morēnas mikrolinearitātes pētījumu primārās literatūras apskats

Paper (micro fabric application)	Till type  Thinsection orientation	Measurements  Statistical indicators	Spatial distribution	Sorting effects  Micro fabric of different grain sizes	Micro fabric versus macro fabric and ice movement direction	Conclusions	Comments
Hart <i>et al.</i> , 2004  (primary method)	Modern subglacial deformation tills  Three orthogonal sections aligned according to ice movement direction	100 largest clasts in whole slide and up to 100 clasts in homogenous areas and specific features, by manually selecting the grains in a digital image to be measured automatically.  Tukey test (a variety of $\chi^2$ test) to calculate whether micro fabric is anisotropic and R-mag – a resultant mean vector length	Stronger micro fabric along the larger clasts.	Better sorting (fewer large clasts) will led to deformation tills with stronger elements as large clasts will induce rotation structures and disorientation of smaller ones  Measurement of larges clasts in studied thinsection areas is deemed to exclude the blurring effects of smaller particles rotating around large ones	Not mentioned	Some samples exhibited very highly oriented microfabric with a small dip upglacier. Better sorted deformation tills exhibit stronger microfabric compared to less sorted tills. The till deformation is a patchwork of simple shear and rotational structures.	
Roberts, Hart (2005)  (secondary method)	Deformation till  Vertical	Minimum of 30 sand-size grains, the measurement methodology is not specified.  Anisotropy – low or high	Not specified			Micro fabric anisotropy – generally low, that is well expressed preferred orientation.	

Paper (micro fabric application)	Till type Thinsection orientation	Measurements Statistical indicators	Spatial distribution	Sorting effects Micro fabric of different grain sizes	Micro fabric versus macro fabric and ice movement direction	Conclusions	Comments
Carr, Rose, 2003  (primary topic)	Subglacial tills  Horizontal	Sand-sized grains with a-b axis ratio $\geq 1.5$ in three size-classes: 5–1 mm, 1000–500 $\mu\text{m}$ and 500–250 $\mu\text{m}$ ; 28 to 91 grains measured in a projection of thinsection.  after Curray (1956): orientation of resultant vector and vector magnitude	A considerable variations from thinsection to thinsection has been identified and were explained by sampling positions in stoss and lee sides of prominent boulder	Not studied  Progressive decrease in fabric strength with decreasing particle size. A relationship between grain size and dominant orientation direction is observed with dominant mode switching from transverse to parallel orientation and back.	Only 56% (out of 32 sets of measurements) dominant micro fabric orientation are parallel to ice movement direction	Particles of different size are rarely oriented consistently and in relation to ice flow direction.	Authors suggest that relation of different size-particles orientation can be used to identify reconstruct the deformation history of sediments
Ostry, Deane, 1963  (primary topic)	Subglacial tills  Horizontal	100 elongated coarse fragments in thinsection measured using microscope with rotational stage  Visual inspection of rose diagrams	Use of several samples from one location is suggested	Not studied  Not studied	Most of the 32 studied cases demonstrated striking similarity between shape of rose diagrams of macro fabric (elongated pebbles 1 to 20 cm large) and micro fabric	Micro fabric measurements in thinsections can be used as an effective substitution for laborious till macro fabric measurements in the field.	This is one of the first papers advocating that till micro fabric and macro fabric orientation is similar
Carr, 1999  (secondary method)	Subglacial till  Vertical	Up to 200 sand size grains measured in thin-section projections and visualised as half-rose diagrams  Calculating vector mean and vector magnitude	Not studied	Not studied  Not studied	Not studied	The sub-horizontal or bi-modal micro fabric distribution is indication that sediments were subjected to uni-modal stress field.	Some of the samples were taken by vibration corer that can significantly affect the micro fabric distribution in poorly lithified sediments.  Micro fabric in the Holocene sediments was uni-modal, sub-vertical, contrasting to sub horizontal sometimes bi-modal micro fabric distribution in older glacial or glacially affected sediments.

Paper (micro fabric application)	Till type Thinsection orientation	Measurements Statistical indicators	Spatial distribution	Sorting effects Micro fabric of different grain sizes	Micro fabric versus macro fabric and ice movement direction	Conclusions	Comments
Thomason, Iverson, 2006  (primary topic)	Till sheared ring-shear apparatus; two subglacial tills were tested  Vertical	All particles with long axis greater than 0.1mm in several microphotographs (100 to 300 grains) using NIH Image software (freeware)  An eigenvalue method suggested by Mark (1973) and adopted for two dimensions	Strong mono-modal and consistent micro fabric was developed in the shear zone in contrast to random orientation in un-sheared sediments	The steady-state fabric strength was similar for both tills, but was faster attained in less-well sorted till (Batestown Member till: 17% gravel, 49% sand, 34% silt/clay) than in the better sorted till ( <i>Douglas Member till: 5% gravel, 72% sand, 23% silt/clay</i> ).  Slightly stronger micro fabric was observed for larger grains (>250µm) than for smaller ones (100-250 µm)	The micro fabric was similar but weaker than the macro fabric developed in previous experiments (Hooyer, Iverson, 2000)	Stable-state up-shear dipping (12°) mono-modal preferred micro fabric orientation is attained after shear strain of 7 to 39 with S1 eigenvalues of 0.71–0.74. Fabric strength did not decrease until maximum shear strain of 108 achieved in experiments.  The micro fabric strength can be used as indicator of strain rate of the diamicton.	
Johnson, 1983  (primary topic)	glaciolacustrine clays or deformation till (clay content up to 85%)  Horizontal section and vertical section cut in the direction of major micro fabric mode in horizontal section	50 to 150 grains were measured on the projection of thinsection, with elongation ration no less than 1.5  Visualisation in rose diagrams and half-rose diagrams. The major mode was determined using moving average technique and fitting ellipse template.	Not studied	Samples with small sand content (3-6%) tended to have transverse, sandy samples (5-14%) tended to have parallel micro fabric orientation relative to ice advance direction, although the relation is not universal and overlap was observed  Not studied	In most samples dominant micro fabric orientation is either perpendicular or parallel to independently known ice movement direction. Only two out of 25 samples have not majore micro fabric mode.	Micro fabric is related to ice advance direction. It sees that in a case of clay-rich tills in creased sand content facilitates development of parallel micro fabric opposite to transverse micro fabric in tills with smaller clay content.	A preferred transverse orientation of micro fabric was observed in cases when micro foliation was observed, that coincides with large clay content.

<b>Paper (micro fabric application)</b>	<b>Till type</b>	<b>Measurements</b>	<b>Spatial distribution</b>	<b>Sorting effects</b>	<b>Micro fabric versus macro fabric and ice movement direction</b>	<b>Conclusions</b>	<b>Comments</b>
	<b>Thinsection orientation</b>	<b>Statistical indicators</b>		<b>Micro fabric of different grain sizes</b>			
Principato <i>et al.</i> , 2005  (secondary method)	Basal till and glaciomarine deposits, dominantly silt and clay rich sediments with sand content in range form approximately 20-60%	anisotropy of magnetic susceptibility (AMS)					A indicator of basal till is sheared – anisotropic – micro fabric that is in contrast to isotropic fabric of un-sheared sediments deposited in water.
	Not applicable						
Evenson, 1970  (a method paper)	Not applicable  Horizontal and vertical, parallel to major mode of horizontal apparent micro fabric	In the projection using ellipse templates or major/minor projections  Visual inspection or vector mean method	Not studied	Not studied  Not studied	Stated excellent agreement of micro fabric and macro fabric orientation, but not actually studied	An introduction of method	
Svärd, Johnson, 2003  (conference thesis)  (primary method)	Sandy basal till of recent continental glaciation in North America  Not specified	Not specified  Eigenvalue as fabric strength indicator	Not studied	Not studied  Not studied	Micro fabric of sand size grains predominantly parallel to macro fabric. Fabric strength measured as eigenvalues did not correlated for macro fabric and micro fabric.		

Paper (micro fabric application)	Till type Thinsection orientation	Measurements Statistical indicators	Spatial distribution	Sorting effects Micro fabric of different grain sizes	Micro fabric versus macro fabric and ice movement direction	Conclusions	Comments
Hart, 2007	Chalk-rich (in some cases more than 70%) sandy subglacial deformation till, Anglian glaciation, oxygen stable isotope stage (MIS) 12  Three mutually perpendicular thins sections aligned according to local ice movement direction as indicated by macro fabric data. Unfortunately the micro fabric observed in differently oriented thinsections was not discussed sufficiently in the paper.	Semi-automated procedure of measuring up to 100 long axis of sand grains using VIPS software (Cupitt, Martinez, 1996) in: (a) whole slide; (b) homogeneous; (c) special areas of interest.  Tukey test (a variety of $\chi^2$ test) with two degrees of freedom for bipolar orientation data	Different micro fabric strength between bands of different composition was observed.	The grain size distribution was evaluated by calculating the standard deviation of the size of micro fabric measurement data. A strong correlation is found between the micro fabric strength and this sorting indicator. Tills with wide grain size distributions have weaker micro fabric. The opposite is observed in banded tills where chalk-rich laminas have stronger micro fabric than the sandy ones despite wider grain size distribution.  Fine-grained, chalk-rich bands in banded till had stronger micro fabric than coarse-grained sandy bands.	Not described	Results suggest that fabric strength (at all scales) is determined by the combined processes of rotation and/or attenuation within the deforming layer and the resultant strength depends on sorting and grain size.	The fabric strength difference in sandy bands and chalk-rich bands in banded till probably is due to different internal friction angle in sandy and chalk-rich diamicton. The chalk-rich bands probably were weaker and underwent plastic deformation whilst stronger sandy bands behaved as a competent body.  From the photographs in article it seems that chalk-rich bands in micro-scale are matrix-supported and sandy ones skeleton-supported.

Paper (micro fabric application)	Till type Thinsection orientation	Measurements Statistical indicators	Spatial distribution	Sorting effects Micro fabric of different grain sizes	Micro fabric versus macro fabric and ice movement direction	Conclusions	Comments
Carr, Goddard, 2007  (primary topic)	Deformation till of a recent surge of Vestari-Hagafellsjökull glacier, Iceland  Orthogonal thinsections sets were prepared; micro fabric data of horizontal sections is only presented in the paper	Fabric measurement was split in size classes – a-axis: 8-16 mm and 16-32 mm (measured in the field as macrofabric); 4-8 mm; 2-4 mm; 1-2 mm; 0.5-1 mm; 0.25-0.5 mm – in thinsections. All grains longer than 2 mm present in thinsection were measured and more than 32 grains in each class smaller than 2mm were measured using sampling gird. A projection microscope was used.  Vector mean and vector magnitude was calculated for micro fabric (<8mm) data and eigenvalue analyst was used for macro fabric data (>8mm).	Not studied	Not studied  A clear relationship between grain size and orientation was observed: the 16-32mm size clasts were consistently oriented parallel to ice advance direction and 8-16 mm were perpendicular to it. The micro fabric was not as well expressed, but inconsistent orientation among size classes was observed as well.	A micro fabric was weaker compared to macro fabric. A transverse or parallel of major modes of orientation was observed, different for different sized grains.	It was suggested that particle-size had a significant control on the dominant orientation and it was likely that often observed multimodal distribution was a result of different-size particles having different dominant orientation. In most cases the fabric modes were either parallel or transverse to ice advance direction. The findings that fabric particle orientation was according to March model should be treated with caution as transverse orientation (Jeffery's and Taylor models) in some size-classes were predominant.	The weak leg of the study was small measurement number: in most cases 50 or less.
Carr, 2001  (primary method)	Sandy undisturbed glaciomarine sediments, glacially over-ridden glaciomarine sediments and modern subglacial clay-rich till  Vertical, orientation not specified	Using projection microscope  Visualisation as half-rose diagrams	Not studied	Not studied  Not discussed, but it seems to be comparable	Not studied	A bimodal micro fabric distribution in vertical sections observed for deformation till. A sub horizontal micro fabric was reported for glaciomarine deposits.	



Paper (micro fabric application)	Till type Thinsection orientation	Measurements Statistical indicators	Spatial distribution	Sorting effects Micro fabric of different sizes	Micro fabric versus macro fabric and ice movement direction	Conclusions	Comments
Stroeven <i>et al.</i> , 2001, 2005  (primary topic, methodology paper)	Antarctic tillite  Two an-orthogonal vertical sections	Directed secants intersection number with grain boundaries circle with diameter 7.5mm (manual procedure) of grains >120µm and 340x340 pixels area for automated procedure  Visualised as rose diagrams and mode determined by curve-fitting algorithm for second order polynomial. The 3D plunge was calculated from apparent plunges in two vertical sections.	Inconsistent in short distances (with in a single thinsection). A vague structural boundary was indentified.	Not studied  Not studied	Not studied	Automated procedure did not produced agreeable results. A steeply dipping (68°) and spatially variable micro fabric were interpreted as shear fabric.  A large number of micro fabric samples were required to reconstruct the reliable macro-structural information.	It was discussed that till was extremely heterogeneous sediment in all scales and therefore it was impossible to define the sample size need for reliable measurement of its properties.
Hart, 2006  (one of primary topics)	Modern, fluted deformation till from small outlet glacier in Norway  Three mutually perpendicular thinsections aligned according to ice advance direction	Semi-automated procedure of measuring up to 100 long axis of sand grains using VIPS software (Cupitt and Martinez, 1996) in: (a) whole slide; (b) homogeneous; (c) special areas of interest.  Tukey test (a variety of $\chi^2$ test) and R-mag – strength of variation around the mean for anisotropic samples	A „milonite” structure was identified as zone of angular, elongated grains aligned in the same direction as well as grain alidgements. The fabric strength was varied in different identified textures.	According to presented data, stronger micro fabric was observed for fine grained, better sorted sediments.  Sediments composed of similar-size grains (better sorted) tended to have stronger micro fabric in comparision to less well sorted sediments.			When excluding two extremely large $\chi^2$ values from the reported data a good inverse linear correlation ( $R^2=0.58$ ) can be observed between the grain size standard devotion (SD) and $\chi^2$ values. A trend for stronger fabric is observed for smaller measured average grain sizes ( $R^2=0.69$ and $0.71$ for slide scale and 40x magnification respectively) as well.

Paper (micro fabric application)	Till type Thinsection orientation	Measurements Statistical indicators	Spatial distribution	Sorting effects Micro fabric of different grain sizes	Micro fabric versus macro fabric and ice movement direction	Conclusions	Comments
Thomason, Iverson, 2009 (primary topic)	Pleistocene till, Lake Michigan lobe, Laurentide ice sheet, 20 and 50 km up-glacier margin	AMS and apparent sand particle orientation in thinsections along a profile, with 0.2m intervals.  Sand grain measurement was done according methodology of Evenson (1971) in two orthogonal, horizontal and vertical thinsections. All particles with long axis $\geq 0.1$ mm and aspect ratio $\geq 1.5$ were measured in five to seven microphotographs of every thinsection. The number of measured grains is not indicated. Eigenvalues (Mark, 1973) were calculated for vertical apparent sand grain orientation and AMS fabric of 25 samples collected at each sampling depth.	In vertical profile a gradual shift of dominant micro fabric orientation was observed, interpreted as representing the gradual change of local ice movement direction. AMS fabric exhibited more consistent results than the apparent sand grain orientation. From sample to sample the sand fabric strength was variable. In vertical sections random to strong micro fabric was observed with dominant orientation in sub-horizontal to almost vertical direction.	Not studied.  Not studied.  Difficult to extract any credible information from presented data.	Not studied.	The micro fabric was deemed to be indicative of subglacial deformation simple shear direction as suggested by experimental results. The micro fabric indicated that deformation depth was only few decimetres and that only approximately 50% of till thickness had undergone simple shearing to moderate value of 7 to 30 needed to attain stable-state micro fabric orientation at the last stage of deformation.	
Carr <i>et al.</i> , 2000 (a method paper, microfabric studies is one of the methods)	Pleistocene basal till and glacio-marine sediments  Vertical sections, with non-specified orientation and a single horizontal section.	Measured using projection microscope	Not studied	Not studied  Not studied	Not studied	Argued that sub-vertical microfabric in diamicton was indicative of sand grain falling through still water column (glaciomarine sediments). Subhorizontal microfabric was suggested to be indicative of deformation till.	It could be inferred that the subverted sand-grain microfabric should develop only when there was fine-grained matrix where sand grains could slowly settle and the sedimentation occurred in truly standing waters.

Paper (micro fabric application)	Till type Thinsection orientation	Measurements Statistical indicators	Spatial distribution	Sorting effects Micro fabric of different sizes	Micro fabric versus macro fabric and ice movement direction	Conclusions	Comments
Carr <i>et al.</i> , 2006 (one of the methods)	Pleistocene basal till and glacio-marine sediments  Mostly vertical, with non-specified orientation, and some horizontal. Microfabric studied only for vertical sections.	Measured using projection microscope  Measured at least 50 randomly selected 0.25 to 1.00 mm sand grains; visual interpretation of half-rose diagrams	Not studied	Not studied  Not studied	Not studied		The micromorphological results supports the suggestion of Carr (1999) and Carr et al. (2000), that sub-vertical microfabric is assumed for water-lain sediments; non-vertical unimodal or bi-modal distribution is considered to be indicative of unidirectional (glacial) stress. In some cases very weak subhorizontal secondary mode is observed in the sections of water-lain sediments.
Chaolu, Zhijiu, 2001 (Primary topic)	Subglacial and end moraine till of latest (Wangfeng) glacial advance in Tien Shan, China  Three mutually perpendicular sections: horizontal, longitudinal and transverse	Particles 0.25 -5.0mm and 0.25-2.0mm long and elongated voids 0.1-0.5mm long), and aspect ration >1.5, measured using polarisation microscope with rotating stage; 32-117 particles and 31-155 voids were measured in each thinsection.  The data was grouped in 10° intervals and plotted as rose diagrams. $\chi^2$ ( <i>chi</i> ) test and percents of particles in a 10° was used to evaluated the significance of orientation. The three neighbouring 10° intervals with larges particle amount were summed to evaluate fabric strength.	Strong fabric in stoss (proximal) and weak fabric in the lee (distal) sides of roche moutonnées and rock core of drumlin	Not studied  Not studied	In stoss side of a drumlin a transverse preferred orientation in horizontal section is reported. This might be due to tabular-shaped nature of the particles (schist)	Strong microfabric is suggested for deformation till, and weak in the lee sides of small landforms	

## Appendix 2

The summary statistics of microfabric distribution in the artificially sedimented sample  
Mikrolinearitātes dominējošās orientācijas statistikas kopsavilkums mākslīgi izgulsnētajā paraugā

Sample No.	Sample description	Thin section no. and orientation	Microfabric description									
			Fabric strength and spread <sup>2</sup>					Comments on distribution				
			R=21mm $n/S_1/V_1^1$	R=2.6mm		R=1.3mm			R=2.6mm	R=1.3mm		
				N	$S_1 > 0.6$	$S_1 > 0.7$	N	$S_1 > 0.6$	$S_1 > 0.7$			
Sedimentation experiment	Laminated diamicton with flame (fluidisation) structures and dropstones	Single vertical section	2248								Subhorizontal preferred orientation with secondary mode around 130°.	Subhorizontal orientation, flame not expressed; e secondary mode around 130°, representing the sediment bulb induced by the dropstones
			0,649	98	85%	45%	87	80%	50%			
			89									

<sup>1</sup> The preferred orientation  $V_1$  direction for verticals section is counted from vertical direction; for horizontal sections – from N

<sup>2</sup> The measured value is rounded to nearest five degrees as slight errors could be introduced during sample processing

### Appendix 3

The statistics of average orientation of different-size grains in the artificially sedimented sample  
 Dažādu izmēru daļiņu orientācijas statistikas kopsavilkums mākslīgi izgulsnētajā paraugā

Sample No.	index	Equivalent circle diameter A (mm) after Francus (1998)								
		All sizes	0.055-0.065	0.065-0.077	0.077-0.092	0.092-0.109	0.109-0.130	0.130-0.154	0.154-0.184	0.184-0.218
			125-177	177-250	250-354	354-500	500-707	707-1000	1000-1414	1414-2000
Sedimentation experiment	N	2248	813	587	395	234	128	61		
	S <sub>1</sub>	0.649	0.629	0.637	0.702	0.644	0.685	0.691	No data	No data
	V <sub>1</sub>	89°	86°	91°	89°	91°	94°	92°		

## Appendix 4

Microfabric strength and orientation variations of the eigenvector values at samples from Ziemupe site  
Mikrolinearitātes dominējošās orientācijas statistikas kopsavilkums paraugos, kas ievākti Ziemupes atsegumā

Sample No.	Sample description	Thinsection No. orientation, and material	Microfabric description <sup>3</sup>								Comments on distribution		
			R = 21mm n/S <sub>1</sub> /V <sub>1</sub> <sup>4</sup>	Presents of diagrams <sup>5</sup>						R = 2.6 mm			R = 1.3 mm
				R = 2.6 mm		R = 1.3 mm		R = 2.6 mm		R = 1.3 mm			
				n	S <sub>1</sub> > 0.6	S <sub>1</sub> > 0.7	n	S <sub>1</sub> > 0.6	S <sub>1</sub> > 0.7				
ZP1	Contact between upper till and lower till	ZP1-H; facing up sand stringer	924 0.542 83°	31	15%	0	62	30%	1				
		diamicton	363 0.523 2°	21	1	0	0	No data	No data				
		ZP1-1 (right part); facing SEE	278 0.572 94°	36	50%	0	4	3	0	Data spread around horizontal direction	All data belongs to the same domain		
		ZP1-2; facing NEE sand stringer	204 0.662 80°	11	10	4	8	7	4		All diagrams within <30°		
		diamicton	555 0.531 60°	32	80%	0	0	No data	No data	Data mostly in direction 0° to 90°			
ZP2	Middle part of upper till	ZP2-H (right part); facing up	687 0.523 172°	84	25%	1	38	20%	0	Diagrams with S <sub>1</sub> >0.6 spread across 40° to 125°	Diagrams with S <sub>1</sub> >0.6 spread across 0° to 75°		

<sup>3</sup> The measured value is rounded to nearest five degrees as slight errors could be introduced during sample processing

<sup>4</sup> The preferred orientation V<sub>1</sub> direction for verticals section is counted from vertical direction

<sup>5</sup> Presents are round to nearest 5%.



Sample No.	Sample description	Thinsection No. orientation, and material	Microfabric description <sup>3</sup>								Comments on distribution		
			R = 21mm n/S <sub>1</sub> /V <sub>1</sub> <sup>4</sup>	Presents of diagrams <sup>5</sup>						R = 2.6 mm			R = 1.3 mm
				R = 2.6 mm		R = 1.3 mm		R = 2.6 mm		R = 1.3 mm			
				n	S <sub>1</sub> > 0.6	S <sub>1</sub> > 0.7	n	S <sub>1</sub> > 0.6	S <sub>1</sub> > 0.7				
		ZP2-1 (lower part); facing N	817 0.576 87°	53	45%	0	70	55%	5%	All data clustered in direction between 60° and 110°	Diagrams with S <sub>1</sub> >0.6 spread across 50° to 115°		
		ZP2-2 (right part); facing E	609 0.592 82°	67	50%	1	70	55%	5%	Most of data clustered in direction between 50° and 110°	Most of data clustered in direction between 50° and 110°		
ZP3	Lower till, below the contact of upper and lower till	ZP3-H; facing up	330 0.631 96°	21	95%	1	0	No data	No data	Data spread between 65° and 120°			
		ZP3-1 (upper part); facing S	236 0.572 111°	37	20%	0	3	2	0	Data spread between 90° and 160°			
		ZP3-2; facing W	479 0.522 10°	28	10%	0	11	3	0				
ZP4	Lower till	ZP4-H (left part); facing up	733 0.558 70°	57	40%	0	48	65%	5%				
		ZP4-1; facing S	4450 0.558 79°	154	25%	0	367	45%	5%				
		ZP4-2; facing E	4162 0.539 102°	131	5%	0	312	50%	4		Data pointing to all directions		
ZP5	Upper till, above the contact of upper and lower till	ZP5-H; facing up	570 0.540 3°	31	10%	0	2	0	0	All results confined from -50° to 50° sector			
		ZP5-1; facing E	402 0.569 90°	27	20%	1	0	No data	No data	Strongest fabric confined from 65° to 115°			

Sample No.	Sample description	Thinsection No. orientation, and material	Microfabric description <sup>3</sup>						Comments on distribution		
			R = 21mm n/S <sub>1</sub> /V <sub>1</sub> <sup>4</sup>	Presents of diagrams <sup>5</sup>					R = 2.6 mm	R = 1.3 mm	
				R = 2.6 mm		R = 1.3 mm				R = 2.6 mm	R = 1.3 mm
				n	S <sub>1</sub> > 0.6	S <sub>1</sub> > 0.7	n	S <sub>1</sub> > 0.6	S <sub>1</sub> > 0.7		
		ZP5-2; facing S	679 0.533 5°	41	15%	0	2	2	1		
ZP6	Upper part of shear zone below upper till	ZP6-H-2; horizontal Diamicton band	1706 0.526 98°	90	5%	0	62	30%	2	Diagrams with S <sub>1</sub> >0.6 confined to 60° to 120°	Diagrams with S <sub>1</sub> >0.6 (except two) confined to 70° to 140°
		ZP6-1-1; facing SWW diamicton band	607 0.574 103°	35	25%	0	14	7	2	Diagrams with S <sub>1</sub> >0.6 (except one) confined to 90° to 115°; diagrams with weaker fabric are shifting towards wide angle (V <sub>1</sub> >90°)	Diagrams with S <sub>1</sub> >0.6 confined to 70° to 110°
		ZP6-1-2; not analysed Sand band	3871 0.641 103°	88	85%	5%	245	85%	15%	Most of diagrams confine from 90° to 115°	Most of diagrams confine from 80° to 130°
		Diamicton band	1144 0.584 96°	66	50%	0	16	8	1	Diagrams with S <sub>1</sub> >0.6 confined to 75° to 115°; diagrams with weaker fabric are shifting towards wider angle (V <sub>1</sub> >90°)	Diagrams with S <sub>1</sub> >0.6 confined to 75° to 125°
		ZP6-2-1; not analysed Sand band and diamicton band	No data								
		ZP6-2-2 Diamicton	228 0.521 35°	4	0	0	6	0	0		

Sample No.	Sample description	Thinsection No. orientation, and material	Microfabric description <sup>3</sup>								
			R = 21mm n/S <sub>1</sub> /V <sub>1</sub> <sup>4</sup>	Presents of diagrams <sup>5</sup>						Comments on distribution	
				R = 2.6 mm			R = 1.3 mm			R = 2.6 mm	R = 1.3 mm
				n	S <sub>1</sub> > 0.6	S <sub>1</sub> > 0.7	n	S <sub>1</sub> > 0.6	S <sub>1</sub> > 0.7		
ZP7	Lower part of shear zone below upper till	ZP7-H-1; facing down Fine sand with silty matrix and some coarse sand grains	1180 0.541 169°	49	15%	0	61	15%	0	Diagrams with S <sub>1</sub> >0.6 confined to -35° to 5°	Diagrams with S <sub>1</sub> >0.6 confined to -30° to 25°
		ZP7-H-3; horizontal Sand with rounded patches of diamicton, that are protrusions from diamicton band within shear zone cut by the plane of thinsection	1666 0.513 168°	77	15%	0	73	35%	2	Diagrams with S <sub>1</sub> >0.6 pointing in all directions with some clustering around 0°	Diagrams with S <sub>1</sub> >0.6 pointing in all directions
		ZP7-H-3-2; facing up Fine sand	2858 0.544 23°	60	10%	0	164	20%	0	Diagrams with S <sub>1</sub> >0.6 confined to -25° to 50°	Diagrams with S <sub>1</sub> >0.6 confined to -25° to 50°
		ZP7-H-5; facing up Fine sand	1370 0.529 16°	40	15%	0	87	20%	0	Diagrams with weaker fabric are shifting towards wider angle (V <sub>1</sub> >90°)	Diagrams with S <sub>1</sub> >0.6 confined to -20° to 50°
		ZP7-1-1; not analysed	No data								
		ZP7-1-2; facing NNW Sand band with few diamicton boudins	5472 0.668 97°	121	100%	15%	349	95%	25%	Diagrams with S <sub>1</sub> >0.6 confined to 75° to 115°; diagrams with weaker fabric are shifting towards narrower angle (V <sub>1</sub> <90°)	Diagrams with S <sub>1</sub> >0.6 confined to 65° to 120°
		ZP7-2-1; facing NEE: A band of sands	755 0.726 97°	25	100%	75%	43	100%	80%	All diagrams confined to 80° to 110°;	All diagrams confined to 85° to 115°;

Sample No.	Sample description	Thinsection No. orientation, and material	Microfabric description <sup>3</sup>								
			R = 21mm n/S <sub>1</sub> /V <sub>1</sub> <sup>4</sup>	Presents of diagrams <sup>5</sup>						Comments on distribution	
				R = 2.6 mm			R = 1.3 mm			R = 2.6 mm	R = 1.3 mm
				n	S <sub>1</sub> > 0.6	S <sub>1</sub> > 0.7	n	S <sub>1</sub> > 0.6	S <sub>1</sub> > 0.7		
	A band of diamicton		865 0.634 97°	47	85%	20%	28	60%	10%	Diagrams with S <sub>1</sub> >0.6 confined to 80° to 110°; diagrams with weaker fabric are shifting towards narrower angle (V <sub>1</sub> <90°)	Diagrams with S <sub>1</sub> >0.6 confined to 75° to 130°
	ZP7-2-2; facing NEE Sand with string of till (diamicton) boudins, that is embedded in finer sand band		4516 0.680 97°	120	>95%	35%	28	>95%	35%	All diagrams except 1 confined to 85° to 110°	Diagrams with S <sub>1</sub> >0.6 confined to 80° to 120°

## Appendix 5

Identification and general microfabric statistics calculated according to eigenvalue method for thin section samples collected at the  
Plašumi gully site

Plašumu gravas atsegumā ievākto plānslīpējumu paraugu identifikācija un vispārīga mikrolinearitātes sadalījuma statistika,  
aprēķināta izmantojot eigevektoru metodi

Sample No. and description	Thin section No. and orientation	Microfabric description <sup>6</sup>							Comments on distribution	
		R = 21 mm n/S <sub>1</sub> /V <sub>1</sub> <sup>7</sup>	Fabric strength and spread							
			R = 2.6 mm		R = 1.3 mm					
			n	S <sub>1</sub> > 0.6	S <sub>1</sub> > 0.7	n	S <sub>1</sub> > 0.6	S <sub>1</sub> > 0.7		
Ps6	Ps6-1; facing N	No data								
Upper till, near the 23,540 m costal profile mark, 2 m below the top of the upper till	Ps6-2; facing E	1720 0.561 76°	91	30%	1	27	45%	0		
	Ps7	Ps7-1-H; facing up	1262 0.522 92°	58	2	0	51	20%	1	
Upper till near the 23,540 m costal profile mark, 1m below the top of the upper till	Ps7-1-1; facing NE	2407 0.555 103°	108	30%	0	120	45%	1		
	Ps7-1-2; facing SE	1651 0.564 81°	70	30%	0	86	55%	5%		
	Ps7-2-H; facing up	2554 0.524 92°	105	10%	0	161	35%	0		
	Ps7-2-1; facing E	1963 0.546 104°	88	20%	0	90	40%	0		

<sup>6</sup> The measured value is rounded to nearest five degrees as slight errors could be introduced during sample processing

<sup>7</sup> The preferred orientation V<sub>1</sub> direction for verticals section is counted from vertical direction

Sample No. and description	Thin section No. and orientation	Microfabric description <sup>6</sup>							Comments on distribution	
		R = 21 mm n/S <sub>1</sub> /V <sub>1</sub> <sup>7</sup>	Fabric strength and spread			R = 1.3 mm				
			n	S <sub>1</sub> > 0.6	S <sub>1</sub> > 0.7	n	S <sub>1</sub> > 0.6	S <sub>1</sub> > 0.7		
Ps8 Upper till near the 23 540m costal profile mark, 0.4m below the top of upper till	Ps8-H; facing up	1023 0.529 73°	61	30%	1	6	1	0		

## Appendix 6

An apparent orientation of different-sized grains observed in the thin section samples from Plašumi gully site  
Dažāda izmēra graudu šķietamās orientācijas statistika plānslīpējumu paraugos no Plašumu gravas apkārtnes

Sample No.	Equivalent circle diameter A (mm) after Francus (1998)									
	All sizes	0.055-0.065	0.065-0.077	0.077-0.092	0.092-0.109	0.109-0.130	0.130-0.154	0.154-0.184	0.184-0.218	
Horizontal sections										
Ps7-1-H	n	1262	357	276	214	141	103	80	53	38
	S <sub>1</sub>	0.522	0.527	0.545	0.523	0.518	0.522	0.531	0.598	0.587
	V <sub>1</sub>	92°	77°	103°	143°	84°	112°	13°	72°	87°
Ps7-2-H	n	2554	744	565	449	284	236	126	86	64
	S <sub>1</sub>	0.524	0.538	0.517	0.542	0.526	0.537	0.541	0.590	0.539
	V <sub>1</sub>	92°	79°	121°	101°	75°	113°	103°	22°	95°
Ps8-H	n	1023	268	220	194	129	89	65	30	
	S <sub>1</sub>	0.529	0.510	0.563	0.541	0.604	0.513	0.573	0.580	No data
	V <sub>1</sub>	73°	14°	54°	59°	100°	112°	75°	115°	
Vertical sections										
Ps6-2	n	1720	455	372	317	231	148	95	60	42
	S <sub>1</sub>	0.561	0.536	0.575	0.568	0.564	0.593	0.577	0.619	0.724
	V <sub>1</sub>	76°	77°	88°	68°	65°	54°	88°	76°	104°
Ps7-1-1	n	2407	726	545	420	279	202	115	75	45
	S <sub>1</sub>	0.555	0.557	0.552	0.552	0.571	0.564	0.543	0.592	0.546
	V <sub>1</sub>	103°	106°	92°	100°	102°	120°	102°	103°	121°
Ps7-1-2	n	1651	439	365	311	198	137	108	54	39
	S <sub>1</sub>	0.564	0.557	0.549	0.586	0.574	0.567	0.584	0.633	0.537
	V <sub>1</sub>	81°	70°	86°	77°	84°	95°	91°	89°	47°
Ps7-2-1	n	1963	560	436	337	248	160	100	74	48
	S <sub>1</sub>	0.546	0.526	0.562	0.553	0.581	0.550	0.528	0.570	0.614
	V <sub>1</sub>	104°	79°	109°	115°	114°	92°	99°	97°	91°



## Appendix 7

Summary of measured microfabric orientation in the samples from sandy diamicton at Strante site  
4.9. tabula. Mikrolinearitātes mērījumu kopsavilkums smilšainajā diamiktonā no Strantes atseguma

Sample No.	Sample description	Thin section no. and orientation	Microfabric description <sup>8</sup>								
			R = 21 mm $n/S_1/V_1$ <sup>9</sup>	Fabric strength and spread						Comments on distribution	
				R = 2.6 mm			R = 1.3 mm			R = 2.6 mm	R = 1.3 mm
N	$S_1 > 0.6$	$S_1 > 0.7$	N	$S_1 > 0.6$	$S_1 > 0.7$						
2n	Sandy diamicton, sample collected 1 m above the lower boundary of sandy diamicton, at 30,730 m of the costal profile	2n-H; horizontal (top to the 30°)	1833 0.560 163° <sup>10</sup>	90	35%	2	29	50%	0	A secondary maximum at ~60°	
		2n-1; facing 200° (SSW)	1651 0.585 80°	98	50%	0	2	0	0	A “glass ceiling” around $S_1 \sim 0.67$	
		2n-2; facing 290° (NWW)	1318 0.589 102°	68	55%	0	21	60%	0	A “glass ceiling” around $S_1 \sim 0.66$	
3n	Sandy diamicton, sample collected 0,5 m above the lower boundary of the sandy diamicton, at 30,730 m of the costal profile	3n-H; facing up (top to the N)	3155 0.573 84°	139	20%	0	134	75%	5%	The diagrams with strongest fabric are clustered; summary orientation confined to 46°-140° sector	Domain-like distribution
		3n-1; facing S	3150 0.551 99°	128	25%	0	184	40%	<5%		Domain-like distribution
		3n-2; facing W	2391 0.589 98°	101	45%	0	127	55%	5%		

<sup>8</sup> The measured value is rounded to nearest five degrees as slight errors could be introduced during sample processing

<sup>9</sup> The preferred orientation  $V_1$  direction for verticals section is counted from vertical direction

<sup>10</sup> Corrected for the thinsection orientation

Sample No.	Sample description	Thin section no. and orientation	Microfabric description <sup>8</sup>							Comments on distribution	
			R = 21 mm n/S <sub>1</sub> /V <sub>1</sub> <sup>9</sup>	Fabric strength and spread						R = 2.6 mm	R = 1.3 mm
				R = 2.6 mm		R = 1.3 mm					
N	S <sub>1</sub> >0.6	S <sub>1</sub> >0.7	N	S <sub>1</sub> >0.6	S <sub>1</sub> >0.7						
4n	Sandy diamicton, sample collected just above the lower boundary of the sandy diamicton, at 30,730 m of the costal profile	4n-H; horizontal (top – not known)	2349 0.528 Not known	119	15%	0	81	25%	0		
		4n-1; vertical section orthogonal to 4n-2	2733 0.549 102°	106	30%	0	172	60%	2	A secondary maximum at ~20°	For most diagrams with S <sub>1</sub> > 0.6; V <sub>1</sub> is in one of two broad modes: 0° to 50°, and 80° to 140° corresponding to fold structures in thin section. A “glass ceiling” around S <sub>1</sub> ~0.69, few S <sub>1</sub> values are above
		4n-2; vertical section orthogonal to 4n-1	Not processed due to low quality								
5n	Bands of fine sand and silt, formed as a result of macroscale deformation at the base of the sandy diamicton, at the 30,730 m mark of the coastal profile	5n-1; vertical, non specified	1863 0.747 71°	79	90%	70%	77	100%	100%		For diagrams with S <sub>1</sub> < 0.7; V <sub>1</sub> is confined in the sector from 30° to 70°; for diagrams with S <sub>1</sub> > 0.7; V <sub>1</sub> is confined from 62° to 83°. Diagrams with low S <sub>1</sub> values forms fold-like pattern.
		5n-2; vertical not specified	460 0.667 90°	18	90%	35%	17	80%	10%		

Sample No.	Sample description	Thin section no. and orientation	Microfabric description <sup>8</sup>							Comments on distribution	
			R = 21 mm n/S <sub>1</sub> /V <sub>1</sub> <sup>9</sup>	Fabric strength and spread						R = 2.6 mm	R = 1.3 mm
				R = 2.6 mm		R = 1.3 mm					
N	S <sub>1</sub> >0.6	S <sub>1</sub> >0.7	N	S <sub>1</sub> >0.6	S <sub>1</sub> >0.7						
01k	Sandy diamicton, sample collected at the base of the layer, at the 30,710 m coastal profile mark	01k-H; facing up (top to the 36°)	1258 0.529 119° <sup>11</sup>	82	20%	0	22	45%	1		A fold-like distribution
		01k-1; facing SW (216°)	1676 0.647 94°	69	90%	10%	81	80%	20%		
		01k-2; facing 306° (NW) Data from polarised light mosaic image with buffer lines	3539 0.615 83°	178	70%	1	113	65%	15%		A “glass ceiling” around S <sub>1</sub> ~0.68; only few data are above
		Data from plain light photomerge image	1366 0.623 80°	89	75%	15%	17	9	2		
02k	Sandy diamicton, sample collected 1 m above the base of the layer, at the 30,710 m coastal profile mark	02k-H; facing up (top to the N)	2532 0.598 104°	124	60%	1	92	55%	10%		A “glass ceiling” around S <sub>1</sub> ~0.70
		02k-1, vertical not specified (S or N)	1512 0.641 90°	110	85%	20%	n	n	n		
		02k-2, vertical, facing E	1528 0.612 92°	104	65%	5%	5	4	0		

<sup>11</sup> Corrected for the thin section orientation

## Appendix 8

The summary statistic of the apparent orientation of the different-sized sand grains (orientation not corrected for thin section orientation)

4.10. tabula. Dažāda izmēra smilts graudu šķietamās orientācijas statistikas kopsavilkums (orientācija nav koriģēta atbilstoši plānslīpējuma orientācijai)

Sample No.	n/S <sub>1</sub> /V <sub>1</sub> <sup>12</sup>	Equivalent circle diameter A (mm) after Francus (1998)								
		All sizes	0.055-0.065	0.065-0.077	0.077-0.092	0.092-0.109	0.109-0.130	0.130-0.154	0.154-0.184	0.184-0.218
2n-H	n	1833	737	488	270	171	73	53		
	S <sub>1</sub>	0.560	0.540	0.585	0.580	0.540	0.588	0.588	No data	No data
	V <sub>1</sub>	133°	137°	128°	140°	133°	109°	145°		
2n-1	n	1561	656	411	223	109	75	47		
	S <sub>1</sub>	0.585	0.572	0.589	0.573	0.558	0.681	0.657	No data	No data
	V <sub>1</sub>	80°	80°	85°	72°	70°	84°	88°		
2n-2	n	1318	570	343	210	74	56			
	S <sub>1</sub>	0.589	0.577	0.605	0.564	0.620	0.645	No data	No data	No data
	V <sub>1</sub>	102°	101°	104°	93°	102°	114°			
3n-H	n	3155	1187	809	461	283	184	114	81	36
	S <sub>1</sub>	0.573	0.569	0.580	0.569	0.560	0.540	0.667	0.647	0.561
	V <sub>1</sub>	84°	81°	91°	78°	79°	66°	92°	88°	80°
3n-1	n	3150	1235	829	502	262	182	73	45	
	S <sub>1</sub>	0.551	0.558	0.549	0.569	0.541	0.537	0.549	0.560	No data
	V <sub>1</sub>	99°	103°	102°	83°	88°	127°	121°	96°	
3n-2	n	2391	944	616	368	196	115	86	38	
	S <sub>1</sub>	0.589	0.592	0.598	0.588	0.583	0.575	0.574	0.663	No data
	V <sub>1</sub>	98°	103°	90°	102°	103°	87°	102°	78°	
4n-H	n	2349	893	585	343	224	129	87	56	32
	S <sub>1</sub>	0.528	0.520	0.563	0.509	0.538	0.543	0.532	0.522	0.563
	V <sub>1</sub>	83°	83°	79°	68°	118°	93°	8°	61°	81°
4n-1	n	2733	948	700	471	265	158	109	56	
	S <sub>1</sub>	0.549	0.551	0.551	0.571	0.532	0.565	0.520	0.577	No data
	V <sub>1</sub>	102°	103°	97°	115°	73°	94°	84°	107°	

<sup>12</sup> The preferred orientation V<sub>1</sub> direction for verticals section is counted from vertical direction

Sample No.	n/S <sub>1</sub> /V <sub>1</sub> <sup>12</sup>	Equivalent circle diameter A (mm) after Francus (1998)								
		All sizes	0.055-0.065	0.065-0.077	0.077-0.092	0.092-0.109	0.109-0.130	0.130-0.154	0.154-0.184	0.184-0.218
5n-1	n	1863	787	521	293	154	72			
	S <sub>1</sub>	0.747	0.730	0.756	0.744	0.776	0.779	No data	No data	No data
	V <sub>1</sub>	71°	71°	69°	71°	72°	77°			
5n-2	n	460	185	121	86	47				
	S <sub>1</sub>	0.667	0.682	0.680	0.665	0.626	No data	No data	No data	No data
	V <sub>1</sub>	90°	92°	94°	79°	91°				
01k-H	n	1258	553	317	180	94	65			
	S <sub>1</sub>	0.529	0.523	0.551	0.537	0.506	0.549	No data	No data	No data
	V <sub>1</sub>	83°	89°	85°	68°	159°	100°			
01k-1	n	1676	681	453	215	163	92	54	33	
	S <sub>1</sub>	0.647	0.646	0.636	0.644	0.657	0.675	0.712	0.690	No data
	V <sub>1</sub>	94°	94°	97°	98°	91°	94°	89°	80°	
01k-2 <sup>13</sup> (buffer-lines)	n	3539	1593	937	459	271	136	79	49	
	S <sub>1</sub>	0.615	0.613	0.605	0.601	0.635	0.602	0.683	0.748	No data
	V <sub>1</sub>	83°	83°	83°	79°	86°	85°	88°	80°	
01k-2 <sup>14</sup> (photomerge)	n	1366	521	328	217	133	75	51		
	S <sub>1</sub>	0.623	0.599	0.602	0.667	0.643	0.684	0.663	No data	No data
	V <sub>1</sub>	80°	85°	73°	81°	80°	85°	77°		
02k-H	n	2532	1044	662	358	201	124	71	48	
	S <sub>1</sub>	0.598	0.586	0.593	0.619	0.578	0.643	0.649	0.647	No data
	V <sub>1</sub>	104°	102°	106°	100°	110°	106°	106°	106°	
02k-1	n	1512	572	352	213	160	90	64	41	
	S <sub>1</sub>	0.641	0.621	0.664	0.613	0.660	0.673	0.670	0.691	No data
	V <sub>1</sub>	90°	93°	90°	93°	86°	90°	88°	75°	
02k-2	n	1528	635	336	246	129	96	58		
	S <sub>1</sub>	0.612	0.614	0.604	0.588	0.661	0.602	0.649	No data	No data
	V <sub>1</sub>	92°	93°	91°	94°	91°	79°	100°		

<sup>13</sup> polarised light image, mosaic image with buffer lines

<sup>14</sup> plain light photomerge image

## Appendix 9

Summary of measured microfabric orientation in the samples from upper basal till and suspected waterlain till at the Sensala site. An early version of calculation algorithm was used in this case where the number of measurements assigned to any grid point is not saved, but in no case the number of measurements for a considered diagram is less than 30

Mikrolinearitātes mērījumu kopsavilkums paraugos, kas ievākti no Sensalas atseguma augšējās, bazālās morēnas un domājamās ūdenī izgulsnētās morēnas. Aprēķinu veikšanai tika izmantot agrīna algoritma versija, kas nesaglabāja režģa punktam piekrītošo mērījumu skaitu, tomēr statistiskie parametri režģa punktam ir aprēķināti tikai, ja atbilstošo mērījumu skaits nav mazāks kā 30

Sample No.	Sample description	Thin section No. and orientation	Microfabric description <sup>15</sup>								
			R = 21 mm (summary orientation) <sup>16</sup> S <sub>1</sub> /V <sub>1</sub> /coments	Presents of diagrams <sup>17</sup>						Comments on distribution	
				R = 2.6 mm			R = 1.3 mm			R = 2.6 mm	R = 1.3 mm
n	S <sub>1</sub> > 0.6	S <sub>1</sub> > 0.7	n	S <sub>1</sub> > 0.6	S <sub>1</sub> > 0.7						
043	Massive diamicton with coarse sand stringer collected from the upper till at the Sensala site near the -17,550 m profile mark	043-1(H) horizontal section	0.528 V <sub>1</sub> – not known forms an angle of ~30° to the coarse sand stringer	124	20%	0%	67	45%	1	Rather weak fabric (S <sub>1</sub> = 0.5 to 0.6, rarely reaching >0.6), with recognisable domains of preferred orientation	Well expressed domain structure. A fold-like or rotation structure can be recognised. S <sub>1</sub> value usually around 0.5 to 0.6, in some cases <0.6

<sup>15</sup> The measured value is rounded to nearest five degrees as slight errors could be introduced during sample processing

<sup>16</sup> The preferred orientation V<sub>1</sub> direction for verticals section is counted from vertical direction

<sup>17</sup> Usually there is more than 100 diagrams in the case of grid resolution R = 2.6mm and R = 1.3mm; in the latter case, not all grid points have sufficient data density (30) for preferred orientation to be calculated with some confidence, thus the diagram number in both grid resolutions often are similar. Presents are round to nearest 5%.

Sample No.	Sample description	Thin section No. and orientation	Microfabric description <sup>15</sup>								Comments on distribution	
			R = 21 mm (summary orientation) <sup>16</sup> S <sub>1</sub> /V <sub>1</sub> /coments	Presents of diagrams <sup>17</sup>								
				R = 2.6 mm			R = 1.3 mm					
				n	S <sub>1</sub> > 0.6	S <sub>1</sub> > 0.7	n	S <sub>1</sub> > 0.6	S <sub>1</sub> > 0.7	R = 2.6 mm	R = 1.3 mm	
		043-2 vertical section	0.613 92°	152	70%	5%	127	90%	20%	Subhorizontal preferred orientation in whole thin section area.	Domain-like structure can be recognised with domains of subhorizontal, strong fabric and domains of weak fabric and random orientation.	
		043-3 vertical section	0.557 98°	114	30%	2	105	50%	5%	Up to 1 cm large domains of subhorizontal and random orientation can be identified; rather weak fabric.	Domain-like distribution with the strongest fabric being in domains with preferred subhorizontal orientation. Wide variation of fabric strength.	
044	Massive diamicton sample from upper till 3m below the surface, collected near -17,550 m profile mark.	044-1(H); horizontal section	0.532 54°	153	10%	3	26	55%	0		Evident domain pattern of moderate size (~1cm) and lineation zones coinciding with direction of summary orientation. Sometimes fold like distribution.	



Sample No.	Sample description	Thin section No. and orientation	Microfabric description <sup>15</sup>							Comments on distribution	
			R = 21 mm (summary orientation) <sup>16</sup>	Presents of diagrams <sup>17</sup>							
			S <sub>1</sub> /V <sub>1</sub> /coments	R = 2.6 mm		R = 1.3 mm			R = 2.6 mm	R = 1.3 mm	
			n	S <sub>1</sub> > 0.6	S <sub>1</sub> > 0.7	n	S <sub>1</sub> > 0.6	S <sub>1</sub> > 0.7			
072	Massive diamicton with fine sandy silt stringer (with obvious deformation structures in the microscale) from the middle part (1.5 m below the till top) of upper till near the - 17,600 m mark	072-H; facing down	0.677 ~340°	102	95%	0%	77	90%	5%	Uniform and strong fabric with little variations.	Strong, uniform microfabric with some unexpressed domains of weaker orientation.
		072-1, facing to the 75°	= 0.628 ~76°	229	80%	10%	291	80%	20%	Some domain structure can be identified with slight variations in preferred orientation	Some domain structure can be identified with slight (~30°) variations in preferred orientation. A microfabric distribution around the gravel grain indicative of pervasive deformation is identified. Steeper dipping microfabric is observed in where sandy silt material and diamicton is mixed.

Sample No.	Sample description	Thin section No. and orientation	Microfabric description <sup>15</sup>								
			R = 21 mm (summary orientation) <sup>16</sup> S <sub>1</sub> /V <sub>1</sub> /coments	Presents of diagrams <sup>17</sup>						Comments on distribution	
				R = 2.6 mm			R = 1.3 mm			R = 2.6 mm	R = 1.3 mm
				n	S <sub>1</sub> > 0.6	S <sub>1</sub> > 0.7	n	S <sub>1</sub> > 0.6	S <sub>1</sub> > 0.7		
	072-2, facing to the 330°		0.643 ~49°	174	85%	15%	174	90%	30%	~85% of diagrams S <sub>1</sub> >0.6 and 15% above 0.7 out of 174. Uniformly oriented microfabric with some bending of it in the zone of sandy silt stringer and diamicton mixing.	~90% of diagrams S <sub>1</sub> >0.6 and 30% above 0.7 out of 174. Uniform microfabric orientation, with slight undulations in the sandy slit stringer and diamicton mixing zone.
076b <sup>18</sup>	Massive diamicton in the bottom part and coarse sand lamina at the top, collected ~1.5 m below the top of upper till near - 17,600 m profile mark.	076b-H; facing up	Strong preferred orientation to the NNW	-	No data	No data	No data	No data	No data	No data	
		076b-1; facing to the NNE	~ 30° deviating from vertical in diamicton part and sub horizontal in sand part	-	No data	No data	No data	No data	No data	No data	
		076b-2; facing to the SSW	Sub-vertical moderately strong in diamicton part and steeply dipping in sand part	-	No data	No data	No data	No data	No data	No data	

<sup>18</sup> Only approximate microfabric data is extracted from Kalvāns (2004)

Sample No.	Sample description	Thin section No. and orientation	Microfabric description <sup>15</sup>								Comments on distribution	
			R = 21 mm (summary orientation) <sup>16</sup> S <sub>1</sub> /V <sub>1</sub> /coments	Presents of diagrams <sup>17</sup>								
				R = 2.6 mm			R = 1.3 mm					
				n	S <sub>1</sub> > 0.6	S <sub>1</sub> > 0.7	n	S <sub>1</sub> > 0.6	S <sub>1</sub> > 0.7	R = 2.6 mm	R = 1.3 mm	
071a	Massive diamicton collected ~2 m below the top of upper till at Sensala site near the profile mark - 17,600 m.	071a-H; facing down	0.647 28 <sup>o19</sup>	187	90%	20%	250	85%	45%	All the diagrams S <sub>1</sub> >0.7 are confined to <50° wide sector	All the diagrams S <sub>1</sub> >0.7 are confined to <50° wide sector	
		071a-1; facing to the N	0.533 148°	188	15%	0%	144	15%	0%	Preferred orientation in strongest fabric domains pointing approximately in the same direction: all diagrams with S <sub>1</sub> >0.6 are confined to ~60° wide sector. A fold-like or rotation structure can be recognised.	Domain like structure; bending around gravel grains.	
		071a-2; facing to the E	0.628 120°	174	80%	11%	186	85%	25%	Uniform and strong fabric with little variations.	Uniformly oriented in the same direction (domain-like structure in thin section scale not observed).	

<sup>19</sup> Real orientation, after conversion from “facing down” to “facing up” projection

Sample No.	Sample description	Thin section No. and orientation	Microfabric description <sup>15</sup>								Comments on distribution	
			R = 21 mm (summary orientation) <sup>16</sup>	Presents of diagrams <sup>17</sup>								
			S <sub>1</sub> /V <sub>1</sub> /coments	R = 2.6 mm		R = 1.3 mm			R = 2.6 mm		R = 1.3 mm	
				n	S <sub>1</sub> > 0.6	S <sub>1</sub> > 0.7	n	S <sub>1</sub> > 0.6	S <sub>1</sub> > 0.7			
071b	See 071a	071b-H; facing up (extremely dense thin section)	0.677 30°	39	90%	50%	0	No data	No data	Uniform and strong fabric with little variations.	Insufficient data density due to low thin section quality (with minimum data points in a single diagram se to 30)	
		071b-1; facing W	0.679 72°	186	95%	35%	126	100%	50%	All diagrams except three outlier with S <sub>1</sub> >0.7 are confined to 35° sector.	Asymmetric fabric distribution is observed around the gravel grain – at the S side subhorizontal fabric are knocking in the 60° steep, down-facing gravel grain side and bending around curved N side.	

Sample No.	Sample description	Thin section No. and orientation	Microfabric description <sup>15</sup>								
			R = 21 mm (summary orientation) <sup>16</sup> S <sub>1</sub> /V <sub>1</sub> /coments	Presents of diagrams <sup>17</sup>						Comments on distribution	
				R = 2.6 mm			R = 1.3 mm			R = 2.6 mm	R = 1.3 mm
				n	S <sub>1</sub> > 0.6	S <sub>1</sub> > 0.7	n	S <sub>1</sub> > 0.6	S <sub>1</sub> > 0.7		
071b-2;	facing S	0.559 4°	149	30%	0%	133	45%	5%	Rather consistent orientation of strongest fabric diagrams, preferred orientation domains can be identified; bending of fabric around the surface of the large (>1cm), partly sectioned gravel grain	Domains of relatively strong and poor preferred orientation can be identified; if minimum number of measurements in single diagram are set to 10, clearly defined zone of microfabric bending around partly sectioned gravel grain with microfabric discontinuity	

Sample No.	Sample description	Thin section No. and orientation	Microfabric description <sup>15</sup>								Comments on distribution	
			R = 21 mm (summary orientation) <sup>16</sup> S <sub>1</sub> /V <sub>1</sub> /coments	Presents of diagrams <sup>17</sup>			Presents of diagrams <sup>17</sup>					
			n	S <sub>1</sub> > 0.6	S <sub>1</sub> > 0.7	n	S <sub>1</sub> > 0.6	S <sub>1</sub> > 0.7	R = 2.6 mm	R = 1.3 mm		
091	Banded till: diamicton interlayered with silt-rich sand often with flow structures, sample collected 1 m below the top of upper till near - 17,685 m profile mark	091-H; facing up	0.532 160°	185	15%	1	145	40%	4	Few domains with stronger preferred orientation can be identified. Diagrams with S <sub>1</sub> > 0.6 are confined to ~80° wide sector	The preferred orientation is strong at the E and W sides of a gravel grain, roughly coinciding with average microfabric orientation in the section and weak and bending in the S and N sides of a gravel grain. Several fold-like structures and moderately large (~1cm) microfabric domains are observed.	
		091-1; facing to the NNE	0.573 120°	145	35%	2	184	45%	5	Relatively weak fabric is rather consistent and by far most of the diagrams are confined to the 40° wide sector.	The preferred orientation spread is considerably large than in case of R <sub>1</sub> =2.6mm. Strong domain-like pattern emerges, with elongated zones of well developed preferred orientation.	

Sample No.	Sample description	Thin section No. and orientation	Microfabric description <sup>15</sup>								Comments on distribution	
			R = 21 mm (summary orientation) <sup>16</sup> S <sub>1</sub> /V <sub>1</sub> /coments	Presents of diagrams <sup>17</sup>						R = 2.6 mm		
				R = 2.6 mm			R = 1.3 mm					
				n	S <sub>1</sub> > 0.6	S <sub>1</sub> > 0.7	n	S <sub>1</sub> > 0.6	S <sub>1</sub> > 0.7			
	091-2; facing to the SEE	0.550 82°	190	20%	1	166	45%	1	Most of the diagrams with S <sub>1</sub> > 0.6 are confined to ~50° wide sector. Domain-like pattern with bending preferred orientation can be identified, domain size exceeds 1cm.	Rather chaotic preferred orientation and on large (>1cm) domain of consistent preferred orientation.		
092	Banded till: diamicton with interbedded silt-rich sand often with flow structures, sample collected 1.3 m below the top of upper till near - 17,685 m profile mark	092-H; facing up	0.525 159°	105	15%	0%	154	35%	5	Weak fabric however domain-like structure can be identified.	Rather well defined small (few mm) domains with contrasting preferred orientation.	
		092-1; facing to the E	0.576 97°	240	35%	1	602	55%	5%	Rather consistent although predominantly weak microfabric in the sandy part and more chaotic in the diamicton part	The microfabric along the contact between diamicton and sand largely follows the surface bending of it. Domain pattern can be identified.	



Sample No.	Sample description	Thin section No. and orientation	Microfabric description <sup>15</sup>							Comments on distribution	
			R = 21 mm (summary orientation) <sup>16</sup> S <sub>1</sub> /V <sub>1</sub> /coments	Presents of diagrams <sup>17</sup>							
				n	S <sub>1</sub> > 0.6	S <sub>1</sub> > 0.7	n	S <sub>1</sub> > 0.6	S <sub>1</sub> > 0.7	R = 2.6 mm	R = 1.3 mm
092-2;	facing to the N	092-2;	0.589 123°	201	45%	1	314	70%	10%	Most of the diagrams with S <sub>1</sub> > 0.6 are confined to ~45° wide sector. Preferred orientation considerably more consistent in the sandy part than in diamicton part. A fold-like distribution is observed in the sandy part. However it does not coincide with visually observed fold structure.	The preferred orientation spread is similar for both R=1.3mm and R=2.6mm resolutions. Large (>1cm) domains with unexpressed or consistent orientation.
017	Base of water-lain till above its contact with fine sands near the - 17,940 m mark of the costal profile.	017-1 Vertical section	0.601 104°	167	60%	4	453	65%	10%	Rather uniform fabric.	A glass ceiling can be identified at S <sub>1</sub> ~0.75; rather uniform fabric with fabric bending around a gravel grain.

Sample No.	Sample description	Thin section No. and orientation	Microfabric description <sup>15</sup>								Comments on distribution	
			R = 21 mm (summary orientation) <sup>16</sup> S <sub>1</sub> /V <sub>1</sub> /coments	Presents of diagrams <sup>17</sup>			Presents of diagrams <sup>17</sup>					
				n	S <sub>1</sub> > 0.6	S <sub>1</sub> > 0.7	n	S <sub>1</sub> > 0.6	S <sub>1</sub> > 0.7	R = 2.6 mm	R = 1.3 mm	
042	Collected from glaciotectionally deformed section of the water-lain till near the - 17,640 m mark of the costal profile.	042-3 Horizontal section	0.603 73°	109	65%	1	295	70%	10%	A trend is observed for fabric strength increases for diagrams from ~45° (generally weaker fabric) towards 95° (generally stronger fabric, covering most of the data.	Similar fabric strength increases as in case of R = 2.6 mm: the weakest fabric near the ~20°, the strongest - near ~100°.	
		042-1 Vertical section	0.571 125°	98	25%	1	258	45%	6			Dominant mode around 120°; secondary mode around 180°
		042-2 Vertical section	0.533 175°	136	10%	0	336	30%	12			Rather good expressed dominant mode around 0°.